Identification des producteurs d'alcénones dans le registre sédimentaire du Cénozoïque : implications pour l'utilisation des proxys de paléo-température (UK' 37) et de paléo-pCO2 (p37 : 2)

Julien Plancq

N° d'ordre 37-2013 Année 2013

THESE DE L'UNIVERSITE DE LYON

Présentée devant

L'UNIVERSITE CLAUDE BERNARD LYON 1

et

ECOLE DOCTORALE
EVOLUTION ECOSYSTEMES MICROBIOLOGIE MODELISATION (E2M2)

pour l'obtention du

DIPLOME DE DOCTORAT

(arrêté du 7 août 2006)

soutenue publiquement le 13 mars 2013

par

Mr PLANCQ Julien

Identification des producteurs d'alcénones dans le registre sédimentaire du Cénozoïque: implications pour l'utilisation des proxys de paléo-température ($U^{K'}_{37}$) et de paléo-pCO_2 ($\varepsilon_{p37:2}$)

Directeur de thèse : Dr Vincent GROSSI (Université Claude Bernard Lyon 1, France)
Co-directeur de thèse : Pr Emanuela MATTIOLI Université Claude Bernard Lyon 1, France)

JURY :

Pr Antoni ROSELL-MELÉ	(Université Autonome de Barcelone, Espagne)	Rapporteur
Dr Luc BEAUFORT	(CEREGE, France)	Rapporteur
Dr Guillemette MÉNOT	(CEREGE, France)	Examinateur
Dr Gudrun BORNETTE	(Université Claude Bernard Lyon 1, France)	Examinateur
Dr Vincent GROSSI	(Université Claude Bernard Lyon 1, France)	Directeur
Pr Emanuela MATTIOLI	(Université Claude Bernard Lyon 1, France)	Co-directeur
Dr Bernard PITTET	(Université Claude Bernard Lyon 1, France)	Invité

N° d'ordre 37-2013 Année 2013

THESE DE L'UNIVERSITE DE LYON

Présentée devant

L'UNIVERSITE CLAUDE BERNARD LYON 1

et

ECOLE DOCTORALE
EVOLUTION ECOSYSTEMES MICROBIOLOGIE MODELISATION (E2M2)

pour l'obtention du

DIPLOME DE DOCTORAT

(arrêté du 7 août 2006)

soutenue publiquement le 13 mars 2013

par

Mr PLANCQ Julien

Identification des producteurs d'alcénones dans le registre sédimentaire du Cénozoïque: implications pour l'utilisation des proxys de paléo-température ($U^{K'}_{37}$) et de paléo-pCO_2 ($\varepsilon_{p37:2}$)

Directeur de thèse : Dr Vincent GROSSI (Université Claude Bernard Lyon 1, France)
Co-directeur de thèse : Pr Emanuela MATTIOLI Université Claude Bernard Lyon 1, France)

JURY :

Pr Antoni ROSELL-MELÉ	(Université Autonome de Barcelone, Espagne)	Rapporteur
Dr Luc BEAUFORT	(CEREGE, France)	Rapporteur
Dr Guillemette MÉNOT	(CEREGE, France)	Examinateur
Dr Gudrun BORNETTE	(Université Claude Bernard Lyon 1, France)	Examinateur
Dr Vincent GROSSI	(Université Claude Bernard Lyon 1, France)	Directeur
Pr Emanuela MATTIOLI	(Université Claude Bernard Lyon 1, France)	Co-directeur
Dr Bernard PITTET	(Université Claude Bernard Lyon 1, France)	Invité

Remerciements

Les gens qui me connaissent savent que je ne suis pas une personne très expressive… Mais j'attache beaucoup d'importance aux personnes qui m'entourent, et plus particulièrement à celles qui m'ont aidées et soutenues durant ces années de thèse (et plus). C'est pourquoi je tenais vraiment à les remercier, ce que je vais essayer de faire dans les lignes qui suivent…

Dans un premier temps, je remercie toutes les personnes que je vais oublier de citer. J'espère qu'elles ne m'en voudront pas !

Je voudrais remercier Antoni Rosell-Melé, Luc Beaufort, Guillemette Ménot, Gudrun Bornette et Bernard Pittet d'avoir accepté de faire partie de mon jury de thèse et qui me font l'honneur de juger mon travail.

Un grand merci, chaleureux et sincère, à mes directeurs de thèse, Emanuela et Vincent. Une thèse ce n'est pas facile tous les jours, mais quand on est bien encadré, ça aide beaucoup ! Et, dans mon cas, je n'ai vraiment pas à me plaindre…
Merci à Vincent pour sa constante bonne humeur, son humour douteux mais qui donne toujours la pêche, et son « investissement » dans ma formation à la géochimie organique. Merci d'avoir été toujours présent quand il le fallait, pour m'avoir poussé à m'exprimer et à m'affirmer, et pour m'avoir rappelé qu'il ne fallait « rien lâcher » même dans les moments difficiles.
Merci à Emanuela, qui me suit depuis le M1 et que je considère un peu comme ma « maman scientifique » (et je ne suis pas le seul !). Je la remercie pour sa gentillesse, sa grande disponibilité, son optimisme et son écoute. Merci d'avoir toujours cru en moi et de m'avoir poussé à prendre confiance en moi.
Merci à vous deux, vous m'avez beaucoup appris sur le plan scientifique mais aussi sur le plan humain !

Je tiens également à remercier toutes les personnes du Laboratoire de Géologie de Lyon que j'ai côtoyées tout au long de ces années et qui m'ont aidé (des fois sans le savoir) au travers de discussions et de coups de pouce. Je pense notamment à Bernard (pour ses conseils et remarques avisés, et son aide précieuse sur le terrain en Sicile), Gilles, Alex, Stéphane, Claude, Seb (pour notre discussion autour d'une bouteille de rhum), Philippe, Murielle (Mumu), Romain, Nico C., Nicolas O., Samuel, … et j'en passe ! J'ai également une pensée pour Dominique qui nous a quitté bien trop tôt.

Je remercie plus particulièrement tous les membres du R4 pour avoir animé cet étage, notamment lors des pauses café, et qui ont contribué à faire de ce labo un endroit agréable où travailler ! Merci aussi à Claire qui, outre les nombreuses aides administratives, m'a permis de maintenir mon niveau aux mots fléchés ! Et merci à Nath, qui n'est plus au labo depuis, mais qui m'a notamment permis de développer ma culture cinématographique.

Je remercie très chaleureusement Fabienne (Fafa), le pilier du R4 sans qui les pauses café n'existeraient pas! Mais je ne la remercie pas seulement pour ça… Merci pour tous tes sages conseils, ta bonne humeur, ton humour, ton soutien quotidien et ton écoute lors de mes moments de doute. Merci tout simplement d'avoir été là !

Je voudrais aussi remercier tous les anciens et nouveaux doctorants/étudiants qui se sont succédés au cours de ces trois années : Ronan (et Gaïa bien sûr !), Thomas, Raphaël,

Guillaume (maintenant maître de conférences, si si je vous jure !), Jérémy, Vincent, Baptiste (qui a le don de poser LA question qui remet tout en cause mais qui n'en demeure pas moins une personne de très bon conseil), les vénézuéliens María, Jesús et Jacky, Adrien, Eva... La relève semble bien assurée notamment avec Julien C. (qui me fait relativiser sur mon côté sudiste), Marie (la casse cou !), Anaïs (qui me fait travailler mon répondant), Margaux, Aurélien, Jorge, Samer, …

Je remercie aussi toute l'équipe de fouille de Belmont avec qui j'ai passée deux étés inoubliables !

Un grand merci aux personnes extérieures au laboratoire avec qui j'ai pu travailler. Merci à Agata di Stefano (Catane, Italie) pour m'avoir préformé aux nanofossiles du Cénozoïque. Merci à Antonio Caruso (Palerme, Italie) pour son aide précieuse sur le terrain en Sicile. Merci à Laurent Simon (LEHNA, Université Lyon 1) pour les analyses du TOC et ses conseils sur l'aspect statistique. Merci à Jorijntje Henderiks (Uppsala, Suède) pour m'avoir accueilli dans son laboratoire et m'avoir donné un aperçu de la biométrie (et de son importance dans les reconstructions de pCO_2 !).

Je remercie tous mes amis de ma promo de Master PSP et qui ne m'ont jamais quitté ! Fabien, le « gars parfait » un peu tête en l'air mais dont les petits coups de fil en fin de thèse m'ont bien fait plaisir; Elsa, pour sa grande écoute et sa confiance sans failles, et qui m'a surtout converti à la cachaça !
Un merci tout particulier à Anne-Sabine, ma coloc de bureau depuis le M2 et qui finalement est un peu la sœur que je n'ai jamais eu. Merci pour tout: le soutien dans les moments difficiles, la petite bière à l'improviste « juste histoire de », les longues discussions où j'arrive à me livrer, les délires,… Bref merci pour tout (je m'arrête là sinon ça va tourner au mélodramatique !).

J'ai également une pensée pour tous mes amis qui ne m'ont pas directement aidé durant ma thèse, mais avec qui j'ai vécu des moments inoubliables que ce soit sur Lyon et ailleurs ! Merci donc à Ju M. (pour ses soirées « juste un verre » qui finissent à 5h du mat), Julien C. (pour son open bar à Hôtel de Ville), Kévin (pour nos discussions et pour avoir relu mon intro!), Mimi (pour son soutien, son optimisme, sa gentillesse), Anaïs, Nath, Marie…
Je remercie aussi mes amis du sud qui me suivent depuis le collège et qui m'apportent beaucoup, chacun à leur manière. Merci à Rémy, Julie, Jean, JC, Aurélie, Marion, Noëlie, JP, Loïc,...
Merci à Erwin, qui depuis la Licence, essaye de refaire mon éducation (sans trop y arriver) ! (A ce moment même, je ne peux pas m'empêcher de penser à notre petit délire : AAAAAAAAAAHHHHHHH !!!!).

Enfin, un grand merci ma famille, et plus particulièrement à mes parents et mes frères. Mes parents m'ont toujours soutenu dans mon désir précoce de faire des longues études. Ils n'ont jamais douté de mon choix d'orientation et se sont réellement investis pour que je puisse atteindre mes objectifs, et je les en remercie.

Identification des producteurs d'alcénones dans le registre sédimentaire du Cénozoïque: implications pour l'utilisation des proxys de paléo-température ($U^{K'}_{37}$) et de paléo-pCO_2 ($\varepsilon_{p37:2}$).

Les alcénones sont largement utilisées comme proxys pour estimer des températures d'eaux de surface océanique ou des pressions partielles de CO_2 (pCO_2) dans des périodes anciennes. Dans les océans actuels, ces cétones à longues chaînes carbonées sont essentiellement produites par les coccolithophoridés *Emiliania huxleyi* et *Gephyrocapsa oceanica*. Il existe toutefois un écart temporel important entre le premier enregistrement sédimentaire des alcénones au Crétacé (~120 Ma) et la première apparition des producteurs actuels (< 2 Ma). Il apparaît donc essentiel d'identifier les producteurs anciens d'alcénones afin d'assurer la fiabilité des proxys environnementaux basés sur ces biomarqueurs pour les périodes pré-quaternaires. Cette thèse présente trois cas d'étude correspondant à des périodes clés de l'évolution de la famille des Noëlaerhabdaceae, qui comprend les ancêtres cénozoïques des producteurs actuels d'alcénones. La comparaison entre le contenu en alcénones (distribution et concentrations) et les abondances relatives et absolues des différentes espèces de Noëlaerhabdaceae dans des sédiments marins datant de l'Eocène-Oligocène (35-31 Ma), de l'Oligocène-Miocène (25-16 Ma) et du Pliocène supérieur (3,6-2,6 Ma) montre que, contrairement aux hypothèses précédentes, *Reticulofenestra* n'était pas le seul genre responsable de la production d'alcénones au Cénozoïque. Les résultats démontrent également qu'il est essentiel d'identifier avec précision les producteurs et la taille de leur cellule pour les estimations de pCO_2. Au contraire, l'identification formelle des producteurs ne semble pas indispensable pour obtenir des estimations de températures cohérentes.

Identification of alkenone producers in the Cenozoic sedimentary record: implications for the use of paleo-temperature ($U^{K'}_{37}$) and paleo-pCO_2 ($\varepsilon_{p37:2}$) proxies

Alkenones have been widely used as proxies for the reconstruction of sea surface temperatures and of partial pressure of CO_2 (pCO_2) in ancient periods. In modern oceans, these long-chain ketones are mainly produced by the coccolithophores *Emiliania huxleyi* and *Gephyrocapsa oceanica*. However, there is a huge gap between the first record of alkenones in the Cretaceous (~120 Ma) and the first occurrence of the modern alkenone producers (< 2 Ma). Thus, it seems crucial to identify ancient alkenone producers to ensure the applicability of environmental proxies based on these biomarkers in pre-Quaternary sediments. In this PhD thesis, three case studies are considered corresponding to key periods in the evolution history of the Noelaerhabdaceae family, which includes the Cenozoic ancestors of modern alkenone producers. The comparison between alkenone contents (distribution and concentrations) and Noelaerhabdaceae species-specific relative and absolute abundances in marine sediments dating back to the Eocene-Oligocene (35-31 Ma), the Oligocene-Miocene (25-16 Ma) and the late Pliocene (3.6-2.6 Ma) shows that, contrary to common assumptions, *Reticulofenestra* was not the only genus responsible for alkenone production during the Cenozoic. Results also underscore the importance of a careful identification of alkenone producers and of their cell size for pCO_2 reconstructions for pre-Quaternary periods. On the contrary, the identification of producers does not seem essential to obtain consistent paleo-temperature estimates.

DISCIPLINE : Sciences de la Terre, micropaléontologie, géochimie organique

MOTS-CLES/KEYWORDS

Cénozoïque, alcénones, Noëlaerhabdaceae, producteurs, $U^{K'}_{37}$, $\varepsilon_{p37:2}$
Cenozoic, alkenones, Noelaerhabdaceae, producers, $U^{K'}_{37}$, $\varepsilon_{p37:2}$

Laboratoire de Géologie de Lyon : Terre, Planètes, Environnement
UMR CNRS 5276 (CNRS, ENS, Université Lyon 1)
Université Claude Bernard Lyon 1
Campus de la Doua, bât. GEODE
2, rue Raphaël Dubois
69622 Villeurbanne Cedex ; France

Table des matières

Introduction générale

Mieux étudier le passé pour mieux comprendre le futur

Le contexte actuel de réchauffement climatique dû aux fortes émissions anthropiques de gaz à effet de serre (essentiellement le dioxyde de carbone, CO_2) inquiète de plus en plus la communauté scientifique. Cette dernière tente de prévoir la réponse des écosystèmes et l'évolution du climat suite à un apport massif de dioxyde de carbone dans l'atmosphère et l'hydrosphère. Ainsi, de plus en plus d'études s'intéressent à la reconstitution environnementale et climatique de périodes anciennes, durant lesquelles les concentrations atmosphériques en CO_2 étaient comparables à ce qu'elles pourraient être à la fin du 21ème siècle. A ce titre, le Pliocène moyen (~3-3,3 Ma[1]) est considéré comme le modèle le plus récent auquel pourrait ressembler la Terre à la fin du 21ème siècle (Jansen et al., 2007). L'étude des climats de périodes géologiques anciennes semble donc nécessaire pour mieux comprendre et appréhender le climat futur.

Puisqu'il n'est pas possible d'accéder directement aux informations climatiques et océanographiques (température et salinité des eaux océaniques, concentrations atmosphériques en CO_2, etc.) pour les temps anciens, il est nécessaire d'utiliser des données ou des outils indirects, appelés « proxys[2] ». A l'heure actuelle, un des proxys (paléo-) environnementaux les plus couramment utilisés depuis les années 1970 est sans doute la composition en isotopes stables de l'oxygène ($\delta^{18}O$) du test calcaire des foraminifères, qui permet d'estimer la température de l'eau dans laquelle vivait ces micro-organismes (Hecht, 1976; Mix, 1987). Toutefois, de nombreux facteurs, telles que la variation de salinité des eaux océaniques ou les modifications de niche écologique, peuvent influencer les valeurs de $\delta^{18}O$ et biaiser la reconstruction des températures basée sur ce proxy.

Les alcénones : une alternative aux proxys « classiques » ?

A la fin des années 1980, la découverte de lipides à longue chaîne carbonée, les alcénones, a permis de mettre en place un nouveau proxy de température des eaux océaniques de surface, l'$U^{K'}_{37}$, et un nouveau proxy de pression partielle de CO_2 atmosphérique (pCO_2), l'$\varepsilon_{p37:2}$. L'$U^{K'}_{37}$ qui semblait être indépendant des variations de salinité et des modifications de niche écologique de l'organisme producteur, présenta alors une réelle alternative aux proxys

[1] Tous les âges dans ce manuscrit font référence à Gradstein et al. (2012).
[2] Le mot proxy est un nom commun anglais, étymologiquement proche du nom commun français « procuration ». En anglais: proxy (singulier), proxies (pluriel); en français: proxy (singulier), proxys (pluriel).

classiques de température, tel que le $\delta^{18}O$ des foraminifères. De même, l'$\varepsilon_{p37:2}$ permit de pallier aux lacunes d'enregistrement des autres proxys de pCO_2, comme par exemple les stomates des végétaux terrestres. Depuis, de très nombreux travaux ont présenté des reconstitutions paléo-environnementales basées sur ces molécules organiques pour les périodes quaternaires mais également pré-quaternaires (e.g., Bard et al., 1997; Henderiks et Bollmann, 2004; Pahnke et Sachs, 2006; Figure 0-1).

Les alcénones sont actuellement produites par un nombre restreint d'algues haptophytes unicellulaires de l'ordre des Isochrysidales, qui inclut les coccolithophoridés (haptophytes calcifiantes) *Emiliania huxleyi* et *Gephyrocapsa oceanica* (Marlowe et al., 1984; Volkman et al., 1980, 1995). Les proxys de température et de pCO_2 basés sur les alcénones ont donc été calibrés sur les espèces *E. huxleyi* et *G. oceanica* en culture (e.g., Conte et al, 1998; Popp et al., 1998; Riebesell et al., 2000) ou à partir de sédiments océaniques de surface (e.g., Rosell-Melé et al., 1995; Müller et al., 1998). Or, il existe un écart temporel significatif entre le premier enregistrement sédimentaire des alcénones au Crétacé inférieur (~120 Ma; Farrimond et al., 1986; Brassell et al., 2004) et la première apparition des producteurs actuels d'alcénones (0,27 Ma pour *E. huxleyi* [Thierstein et al., 1977] et 1,85 Ma [Pujos-Lamy, 1977] pour *G. oceanica*). Puisque *E. huxleyi* et *G. oceanica* ne peuvent pas être responsables de la production d'alcénones sur l'ensemble du Cénozoïque et au Mésozoïque, il semble donc primordial d'identifier les producteurs anciens, afin de garantir l'application des proxys basés sur ces lipides dans des sédiments pré-datant l'apparition des producteurs actuels.

Suite à l'observation de la présence concomitante de coccolithes du genre *Reticulofenestra* et d'alcénones dans des sédiments datant depuis l'Eocène (56-33,9 Ma), Marlowe et collaborateurs (1990) ont suggéré que le producteur d'alcénones le plus probable pendant le Cénozoïque devait faire partie du genre *Reticulofenestra* qui, comme *Emiliania* et *Gephyrocapsa*, appartient à la famille des Noëlaerhabdaceae. Mais cette hypothèse n'a jamais vraiment été démontrée et ne s'est pas appuyée sur une quantification absolue des concentrations en alcénones et des abondances de *Reticulofenestra*.

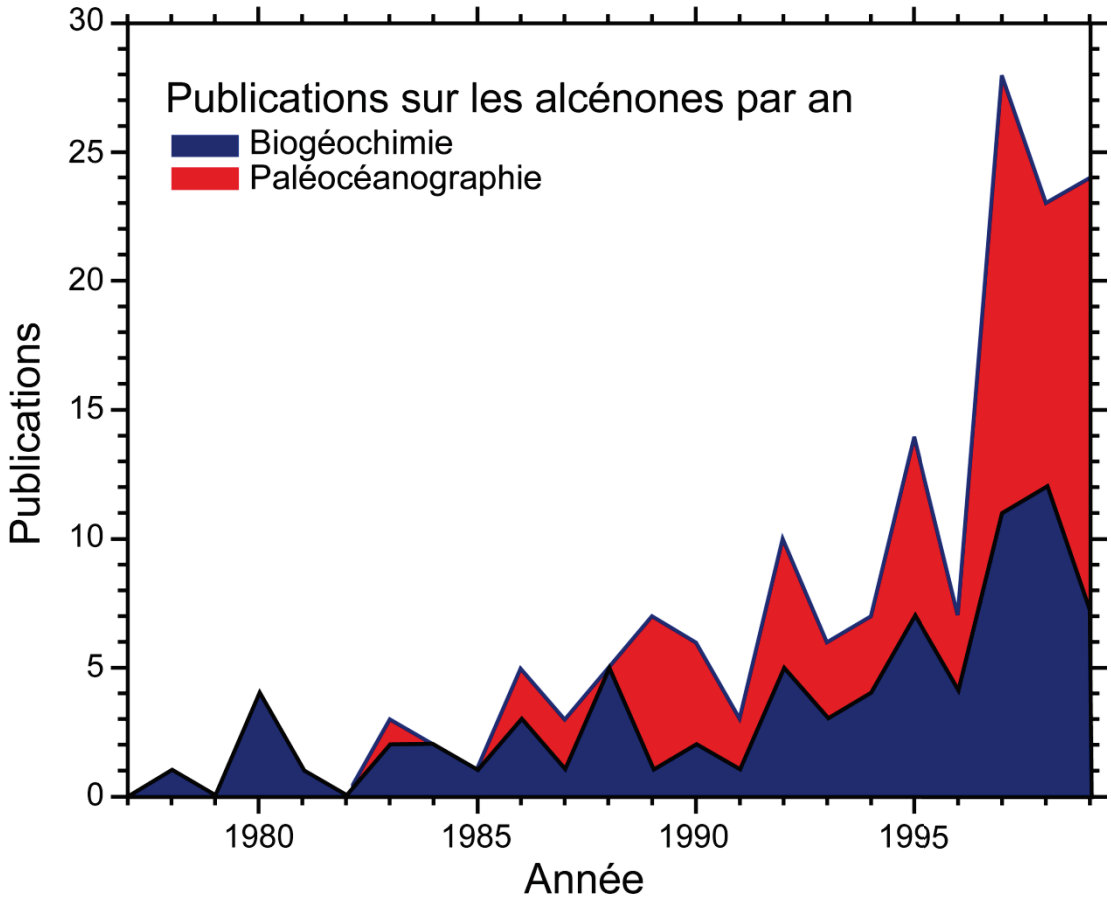

Figure 0-1. Les papiers de biogéochimie traitent de la structure, de la présence et de la préservation des alcénones dans l'environnement. Les papiers de paléocéanographie sont des applications des proxys basés sur les alcénones dans des études paléo-environnementales (modifié d'après Eglinton et al., 2001).

Objectifs de la thèse

Ce travail de thèse a donc pour objectifs d'apporter des éléments de réponses aux questions suivantes: quelles étaient les espèces productrices d'alcénones au cours du Cénozoïque ? L'hypothèse de Marlowe et collaborateurs (1990) est-elle vérifiée et généralisable ? L'identification formelle des producteurs anciens d'alcénones est-elle essentielle pour l'utilisation des proxys basés ces lipides ($U^{K'}_{37}$ et $\varepsilon_{p37:2}$) dans des sédiments pré-datant l'apparition des producteurs actuels ?

Pour tenter de répondre à ces questions, une double approche couplant des méthodes de géochimie organique et de micropaléontologie quantitative a été envisagée[3]. La quantification absolue des concentrations en alcénones et des assemblages de coccolithes (plus

[3] Les principales méthodes utilisées au cours de ce travail de thèse sont détaillées en Annexe 1.

particulièrement des Noëlaerhabdaceae) a été entreprise dans les mêmes sédiments. Les profils de variations des concentrations en alcénones et des abondances (relatives et absolues) des différentes espèces de Noëlaerhabdaceae ont ensuite été comparés pour tenter de déceler une co-variation entre les alcénones et une espèce particulière de coccolithe (identifiée alors comme producteur potentiel). Pour cette approche, de bonnes conditions de préservation sont bien évidemment essentielles, afin d'éviter un biais dans les profils de variations suite à une dégradation (ou une préservation) préférentielle des alcénones par rapport aux coccolithes (et inversement). Une telle approche a été utilisée auparavant dans des sédiments quaternaires (e.g. Müller et al., 1997; Weaver et al., 1999), et quelques rares études l'ont appliquée à des sédiments plus anciens (Pliocène, 5,33-2,59 Ma; Bolton et al., 2010; Beltran et al., 2011). Cependant, ces dernières ne présentent pas de quantifications absolues (en spécimens par gramme de sédiment) des différentes espèces de Noëlaerhabdaceae.

De plus, dans ce travail de thèse, toutes les alcénones présentes dans les sédiments ont été quantifiées individuellement, dans le but d'observer d'éventuelles variations dans la distribution des différentes alcénones et ainsi déceler d'éventuels changements de producteurs et/ou de conditions environnementales (variations de température, de concentrations en nutriments, etc).

Les sédiments analysés dans ce travail de thèse proviennent de forages profonds (Deep Sea Drilling Project, DSDP) en Atlantique et Pacifique et d'affleurements de Sicile. Le choix des échantillons a été guidé par le fait qu'ils couvrent des périodes clés de l'évolution des Noëlaerhabdaceae (Figure 0-2), mais aussi parce que des études antérieures ont indiqué la présence d'alcénones dans ces échantillons. La présence d'alcénones est en effet un point crucial pour mener à bien ce travail.

Ce manuscrit s'articule autour de cinq chapitres, dont trois écrits sous forme d'articles de recherche (publié, soumis ou en préparation).

Le **chapitre 1** présente un état de l'art sur les alcénones et sur leur utilisation en tant que proxys paléo-environnementaux.

Les trois chapitres suivants présentent des études paléo-environnementales couvrant trois périodes clés de l'évolution des Noëlaerhabdaceae (Figure 0-2).

Le **chapitre 2** couvre la transition Eocène-Oligocène (34,8-30,7 Ma) du Site DSDP 511 (Atlantique Sud). L'étude couplée des variations de températures des eaux océaniques de surface (SSTs) reconstruites à partir de l'$U^{K'}_{37}$, des concentrations en carbonate de calcium et

en biomarqueurs lipidiques, et des flux de nannofossiles[4], permet de mieux caractériser les changements de température et de productivité survenant au Site 511 autour de la limite Eocène-Oligocène. La comparaison entre les températures dérivées de l'$U^{K'}_{37}$ et celles dérivées d'autres proxys permet de discuter de la nécessité ou non de l'identification des producteurs d'alcénones au sein des Noëlaerhabdaceae pour l'application de l'$U^{K'}_{37}$ dans ces sédiments paléogènes.

Le **chapitre 3** s'intéresse à la transition Oligocène-Miocène (25-16 Ma) du Site DSDP 516 (Atlantique Sud). Dans une première partie (3.1), une étude sur les variations d'abondances absolues des assemblages de Noëlaerhabdaceae à différentes latitudes de l'Océan Atlantique et de l'Océan Pacifique montre un changement global dans les assemblages. Cette première partie de chapitre a été soumise pour publication au journal Marine Micropaleontology. Dans la deuxième partie (3.2), la comparaison entre les concentrations en alcénones et les abondances relatives et absolues des différentes espèces de Noëlaerhabdaceae permet une identification précise des producteurs d'alcénones au Site DSDP 516 à la transition Oligocène-Miocène. Ce travail montre que les espèces productrices ne sont pas forcément celles identifiées précédemment dans la littérature. Les implications sur l'estimation des paléo-pCO_2 basées sur les alcénones sont discutées. Cette deuxième partie de chapitre correspond à un article publié dans la revue Paleoceanography (Plancq et al., 2012).

Le **chapitre 4** se focalise sur le Pliocène supérieur (3,6-2,6 Ma) du sud-ouest de la Sicile. Cette étude discute des conditions environnementales régnant lors du dépôt de niveaux riches en matière organique (sapropèles), en s'appuyant sur les variations des SST dérivées de l'$U^{K'}_{37}$, sur les flux d'alcénones et sur la composition et les flux des assemblages de nannofossiles. L'identification des producteurs d'alcénones et la possibilité de l'utilisation de l'$U^{K'}_{37}$ dans ces sédiments pliocènes sont également discutées.

Le **chapitre 5** présente les grandes conclusions de ce travail de thèse et certaines perspectives.

Enfin, le manuscrit se termine par des annexes présentant les principales méthodes utilisées au cours de ce travail (**Annexe 1**) et la taxonomie utilisée pour les Noëlaerhabdaceae (**Annexe 2**).

[4] Les nannofossiles incluent les coccolithes (écailles calcaires produites par les coccolithophoridés) et les nannolithes (d'origine incertaine, *incertae sedis*).

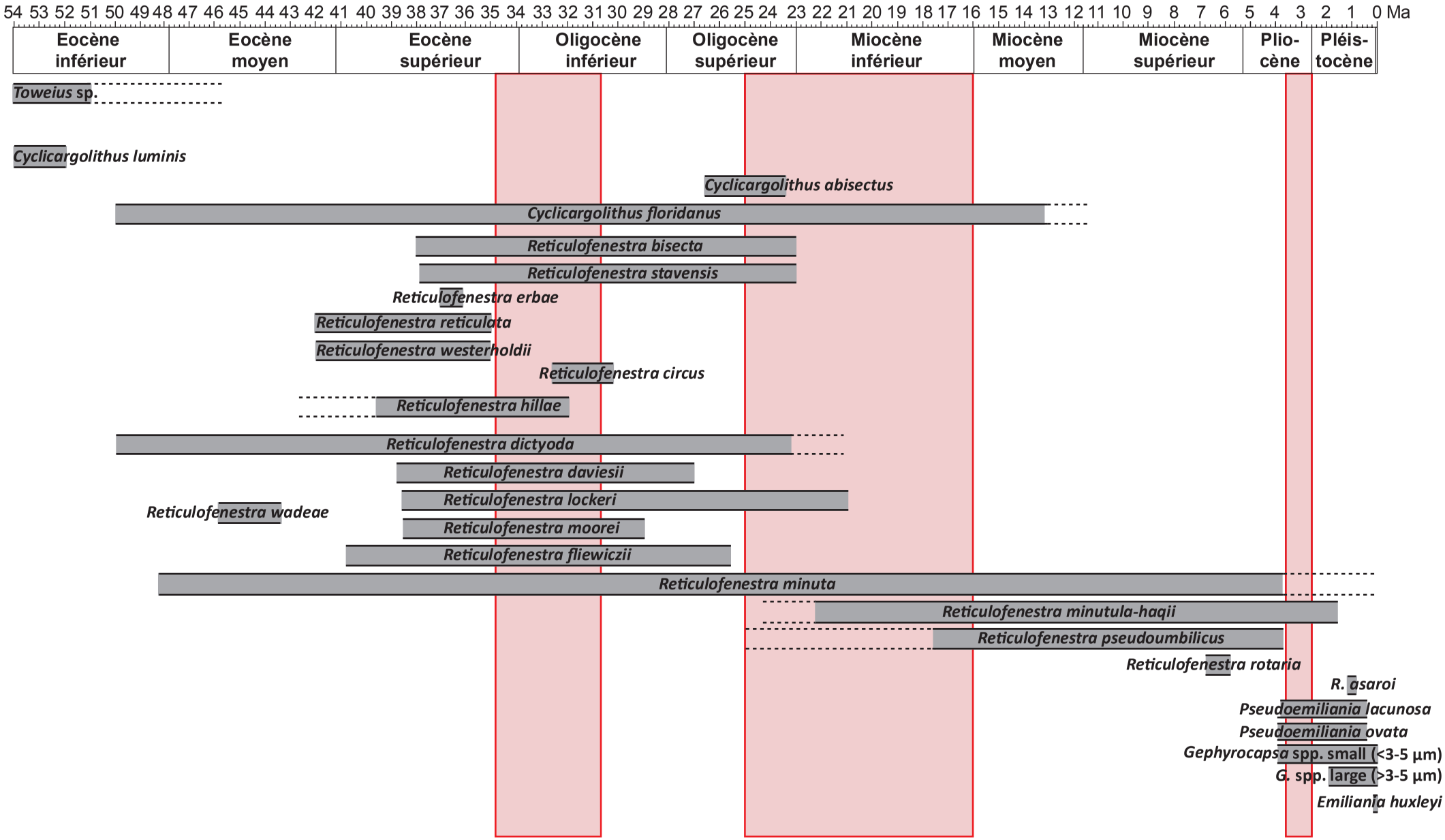

Figure 0-2. Répartition stratigraphique des principales espèces de Noëlaerhabdaceae au cours du Paléogène et du Néogène montrant les principales périodes de diversification au sein de la famille (modifié d'après Young, 1998; Bown et Dunkley Jones, 2012). Les bandes grises indiquent les répartitions stratigraphiques bien définies, les bandes en pointillés les répartitions discutables. Les bandes rouges indiquent les intervalles de temps étudiés dans ce travail de thèse.

Références

Bard, E., Rostek, F., Sonzogni, C., 1997. Interhemispheric synchrony of the last deglaciation inferred from alkenone paleothermometry. Nature 385, 707-710, doi:10.1038/385707a0.

Beltran, C., Flores, J.-A., Sicre, M.-A., Baudin, F., Renard, M., de Rafélis, M., 2011. Long chain alkenones in the Early Pliocene Sicilian sediments (Trubi Formation-Punta di Maiata section): implications for the alkenone paleothermometry. Palaeogeography Palaeoclimatology Palaeoecology 308 (3–4), 253–263.

Bolton, C.T., Lawrence, K.T., Gibbs, S.J., Wilson, P.A., Cleaveland, L.C., Timothy, D., Herbert, T.D., 2010. Glacial-interglacial productivity changes recorded by alkenones and microfossils in late Pliocene eastern equatorial Pacific and Atlantic upwelling zones. Earth and Planetary Science Letters 295, 401-411.

Bown, P.R., Dunkley Jones, T., 2012. Calcareous nannofossils from the Paleogene equatorial Pacific (IODP Expedition 320 Sites U1331-1334). Journal of Nannoplankton Research 32 (2), 3-51.

Brassell, S.C., Dumitrescu, M., ODP Leg 198 Shipboard Scientific Party, 2004. Recognition of alkenones in a lower Aptian porcellanite from the west-central Pacific. Organic Geochemistry 35, 181-188.

Conte, M.H., Thompson, A., Lesley, D., Harris, R.P., 1998. Genetic and physiological influences on the alkenone/alkenoate versus growth temperature relationship in *Emiliania huxleyi* and *Gephyrocapsa oceanica*. Geochimica et Cosmochimica Acta 62 (1), 51-68.

Eglinton, T., Conte, M., Eglinton, G., Hayes, J., 2001. Proceedings of a workshop on alkenone-based paleoceanographic indicators. Geochemistry, Geophysics, Geosystems 2 (1). doi: 10.1029/2000GC000122. issn: 1525-2027.

Farrimond, P., Eglinton, G., Brassell, S.C., 1986. Alkenones in Cretaceous black shales, Blake-Bahama Basin, western North Atlantic. Organic Geochemistry 10, 897-903.

Gradstein, F.M., Ogg, J.G., Schmitz, M., Ogg, G. (Eds), 2012. The Geologic Time Scale 2012. Elsevier, 2012, 1176 pp.

Hecht, A., 1976. The oxygen isotope record of foraminifera in deep sea sediments. In: Hedley, R.H., Adams, C.G. (Eds), Foraminifera. Academic Press, New York, pp. 1-43.

Henderiks, J., Bollmann, J., 2004. The *Geophyrocapsa* sea surface paleothermometer put to the test: comparison with alkenone and foraminifera proxies off NW Africa. Marine Micropaleontology 50, 161-184.

Jansen, E., Overpeck, J., Briffa, K.R., Duplessy, J.-C., Joos, F., Masson-Delmotte, V., Olago, D., Otto-Bliesner, B., Peltier, W.R., Rahmstorf, S., Ramesh, R., Raynaud, D., Rind, D., Solomina, O., Villalba, R., Zhang, Z., 2007. Palaeoclimate. In: Solomon, S. et al. (Eds), Climate Change 2007: The Physical Science Basis. Contribution of Working Group I to the Fourth Assessment Report of the Intergovernmental Panel on Climate Change. Cambridge University Press, pp. 433-497.

Marlowe, I.T., Brassell, S.C., Eglinton, G., Green, J.C., 1984. Long chain unsatured kenones and esters in living algae and marine sediments. Organic Geochemistry 6, 135-141.

Marlowe, I.T., Brassell, S.C., Eglinton, G., Green, J.C., 1990. Long-chain alkenones and alkyl alkenoates and the fossil coccolith record of marine sediments. Chemical Geology 88, 349-375.

Mix, A.C., 1987. The oxygen isotope record of glaciation. In: Ruddiman, W.F., Wright, H.E. (Eds), North America and adjacent Oceans during the last deglaciation: The geology of North America v.K-3. Geological Society of America, pp. 111-135.

Müller, P.J., Cepek, M., Ruhland, G., Schneider, R.R., 1997. Alkenone and coccolithophorid species changes in Late Quaternary sediments from the Walvis Ridge: Implications for the alkenone paleotemperature method. Palaeogeography Palaeoclimatology Palaeoecology 135, 71–96.

Müller, P.J., Kirst, G., Rulhand, G., von Storch, I., Rosell-Melé, A., 1998. Calibration of the alkenone paleotemperature index $U^{K'}_{37}$ based on core-tops from the eastern South Atlantic and the global ocean (60°N-60°S). Geochimica et Cosmochimica Acta 62 (10), 1757-1772.

Pahnke, K., Sachs, J.P., 2006. Sea surface temperatures of southern midlatitudes 0-160 kyr B.P. Paleoceanography 21, PA2003, doi: 10.1029/2005PA001191.

Plancq, J., Grossi, V., Henderiks, J., Simon, L., Mattioli, E., 2012. Alkenone producers during late Oligocene–early Miocene revisited. Paleoceanography 27, PA1202, doi:10.1029/2011PA002164.

Popp, B.N., Laws, E.A., Bidigare, R.R., Dore, J.E., Hanson, K.L., Wakeham, S.G., 1998. Effect of phytoplankton cell geometry on carbon isotopic fractionation. Geochimica et Cosmochimica Acta 62, 69–77.

Pujos-Lamy, A., 1977. Essai d'établissement d'une biostratigraphie du nannoplancton calcaire dans le Pleistocène de l'Atlantique Nord-oriental. Boreas 6, 323-331.

Riebesell, U., Revill, A.T., Hodsworth, D.G., Volkman, J.K., 2000. The effects of varying CO_2 concentration on lipid composition and carbon isotope fractionation in *Emiliania huxleyi*. Geochimica et Cosmochimica Acta 64, 4179-4192.

Rosell-Melé, A., Eglinton, G., Pflaumann, U., Sarnthein, M., 1995. Atlantic core-top calibration of the $U^{K'}_{37}$ index as a sea surface paleotemperature indicator. Geochimica et Cosmochimica Acta 59, 3099-3107.

Thierstein, H.R., Geitzenauer, K.R., Molfino, B., 1977. Global synchroneity of late Quaternary coccolith datum levels: Validation by oxygen isotopes. Geology 5, 400-404.

Volkman, J.K., Barrett, S.M., Blackburn, S.I., Sikes, E.L., 1995. Alkenones in *Gephyrocapsa oceanica*: Implications for studies of paleoclimate. Geochimica et Cosmochimica Acta 59, 513-520.

Volkman, J.K., Eglinton, G., Corner, E.D.S., Forsberg, T.E.V., 1980. Long-chain alkenes and alkenones in the marine coccolithphorid *Emiliania huxleyi*. Phytochemistry 19, 2619-2622.

Weaver, P.P.E., Chapman, M.R., Eglinton, G., Zhao, M., Rutledge, D., Read, G., 1999. Combined coccolith, foraminiferal and biomarker reconstruction of paleoceanographic conditions over the past 120 kyr in the northern North Atlantic (59°N, 23°W). Paleoceanography 14, 336-349.

Young, J.R., 1998. Neogene. In: Bown, P.R. (Ed.), Calcareous Nannofossil Biostratigraphy. British Micropalaeontology Society Publication Series, Kluver Academic Publishers, Cambridge, pp. 5.

Chapitre 1
Exposé bibliographique

1.1. Structure des alcénones

Les alcénones sont des cétones à longue chaîne carbonée (35 à 41 atomes de carbone) possédant 1 à 5 doubles liaisons carbone-carbone (ou insaturations). Les alcénones les plus abondantes dans les haptophytes et les sédiments marins actuels sont les alcénones di- et tri-insaturées à 37-39 atomes de carbone (Figure 1-1). La nomenclature des alcénones les plus communes ainsi que leurs abréviations (utilisées dans ce manuscrit) sont présentées dans la Table 1-1.

Ces molécules présentent des caractéristiques chimiques assez particulières pour des lipides :

- une grande longueur de chaîne carbonée (35 à 41 atomes de carbone);
- une stéréochimie des doubles liaisons *trans* (E) et non pas *cis* (Z) comme dans la majorité des lipides (Rechka et Maxwell, 1988);
- un espacement de leurs insaturations allant de 3 à 5 groupements méthylènes CH_2 (e.g., de Leeuw et al., 1980; Xu et al., 2001; Rontani et al., 2006).

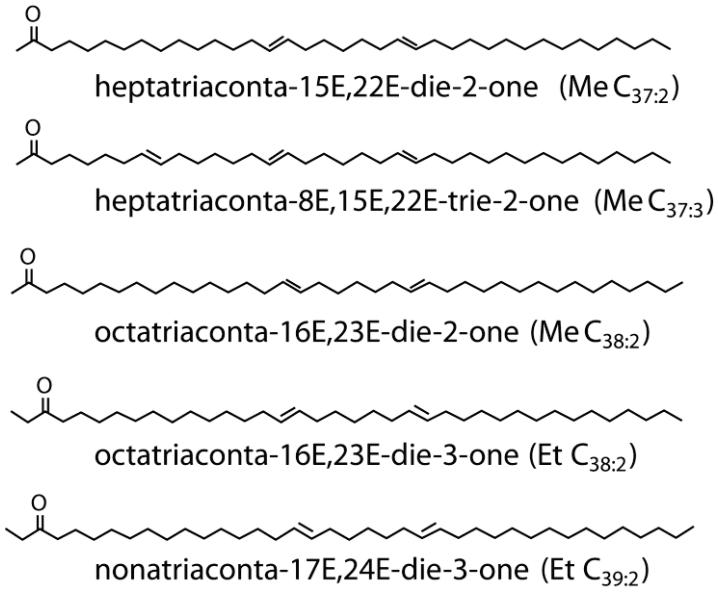

Figure 1-1. Structure chimique des alcénones les plus communes.

Les alcénones ont été identifiées pour la première fois en 1978 par Boon et collaborateurs dans des sédiments provenant de la dorsale de Walvis (sud-ouest de l'Afrique). De nombreuses études ont ensuite mis en évidence l'ubiquité de ces lipides dans le domaine océanique (e.g., Volkman et al., 1980b; Westbroek et al., 1993; Rosell-Melé et al., 1994), mais aussi leur présence dans des environnements lacustres (Li et al., 1996; Theissen et al.,

2005) ou dans les mers fermées (Freeman et Wakeham, 1992; Schulz et al., 2000; Lopez et al., 2005).

Nom	Abréviation
Heptatriacontadien-2-one	$MeC_{37:2}$
Heptatriacontatrien-2-one	$MeC_{37:3}$
Heptatriacontatetra-2-one	$Me_{C37:4}$
Octatriacontadien-2-one	$MeC_{38:2}$
Octatriacontatrien-2-one	$MeC_{38:3}$
Octatriacontadien-3-one	$EtC_{38:2}$
Octatriacontatrien-3-one	$EtC_{38:3}$
Nonatriacontadien-3-one	$EtC_{39:2}$
Nonatriacontatrien-3-one	$EtC_{39:3}$

Table 1-1. Noms et abréviations des alcénones les plus communes.

Les alcénones sont également considérées comme relativement résistantes aux processus de biodégradation en comparaison à d'autres lipides (comme les acides gras ou les stérols) du fait de leur structure particulière (grande longueur de chaîne, doubles liaisons de configuration *trans*, espacement des doubles liaisons par plusieurs groupements méthylènes) (Sun et Wakeham, 1994; Gong et Hollander, 1997, 1999). Ces lipides sont d'ailleurs préservées dans des sédiments anciens datant du Cénozoïque (Pliocène, Miocène, Oligocène, Eocène, 0-65 Ma; e.g., Boon et al., 1978; Marlowe et al., 1984a; Marlowe et al., 1990), et du Crétacé inférieur (Aptien, Albien, ~105-120 Ma; Farrimond et al., 1986; Brassell et al., 2004).

Il est à noter que la présence d'alcènes (hydrocarbures insaturés) et d'esters éthyliques et méthyliques (alcénoates) avec des structures chimiques apparentées aux alcénones a également été reportée dans la plupart des souches d'haptophytes étudiées (par exemple *Emiliania huxleyi*; cf. paragraphe 1.2) et dans des sédiments marins (e.g., de Leeuw et al., 1980; Volkman et al., 1980a; Marlowe et al., 1984a; Conte et al., 1998; Rieley et al., 1998; Grossi et al., 2000).

1.2. Les producteurs actuels d'alcénones

Actuellement, les alcénones sont produites de façon spécifique par des algues planctoniques micrométriques unicellulaires de l'embranchement Haptophyta, de la classe des Prymnesiophyceae et de l'ordre des Isochrysidales (Billard et Inouye, 2004). Les Isochrysidales comprennent la famille des Noëlaerhabdaceae et la famille des Isochrysidaceae (Table 1-2).

Dans la famille des Noëlaerhabdaceae, les alcénones ont été reportées chez les coccolithophoridés *Emiliania huxleyi* (Volkman et al., 1980a,b) et *Gephyrocapsa oceanica* (Volkman et al., 1995) qui sont prédominantes dans les assemblages actuels de nannoplancton (Figure 1-2). Les coccolithophoridés ont la particularité de sécréter autour de leur cellule plusieurs plaques de carbonate de calcium (coccolithes) formant un test appelé coccosphère (Pienaar, 1994). Elles jouent donc un rôle important dans le cycle du carbone, puisque ce sont les seuls organismes à participer simultanément à la pompe du carbone via la photosynthèse et à la contre-pompe du carbone via la production de carbonate de calcium (Rost et Riebesell, 2004). Ainsi il est estimé que la moitié du carbonate pélagique dans l'océan actuel est produite par ces micro-algues marines (Milliman, 1993), notamment par le biais de blooms saisonniers (multiplication massive d'une espèce sur une courte période suite à des conditions environnementales favorables).

Les alcénones ont également été détectées chez des haptophytes non-calcifiantes de la famille des Isochrysidaceae, typiques d'environnements côtiers ou lacustres: *Chrysotila lamellosa* (Marlowe et al., 1984a,b; Rontani et al., 2004) et *Isochrysis galbana* (Marlowe et al., 1984a,b, 1990).

Odre des ISOCHRYSIDALES	
Famille des ISOCHRYSIDACEAE	Famille des NOËLAERHABDACEAE
Genre *Chrysotila* *Chrysotila lamellosa* ***** ***Chrysotila sipitata*** Genre *Dicrateria* *Dicrateria gilva* ***Dicrateria inornata*** Genre *Isochrysis* ***Isochrysis galbana* *** *Isochrysis littoralis*	Genre *Emiliania* ***Emiliania huxleyi* *** Genre *Gephyrocapsa* *Gephyrocapsa crassipons* *Gephyrocapsa ericsonii* *Gephyrocapsa muellerae* ***Gephyrocapsa oceanica* *** *Gephyrocapsa ornata* Genre *Reticulofenestra* *Reticulofenestra maceria* *Reticulofenestra parvula* *Reticulofenestra sessilis* *Reticulofenestra punctata*

Table 1-2. Taxonomie des Isochrysidales actuelles. Les espèces en gras sont les espèces types. Les astérisques indiquent les espèces pour lesquelles la présence d'alcénones a été reportée.

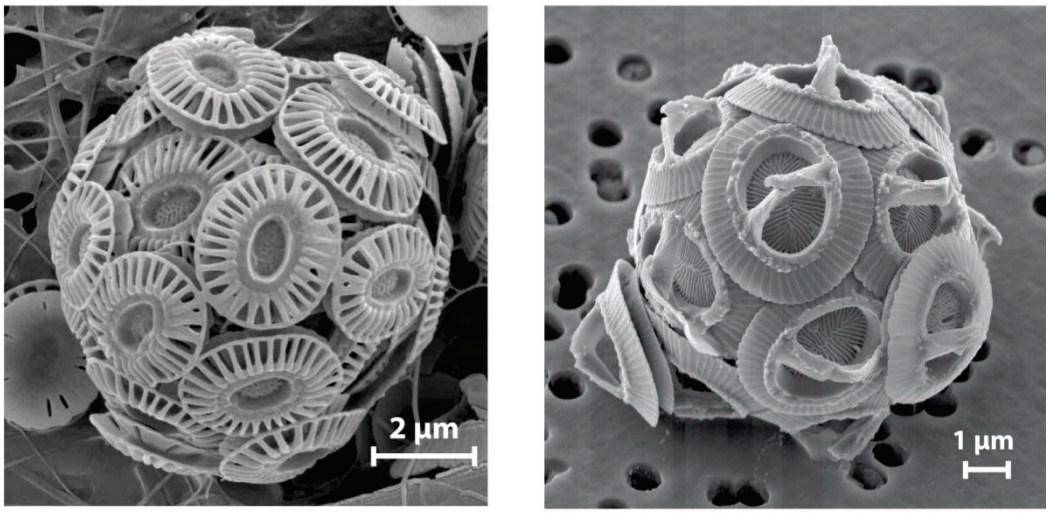

Figure 1-2. Photographies au microscope électronique à balayage (MEB) des coccolithophoridés *Emiliania huxleyi* (à gauche; photographie de J. Young) et *Gephyrocapsa oceanica* (à droite; photographie de NEON ja).

Deux distributions « types » d'alcénones ont été mises en évidence jusqu'à présent (Figure 1-3).

Le premier type (A) est caractéristique des haptophytes marines *Emiliania huxleyi* et *Gephyrocapsa oceanica* et comprend des alcénones en MeC_{37}, Me- et EtC_{38}, Me- et en EtC_{39} (Figure 1-3). Le type B est caractérisé par une forte concentration de l'alcénone en $MeC_{37:4}$ (Figure 1-3) et par la présence d'alcénones à chaînes plus courtes (C_{35}-$_{36}$) et possédant de 1 à 5 insaturations (Schulz et al., 2000; Xu et al., 2001; Sun et al., 2007; Jaraula et al., 2010). Ce profil est rencontré dans des environnements particuliers (lacustres, côtiers, hypersalins ou froids) et pourrait témoigner de la contribution d'haptophytes non-calcifiantes (comme *Chrysotila lamellosa*) ou d'espèces encore non connues mais phylétiquement proches des autres espèces productrices (Marlowe et al., 1990; Coolen et al., 2004; Rontani et al., 2004; Jaraula et al., 2010; Theroux et al., 2010; Toney et al., 2012).

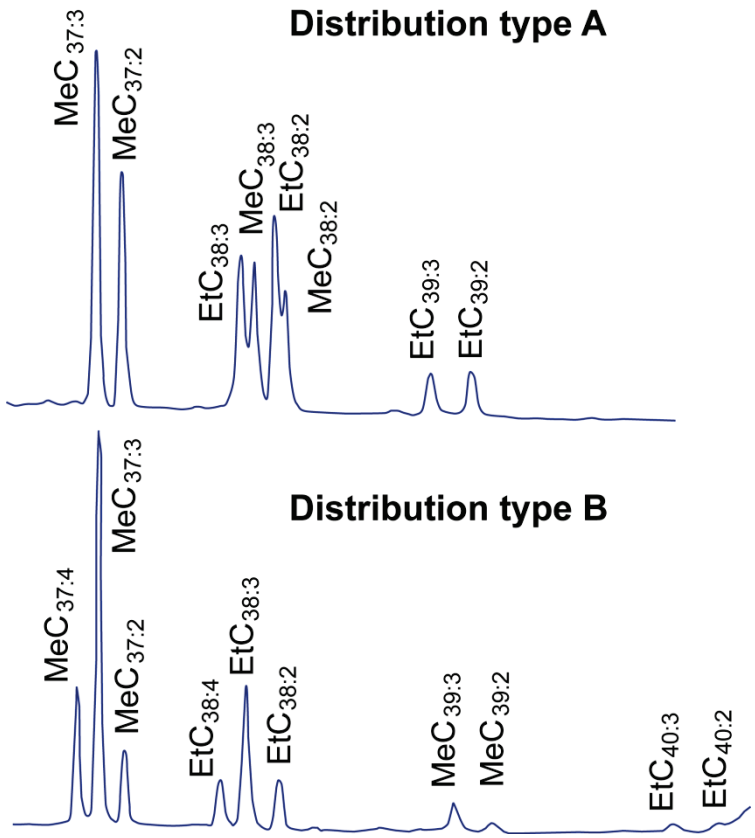

Figure 1-3. Chromatogrammes illustrant les deux types de distributions d'alcénones. Le type A est caractéristique d'environnements océaniques, alors que le type B est rencontré dans des environnements côtiers ou lacustres (modifié d'après Grimalt et Lopez, 2007).

De même, des études sur la position des doubles liaisons ont permis de distinguer trois catégories d'alcénones (Xu et al., 2001; Lopez et al., 2005; Prahl et al., 2006; Rontani et al., 2006) :

- La première comprend les alcénones « classiques » di- et tri-insaturées (MeC_{37}, MeC_{38}, EtC_{38}, MeC_{39}, EtC_{39}). Les doubles liaisons sont séparées de 5 groupements méthylènes et la première double liaison est située en position Δ14 (c'est-à-dire à 14 atomes de carbones en partant du groupement carbonyle C=O).

- La deuxième catégorie comprend les alcénones à chaîne plus courte (C_{35}-C_{36}) trouvées dans des sédiments de mer Noire et dans la souche *E. huxleyi* CCMP1742. Les doubles liaisons sont séparées par 5 groupements méthylènes et la première double liaison est située en position Δ12.

- La troisième catégorie comprend des alcénones dont les doubles liaisons sont séparées par 3 groupements méthylènes et dont la première double liaison est située en position Δ14. Ces alcénones ont été retrouvées dans des sédiments de la mer Noire, de la mer de Ligure et dans la souche *G. oceanica* JB-02.

1.3. Rôle physiologique des alcénones

La fonction des alcénones reste encore incertaine. La localisation de ces lipides dans les membranes cytoplasmiques suggère que les alcénones joueraient un rôle dans la régulation de la rigidité et de la fluidité de la membrane (Prahl et al., 1988; Brassell, 1993). La localisation des alcénones dans les membranes cellulaires a cependant été remise en question par Conte et Eglinton (1993).

Un autre hypothèse, la plus probable, est que les alcénones jouent un rôle de stockage d'énergie dans le métabolisme du phytoplancton (Epstein et al., 2001). Cette hypothèse a été confirmée par l'observation en cultures d'une variation de la concentration en alcénones en réponse à une carence nutritive ou à une limitation de lumière (Bell et Pond, 1996; Pond et Harris 1996; Epstein et al., 2001; Versteegh et al., 2001; Prahl et al., 2003; Eltgroth et al., 2005). En 2005, les travaux d'Eltgroth et collaborateurs ont permis de localiser les alcénones dans les chloroplastes et les vésicules cytoplasmiques des haptophytes. Ces auteurs ont alors suggéré que les alcénones sont fabriquées dans les chloroplastes et exportées dans les vésicules cytoplasmiques, afin d'y être stockées ou utilisées pour le métabolisme.

1.4. Proxys environnementaux basés sur les alcénones

Les alcénones sont couramment utilisées pour des reconstitutions paléo-environnementales car elles permettent d'estimer deux paramètres climatiques importants dans le passé: la température des eaux océaniques de surface et la concentration en dioxyde de carbone atmosphérique (pCO_2) au moment de la croissance de l'organisme producteur. Ces deux paramètres environnementaux sont estimés à l'aide de proxys basés respectivement sur la distribution des alcénones en C_{37} et sur la composition en isotopes stables du carbone des alcénones en C_{37}.

1.4.1. Le proxy de température ($U^{K'}_{37}$)

Des expérimentations *in vitro* sur des cultures d'*E. huxleyi* ont permis de mettre en évidence une relation linéaire entre la température de croissance de la culture et le degré d'insaturation des alcénones en C_{37} (Marlowe, 1984; Prahl et Wakeham, 1987; Prahl et al., 1988). Ainsi, une diminution de la température résulte en une augmentation de la proportion relative des alcénones $C_{37:3}$ par rapport aux alcénones $C_{37:2}$, et inversement (Figure 1-4).

L'ubiquité des alcénones dans les sédiments marins récents et anciens a permis l'établissement du ratio U^{K}_{37} (pour C_{37} Unsaturated Ketones ratio), permettant de déterminer la température des eaux océaniques de surface au moment de la croissance de l'organisme producteur (Brassell et al., 1986). Le ratio est défini comme suit :

$$\mathbf{U^{K}_{37} = ([C_{37:2}] - [C_{37:4}]) / ([C_{37:2}] + [C_{37:3}] + [C_{37:4}])} \quad (1)$$

Prahl et Wakeham (1987) ont par la suite simplifié le rapport U^{K}_{37} et proposé le rapport $U^{K'}_{37}$, en enlevant de la relation (1) l'alcénone en $C_{37:4}$ qui est rare dans la plupart des sédiments marins :

$$\mathbf{U^{K'}_{37} = ([C_{37:2}]) / ([C_{37:2}] + [C_{37:3}])} \quad (2)$$

De nombreuses études ont ensuite confirmé l'adéquation entre les températures dérivées de l'$U^{K'}_{37}$ et celles dérivées du $\delta^{18}O$ des foraminifères (e.g., Brassell et al., 1986; ten Haven et al., 1987; Eglinton et al., 1992). Prahl et collaborateurs (1988) furent les premiers à proposer une calibration de l' $U^{K'}_{37}$ basée sur des cultures d'*E. huxleyi*. Plus tard, des analyses sur des sédiments de surface provenant de divers sites océaniques (e.g., Sikes et al., 1991; Rosell-Melé et al., 1995; Pelejero et Grimalt, 1997) ont permis la mise au point d'une calibration globale, applicable dans la plupart des aires océaniques (Müller et al., 1998; Figure 1-4).

Facteurs pouvant affecter les valeurs de l'$U^{K'}_{37}$

S'il est admis que l'$U^{K'}_{37}$ reflète les températures océaniques de surface, plusieurs études ont montré que la profondeur de production des alcénones dans la zone photique des océans varie de manière régionale et saisonnière. Ainsi, les alcénones peuvent être produites dans la couche mixte de surface dans l'Atlantique Nord (Conte et al., 2001) et dans les hautes et basses latitudes du Pacifique (Ohkouchi et al., 1999), ou au niveau de la thermocline superficielle dans les latitudes moyennes du Pacifique (Ohkouchi et al., 1999). Par ailleurs, même si la production d'alcénones montre un fort contrôle saisonnier (plus forte production notamment au printemps, correspondant à un bloom des haptophytes), ce qui peut biaiser les estimations de températures (Sikes et Volkman, 1993), l'$U^{K'}_{37}$ enregistré dans les sédiments reflète dans la plupart des aires étudiées la température moyenne annuelle des eaux de surface (Rosell-Melé et al., 1995; Müller et Fischer, 2001; Prahl et al., 2005).

Il a également été observé que les variations génétiques au sein des haptophytes peuvent influencer l'$U^{K'}_{37}$, puisque la calibration du proxy de température diffère entre les espèces productrices d'alcénones (e.g., Volkman et al., 1995; Conte et al., 1998; Popp et al., 1998). De même, une variabilité a été observée en réponse à des facteurs environnementaux, telle que la disponibilité en nutriments et en lumière (photopériode) (e.g., Epstein et al., 1998; Prahl et al., 2003). Ainsi, un stress nutritif conduit à une diminution des valeurs de l'$U^{K'}_{37}$ alors qu'un stress prolongé à l'obscurité résulte en une augmentation des valeurs de l'$U^{K'}_{37}$ (Prahl et al., 2003).

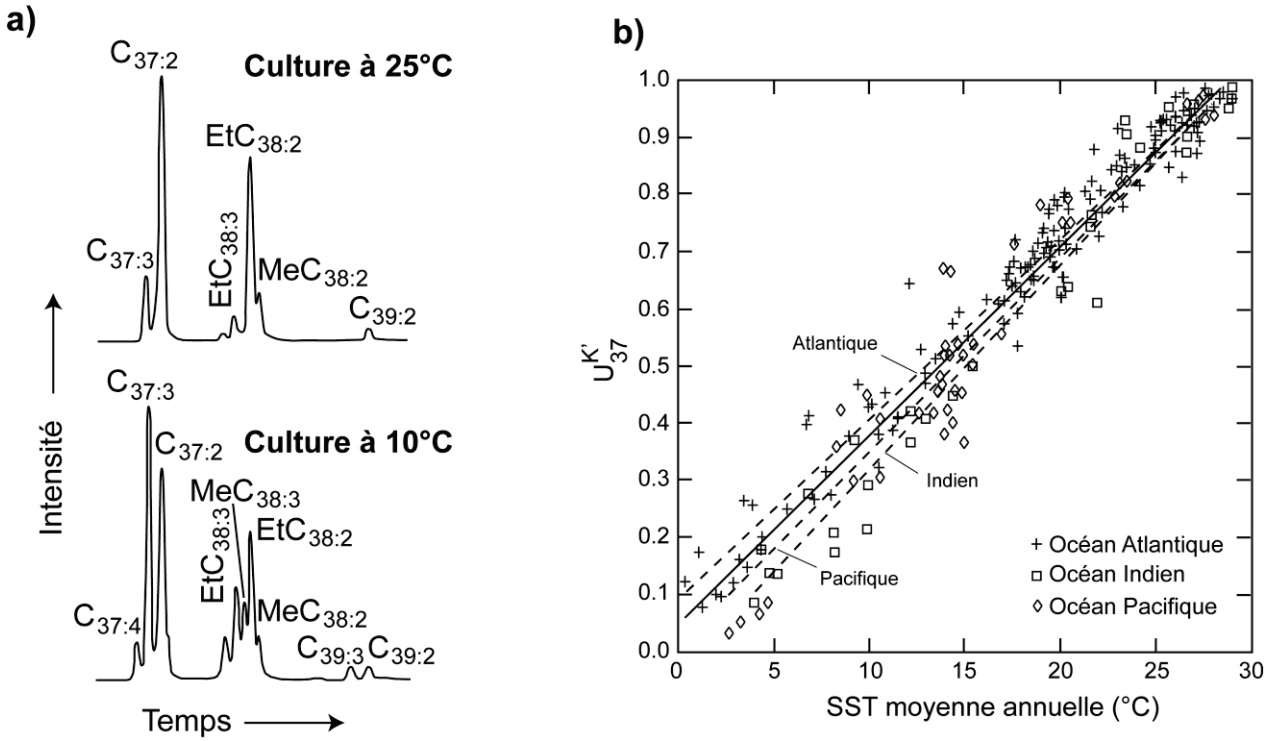

Figure 1-4. **(a)** Chromatogrammes partiels des alcénones produites par *Emiliania huxleyi* (souche 55a) à deux températures différentes, montrant l'augmentation de la proportion des alcénones en $C_{37:3}$ à basse température (modifié d'après Prahl et al., 1988). **(b)** Relation linéaire entre les températures moyennes annuelles des eaux océaniques de surface (SST) et l'$U^{K'}_{37}$ pour des sédiments de surface provenant de diverses zones océaniques entre 60°S et 60°N. La calibration globale (trait plein) a pour équation: $U^{K'}_{37} = 0.033 \times SST + 0.044$ (modifié d'après Müller et al., 1998).

1.4.2. Le proxy de pression partielle de CO_2 ($\varepsilon_{p37:2}$)

Selon la loi de Henry (1803), la concentration en dioxyde de carbone dissous dans l'eau de mer ($[CO_{2(aq)}]$) est proportionnelle à la concentration en dioxyde de carbone atmosphérique (pCO_2):

$$\mathbf{[CO_{2(aq)}] = K_0 \times pCO_2}$$

où K_0 est le coefficient de solubilité du CO_2 dépendant de la salinité et de la température.

L'estimation des concentrations en $CO_{2(aq)}$ dans le passé permet donc d'accéder à des paléo-pCO_2. Cette estimation est faite à partir du fractionnement isotopique du carbone qui se produit entre le CO_2 ambiant, c'est-à-dire le $CO_{2(aq)}$, et la cellule algaire pendant la photosynthèse des haptophytes (Jasper et Hayes, 1990; Jasper et al., 1994; Bidigare et al., 1997, 1999; Pagani et al., 1999). Ce fractionnement, noté ε_p, est exprimé selon la relation suivante :

$$\mathbf{\varepsilon_p = \varepsilon_f - b/[CO_{2(aq)}]}$$

où: ε_p est obtenu par la différence entre la composition isotopique en carbone ($\delta^{13}C$) du $CO_{2(aq)}$ et celle de la biomasse algaire (Figure 1-5). L'ε_p est communément noté $\varepsilon_{p37:2}$ puisque le $\delta^{13}C$ de la biomasse algaire est estimé égal au $\delta^{13}C$ de l'alcénone $C_{37:2}$. Le $\delta^{13}C$ du carbonate des foraminifères planctoniques permet quant à lui d'estimer le $\delta^{13}C$ du $CO_{2(aq)}$ (Pagani et al., 1999).

ε_f est le fractionnement isotopique lié à toutes les réactions de fixation du carbone (ε_f = 25 ‰; Popp et al., 1998)

Le terme b représente tous les facteurs physiologiques (taille de la cellule, taux de croissance, concentration en nutriments) pouvant affecter le fractionnement isotopique total (ε_p) (Laws et al., 1995; Popp et al., 1998).

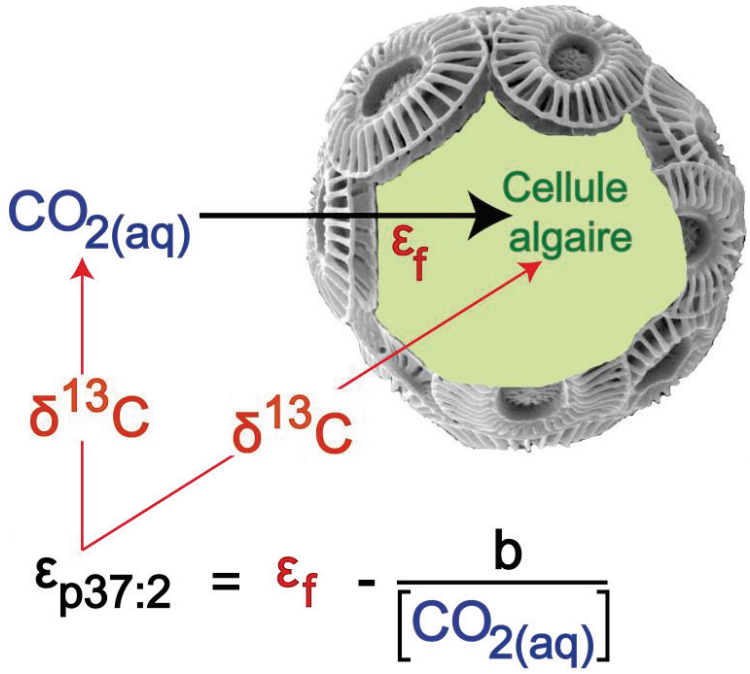

Figure 1-5. Schématisation du fractionnement isotopique en carbone ($\varepsilon_{p37:2}$) se produisant entre le CO_2 ambiant ($CO_{2(aq)}$) et la cellule algaire lors de la phostosynthèse.

Généralement, la concentration en phosphate (PO_4^{3-}) des eaux océaniques de surface, qui influence directement le taux de croissance algaire, est utilisée pour estimer la valeur du terme b (Bidigare et al., 1997, 1999; Pagani et al., 1999). Dans les océans modernes, ce terme est en effet fortement corrélé à la concentration en phosphate selon la relation:

$$\mathbf{b = 84{,}07 + 118{,}52 \times [PO_4^{3-}]}$$

Pour les sites oligotrophiques (pauvres en nutriments), l'influence du taux de croissance des haptophytes sur l' $\varepsilon_{p37:2}$ est considérée comme négligeable (Pagani et al., 2005).

Influence de la taille de la cellule des haptophytes

En considérant que, pour des concentrations similaires de $CO_{2(aq)}$, le fractionnement isotopique ε_p est moins important pour les grandes cellules phytoplanctoniques (avec un faible taux de croissance) que pour les petites cellules (avec un taux de croissance élevé) (Laws et al., 1995; Popp et al., 1998), le terme b peut être corrigé en prenant en compte la taille de la cellule (Henderiks et Pagani, 2007):

$$\mathbf{b' = b \times [V{:}SA_{fossil}/V{:}SA_{Ehux}]}$$

où: $V:SA_{fossil}$ est le ratio entre le volume (V) et l'aire de la surface (SA) de la cellule. Ce ratio est estimé à partir de la morphologie du coccolithe (fossile), le diamètre moyen de la cellule des coccolithophoridés (D_{cell}) étant linéairement corrélé à la longueur du coccolithe ($L_{coccolith}$) (Henderiks et Pagani, 2007; Henderiks, 2008):

$$\mathbf{D_{cell} = 0{,}55 + 0{,}88 \times L_{coccolith}} \quad r^2 = 0{,}82;\ p<0{,}0001$$

Le volume de la cellule (V) et l'aire de la surface (SA) sont alors calculés en considérant une simple géométrie sphérique.

$V:SA_{Ehux}$ est une valeur constante correspondant aux dimensions de la cellule d'*Emiliania huxleyi* en culture ($V:SA_{Ehux} = 0{,}9 \pm 0{,}1$ µm; Popp et al., 1998).

Les concentrations en CO_2 dans l'eau de mer pour les périodes anciennes peuvent alors être estimées en utilisant la nouvelle relation suivante :

$$\mathbf{[CO_{2(aq)}] = b'/ (\varepsilon_f - \varepsilon_{p37:2})}$$

1.5. Distribution des alcénones dans le registre sédimentaire

Le premier enregistrement sédimentaire des alcénones remonte à l'Aptien (Crétacé inférieur, ~120 Ma; Brassell et al., 2004). Une différence majeure dans la distribution des alcénones est observée entre les sédiments cénozoïques (post-Eocène) et les sédiments crétacés (anté-Eocène) (Farrimond et al., 1986; Brassell et al., 2004). Alors que les sédiments post-Eocène présentent essentiellement des alcénones en C_{37}-C_{38} ($MeC_{37:2}$, $MeC_{37:3}$, Et- et $MeC_{38:2}$, Et- et $MeC_{38:3}$, $EtC_{39:2}$ et $EtC_{39:3}$), les sédiments anté-Eocène sont caractérisés par des abondances élevées d'alcénones en C_{39}-C_{40} ($MeC_{37:2}$, $EtC_{38:2}$, $MeC_{39:2}$, $EtC_{40:2}$, $MeC_{41:2}$) (Figure 1-6). Cette différence de distribution est difficilement attribuable à des processus diagénétiques qui auraient préférentiellement dégradé certaines alcénones par rapport à d'autres, comme le suggère dans ces sédiments la présence d'autres composés très facilement dégradables. Ce changement de profil de distribution suggère plutôt que les producteurs d'alcénones au Crétacé appartenaient à une famille différente des producteurs cénozoïques.

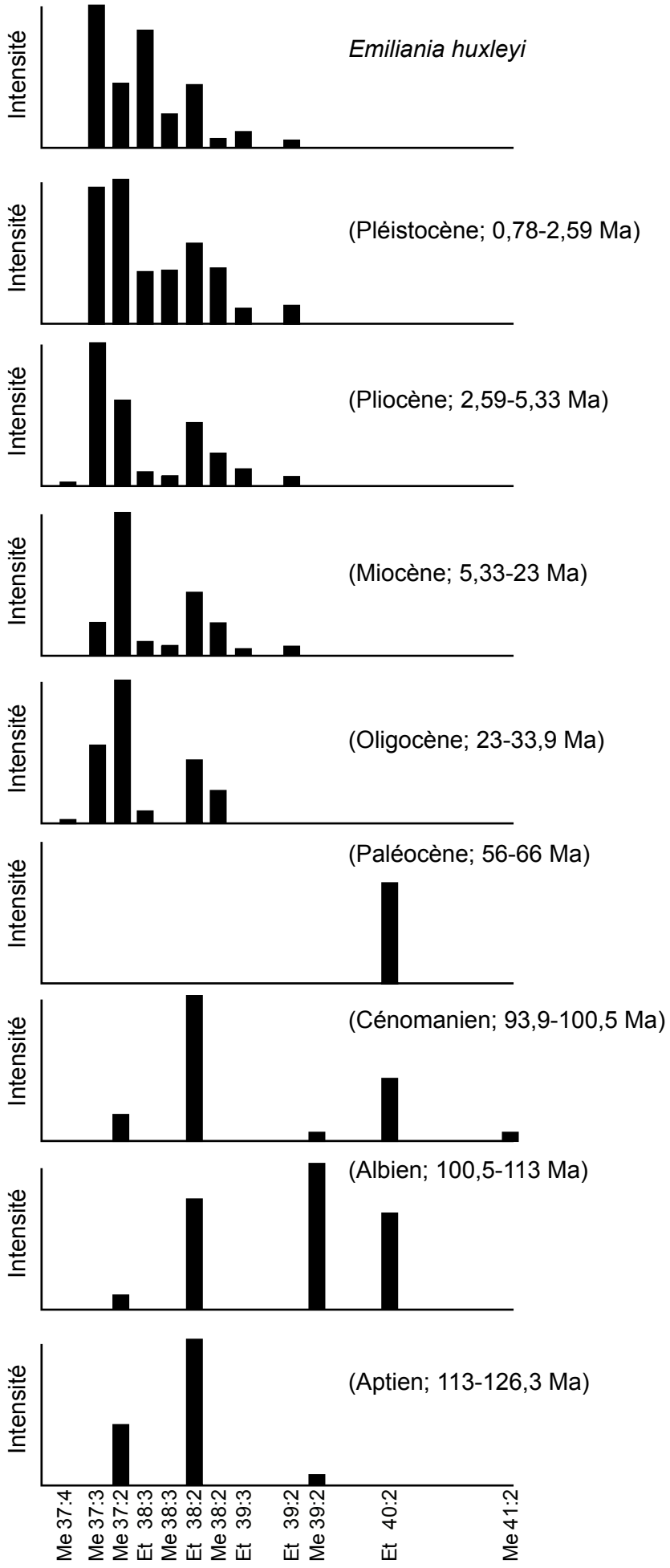

Figure 1-6. Profils de distribution des alcénones au Crétacé et au Cénozoïque (modifié d'après Farrimond et al., 1986).

Par ailleurs, Brassell et collaborateurs (2004; 2012) ont suggéré que la détection des alcénones tri-insaturées uniquement à partir de l'Eocène inférieur pouvait être expliquée par un changement à cette époque du mode de biosynthèse des alcénones, en relation avec l'évolution des haptophytes ou en réponse à un changement climatique majeur tel que le refroidissement global se produisant après l'Optimum climatique de l'Eocène inférieur (~50 Ma).

1.6. Quels étaient les producteurs d'alcénones au cours du Cénozoïque ?

Depuis l'étude de Marlowe et collaborateurs (1990), le genre *Reticulofenestra,* qui comme *Emiliania* et *Gephyrocapsa* appartient à la famille des Noëlaerhabdaceae (Table 1-3), est considéré comme le producteur d'alcénones le plus probable pendant le Cénozoïque. Marlowe et collaborateurs (1990) se sont en effet appuyés sur la présence concomitante des coccolithes de *Reticulofenestra* et d'alcénones dans des sédiments datant depuis l'Eocène (56-33.9 Ma). Mais si des données moléculaires (Fujiwara et al., 2001; Sáez et al., 2004) et micropaléontologiques (Young, 1990, 1998; Young et Bown, 1997) ont montré que le genre *Reticulofenestra* était phylétiquement proche des producteurs actuels, cette hypothèse n'a jamais vraiment été démontrée. De plus, certains genres (tel que *Cyclicargolithus*) ont pu être éludés[1] (Table 1-3).

FAMILLE NOËLAERHABDACEAE	
Genre *Pseudoemiliania*	**Genre *Reticulofenestra***
Pseudoemiliania lacunosa	*Reticulofenestra pseudoumbilicus*
Pseudoemiliania ovata	*Reticulofenestra haqii*
	Reticulofenestra minutula
Genre *Cyclicargolithus*	*Reticulofenestra minuta*
Cyclicargolithus abisectus	*Reticulofenestra asanoi*
Cyclicargolithus floridanus	*Reticulofenestra bisecta*
Cyclicargolithus luminis	*Reticulofenestra daviesii*
	Reticulofenestra clatrata
Genre *Dictyococcites*	*Reticulofenestra dictyoda*
Dictyococcites antarcticus	*Reticulofenestra lockeri*
Dictyococcites hesslandii	
Dictyococcites spp.	

Table 1-3. Taxonomie des Noëlaerhabdaceae au Cénozoïque (liste non exhaustive).

[1] La taxonomie des Noëlaerhabdaceae au Cénozoïque reste à ce jour sujet à discussion. Pour plus de détails sur la taxonomie utilisée dans ce travail, se référer à l'Annexe 2.

L'identification formelle des producteurs d'alcénones au Cénozoïque semble primordiale pour assurer l'application des proxys basés sur ces lipides ($U^{K'}_{37}$, $\varepsilon_{p37:2}$) dans des sédiments pré-datant l'apparition des producteurs actuels. C'est donc aux questions *« Quels étaient les producteurs d'alcénones au cours du Cénozoïque ? L'hypothèse de Marlowe et collaborateurs (1990) est-elle vérifiée et généralisable ? L'identification formelle des producteurs anciens d'alcénones est-elle essentielle pour l'utilisation des proxys basés ces lipides dans des sédiments pré-datant l'apparition des producteurs actuels ?»* que ce travail de thèse va tenter de répondre au travers de trois cas d'études présentés dans les chapitres suivants.

Références

Bell, M.V., Pond, D., 1996. Lipid composition during growth of motile and coccolith forms of *Emiliania huxleyi*. Phytochemistry 41, 465–471.

Bidigare, R.R., Fluegge, A., Freeman, K.H., Hanson, K.L., Hayes, J.M., Hollander, D., Jasper, J.P., King, L.L., Laws, E.A., Milder, J., Millero, F.J., Pancost, R., Popp, B.N., Steinberg, P.A., Wakeham, S.G., 1997. Consistent fractionation of ^{13}C in nature and in the laboratory: Growth-rate effects in some haptophyte algae. Global Biogeochemistry Cycles 11, 279–292 (Correction, Global Biogeochemistry Cycles, 13, 251– 252, 1999).

Bidigare, R.R., Hanson, K.L., Buesseler, K.O., Wakeham, S.G., Freeman, K.H., Pancost, R.D., Millero, F.J., Steinberg, P., Popp, B.N., Latasa, M., Landry, M.R., Laws, E.A., 1999. Iron stimulated changes in ^{13}C fractionation and export by equatorial Pacific phytoplankton: Toward a paleogrowth rate proxy. Paleoceanography 14, 589-595.

Billard, C., Innouye, I. 2004. What is new in coccolithophore biology? In: Thierstein, H.R., Young, J.R. (Eds), Coccolithophores From molecular processes to global impact. Springer, 1-29.

Boon, J.J.V.D., Meer, F.W., Schuyl, P.J.W., de leeuw, J.W., Schenck, P.A., Burlingame, A.L., 1978. Organic geochimical analysis of core samples from site 362 Walvis Ridge, DSDP leg 40. In: Bolli, H.M., Ryan, W.B.F. (Eds), Initial reports of the deep sea drilling project. U.S. Governement printing office, Washington, pp. 627-637.

Brassell, S.C., 1993. Applications of biomarkers for delineating marine paleoclimate fluctuations during the Quaternary. In: Engel, M.H., Macko, S.A. (Eds), Organic Geochemistry, Plenum, New York, pp. 699-738.

Brassell, S.C., 2012. A temporal limit on the alkenone paleotemperature proxy. Poster presentation, AGU Fall Meeting 2012.

Brassell, S.C., Dumitrescu, M., ODP Leg 198 Shipboard Scientific Party, 2004. Recognition of alkenones in a lower Aptian porcellanite from the west-central Pacific. Organic Geochemistry 35, 181-188.

Brassell, S.C., Eglinton, G., Marlowe, I.T., Pflaumann, U., Sarnthein, M., 1986. Molecular stratigraphy: a new tool for climatic assessment. Nature 320, 129-133.

Conte, M.H., Eglinton, G., 1993. Alkenone and alkenoate distributions within the euphotic zone of the eastern North Atlantic: correlation with production temperature. Deep Sea Research I 40, 1935–1961.

Conte, M.H., Thompson, A., Lesley, D., Harris, R.P., 1998. Genetic and physiological influences on the alkenone/alkenoate versus growth temperature relationship in *Emiliania huxleyi* and *Gephyrocapsa oceanica*. Geochimica et Cosmochimica Acta 62 (1), 51-68.

Conte, M.H., Weber, J.C., King, L.L.,Wakeham, S.G., 2001. The alkenone temperature signal in western north Atlantic surface waters. Geochimica et Cosmochimica Acta 65, 4275-4287.

Coolen, M.J.L., Muyzer, G., Rijpstra, W.I.C., Schouten, S., Volkman, J.K, Damste, J.S.S., 2004. Combined DNA and lipid analyses of sediments reveal changes in Holocene haptophyte and diatom populations in an Antarctic lake. Earth and Planetary Science Letters 223, 225-239.

de Leeuw, J.W., van der Meer, J.W., Rijpstra, W.I.C., Schenck, P.A., 1980. On the occurence and structural identification of long chain ketones and hydrocarbons in sediments. In: Douglas, A.G., Maxwell, J.R. (Eds), Advances in organic geochemistry. Pergamon Press, Oxford, pp. 211-217.

Eglinton, G., Bradshaw, S.A., Rosell-Melé, A., Sarnthein, M., Pflaumann, U., Tiedemann, R., 1992. Molecular record of secular sea surface temperature: Changes on 100-year timescales for Glacial Termination-I, Termination-II and Termination-IV. Nature 356, 423-426.

Eltgroth, ML, Watwood, RL, Wolfe, GV, 2005. Production and cellular localisation of neutral long chain lipids in the Haptophyte algae *Isochrysis galbana* and *Emiliania huxlyei*. Journal of Phycology 41, 1000-1009.

Epstein, B.L., D'Hondt, S., Hargraves, P.E., 2001. The possible role of C_{37} alkenones in *Emiliania huxleyi*. Organic Geochemistry 32, 867-875.

Epstein, B.L., D'Hondt, S., Quinn, J.G., Zhang, J., Hargraves, P.E., 1998. An effect of dissolved nutrient concentrations on alkenone-based temperature estimates. Paleoceanography 13, 122–126.

Farrimond, P., Eglinton, G., Brassell, S.C., 1986. Alkenones in Cretaceous black shales, Blake-Bahama Basin, western North Atlantic. Organic Geochemistry 10, 897-903.

Freeman, K.H., Wakeham, S.G., 1992. Variations in the distributions and isotopic compositions of alkenones in Black Sea particles and sediments. Organic Geochemistry 19, 277-285.

Fujiwara, S., Tsuzuki, M., Kawachi, M., Minaka, N., Inouye, I., 2001. Molecular phylogeny of the Haptophyta based on the *rbc*L gene and sequence variation in the spacer region of the rubisco operon. Journal of Phycology 37, 121-129.

Gong, C., Hollander, D.J., 1997. Differential contribution of bacteria to sedimentary organic matter in oxic and anoxic environments, Santa Monica Basin, California. Organic Geochemistry 26, 545-563.

Gong, C., Hollander, D.J., 1999. Evidence for differential degradation of alkenones under contrasting bottom water oxygen conditions: Implication for paleotemperature reconstruction. Geochimica et Cosmochimica Acta 63, 405-411.

Grimalt, J.O., Lopez, J.F., 2007. Paleoceanography, biological proxies-Alkenone paleothermometry from coccoliths. Encyclopedia of Quaternary Science, Elsevier, 1610-1618.

Grossi, V., Raphel, D., Aubert, C., Rontani, J.-F., 2000. The effect of growth temperature on the long-chain alkenes composition in the marine coccolithophorid *Emiliania huxleyi*. Phytochemistry 54, 393-399.

Henderiks, J., 2008. Coccolithophore size rules - reconstructing ancient cell geometry and cellular calcite quota from fossil coccoliths. Marine Micropaleontology 67, 143-154.

Henderiks, J., Pagani, M., 2007. Refining ancient carbon dioxide estimates: significance of coccolithophore cell size for alkenone-based pCO_2 records. Paleoceanography 22 (PA3202). doi:10.1029/2006PA001399.

Henry, W., 1803. Experiments on the Quantity of Gases Absorbed by Water, at Different Temperatures, and under Different Pressures. Philosophical Transactions of the Royal Society of London 93, 29-42.

Jaraula, C.M.B., Brassell, S.C., Morgan-Kiss, R.M., Doran, P.T., Kenig, F., 2010. Origin and tentative identification of tri to pentaunsaturated ketones in sediments from lake Fryxell, East Antarctica. Organic Geochemistry 41, 386-397.

Jasper, J.P., Hayes, J.M., 1990. A carbon isotope record of CO_2 levels during the late Quaternary. Nature 347, 462-464.

Jasper, J.P., Hayes, J.M., Mix, A.C., Prahl, F.G., 1994. Photosynthetic fractionation of ^{13}C and concentrations of dissolved CO_2 in the central equatorial Pacific during the last 255,000 years. Paleoceanography 9, 781-798.

Laws, E.A., Popp B.N., Bidigare, R.R., Kennicutt, M.C., Macko, S.A., 1995. Dependence of phytoplankton carbon isotopic composition on growth rate and $[CO_2]_{aq}$: theoretical considerations and experimental results. Geochimica et Cosmochimica Acta 59*,* 1131–1138.

Li, J.G., Philp, R.P., Pu, F., Allen, J., 1996. Long-chain alkenones in Qinghai Lake sediments. Geochimica et Cosmochimica Acta 60, 235-241.

Lopez, J.F., de Oteyza, T.G., Teixidor, P., Grimalt, J.O., 2005. Long chain alkenones in hypersaline and marine coastal microbial mats. Organic Geochemistry 36, 861-872.

Marlowe, I.T., Brassell, S.C., Eglinton, G., Green, J.C., 1984a. Long chain unsatured kenones and esters in living algae and marine sediments. Organic Geochemistry 6, 135-141.

Marlowe, I.T., Brassell, S.C., Eglinton, G., Green, J.C., 1990. Long-chain alkenones and alkyl alkenoates and the fossil coccolith record of marine sediments. Chemical Geology 88, 349-375.

Marlowe, I.T., Green, J.C., Brassell, S.C., Eglinton, G., Course, P.A., 1984b. Long chain (n-C_{37}-C_{39}) alkenones in the Prymnesiophyceae. Distribution of alkenones and other lipids and their taxonomic significance. British Phycology Journal 19 (3), 203-216.

Milliman, J.D., 1993. Production and accumulation of calcium carbonate in the ocean: budget of a nonsteady state. Global Biogeochemistry Cycles 7, 927-957.

Müller, P.J., Fischer, G., 2001. A 4-year sediment trap record of alkenones from the filamentous upwelling region off Cape Blanc, NW Africa and a comparison with distributions in underlying sediments. Deep-Sea Research Part I-Oceanographic Research Papers 48, 1877-1903.

Müller, P.J., Kirst, G., Rulhand, G., von Storch, I., Rosell-Melé, A., 1998. Calibration of the alkenone paleotemperature index $U^{K'}_{37}$ based on core-tops from the eastern South Atlantic and the global ocean (60°N-60°S). Geochimica et Cosmochimica Acta 62 (10), 1757-1772.

Ohkouchi, N., Kawamura, K., Kawahata, H., Okada, H., 1999. Depth ranges of alkenone production in the central Pacific Ocean. Global Biogeochemical Cycles 13, 695-704.

Pagani, M., Arthur, M.A., Freeman, K.H., 1999. Miocene evolution of atmospheric carbon dioxide. Paleoceanography 14 (3), 273–292.

Pagani, M., Zachos, J.C., Freeman, K.H., Tripple, B., Bohaty, S., 2005. Marked decline in atmospheric carbon dioxide concentrations during the Paleogene. Science 309, 600–603.

Pelejero, C., Grimalt, J.O., 1997. The correlation between the $U^{K'}_{37}$ index and sea surface temperatures in the warm boundary: The south China Sea. Geochimica et Cosmochimica Acta 61, 4789-4797.

Pienaar, R.N. 1994. Ultrastructure and calcification of coccolithophores. In: Winter, A., Siesser, W.G. (Eds), Coccolithophore. Cambridge (Cambridge University Press), 13-37.

Pond, D.W., Harris, R.P., 1996. The lipid composition of the coccolithophore *Emiliania huxleyi* and its possible ecophysiological significance. Journal of Marine Biology Association United Kingdom 76, 579-594.

Popp, B.N., Laws, E.A., Bidigare, R.R., Dore, J.E., Hanson, K.L., Wakeham, S.G., 1998. Effect of phytoplankton cell geometry on carbon isotopic fractionation, Geochimica et Cosmochimica Acta 62, 69–77.

Prahl, F.G., Muehlhausen, L.A., Zahnle, D.L., 1988. Further evaluation of long-chain alkenones as indicators of paleoceanographic conditions. Geochimica et Cosmochimica Acta 52, 2303-2310.

Prahl, F.G., Popp, B.N., Karl, D.M., Sparrow, M.A., Royer, I.M., 2006. Unusual C_{35} and C_{36} alkenones in paleoceanographic benchmark strain of *Emiliania huxleyi*. Geochimica et Cosmochimica Acta 70, 2856-2867.

Prahl, F.G., Rontani, J.-F., Volkman, J.K., Sparrow, M.A., 2005. Ecology and biogeochemistry of alkenone production at Station ALOHA. Deep-Sea Research Part I-Oceanographic Research Papers 52, 699-719.

Prahl, F.G., Wakeham, S.G., 1987. Calibration of unsaturation patterns in long-chain ketone compositions for paleotemperature assessment. Nature 330, 367-369.

Prahl, F.G., Wolfe, G.V., Sparrow, M.A., 2003. Physiological impacts on alkenone paleothermometry. Paleoceanography 18, doi:10.1029/2002PA000803.

Pujos-Lamy, A., 1977. Essai d'établissement d'une biostratigraphie du nannoplancton calcaire dans le Pleistocène de l'Atlantique Nord-oriental. Boreas 6, 323-331.

Rechka, J.A., Maxwell, J.R., 1988. Characterisation of alkenone temperature indicators in sediments and organisms. Advances in Organic Geochemistry 13, 727-734.

Rieley, G., Teece, M.A., Peakman, T.M., Raven, A.M., Greene, K.J., Clarke, T.P., Murray, M., Leftley, J.W., Campbell, C.N., Harris, R.P., Parkes, R.J., Maxwell, J.R., 1998. Long-chain alkenes of the haptophytes *Isochrysis galbana* and *Emiliania huxleyi*. Lipids 33, 617–625.

Rontani, J.-F., Beker, B., Volkman, J.K., 2004. Long-chain alkenones and related compounds in the benthic haptophyte *Chrysotila lamellosa* Anand HAP 17. Phytochemistry 65, 117-126.

Rontani, J.-F., Prahl, F.G., Volkman, J.K., 2006. Re-examination of the double bond position in alkenones and derivatives: biosynthetic implications. Journal of Phycology 42, 800-813.

Rosell-Melé, A., Carter, J., Eglinton, G., 1994. Distributions of long-chain alkenones and alkyl alkenoates in marine surface sediments from the north east Atlantic. Organic Geochemistry 22, 501-509.

Rosell-Melé, A., Eglinton, G., Pflaumann, U., Sarnthein, M., 1995. Atlantic core-top calibration of the $U^{K'}_{37}$ index as a sea surface paleotemperature indicator. Geochimica et Cosmochimica Acta 59, 3099-3107.

Rost, B., Riebesell, U., 2004. Coccolithophores and the biological pump: responses to environmental changes. In: Thierstein, H.R., Young, J.R. (Eds), Coccolithophores – From Molecular Processes to Global Impact. Springer, New York, 76-99.

Sáez, A.G., Probert, I., Young, J.R., Edvardsen, B., Eikrem, W., Medlin, L.K., 2004. A review of the phylogeny of the Haptophyta. In: Thierstein, H.R., Young, J.R. (Eds), Coccolithophores: From molecular processes to global impact. Springer-Verlag, Berlin Heidelberg, pp. 251–269.

Schulz, H.M., Schoner, A., Emeis, K.C., 2000. Long-chain alkenone patterns in the Baltic Sea: An ocean freshwater transition. Geochimica et Cosmochimica Acta 64, 469-477.

Sikes, E.L., Farrington, J.W., Keigwin, L.D., 1991. Use of the alkenone unsaturation ratio $U^{K'}_{37}$ to determine past sea surface temperatures: Core-top SST calibrations and methodology considerations. Earth and Planetary Science Letters 104, 36-47.

Sikes, E.L., Volkman, J.K., 1993. Calibration of alkenone unsaturation ratios $U^{K'}_{37}$ for paleotemperature estimation in cold polar waters. Geochimica et Cosmochimica Acta 57, 1883-1889.

Sun, Q., Chu, G.Q., Liu, G.X., Li, S., Wang, X.H., 2007. Calibration of alkenone unsaturation index with growth temperature for a lacustrine species, *Chrysotila lamellosa* (Haptophyceae). Organic Geochemistry 38, 1226-1234.

Sun, M.-Y., Wakeham, S.G., 1994. Molecular evidence for degradation and preservation of organic matter in the anoxic Black Sea Basin. Geochimica et Cosmochimica Acta 58, 3395-3406.

ten Haven, H.L., Baas, M., Kroot, M., de Leeuw, J.W., Schenck, P.A., Ebbing, J., 1987. Late Quaternary Mediterranean sapropels, III. Assessment of source of input and paleotemperature as derived from biological markers. Geochimica et Cosmochimica Acta 51, 803-810.

Theissen, K.M., Zinniker, D.A., Moldowan, J.M., Dunbar, R.B., Rowe, H.D., 2005. Pronounced occurrence of long-chain alkenones and dinosterol in a 25,000 year lipid molecular fossil record from Lake Titicaca, South America. Geochimica et Cosmochimica Acta 69, 623-636.

Theroux, S., D'Andrea, W.J., Toney, J., Amaral-Zettler, L., Huang Y., 2010. Phylogenetic diversity and evolutionary relatedness of alkenone-producing haptophyte algae in lakes: implications for continental paleotemperature reconstructions. Earth and Planetary Science Letters 300, 311–320.

Thierstein, H.R., Geitzenauer, K.R., Molfino, B., 1977. Global synchroneity of late Quaternary coccolith datum levels: Validation by oxygen isotopes. Geology 5, 400-404.

Toney, J.L., Theroux, S., Andersen, R.A., Coleman, A., Amaral-Zettler, L., Huang, Y., 2012. Culturing the first 37:4 predominant lacustrine haptophyte: Geochemical, biochemical, and genetc implications. Geochimica et Cosmochimica 78, 51-64.

Versteegh, G.J.M., Riegman, R., de Leeuw, J.W., Jansen, J.H.F., 2001. $U^{K'}_{37}$ values for *Isochrysis galbana* as a function of culture temperature, light intensity and nutrient concentrations. Organic Geochemistry 32, 785-794.

Volkman, J.K., Barrett, S.M., Blackburn, S.I., Sikes, E.L., 1995. Alkenones in *Gephyrocapsa oceanica*: Implications for studies of paleoclimate. Geochimica et Cosmochimica Acta 59, 513-520.

Volkman, J.K., Eglinton, G., Corner, E.D.S., Forsberg, T.E.V., 1980a. Long-chain alkenes and alkenones in the marine coccolithphorid *Emiliania huxleyi*. Phytochemistry 19, 2619-2622.

Volkman, J.K., Eglinton, G., Corner, E.D.S., Sargent, J., 1980b. Novel unsatured straight-chain C_{37}-C_{39} methyl and ethyl ketones in marine sediments and a coccolithophore *Emiliania huxleyi*. In: Douglas, A.G., Maxwell, J.R. (Eds), Advances in Organic Geochemistry. Pergamon Press, Oxford, pp. 219-228.

Westbroek, P., Brown, C.W., Vanbleijswijk, J., Brownlee, C., Brummer, G.J., Conte, M., Egge, J., Fernandez, E., Jordan, R., Knappertsbusch, M., Stefels, J., Veldhuis, M., Vanderwal, P., Young, J., 1993. A model system approach to biological climate forcing: The example of *Emiliania huxleyi*. Global and Planetary Change 8, 27-46.

Xu, L., Reddy, C.M., Farrington, J.W., Frysinger, G.S., Gaines, R.B., Johnson, C.G., Nelson, R.K., Eglinton, T.I., 2001. Identification of a novel alkenone in Black Sea sediments. Organic Geochemistry 32, 633-645.

Young, J.R., 1990. Size variation of Neogene *Reticulofenestra* coccoliths from Indian Ocean DSDP Cores. Journal of Micropaleontology 9, 71–86.

Young, J.R., 1998. Neogene. In: Bown, P.R. (Ed.), Calcareous Nannofossil Biostratigraphy. British Micropalaeontology Society Publication Series, Kluver Academic Publishers, Cambridge, pp. 5.

Young, J.R., Bown, P.R., 1997. Cenozoic calcareous nannoplankton classification. Journal of Nannoplankton Research 19, 36-47.

Chapitre 2

Production d'alcénones et changements environnementaux autour de la limite Eocène-Oligocène : pertinence de l'utilisation du proxy de température $U^{K'}_{37}$

Ce chapitre présente une étude basée sur les sédiments du Site DSDP (Deep Sea Drilling Project) 511 qui couvre la limite Eocène-Oligocène (34,8-30,7 Ma). Ce site, situé sur le Plateau du Falkland au sud-ouest de l'Atlantique Sud (à 2500 m de profondeur) présente l'avantage de couvrir en continu la transition Eocène-Oligocène. De plus, le taux de sédimentation élevé (entre 13 et 66 m/Ma) au Site DSDP 511 a permis un enfouissement rapide de la matière organique, et ainsi sa bonne préservation en comparaison avec d'autres sites océaniques profonds.

La transition Eocène-Oligocène correspond au changement climatique le plus significatif du Cénozoïque puisqu'elle marque le passage d'un climat de type « greenhouse » (globalement chaud) à un climat de type « icehouse » (globalement plus froid), avec l'apparition de glace permanente en Antarctique (e.g., Zachos et al., 2001). La réponse des nannofossiles calcaires à cet événement climatique majeur reste peu étudiée, bien que quelques études aient montré une baisse significative de la diversité spécifique et une augmentation en proportions relatives des taxons d'eaux froides (Persico et Villa, 2004; Dunkley Jones et al., 2008).

Dans cette étude, les températures des eaux de surface (SSTs) reconstruites à partir du rapport d'insaturation des alcénones ($U^{K'}_{37}$) indiquent un refroidissement progressif d'environ 8°C entre 34,4 Ma et 33,5 Ma. Ce refroidissement est associé à une augmentation de la productivité primaire (probablement induite par la mise en place de conditions d'upwelling), comme en témoignent les flux de carbone organique total, de biomarqueurs phytoplanctoniques (alcénones et diols à longues chaînes) et de carbonate/silice. Ces changements environnementaux ont induit un changement dans les assemblages de nannofossiles, plus particulièrement au sein des espèces de *Reticulofenestra*.

La comparaison entre les abondances absolues des différentes espèces de *Reticulofenestra* et les concentrations en alcénones dans les mêmes sédiments ne permet pas une identification claire des producteurs d'alcénones au Site 511 pendant l'Eocène-Oligocène, mais la production par *R. dictyoda*, *R. minuta* et *R. clatrata* reste probable. Les températures dérivées de l'$U^{K'}_{37}$, qui est calibré sur les espèces productrices actuelles, sont cohérentes avec celles dérivées d'autres proxys de température (TEX_{86}; $\delta^{18}O$) au même site et pour le même intervalle de temps. Ceci suggère que la calibration de l'$U^{K'}_{37}$ n'est pas aussi dépendante de l'espèce productrice que ce qu'il avait été suggéré auparavant et/ou que les producteurs anciens d'alcénones au Site 511 étaient phylétiquement proches des producteurs actuels.

Paleoenvironmental changes and applicability of the alkenone paleothermometer during the late Eocene–early Oligocene at DSDP Site 511 (South Atlantic)

Julien Plancq[a]*, Emanuela Mattioli[a], Bernard Pittet[a], Laurent Simon[b] and Vincent Grossi[a]

[a] Laboratoire de Géologie de Lyon : Terre, Planètes, Environnement (UMR 5276), CNRS, Université Lyon 1, Ecole Normale Supérieure Lyon, Campus scientifique de la DOUA, Villeurbanne Cedex, France.

[b] Université de Lyon, UMR5023 Ecologie des Hydrosystèmes Naturels et Anthropisés, Université Lyon 1, ENTPE, CNRS, 6 rue Raphaël Dubois, 69622 Villeurbanne, France.

[*] Corresponding author : J. Plancq, Laboratoire de Géologie de Lyon, UMR 5276, CNRS, Université Lyon 1, Campus de la DOUA, Bâtiment Géode, 69622 Villeurbanne Cedex, France. Tel.: +33 4 72431544. (plancq@pepsmail.univ-lyon1.fr)

Submitted to Paleoceanography

Abstract

This study investigates paleoenvironmental changes at Deep Sea Drilling Project Site 511 (South Atlantic) during the late Eocene–early Oligocene using variations in lipid-biomarker concentrations (long-chain diols, alkenones), in calcareous nannofossil assemblages and in sediment composition (TOC, calcium carbonate, silica percentages). Sea-surface temperatures (SSTs) reconstructed from the alkenone unsaturation index $U^{K'}_{37}$ indicate a progressive cooling (~8°C) from 34.4 Ma to 33.5 Ma. This cooling is associated with an increase in primary productivity (probably induced by upwelling conditions) as attested by fluxes of total organic matter (TOC), of phytoplanktonic biomarkers (long-chain diols) and of silica. These environmental changes induced a shift in nannofossil assemblages, especially within the *Reticulofenestra* genus. The comparison between Noelaerhabdaceae species-specific absolute abundances and alkenone concentrations in the same sedimentary samples does not allow an unequivocal identification of alkenone producers at Site 511 during the late Eocene-early

Oligocene, but alkenone production by *R. dictyoda*, *R. minuta* and *R. clatrata* is likely. SSTs derived from the alkenone unsaturation index, which is calibrated on modern alkenone producer species, are consistent with those derived from other temperature proxies (TEX_{86}; $\delta^{18}O$) at the same site and for the same time interval. This suggests that the $U^{K'}_{37}$ index is less species-dependent than previously suggested and/or that the ancient alkenone producers at Site 511 were phyletically closely related to modern producers.

Keywords: Paleotemperatures, paleoproductivity, $U^{K'}_{37}$, alkenone producers, Eocene-Oligocene, DSDP Site 511.

1. Introduction

The Eocene-Oligocene boundary (EOB; ~ 34 Ma) marks the change from a "greenhouse" climate to an "icehouse" climate with a dramatic cooling event, leading to the formation of a large and permanent ice-sheet on East Antarctica [e.g., *Zachos et al.*, 2001; *Lear et al.*, 2008; *Liu Z. et al.*, 2009]. Causes proposed for this abrupt glaciation include a substantial CO_2 decrease in the atmosphere [*DeConto and Pollard*, 2003; *Pagani et al.*, 2005, 2011], or a decrease in CO_2 combined with an orbital configuration that reduced polar seasonality [*DeConto and Pollard*, 2003; *Coxall et al.*, 2005]. Also, it has been suggested that Antarctic glaciation was the result of the thermal isolation of Antarctica from mid-latitude warm currents as a consequence of the opening of the circumpolar passages (Tasmanian Gateway and Drake Passage) and the onset of the Antarctic Circumpolar Current (ACC) [e.g., *Kennett*, 1977; *Lawver and Gahagan*, 2003; *Persico and Villa*, 2004; *Lagabrielle et al.*, 2009].

The EOB is further associated to a marine biotic turnover [*Aubry*, 1992; *Dunkley Jones et al.*, 2008; *Funakawa and Nishi*, 2008; *Pearson et al.*, 2008; *Villa et al.*, 2008; Wade *and Pearson*, 2008], terrestrial faunal and floral changes [e.g., *Hooker et al.*, 2004; *Jaramillo et al.*, 2006], a reorganization of the carbon cycle [*Shackleton and Kennett*, 1975; *Zachos et al.*, 2001; *Coxall et al.*, 2005; *Merico et al.*, 2008], an increase of marine primary production [*Diester-Haass and Zahn*, 1996; *Salamy and Zachos*, 1999; *Nilsen et al.*, 2003; *Anderson and Delaney*, 2005], a deepening of the Carbonate Compensation Depth (CCD) [*Coxall et al.*, 2005; *Rea and Lyle*, 2005], and a sea-level fall [e.g., *Pekar et al.*, 2002; *Miller et al.*, 2008].

These changes have been well documented notably by oxygen isotope ($\delta^{18}O$) and carbon isotope ($\delta^{13}C$) records from planktonic and benthic foraminifera [e.g. *Kennett and Stott*, 1990; *Diester-Haass and Zahn*, 1996; *Zachos et al.*, 1996, 2001], and by shifts in foraminifera,

radiolarian and nannofossil assemblages [e.g. *Boersma and Premoli Silva*, 1991; *Aubry*, 1992; *Keller et al.*, 1992; *Lazarus and Caulet*, 1993; *Villa et al.*, 2008]. Alkenone-based proxies ($\varepsilon_{p37:2}$; $U^{K'}_{37}$) have also been used to reconstruct variations in partial pressure of CO_2 (pCO_2) and sea surface temperatures (SSTs) during the late Eocene-early Oligocene [*Pagani et al.*, 2005, 2011; *Liu Z. et al.*, 2009]. However, paleoenvironmental changes occurring during the late Eocene-early Oligocene have been mostly documented at a number of deep-sea sites located in the Southern Ocean, whereas only a few studies have investigated lower latitude sites [e.g., *Nilsen et al.*, 2003; *Pagani et al.*, 2005, 2011; *Liu Z. et al.*, 2009].

In the present study, the comparison between alkenone and nannofossil fluxes in sediments from the Deep Sea Drilling Project (DSDP) Site 511 (South Atlantic), which show a good preservation of organic matter, allows discussing the applicability of the alkenone-based temperature proxy ($U^{K'}_{37}$) in sediments pre-dating the first occurrence of modern producers. Then, we quantified and compared contents in nannofossil assemblages, total organic matter, calcium carbonate/silica ratios and lipid biomarkers (alkenones and long-chain diols) with reconstructed alkenone-based sea surface temperatures (SSTs). This multi-proxy approach, based on a more continuous sampling with respect to previous studies [*Liu Z. et al.*, 2009; *Pagani et al.*, 2011], demonstrates that a cooling of sea-surface waters associated with an increase in primary productivity, consistent with the development of upwelling conditions, occurred at Site 511 during the late Eocene-early Oligocene (34.8-30.7 Ma). This induced a shift in nannofossil assemblages, especially within the *Reticulofenestra* genus.

2. Material and methods

2.1. Sampling and age model

DSDP Leg 71 Site 511 (51°S, 46°W) is located in the basin province of the Falkland Plateau, at 2589 m water depth in the southwest Atlantic Ocean (Figure 2-1). We selected a total of 40 sediment samples (mainly diatom ooze and nannofossil diatomaceous ooze) between 10 and 180 meters below the sea floor (mbsf), spanning the latest Eocene-early Oligocene. During this period, Site 511 was at about 2500 m depth and was located at 55°S, 42°W [*Ludwig et al.*, 1983; *Basov and Krasheninnikov*, 1983; *Syke et al.*, 1998].

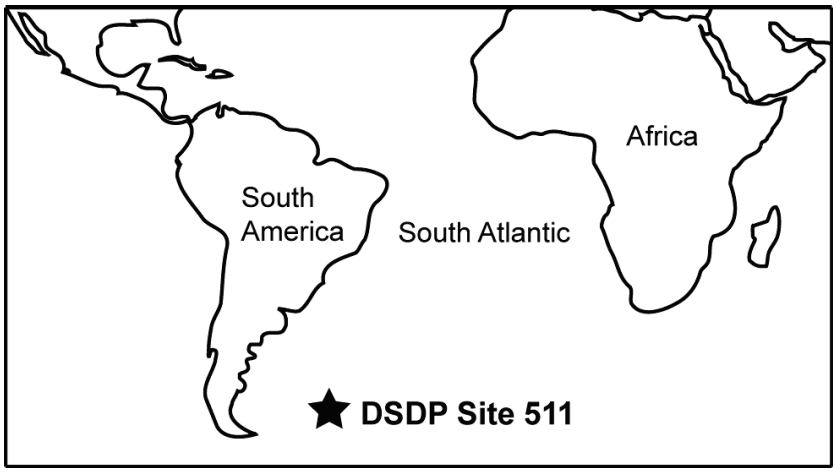

Figure 2-1. Location of DSDP Site 511 in the South Atlantic Ocean.

The age model for DSDP Site 511 used in this study is based on the paleomagnetic data presented by *Salloway* [1983] (Figure 2-2) and on nannofossil data presented here. *Chiasmolithus oamaruensis* is consistently present in all the studied samples, and the last occurrences of *Reticulofenestra umbilica* and *Isthmolithus recurvus* were observed at 15 mbsf and 18 mbsf, respectively. Contrarily to *Liu Z. et al.* [2009] and *Schumacher and Lazarus* [2004], the first occurrences of *Chiasmolithus oamaruensis* and of *Isthmolithus recurvus* were not identified at 177.7 and 180 mbsf, respectively, as these species are present from the base of the interval studied here. All these observations strongly support that this interval is correlative with the magnetic Chron C13 (35-33.16 Ma) and Chron C12 (33.16-30.59 Ma) as defined in the timescale of *Gradstein et al.* [2012] (Figure 2-2). The time interval studied (10-180 mbsf) is thus comprised between 30.7 and 34.8 Ma. Ages of nannofossil bioevents are not integrated in this age model because first and last occurrences can be slightly diachronous [*Backman*, 1987]. The sedimentation rate calculated according to our age model was not constant: 66.8 m/Ma between 109-195 mbsf, 35.5 m/Ma between 14-109 mbsf, and 13.4 m/Ma between 8-14 mbsf. This age-depth model differs from the ones presented by *Schumacher and Lazarus* [2004] and *Liu Z. et al.* [2009] who did not integrate the available magnetostratigraphic data in their age models. Thus, contrarily to previous assumptions, no hiatus or drastic increase in sedimentation rate are supported by our data.

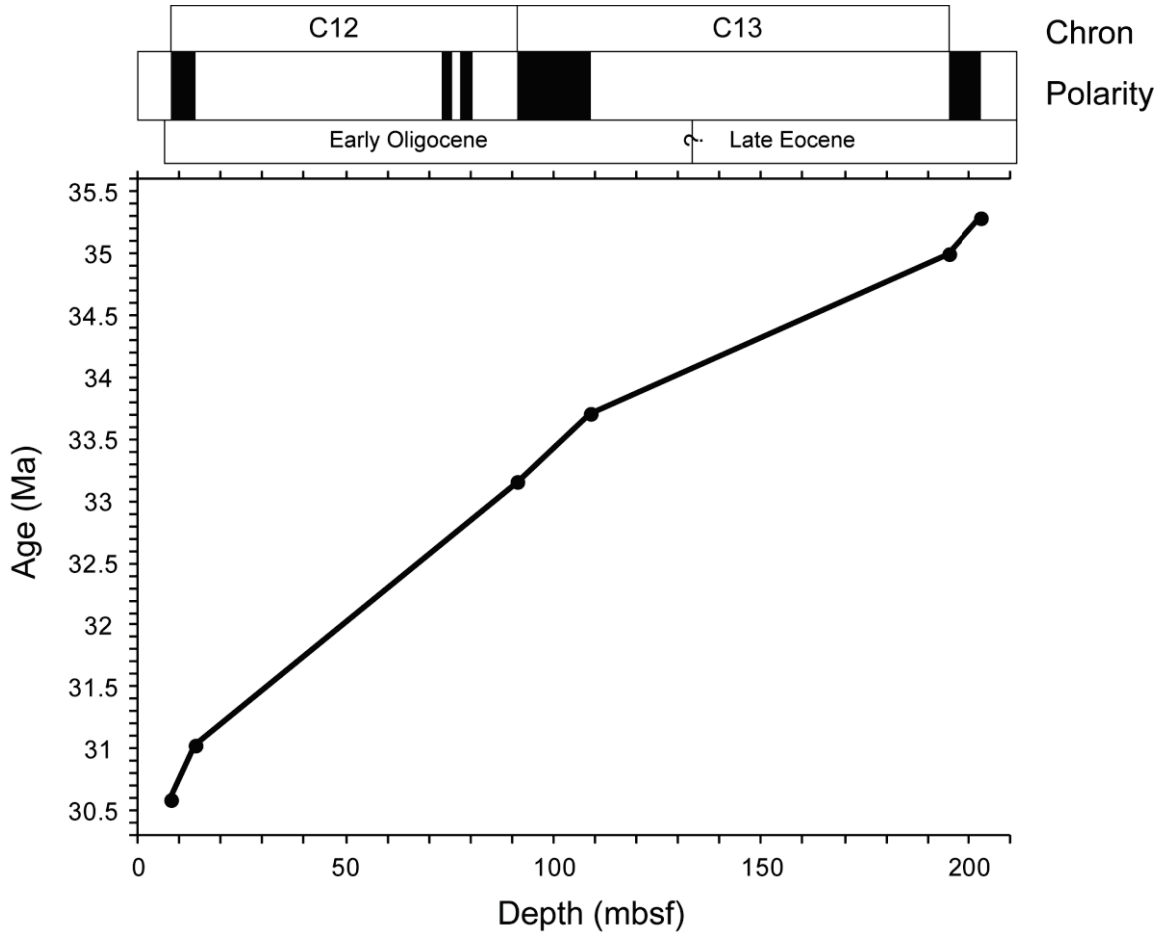

Figure 2-2. Age-depth plot for DSDP Site 511 used in the present study. Paleomagnetic data are from *Salloway* [1983]. Absolute ages are derived from the timescale of *Gradstein et al.* [2012].

2.2. Sediment composition analyses

2.2.1. Total Organic Carbon (TOC)

Sub-samples (ca. 100 mg of ground samples) were acidified *in-situ* with HCl 2N in pre-cleaned (combustion at 450°C) silver capsules until effervescence ceased, dried in an oven (50°C) and wrapped in tin foil before analyses. Duplicate TOC analyses were performed with a Thermo FlashEA 1112 elemental analyzer using aspartic acid (36.09% of carbon) and nicotinamid (59.01% of carbon) as calibration standards. Accuracy was checked using in-house reference material (fine grounded low carbon sediment). The reproducibility achieved for duplicate analyses of all samples was better than 10% (coefficient of variation).

2.2.2. Calcium carbonate ($CaCO_3$)

For each sample, approximately 300 mg of powdered bulk sediment was dissolved using HCl 1N and the amount of CO_2 released from the sample, which is proportional to the calcium carbonate ($CaCO_3$) content, was measured using a Dietrich-Frühling™ calcimeter.

2.2.3. Remaining component

The remaining component of the sediment was calculated as bulk less the TOC content and the $CaCO_3$ content.

2.3. Nannofossil analyses

Slides for calcareous nannofossil quantitative analysis were prepared following the Random Settling method [*Beaufort*, 1991; modified by *Geisen et al.*, 1999]. A small amount of dried sediment powder (5 mg) was mixed with water (with basic pH, over-saturated with respect to calcium carbonate) and the homogenised suspension was allowed to settle for 24 hours onto a cover slide. The slide was dried and mounted on a microscope slide with Rhodopass. Coccolith quantification was performed using a polarizing optical ZEISS microscope (magnification 1000x). A standard number of 400 calcareous nannofossils (coccoliths and nannoliths) were counted in a variable number (between 15 and 30) of field of views. In order to test the reproducibility of our quantification, each slide was counted twice and the repeatability achieved was better than 10 % (coefficient of variation).

Absolute abundance of nannofossils per gram of sediment was calculated using the formula:

$$X = (N.V)/(M.A.H) \quad (1)$$

where X is the number of calcareous nannofossils per gram of sediment; N the number of nannofossils counted in each slide; V the volume of water used for the dilution in the settling device (cm^3); M the weight of powder used for the suspension (g); A the surface considered for nannofossil counting (cm^2); H the height of the water over the cover slide in the settling device (2.1 cm). Species-specific relative abundances (percentages) were also calculated from the total nannofossil content.

2.4. Lipid biomarkers

Each sample (ca. ~15g) was ground and extracted by way of sonication with Dichloromethane (DCM; 5 x 50 mL). Following evaporation of the solvents, the total lipid extract was separated into four lipid fractions of increasing polarity by chromatography over a solid phase extraction (SPE) silica-NH_2 cartridge (0.5 g packing) with hexane (Hex), Hex/DCM (3:1 v/v), DCM/acetone (9:1 v/v) and Methanol (MeOH) as eluents, respectively. Alkenones, eluting in the second fraction, were identified and quantified by gas chromatography/mass spectrometry (GC/MS) and gas chromatography (GC/FID), respectively. Alkenone abundances were determined by GC/FID using hexatriacontane (*n*-C_{36} alkane) as internal standard. Long-chain diols, eluting in the third fraction from the SPE chromatography, were silylated [pyridine/N,O-bis(trimethylsilyl)trifluoroacetamide (BSTFA), 2:1 v/v] before GC/FID and GC/MS analyses. Diol abundances were determined by GC/MS using 1,2-dipalmitoyl glycerol as external standard.

GC/MS analyses were performed on a MD800 Voyager spectrometer interfaced to an HP6890 gas chromatograph equipped with an on-column injector and a DB-5MS column (30 m x 0.25 mm x 0.25 μm). The oven temperature was programmed from 60°C (1 min) to 130°C at 20°C min^{-1}, and then to 310°C (20 min) at 4°C min^{-1}. Helium was used as the carrier gas at constant flow. GC/FID analyses were performed on a HP-6890 Series gas chromatograph configured with an on-column injector and a HP5 (30 m x 0.32 mm x 0.25 μm) capillary column. Helium was used as the carrier gas at constant flow and the oven temperature program was the same as for GC/MS analyses.

2.5. Mass accumulation rates

The calculation of fluxes permits to overcome the effects of a variable sedimentary dilution and to effectively compare data from different intervals in a time-series. The formula introduced by *Davies et al.* [1995] was first used to calculate the mass accumulation rates (MAR):

$$MAR = T.\,[BD-(P.W)] \qquad (2)$$

where MAR is the mass accumulation rate ($g/m^2/yr$), T the sedimentation rate (m/yr), BD the wet bulk density (g/m^3), P the porosity (weight percent) and W the seawater density (1.025 g/cm^3).

Fluxes of $CaCO_3$ (g/m^2/yr), biomarkers (µg/m^2/yr) and coccoliths (specimens/m^2/yr) were then obtained by multiplying the MAR with $CaCO_3$ content (g/g sediment), biomarker concentrations (µg/g sediment) and coccolith abundances (specimens/g sediment).

3. Results

3.1. Sediment composition

The studied samples are characterized by relatively high total organic carbon (TOC) contents for a deep-sea site (0.60 wt%; 0.16 g/m^2/yr on average; Figure 2-3). The TOC fluxes are in average of 0.12 g/m^2/yr between 34.8 and 34.4 Ma but slightly increased thereafter and then remained relatively constant between 34.4 and 31.4 Ma (0.17 g/m^2/yr) before a new decrease afterwards (Figure 2-3).

Calcium carbonate ($CaCO_3$) content is low (in average 9%; 2.4 g/m^2/yr) in all the studied samples (Figure 2-3). During the late Eocene (34.8-34.4 Ma), fluxes were in average of 4.7 g/m^2/yr but drastically decreased and showed lower values between 34.4 and 33.5 Ma (1.9 g/m^2/yr). It should be noted that one single sample at 138.6 mbsf (34.16 Ma) has a very low $CaCO_3$ content (0.8 %; 0.2 g/m^2/yr). During the early Oligocene, fluxes are slightly higher compared to the previous time interval (in average 2.1 g/m^2/yr) with two peaks observed at ~33.2 Ma and ~31.1 Ma (4.9 and 5.9 g/m^2/yr, respectively). Similar temporal variations are observed when relative proportions (%) of $CaCO_3$ are considered (Figure 2-3).

It is assumed that the remaining component of the sediment (i.e. other than TOC and $CaCO_3$) is almost exclusively constituted by biogenic silica. Diatoms and radiolarians are indeed dominant in all the studied samples, as testified by previous studies [*Ludwig et al.*, 1983; *Gombos and Ciesielski*, 1983] and by Scanning Electron Microscope (SEM) pictures (see Plate 2-1 in supplementary data). Silica fluxes were in average of 23.9 g/m^2/yr during the late Eocene (34.8-34.4 Ma) but they increased between 34.4 and 33.5 Ma (24.8 g/m^2/yr), before they became steady (23.6 g/m^2/yr in average) during the early Oligocene (34.8-34.4 Ma; Figure 2-3).

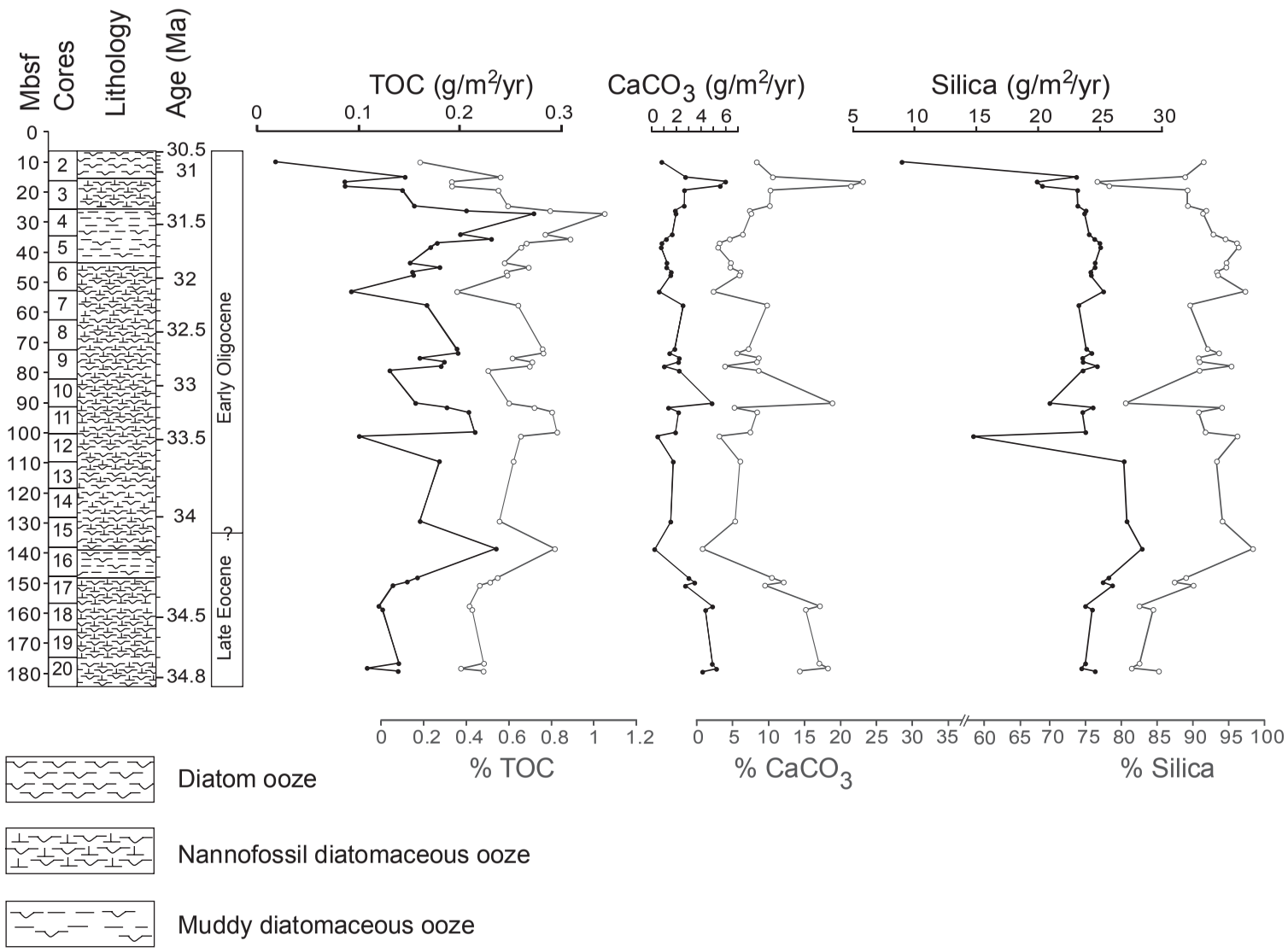

Figure 2-3. Fluxes (dark lines) and relative proportions (gray lines) of Total organic carbon (TOC), calcium carbonate ($CaCO_3$), and silica at DSDP Site 511 during the late Eocene-early Oligocene. Please note that the horizontal scale is different for TOC with respect to $CaCO_3$ and silica. Sample depths (in meters below the sea floor; mbsf), ages, and lithology [from *Ludwig et al.*, 1983] are also indicated.

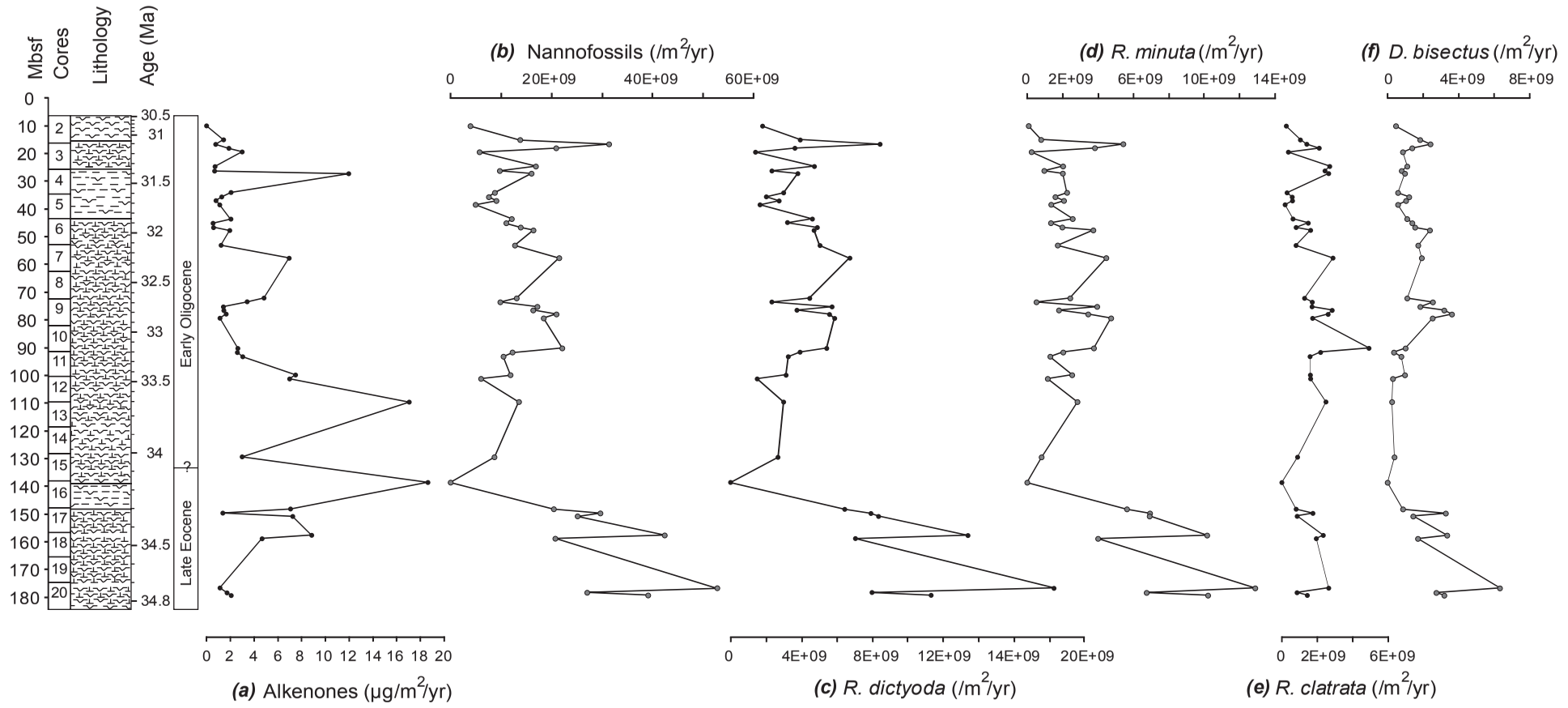

Figure 2-4. Alkenone and nannofossil distributions at DSDP Site 511 during the late Eocene-early Oligocene. Fluxes of ***(a)*** total alkenones, ***(b)*** total nannofossils and of the most abundant Noelaerhabdaceae species (***(c)*** *Reticulofenestra dictyoda*, ***(d)*** *R. minuta*, ***(e)*** *R. clatrata*, ***(f)*** *Dictyococcites bisectus*). Please note that the horizontal scale is different for nannofossils with respect to Noelaerhabdaceae species.

3.3. Coccolith assemblages

Coccolith assemblages are dominated by two genera of the Noelaerhabdaceae Family, namely *Reticulofenestra* and *Dictyococcites*, which account for 70-80% of the total nannofossils. The genus *Reticulofenestra* is mainly represented by the species *R. dictyoda*, *R. minuta* and *R. clatrata*, whereas *D. bisectus* is the main *Dictyococcites* species. Other species of these two genera (*R. hillae*, *R. umbilica*, *R. daviesii*, *R. reticulata* and *D. stavensis*) are present in lower amounts. The remaining nannofossil taxa (*Blackites* spp., *Chiasmolithus* spp., *Clausicoccus* spp., *Coccolithus* spp., *Ericsonia* spp., *Helicosphaera* spp., *Ismolithus recurvus*, *Pontosphaera* spp., *Toweius* spp., *Umbilicosphaera* spp.) account in average for 16% of the total nannofossil assemblage.

The mean nannofossil accumulation rate throughout the investigated interval is 16.9×10^9 nannofossils/m^2/yr. During the late Eocene (34.8-34.3 Ma), fluxes are relatively high (32.2×10^9 nannofossils/m^2/yr) but they drastically decrease and show low values between 34.3 and 33.5 Ma (8.9×10^9 nannofossils/m^2/yr). It should be noted that the sample with 0.8% of $CaCO_3$ at 138.6 mbsf appears barren of nannofossils (34.16 Ma; Figure 2-4). During the early Oligocene, fluxes of nannofossils slightly increase and reach relatively constant values between 33.2 and 30.7 Ma (14.2×10^9 nannofossils/m^2/yr). Fluxes of nannofossils and of each species of *Reticulofenestra* (in particular *R. dictyoda* and *R. minuta*) show in general similar temporal variations (Figure 2-4). A significant and positive linear regression is observed between $CaCO_3$ and nannofossil fluxes (Figure 2-5a), indicating that nannofossils are major carbonate producers at Site 511.

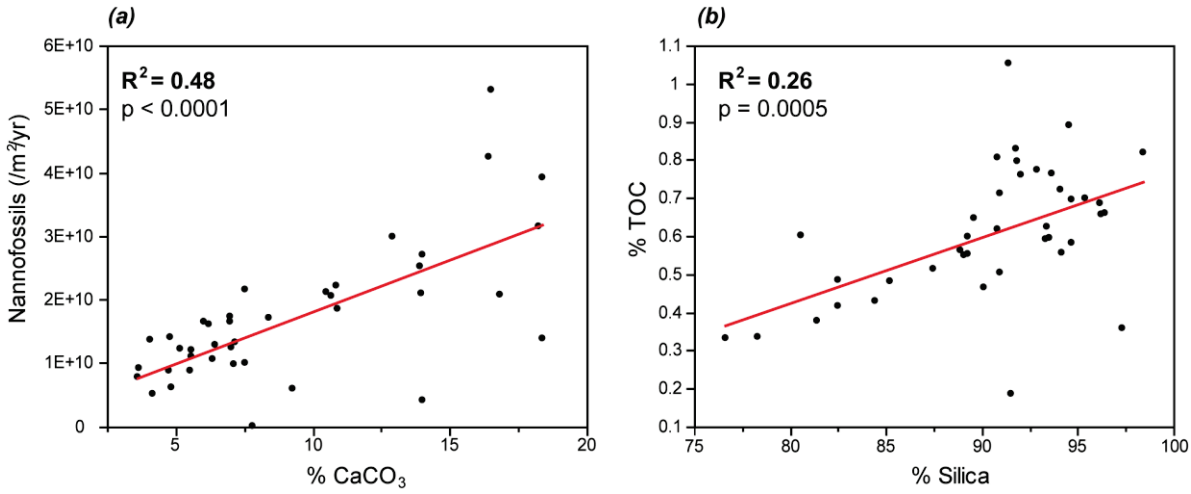

Figure 2-5. Correlations (linear regressions, significance threshold α = 0.05) between ***(a)*** nannofossil fluxes and calcium carbonate ($CaCO_3$) proportions, and between ***(b)*** Total Organic Carbon (TOC) and silica proportions.

3.2. Phytoplanktonic lipids

All studied samples show the presence of two C_{37} and two C_{38} alkenones identified respectively as: heptatriacontatrien-2-one ($MeC_{37:3}$), heptatriacontadien-2-one ($MeC_{37:2}$), octatriacontatrien-3-one ($EtC_{38:3}$) and octatriacontadien-3-one ($EtC_{38:2}$). No significant variation of the proportions of $EtC_{38:3}$ and $EtC_{38:2}$ alkenones is observed through the time interval studied. However, a change in proportions of $C_{37:2}$ and $C_{37:3}$ alkenones occurs at ~ 34 Ma. Higher proportions of $C_{37:2}$ alkenones (34% and 21% for $C_{37:2}$ and $C_{37:3}$ alkenones, respectively) are recorded during the late Eocene (34.8-34 Ma). Conversely, during the early Oligocene (34-30.7 Ma), higher proportions of $C_{37:3}$ alkenones (34% and 23% for $C_{37:3}$ and $C_{37:2}$ alkenones, respectively) are recorded. The $U^{K'}_{37}$ index, which is the ratio between $C_{37:2}$ alkenones and $C_{37:3}$ alkenones ($U^{K'}_{37} = [C_{37:2}]/ [C_{37:2} + C_{37:3}]$) [*Prahl and Wakeham*, 1987], was converted into sea surface temperatures (SSTs) (Figure 2-6), using the calibration of *Liu Z. et al.* [2009], based on global core top sediments [data set from *Conte et al.*, 2006].

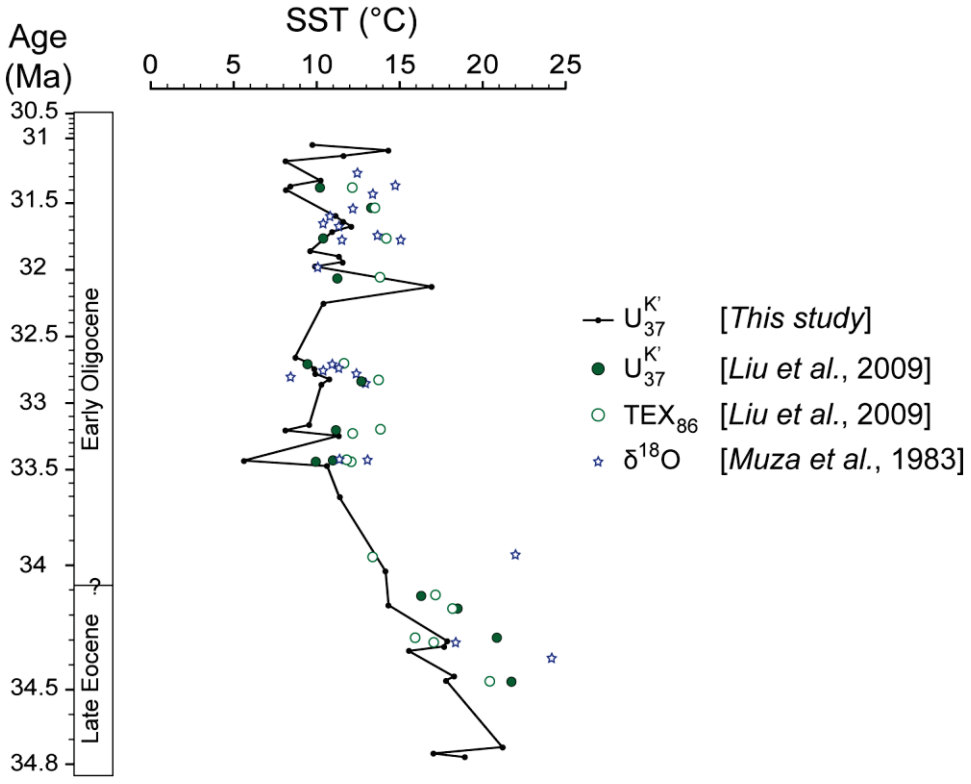

Figure 2-6. Paleo-sea surface temperatures (SSTs) derived from various temperature proxies at DSDP Site 511 during the late Eocene-early Oligocene. SSTs obtained in the present study (black line) are compared with those obtained by *Liu Z. et al.* [2009] using $U^{K'}_{37}$ (filled circles) and the tetraether index TEX_{86} (empty circles) proxies, and with those of *Muza et al.* [1983] who used the stable oxygen isotope composition of planktonic foraminifera ($\delta^{18}O$; blue stars).

SSTs, which are relatively high (ca. 18°C) during the late Eocene, show a regular decrease down to ca. 10°C around the Eocene-Oligocene boundary (34.4-33.4 Ma) and remain relatively constant afterwards (Figure 2-6).

The average flux of alkenones is 3.7 µg/m^2/yr and shows a maximum of 18.6 µg/m^2/yr at about 34.2 Ma (Figure 2-7). A general trend to decreasing alkenone content is observed during the late Eocene-early Oligocene, but three periods of increasing alkenone flux are observed at about 34.3-33.6, 32.7-32.1 and 31.4 Ma (Figure 2-7).

Eight long-chain diols, presumably originating from diatoms [*Rampen et al.*, 2007] and/or from Eustigmatophyte microalgae [*Volkman et al.*, 1999], are also present in all the studied samples. These compounds were respectively identified as: hexacosane-1,12-diol (1,12 C_{26}), hexacosane-1,13-diol (1,13 C_{26}), hexacosane-1,14-diol (1,14 C_{26}), octacosane-1,12-diol (1,12 C_{28}), octacosane-1,13-diol (1,13 C_{28}), octacosane-1,14-diol (1,14 C_{28}), triacontane-1,13-diol (1,13 C_{30}), triacontane-1,14-diol (1,14 C_{30}).

Diols show much lower fluxes (in average 0.5 µg/m^2/yr) than alkenones, with values close to the detection limit between 34.8 and 34.4 Ma, but their production significantly increases between 34.4 and 33.4 Ma (Figure 2-7). Peaks of maximum flux are observed during the early Oligocene at 32.7-32.1 Ma (1.2 µg/m^2/yr) and at 31.4 Ma (4.9 µg/m^2/yr). This overall distribution matches with that of TOC, although higher variations are recorded for diol flux (Figure 2-7).

4. Discussion

A set of observations indicates that variations through time in TOC and lipid-biomarker contents in the studied samples are unlikely the result of potential preservation biases. As biomarker concentrations were converted to fluxes, the effects of a variable dilution of organic matter in different samples can be excluded. Although a majority of organic matter produced in the surface oceans is remineralized before reaching the seafloor, the high sedimentation rate at DSDP Site 511 (35.5-66.8 m/Ma) has likely induced a relatively rapid burial of organic matter into the sediments, thus limiting its oxidation at the water/sediment interface. The variations in TOC and lipid-biomarker contents are thus more likely the result of changes in primary productivity rather than changes in organic matter degradation.

Along with alkenone-based temperatures, we used variations in sediment components ($CaCO_3$, silica, TOC) and in lipid-biomarkers (alkenones, long-chain diols) to infer changes in primary productivity occurring at Site 511. $CaCO_3$ and silica fluxes are currently used as

proxies to trace calcareous (nannossils, foraminifera) and siliceous (diatoms, radiolarian) production, respectively [e.g., *Faul et al.*, 2003; *Nilsen et al.*, 2003]. Alkenones are produced in modern oceans by a few extant unicellular haptophyte algae belonging to the Isochrysidale clade (including the coccolithophores *Emiliania huxleyi* and *Gephyrocapsa oceanica*; *Marlowe et al.*, 1984; *Volkman et al.*, 1980, 1995), but their sedimentary abundances have been widely used as indicators to estimate global primary paleoproductivity [e.g., *Brassell et al.*, 1986; *Brassell*, 1993; *Villanueva et al.*, 1997, 1998; *Weaver et al.*, 1999; *Grimalt et al.*, 2000; *Ternois et al.*, 2001]. The total long-chain diol abundances may also be interpreted as a proxy for phytoplanktonic productivity since eustigmatophytes and diatoms have been identified as potential producers of these biolipids [e.g., *Versteegh et al.*, 1997; *Sinninghe Damsté et al.*, 2003; *Rampen et al.*, 2007].

4.1. Alkenone production and applicability of the $U^{K'}_{37}$ proxy

Sea-surface temperatures at Site 511 were reconstructed using the alkenone-based proxy $U^{K'}_{37}$. However, this proxy has been calibrated on extant coccolithophore cultures (*E. huxleyi* and *G. oceanica*) and/or contemporary core top sediments [e.g., *Prahl and Wakeham*, 1987; *Prahl et al.*, 1988; *Sikes et al.*, 1991; *Conte et al.*, 1995; *Müller et al.*, 1998; *Popp et al.*, 1998; *Riebesell et al.*, 2000], and appears species-dependent [e.g., *Volkman et al.*, 1995; *Conte et al.*, 1998]. It is thus essential to identify ancient alkenone producers to ensure the applicability of this proxy in pre-Quaternary sediments.

4.1.1. Putative alkenone producers at Site 511 during the late Eocene-early Oligocene

To identify ancient alkenone producers, we assume that, under good preservation conditions, the alkenone concentration is related to the number of coccoliths of alkenone-producing species in the same sediment. A similar approach has already been used to identify alkenone producers in sediments of late Quaternary [e.g. *Müller et al.*, 1997; *Weaver et al.*, 1999], Pliocene [e.g. *Bolton et al.*, 2010; *Beltran et al.*, 2011] and Oligocene-Miocene age [*Plancq et al.*, 2012].

The *Reticulofenestra* genus has been suggested as the most probable ancient producer of alkenones based on its continuous co-occurrence with these lipid biomarkers throughout the Cenozoic sediment record [e.g., *Marlowe et al.*, 1990]. At DSDP Site 511, no apparent similar variation is observed between the total alkenone content and abundances of *Reticulofenestra* species (or *Dictyococcites* species), especially between 34.8 and 32.7 Ma where alkenone and coccolith contents seem to be inversely correlated. However, the contribution to alkenone

production of some *Reticulofenestra* species, namely *R. dictyoda*, *R. minuta* and *R. clatrata*, cannot be totally excluded since they show some similar variations with alkenone fluxes during the early Oligocene (32.7-30.5 Ma; Figure 2-4).

Using cultures of *Emiliania huxleyi*, *Sorrosa* [2012] showed that a change of growth temperature from 20°C to 10°C promoted an enhancement of alkenone production but reduced the cell number (and thus the number of coccoliths). A decrease in SSTs associated with the onset of upwelling conditions and the ecological perturbation induced by the competition of coccolithophores with diatoms (see section 4.2) could then explain that the highest alkenone fluxes are contemporary of the lowest coccolith fluxes (34.4-33.4 Ma; Figure 2-4). The end of this perturbation period subsequent to the stabilization of upwelling conditions (33.4-31 Ma; see section 4.2) would explain the following lower alkenone production. Yet, this interpretation remains speculative since the mode of production and the physiological function of alkenones in haptophyte cells is still not clearly understood [*Prahl et al.*, 1988; *Brassell*, 1993; *Bell and Pond*, 1996; *Epstein et al.*, 2001].

The discrepancy between alkenone and coccolith sedimentary contents may also suggest that other alkenone-producing taxa, likely non-calcifying haptophytes, have contributed to alkenone production. Nowadays, certain non-calcifying Isochrysidales, such as *Isochrysis galbana*, also produce alkenones. Although they are not considered as an important source of alkenone in the open ocean since they are believed to be restricted to coastal areas [*Marlowe et al.*, 1990], *Isochrysis* strains are also known from oceanic waters [*Versteegh et al.*, 2001]. So, the distribution and abundances of non-calcifying producers in marine waters are virtually unknown and are probably underestimated [*Liu H. et al.*, 2009]. Thus, at Site 511, the contribution of non-calcifying haptophytes to alkenone production, for which there is no sedimentary record, cannot be excluded.

Coccolith-calcite dissolution during the dissolution event is another possible cause to explain the differences observed between alkenone and coccolith records. However, as dissolution is found to be important only in the sample at 138.6 m, this mechanism can only be invoked for the interval close to the Eocene/Oligocene boundary (see Plate 1 in supplementary data and discussion in section 4.2).

4.1.2. Applicability of the $U^{K'}_{37}$ index

Temperatures derived from the alkenone paleothermometer are interestingly consistent with those derived from other paleotemperature proxies (TEX_{86}; $\delta^{18}O$) all along the sediment section investigated (Figure 2-6). This suggests that the $U^{K'}_{37}$ index is less species-dependent

than previously suggested or that the ancient alkenone producers at Site 511 were phyletically closely related to modern producers. The impact of changes in alkenone producing species on the $U^{K'}_{37}$ index remains poorly studied, although it has been suggested that such changes do not involve significant changes in the $U^{K'}_{37}$-temperature relationship [*Müller et al.*, 1997, 1998; *Villanueva et al.*, 2002]. For example, *Villanueva et al.* [2002] showed that reversals in the Noelaerhabdaceae assemblages (*Gephyrocapsa* and *Emiliania* species) over the last 290 kyrs did not significantly alter $U^{K'}_{37}$ values. On the other hand, molecular [*Fujiwara et al.*, 2001; *Sáez et al.*, 2004] and micropaleontological data [*Marlowe et al.*, 1990; *Young*, 1990, 1998; *Young and Bown*, 1997] suggest very close evolutionary relationships between *E. huxleyi* and *G. oceanica* and their Cenozoic ancestors, such as *Reticulofenestra* (considered as an important alkenone producing genus at Site 511). Thus, although a few studies showed that the calibration of the $U^{K'}_{37}$ ratio is species-dependent [e.g., *Conte et al.*, 1995, 1998; *Popp et al.*, 1998; *Yamamoto et al.*, 2000], genetically-related factors are believed to have a small impact on the alkenone unsaturation of open-ocean producers. All these observations allow a confident use of the $U^{K'}_{37}$ in the Eocene-Oligocene sediments of Site 511, even if the producers are not yet clearly identified.

4.2. Changes in sea-surface temperatures and primary productivity at Site 511

Based on a continuous sampling spanning the late Eocene-early Oligocene boundary, the present data describe a regular decrease in SSTs inferred from 18°C in the late Eocene to 10°C in the early Oligocene (Figure 2-7). This is in good agreement with previous studies that indicated a cooling at Site 511 for this time interval based on the oxygen isotope record of planktonic foraminifera ($\delta^{18}O$) [*Muza et al.*, 1983], on changes in foraminifera or radiolarian assemblages [*Krasheninnikov and Basov*, 1983; *Weaver*, 1983], or on few $U^{K'}_{37}$ and tetraether index (TEX_{86}) measurements [*Liu Z. et al.*, 2009] (Figure 2-6). Also, this sharp cooling event has been recorded in several other oceanic sites [e.g., *Zachos et al.*, 2001; *Coxall et al.*, 2005; *Liu Z. et al.*, 2009].

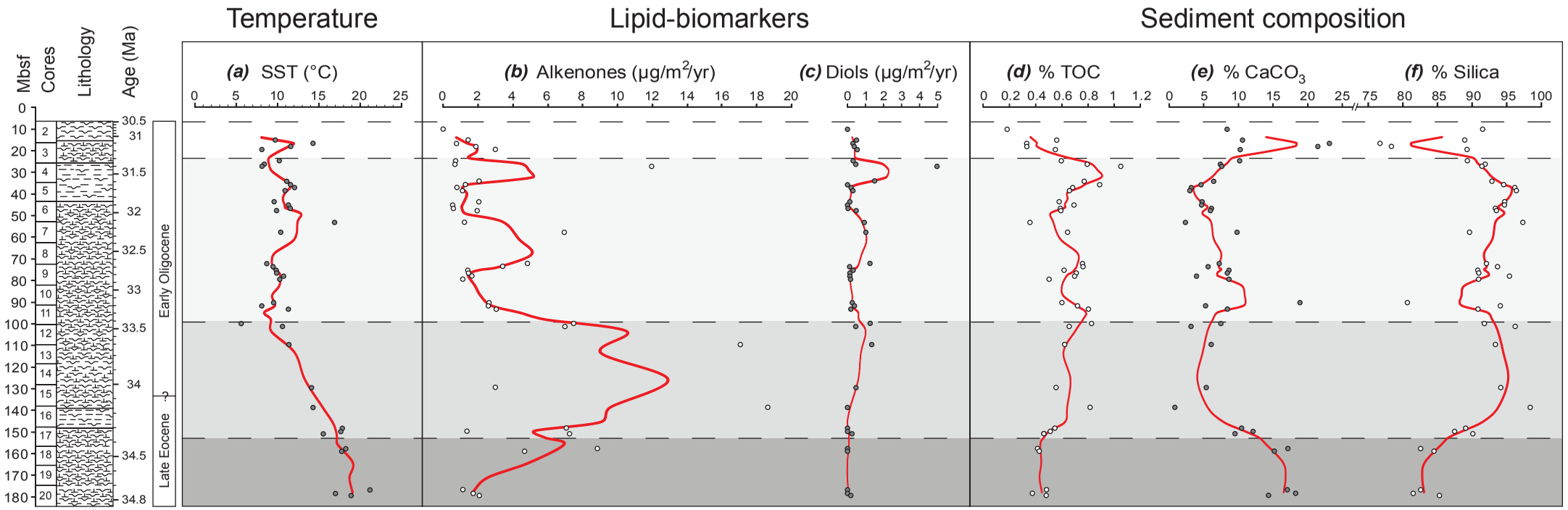

Figure 2-7. Changes in sea-surface temperatures (SSTs) and in primary productivity at DSDP Site 511 during the late Eocene-early Oligocene. Trend curves are 3-points moving average curves. A cooling is recorded in ***(a)*** alkenone-based SSTs (°C) coupled to an increase in primary productivity as attested by variations in lipid-biomarkers (***(b)*** alkenones, ***(c)*** long-chain diols) and by variations in relative proportions (%) of ***(d)*** Total Organic Carbon (TOC), ***(e)*** calcium carbonate ($CaCO_3$) and ***(f)*** silica contents. Please note that the horizontal scale is different for TOC with respect to $CaCO_3$ and silica.

The progressive cooling recorded at DSDP Site 511 is accompanied by a progressive increase in primary productivity through the Eocene-Oligocene boundary (34.4-33.4 Ma), as evidenced by variations in TOC and long-chain diol contents (Figure 2-7). This is supported by higher fluxes of silica, which suggest an enhanced production of siliceous organisms (Figure 2-7). A significant and positive correlation is observed between percentages of TOC and silica (Figure 2-5b), whereas the production of calcareous organisms (mainly nannofossils; Figure 2-5a) was limited, as shown by significantly reduced carbonate contents (Figure 2-7). These observations suggest a change in trophic conditions across the Eocene-Oligocene boundary (34.4-33.4 Ma), probably linked to the onset of an upwelling front that might have been more favorable to the development of diatoms [e.g., *Ziveri et al.*, 1995; *Marañon et al.*, 1996; *Schiebel et al.*, 2004]. Upwelling conditions, resulting from increased cold water production and more vigorous oceanic circulation, have indeed been suggested at Site 511 during this time interval, based on carbon isotopic composition ($\delta^{13}C$) of benthic and planktonic foraminifera and changes in diatom assemblages [*Muza et al.*, 1983; *Weaver*, 1983; *Schumacher and Lazarus*, 2004]. The onset of the Antarctic Circumpolar Current likely played a role in the expansion of subantarctic waters and of upwelling front towards Site 511 [*Muza et al.*, 1983; *Salamy and Zachos*, 1999; *Barker and Thomas*, 2004]. The early Oligocene (33.4-31.3 Ma) still accounts for a period of enhanced primary productivity as evidenced by TOC and long-chain diol fluxes (Figure 2-7). But the slight increase in carbonate content and the steady SSTs seem to indicate more stable sea-surface conditions, maybe linked to a stabilization of upwelling conditions during this period. Finally, an episodic input of warmer water masses can be observed between 31.3 and 31 Ma, as shown by an increase in SSTs and carbonate content (coupled with a decrease in silica proportions; Figure 2-7). This is in good agreement with oxygen isotope data [*Muza et al.*, 1983; *Weaver*, 1983].

An increase in primary productivity across the Eocene-Oligocene boundary is thus highlighted in nannofossil diatomaceous ooze from the DSDP Site 511. Similarly, previous studies inferred an increase in primary productivity during the Eocene-Oligocene at DSDP sites from South Atlantic and Southern Ocean, where sediments are mainly constituted by calcium carbonate [e.g., *Salamy and Zachos*, 1999; *Nilsen et al.*, 2003; *Persico and Villa*, 2004; *Anderson and Delaney*, 2005].

Alkenone fluxes at Site 511 intriguingly show a stratigraphic trend inversely correlated to that of nannofossils (Figure 2-4). Alkenone fluxes would suggest highest primary productivity around the Eocene-Oligocene boundary (34.4-33.4 Ma), whereas nannofossils show their

lowest fluxes during this time interval (Figure 2-4). A sample (138.6 mbsf; 34.16 Ma) is even characterized by very low $CaCO_3$ content (0.8 %) and is barren of nannofossils. It is worth noticing that this sample might correspond to the worldwide dissolution event recorded in different latitudes at ~34 Ma [*Diester-Haass and Zachos*, 2003; *Coxall et al.*, 2005; *Lear et al.*, 2008]. This event, with a duration of 40-60 kyr, is considered integral of the climatic change occurring during the late Eocene-early Oligocene and has been interpreted as a temporary shoaling of the Carbonate Compensation Depth [e.g., *Coxall and Pearson*, 2007]. However, our data suggest that the low nannofossil content in the other samples between 34.4 and 33.4 Ma is unlikely the result of enhanced dilution or dissolution of nannofossils. Nannofossil abundances are indeed expressed in fluxes, avoiding a possible dilution effect on nannofossil abundance by a variable accumulation rate of siliceous organisms in the same sediment. In addition, optical and scanning electron microscopy show that nannofossils are generally well preserved in all other investigated samples (see Plate 2-1 in supplementary data) and that delicate coccoliths that are prone to dissolution, such as *Pontosphaera*, are commonly observed with pristine structures. These observations suggest that the drastic decrease in nannofossil fluxes around the Eocene-Oligocene boundary is more likely an ecological response of coccolithophores, subsequent to the onset of upwelling conditions, rather than the result of enhanced dissolution during this period.

5. Conclusion

The comparison of nannofossil and alkenone contents in sediment samples from DSDP Site 511 does not allow an unequivocal identification of alkenone producers. However, some *Reticulofenestra* species (namely *R. dictyoda*, *R. minuta* and *R. clatrata*) as well as non-calcifying haptophytes could have contributed to alkenone production for the late Eocene-early Oligocene interval. Interestingly, the fact that sea-surface temperatures (SSTs) derived from the $U^{K'}_{37}$ ratio are consistent with temperatures derived from other proxies (TEX_{86}; $\delta^{18}O$) suggests that the calibration of the alkenone-based paleothermometer is less species-dependent than previously supported. In specific cases, such as the present one, the identification of alkenone producers is thus not crucial to better constrain the reconstructions of paleo-SSTs based on alkenones.

Quantitative variations in lipid-biomarkers, TOC, carbonate/silica ratio, nannofossils and alkenone-based sea surface temperatures allow the characterization of paleoenvironmental changes occurring at DSDP Site 511 (South Atlantic) during the late Eocene-early Oligocene.

A progressive cooling coupled to an increase in primary productivity, consistent with the development of upwelling conditions, occurred during the early Oligocene and induced a shift in nannofossil assemblages, especially within the Noelaerhabdaceae species (*R. dictyoda*, *R. minuta*, *D. bisecta*, *R. daviesii*). The opening of the circumpolar passages and the onset of the Antarctic Circumpolar Current very likely influenced environmental conditions at Site 511 and can both explain the temperature decrease of about 8°C and the productivity increase recorded there.

Appendix A: Taxonomic remarks

Taxonomy used in the present work follows Haptophyte phylogeny as revised by *Young and Bown* [1997] and *Sáez et al.* [2004].

A1. Noelaerhabdaceae family

Noelaerhabdaceae (*Jerkovic* [1970], emended by *Young and Bown*, [1997]) is the dominant family in the studied samples and is assumed to include the Cenozoic ancestors of the modern alkenone producers, namely *Emiliania* and *Gephyrocapsa*.

A1.1. Genus *Reticulofenestra*

Coccoliths of the genus *Reticulofenestra* [*Hay et al.*, 1966] are elliptical to subcircular with an open central area and with no slits in the distal shield. The following species were observed in this study:

R. clatrata [*Muller*, 1970]: medium-sized coccolith with large margins and large central area filled by a sieve plate divided by a median suture.

R. daviesii [*Haq*, 1968; *Haq*, 1971]: medium-sized coccoliths (5-8 μm) with plugs in central area.

R. dictyoda [*Stradner* in *Stradner and Edwards*, 1968]: small to large (3-14 μm) elliptical coccoliths with a wide central area.

R. hillae [*Bukry and Percival*, 1971]: large (> 12 μm) elliptical coccolith with a thick-wide collar around a small central opening which scales measuring less than one third of placolith length.

R. minuta [*Roth*, 1970]: small elliptical coccoliths (< 3 μm) with a wide central area.

R. umbilicus [*Levin*, 1965; *Martini and Ritzkowski*, 1968]: very large (> 14 μm, as defined by *Backman and Hermelin* [1986]) elliptical coccoliths with a wide central area.

A1.2. Genus *Dictyococcites*

Elliptical to subcircular coccoliths with a closed (or virtually closed) central area. Although, *Dictyococcites sensu Black* [1967] can be regarded as a heavily calcified synonym of *Reticulofenestra*, the emended diagnosis of *Backman* [1980] clearly separates this genus from *Reticulofenestra*.

D. bisectus [*Hay et al.*, 1966; *Bukry and Percival*, 1971] = *R. bisecta* [*Hay et al.*, 1966; *Roth*, 1970]: highly birefringent elliptical coccoliths (< 10 μm) with a closed central area in the distal shield.

D. stavensis [*Levin and Joerger*, 1976] = *R. stavensis* [*Levin and Joerger*, 1967; *Varol*, 1989]: highly birefringent elliptical coccoliths (> 10 μm) with a closed central area in the distal shield.

A2. Other coccoliths

Other coccoliths that do not belong to the Noelaerhabdaceae family are found in the studied samples are listed here: *Blackites* spp. [*Hay and Towe*, 1962], *Chiasmolithus* spp. [*Hay et al.*, 1966], *Clausicoccus* spp. [*Prins*, 1979], *Coccolithus formosus* [*Kamptner*, 1963; *Wise*, 1973], *Coccolithus pelagicus* [*Wallich*, 1877; *Schiller*, 1930], *Ericsonia* spp. [*Black*, 1964], *Heliscophaera* spp. [*Kamptner*, 1954], *Ismolithus recurvus* [*Deflandre*, 1954], *Pontosphaera* spp. [*Lohmann*, 1902], *Toweius* spp. [*Hay and Mohler*, 1967], *Umbilicosphaera* spp. [*Lohmann*, 1902], *Zygrhablithus* spp. [*Deflandre*, 1959].

A3. Nannoliths

Nannoliths include forms without a distinct rim and for which the peculiar structure cannot be directly related to coccoliths. They are thus considered as *incertae sedis*. Nannoliths found in this study are *Discoaster* spp. [*Tan*, 1927] and *Sphenolithus* spp. [*Grassé*, 1952].

Acknowledgements

This study used Deep Sea Drilling Project samples provided by the Integrated Ocean Drilling Program. We thank Walter Hale from the Bremen Core Repository for his efficiency and availability. We are also grateful to Baptiste Suchéras-Marx who helped to measure the calcium carbonate content.

References

Anderson, L.D., and M.L. Delaney (2005), Middle Eocene to early Oligocene paleoceanography from Agulhas Ridge, Southern Ocean (Ocean Drilling Program Leg 177, Site 1090), *Paleoceanography*, *20*, PA1013, doi:10.1029/2004PA001043.

Aubry, M.P. (1992), Paleogene calcareous nannofossils from the Kerguelen Plateau, Leg 120, in *Proceedings of the Ocean Drilling Program, Scientific Results, College Station, TX (Ocean Drilling Program), vol. 120*, edited by S.W. Wise et al., pp. 471-491, doi:10.2973/odp.proc.sr.120.149.

Backman, J. (1987), Quantitative calcareous nannofossil biochronology of middle Eocene through early Oligocene sediment from DSDP Sites 522 and 523, *Abh. Geol. Bundesanst., 39*, 21-31.

Barker, P.F., and E. Thomas (2004), Origin, signature and palaeoclimatic influence of the Antarctic Circumpolar Current, *Earth-Sci Rev*, *66*, 143-162.

Basov, I.A., and V.A Krasheninnikov (1983), Benthic foraminifers in Mesozoic and Cenozoic sediments of the southwestern Atlantic as indicators of paleoenvironment: Deep Sea Drilling Project Leg 71, *Deep Sea Drill. Proj. Init. Rep., 71*, 739-788.

Beaufort, L. (1991), Adaptation of the random settling method for quantitative studies of calcareous nannofossils, *Micropaleontology*, *37*, 415–418.

Bell, M.V., and D. Pond (1996), Lipid composition during growth of motile and coccolith forms of *Emiliania huxleyi*, *Phytochemistry*, 41, 465–471.

Beltran, C., J.-A. Flores, M.-A. Sicre, F. Baudin, M. Renard, and M. de Rafélis (2011), Long chain alkenones in the Early Pliocene Sicilian sediments (Trubi Formation-Punta di Maiata section): implications for the alkenone paleothermometry, *Palaeogeogr. Palaeoclim. Palaeoecol*, *308* (3–4), 253–263.

Boersma, A., and I. Premoli Silva (1991), Distribution of Paleogene planktonic foraminifera, analogies with the recent?, *Palaeogeogr. Palaeoclimat. Palaeoecol.*, *83*, 29-48.

Bolton, C.T., K.T., Lawrence, S.J. Gibbs, P.A. Wilson, L.C. Cleaveland, D. Timothy, and T.D. Herbert (2010), Glacial-interglacial productivity changes recorded by alkenones and microfossils in late Pliocene eastern equatorial Pacific and Atlantic upwelling zones, *Earth Planet. Sci. Lett.*, *295*, 401-411.

Brassell, S.C. (1993), Applications of biomarkers for delineating marine paleoclimate fluctuations during the Quaternary, in *Organic Geochemistry* edited by M.H. Engel, and S.A. Macko, Plenum, New York, pp. 699–738.

Brassell, S.C., G. Eglinton, I.T. Marlowe, U. Pflaumann, and M. Sarnthein (1986), Molecular stratigraphy: a new tool for climatic assessment, *Nature*, *320*, 129-133.

Conte, M.H., A. Thompson, and G. Eglinton (1995), Lipid biomarker diversity in the coccolithophorid *Emiliania huxleyi* (Prymnesiophycea) and the related species *Gephyrocapsa oceanica*, *J. Phycol.*, *31*, 272–82.

Conte, M.H., A. Thompson, D. Lesley, and R.P. Harris (1998), Genetic and physiological influences on the alkenone/alkenoate versus growth temperature relationship in *Emiliania huxleyi* and *Gephyrocapsa oceanica*, *Geochim. Cosmochim. Acta*, *62* (1), 51-68.

Conte, M.H., M.-A. Sicre, C. Rühlemann, J.C. Weber, S. Schulte, D. Schulz-Bull, and T. Blanz (2006), Global calibration of the alkenone unsaturation index $U^{k'}_{37}$ with surface water production temperature and a comparison of the coretop integrated production temperatures recorded by $U^{k'}_{37}$ with overlying sea surface temperatures, *Geochem. Geophys. Geosyst.*, *72*, 1–22.

Coxall, H.K., P.A. Wilson, H. Pälike, C.H. Lear, and J. Backman (2005), Rapid stepwise onset of Antarctic glaciation and deeper calcite compensation in the Pacific Ocean, *Nature*, *433*, 53–57, doi:10.1038/nature03135.

Coxall, H.K., and P.N. Pearson (2007), The Eocene-Oligocene transition, in *Deep-time perspectives on climate change: marrying the signal from computer models and biological proxies*, edited by M. Williams et al., pp. 351–387, Geol. Soc., London.

Davies, T.A., R.B. Kidd, and T.S. Ramsay-Anthony (1995), A time-slice approach to the history of Cenozoic sedimentation in the Indian Ocean, in *Selected Topics Relating to the Indian Ocean Basins and Margins,* edited by T.A. Davies, M.F. Coffin, and S.W. Wise, Sediment. Geol., 96, 157–179.

DeConto, R., and D. Pollard (2003), Rapid Cenozoic glaciation of Antarctica induced by declining atmospheric CO_2, *Nature*, *421*, 245–249, doi:10.1038/nature01290.

Diester-Haass, L., and J.C. Zachos (2003), The Eocene-Oligocene Transition in the Equatorial Atlantic (ODP Site 925), Paleoproductivity increase and positive $\delta^{13}C$ excursion, in *From Greenhouse to Icehouse: The Marine Eocene-Oligocene Transition*, edited by D.R. Prothero, L.C. Ivany, and E.A. Nesbitt, pp. 397– 416, Columbia Univ. Press, New York.

Diester-Haass, L., and R. Zahn (1996), Eocene-Oligocene transition in the Southern Ocean: History of water mass circulation and biological productivity, *Geology*, *24* (2), 163-166.

Dunkley Jones, T., P.R. Bown, P.N. Pearson, B.S. Wade, H.K. Coxall, and C.H. Lear (2008), Major shifts in calcareous phytoplankton assemblages through the Eocene-Oligocene

transition of Tanzania and their implications for low-latitude primary production, *Paleoceanography*, *23*, PA4204, doi:10.1029/2008PA001640.

Epstein, B.L., S. D'Hondt, and P.E. Hargraves (2001), The possible role of C_{37} alkenones in *Emiliania huxleyi*, *Org. Geochem.*, *32*, 867-875.

Faul, K.L., L.D. Anderson, and M.L. Delaney (2003), Late Cretaceous and early Paleogene nutrient and paleoproductivity records from Blake Nose, western North Atlantic Ocean, *Paleoceanography*, *18*, 1042-1058, doi:10.1029/2001PA000722.

Fujiwara, S., M. Tsuzuki, M. Kawachi, N. Minaka, and I. Inouye (2001), Molecular phylogeny of the Haptophyta based on the *rbc*L gene and sequence variation in the spacer region of the rubisco operon, *J. Phycol.*, *37*, 121-129.

Funakawa, S., and H. Nishi (2008), Radiolarian faunal changes during the Eocene-Oligocene transition in the Southern Ocean (Maud Rise, ODP Leg 113, Site 689) and its significance in paleoceanographic change, *Micropaleontology*, *54* (1), 15-26.

Geisen, M., J. Bollmann, J.O. Herrle, J. Mutterlose, and J.R. Young (1999), Calibration of the random settling technique for calculation of absolute abundance of calcareous nannoplankton, *Micropaleontology*, *45* (4), 437-442.

Gombos, A.M., and P.F. Ciesielski (1983), Late Eocene to early Miocene diatoms from the southwest Atlantic, *Deep Sea Drill. Proj. Init. Rep.*, *71*,583-634.

Gradstein, F.M., J.G Ogg, M. Schmitz, and G. Ogg (2012)*, The Geologic Time Scale 2012,* Elsevier, 2012, 1176 pp.

Grimalt, J.O., J. Rulkötter, M.-A. Sicre, R. Summons, J. Farrington, H.R. Harvey, M. Goñi, and K. Sawada (2000), Modifications of the C_{37} alkenone and alkenoate composition in the water column and sediment: possible implications for sea surface temperatures estimates in paleoceanography, *Geochem. Geophys. Geosyst.*, *1*, doi: 2000GC000053.

Hooker, J.J., M.E. Collinson, and N.P. Sille (2004), Eocene-Oligocene mammalian faunal turnover in the Hampshire Basin, UK: calibration of the global time scale and the major cooling event, *J. Geol. Soc. London*, *161*, 161-172.

Jaramillo, C., M.J. Rueda, and G. Mora (2006), Cenozoic plant diversity in the Neotropics, *Science*, *311*, 1893-1896.

Keller, G., N. MacLeod, and E. Barrera (1992), Eocene–Oligocene faunal turnover in planktic foraminifera, and Antarctic glaciation, in *Eocene-Oligocene Climatic and Biotic Evolution*, edited by D.R. Prothero, and W.A. Berggren, Princeton University Press, New Jersey, pp. 218-244.

Kennett, J.P. (1977), Cenozoic evolution of Antarctic glaciation, the Circum-Antarctic Ocean, and their impact on global paleoceanography, *J. Geophys. Res.*, *82*, 3843-3860.

Kennett, J.P., and L.D. Stott (1990), Proteus and Proto-Oceanus: ancestral Paleogene oceans as revealed from Antarctic stable isotopic results, *Proc. Oc. Drill. Progr., Scient. Res., 113*, 865-880.

Krasheninnikov, V.A., and I.A. Basov (1983), Stratigraphy of Cretaceous sediments of the Falkland Plateau based on planktonic foraminifers, Deep Sea Drilling Project Leg 71, *Deep Sea Drill. Proj. Init. Rep.*, *71*, 789-820.

Lagabrielle, Y., Y. Goddéris, Y. Donnadieu, J. Malavieille, and M. Suarez (2009), The tectonic history of Drake Passage and its possible impacts on global climate, *Earth Planet. Sci. Lett.*, *279*, 197-211.

Lawver, L.A., and L.M. Gahagan (2003), Evolution of Cenozoic seaways in the circum-Antarctic region, *Palaeogeogr. Palaeoclimatol. Palaeoecol.*, *198*, 11–37.

Lazarus, D., and J.P. Caulet (1993), Cenozoic Southern Ocean reconstructions from sedimentologic, radiolarian, and other microfossil data, in *The Antarctic paleoenvironment; a perspective on global change; Part two*, edited by J.P. Kennett and D.A. Warnke, Antarctic Research Series, pp. 145-174.

Lear, C.H., T.R. Bailey, P.N. Pearson, H.K. Coxall, and Y. Rosenthal (2008), Cooling and ice growth across the Eocene-Oligocene transition, *Geology*, *36*, 251–254, doi:10.1130/G24584A.1.

Liu, Z., M. Pagani, D. Zinniker, R. DeConto, M. Huber, H. Brinkhuis, S.R. Shah, M. Leckie, and A. Pearson (2009), Global cooling during the Eocene-Oligocene climate transition, *Science*, *323*, 1187–1190, doi:10.1126/science.1166368.

Liu, H., I. Probert, J. Uitz, H. Claustre, S. Aris-Brosou, M. Frada, F. Not, and C. de Vargas (2009), Extreme diversity in noncalcifying haptophytes explains a major pigment paradox in open oceans, *PNAS*, *106* (31), 12803-12808.

Ludwig, W.G., V.A. Krasheninnikov, and the Shipboard Scientific Party (1983), Site 511, *Deep Sea Drill. Proj. Init. Rep.*, *71*, 21-109.

Marañón, E., E. Fernández, R.P. Harris, and D.S. Harbour (1996), Effects of the diatom-*Emiliania huxleyi* succession on photosynthesis, calcification and carbon metabolism by size-fractionated phytoplankton, *Hydrobiologia*, *317*, 189-199.

Marlowe, I.T., S.C. Brassell, G. Eglinton, and J.C. Green (1984), Long chain unsaturated kenones and esters in living algae and marine sediments, *Org. Geochem.*, *6*, 135-141.

Marlowe, I.T., S.C. Brassell, G. Eglinton, and J.C. Green (1990), Long-chain alkenones and alkyl alkenoates and the fossil coccolith record of marine sediments, *Chem. Geol.*, *88*, 349-375.

Merico, A., T. Tyrrell, and P.A. Wilson (2008), Eocene/Oligocene ocean de-acidification linked to Antarctic glaciation by sea-level fall, *Nature*, *452*, 979-982, doi:10.1038/nature06853.

Miller, K.G., J.V. Browning, M.P. Aubry, B.S. Wade, M.E. Katz, A.A. Kulpecz, and J.D. Wright (2008), Eocene-Oligocene global climate and sea-level changes: St. Stephens Quarry, Alabama, *Geol. Soc. Am. Bull.*, *120*, 34–53, doi:10.1130/B26105.1.

Müller, P.J., M. Cepek, G. Ruhland, and R.R. Schneider (1997), Alkenone and coccolithophorid species changes in Late Quaternary sediments from the Walvis Ridge: Implications for the alkenone paleotemperature method, *Palaeogeogr. Palaeoclimatol. Palaeoecol.*, *135*, 71–96.

Müller, P.J., G. Kirst, G. Rulhand, I. von Storch, and A. Rosell-Melé (1998), Calibration of the alkenone paleotemperature index $U^{K'}_{37}$ based on core-tops from the eastern South Atlantic and the global ocean (60°N-60°S), *Geochim. Cosmochim. Acta*, *62* (10), 1757-1772.

Muza, J.P., D.F. Williams, and S.W. Wise (1983), Paleogene oxygen isotope record for Deep Sea Drilling Sites 511 and 512, subantarctic south Atlantic ocean: paleotemperatures, paleoceanographic changes, and the Eocene/Oligocene boundary event, *Deep Sea Drill. Proj. Init. Rep.*, *71*, 409-422.

Nilsen, E.B., L.D. Anderson, and M.L. Delaney (2003), Paleoproductivity, nutrient burial, climate change and the carbon cycle in the western equatorial Atlantic across the Eocene/Oligocene boundary, *Paleoceanography*, *18* (3), 1057-1068, doi:10.1029/2002PA000804.

Pagani, M., J.C. Zachos, K.H. Freeman, B. Tripple, and S. Bohaty (2005), Marked decline in atmospheric carbon dioxide concentrations during the Paleogene, *Science*, *309*, 600– 603.

Pagani, M., M. Huber, Z. Liu, S.M. Bohaty, J. Henderiks, W. Sijp, S. Krishnan, and R.M. DeConto (2011), The role of carbon dioxide during the onset of Antarctic glaciation, *Science*, *334*, 1261-1264, doi: 10.1126/science.1203909.

Pearson, P.N., I.K. McMillan, B.S. Wade, T. Dunkley Jones, H.K. Coxall, P.R. Bown, and C.H. Lear (2008), Extinction and environmental change across the Eocene-Oligocene boundary in Tanzania, *Geology*, *36*, 179– 182, doi:10.1130/G24308A.1.

Pekar, S.F., N. Christie-Blick, M.A. Kominz, and K.G. Miller (2002), Calibration between eustatic estimates from backstripping and oxygen isotopic records for the Oligocene, *Geology*, *30*, 903–906, doi:10.1130/0091-7613(2002)030<0903:CBEEFB>2.0.CO;2.

Persico, D., and G. Villa (2004), Eocene-Oligocene calcareous nannofossils from Maud Rise and Kerguelen Plateau (Antarctica): Paleoecological and paleoceanographic implications, *Mar. Micropaleontol*., *52*, 153 – 179, doi:10.1016/j.marmicro.2004.05.002.

Plancq, J., V. Grossi, J. Henderiks, L. Simon, and E. Mattioli (2012), Alkenone producers during late Oligocene–early Miocene revisited, *Paleoceanography*, *27*, PA1202, doi:10.1029/2011PA002164.

Popp, B.N., E.A. Laws, R.R. Bidigare, J.E. Dore, K.L. Hanson, and S.G. Wakeham (1998), Effect of phytoplankton cell geometry on carbon isotopic fractionation, *Geochim. Cosmochim. Acta*, *62*, 69– 77.

Prahl, F.G., and S.G. Wakeham (1987), Calibration of unsaturation patterns in long-chain ketone compositions for paleotemperature assessment, *Nature*, *330*, 367-369.

Prahl, F.G., L.A. Muehlhausen, and D.L. Zahnle (1988), Further evaluation of long-chain ketone compositions for paleotemperature assessment, *Geochim. Cosmochim. Acta*, *52*, 2303-2310.

Rampen, S.W., S. Schouten, S.G. Wakeham, and J.S. Sinninghe Damsté (2007), Seasonal and spatial variation in the sources and fluxes of long chain diols and mid-chain hydroxy methyl alkanoates in the Arabian Sea, *Org. Geochem.*, *38*, 165-179, doi: 10.1016/j.orggeochem.2006.10.008.

Rea, D.K., and M.W. Lyle (2005), Paleogene calcite compensation depth in the eastern subtropical Pacific: Answers and questions, *Paleoceanography*, *20*, PA1012, doi:10.1029/2004PA001064.

Riebesell, U., A.T. Revill, D.G. Hodsworth, and J.K. Volkman (2000), The effects of varying CO_2 concentration on lipid composition and carbon isotope fractionation in *Emiliania huxleyi*, *Geochim. Cosmochim. Acta*, *64*, 4179-4192.

Sáez, A.G., I. Probert, J.R. Young, B. Edvardsen, W. Eikrem, and L.K. Medlin (2004), A review of the phylogeny of the Haptophyta, in *Coccolithophores: From molecular processes to global impact*, edited by H.R. Thierstein and J.R. Young, J.R., pp. 251–269, Springer-Verlag, Berlin Heidelberg.

Salamy, K.A., and J.C. Zachos (1999), Latest Eocene-early Oligocene climate change and Southern Ocean fertility: Inferences from sediment accumulation and stable isotope data,

Palaeogeogr. Palaeoclimatol. Palaeoecol., *145*, 61–77, doi:10.1016/S0031-0182(98)00093-5.

Salloway, J.C. (1983), Paleomagnestism of sediments from Deep Sea Drilling Project Leg 71, *Deep Sea Drill. Proj. Init. Rep.*, *71*, 1073-1091.

Schiebel, R., A. Zeltner, U.F. Treppke, J.J. Waniek, J. Bollmann, T. Rixen, and C. Hemleben (2004), Distribution of diatoms, coccolithophores and planktic foraminifers along a trophic gradient during SW monsoon in the Arabian Sea, *Mar. Micropal.*, *51*, 345-371, doi: 10.1016/j.marmicro.2004.02.001.

Schumacher, S., and D. Lazarus (2004), Regional differences in pelagic productivity in the late Eocene to early Oligocene-a comparison of southern high latitudes and lower latitudes, *Palaeogeogr. Palaeoclimatol. Palaeoecol.*, *214*, 243-263, doi:10.1016/j.palaeo.2004.06.018.

Shackleton, N.J., and J.P. Kennett (1975), Paleotemperature history of the Cenozoic and the initiation of Antarctic Glaciation, oxygen and carbon isotope analyses in DSDP Sites 277, 279 and 281, *Deep Sea Drill. Proj. Init. Rep.*, *29*, 599– 612.

Sikes, E.L., J.W. Farrington, and L.D. Keigwin (1991), Use of the alkenone unsaturation ratio U^{K}_{37} to determine past sea surface temperatures: core-top SST calibrations and methodology considerations, *Earth Planet. Sci. Lett.*, *104*, 36-47.

Sinninghe Damsté, J.S., S. Rampen, W. Irene, C. Rijpstra, B. Abbas, G. Muyzer, and S. Schouten (2003), A diatomaceous origin for long-chain diols and mid chain hydroxy methyl alkanoates widely occurring in Quaternary marine sediments: indicators for high-nutrient conditions, *Geochim. Cosmochim. Acta*, *67*, 1339-1348, doi: 10.1016/S0016-7037(02)01225-5.

Sorrosa, J. (2012), Regulation by temperature in coccolithophorids; growth, calcification and alkenone synthesis, Lambert Academic Publishing, U.K., 62 pp.

Syke, T.J.S., J.-Y. Royer, A.T.S Ramsay, and R.B. Kidd (1998), Southern hemisphere palaeobathymetry, in *Geological Evolution of Ocean Basins: Results from the Ocean Drilling Program*, edited by A. Cramp et al., Spec. Publ. Geol. Soc. Lond., vol. 131, pp. 3-42.

Ternois, Y., K. Kawamura, L. Keigwin, N. Ohkouchi, and T. Nakatsuka (2001), A biomarker approach for assessing marine and terrigenous inputs to the sediments of Sea of Okhotsk for the last 27,000 years*, Geochim. Cosmochim. Acta*, *65*, 791–802.

Versteegh, G.J.M., H.J. Bosch, and J.W. De Leeuw (1997), Potential palaeoenvironmental information of C_{24} to C_{36} mid-chain diols, keto-ols and mid-chain hydroxy fatty acids; a critical review, *Org. Geochem.*, *27*, 1-13, doi: 10.1016/s0146-6380(97)00063-6.

Versteegh, G.J.M., R. Riegman, J.W. De Leeuw, and J.H.F. Jansen (2001), $U^{k'}_{37}$ values for *Isochrysis galbana* as a function of culture temperature, light intensity and nutrient concentrations, *Org. Geochem*., *32*, 785-794.

Villa, G., C. Fioroni, L. Pea, S. Bohaty, and D. Persico (2008), Middle Eocene-late Oligocene climate variability: Calcareous nannofossil response at Kerguelen Plateau, Site 748, *Mar. Micropaleontol*., *69*, 173-192.

Villanueva, J., J.O. Grimalt, E. Cortijo, L. Vidal, and L.D. Labeyrie (1997), A biomarker approach to the organic matter deposited in the North Atlantic during the last climatic cycle, *Geochim. Cosmochim. Acta*, *61*, 4633-4646.

Villanueva, J., J.O. Grimalt, L.D. Labeyrie, E. Cortijo, L. Vidal, and J.-L. Turon (1998), Precessional forcing of productivity in the North Atlantic Ocean, *Paleoceanography*, *13*, 561-571.

Villanueva, J., J.A. Flores, and J.O. Grimalt (2002), A detailed comparison of the $U^{k'}_{37}$ and coccolith records over the past 290 kyears: implications to the alkenone paleotemperature method, *Org. Geochem.*, *33*, 897-905.

Volkman, J.K., G. Eglinton, E.D.S. Corner, and T.E.V. Forsberg (1980), Long-chain alkenes and alkenones in the marine coccolithphorid *Emiliania huxleyi*, *Phytochemistry*, *19*, 2619-2622.

Volkman, J.K., S.M. Barrett, S.I. Blackburn, and E.L. Sikes (1995), Alkenones in *Gephyrocapsa oceanica*: Implications for studies of paleoclimate, *Geochim. Cosmochim. Acta*, *59*, 513–520.

Volkman, J.K., S.M. Barrett, and S.I. Blackburn (1999), Eustigmatophyte microalgae are potential sources of C_{29} sterols, C_{22}-C_{28} *n*-alcohols and C_{28}-C_{32} *n*-alkyl diols in freshwater environments, *Org. Geochem.*, *30*, 307–318.

Wade, B.S., and P.N. Pearson (2008), Planktonic foraminiferal turnover, diversity fluctuations and geochemical signals across the Eocene/Oligocene boundary in Tanzania, *Mar. Micropaleontol*., *68*, 244– 255.

Weaver, P.P.E. (1983), An integrated stratigraphy of the Upper Quaternary of the King's Trough flank area NE Atlantic, *Oceanologica Acta*, *6*, 451–456.

Weaver, P.P.E., M.R. Chapman, G. Eglinton, M. Zhao, D. Rutledge, and G. Read (1999), Combined coccolith, foraminiferal, and biomarker reconstruction of paleoceanographic

conditions over the past 120 kyr in the northern North Atlantic (59°N, 23°W), *Paleoceanography*, *14*, 336-349.

Yamamoto, M., Y. Shiraiwa, and I. Inouye (2000), Physiological responses of lipids in *Emiliania huxleyi* and *Gephyrocapsa oceanica* (Haptophyceae) to growth status and their implications for alkenone paleothermometry, *Org. Geochem.*, *31*, 799-811.

Young, J.R. (1990), Size variation of Neogene *Reticulofenestra* coccoliths from Indian Ocean DSDP Cores, *J. Micropaleontol.*, *9*, 71–86.

Young, J.R. (1998), Neogene, in *Calcareous Nannofossil Biostratigraphy*, edited by P.R. Bown, pp. 225-265, Chapman and Hall, Cambridge, U.K.

Young, J.R., and P.R. Bown (1997), Cenozoic calcareous nannoplankton classification, *J. Nannoplankton Res.*, *19*, 36–47.

Zachos, J.C., T.M. Quinn, and K.A. Salamy (1996), High-resolution (104 years) deep-sea foraminiferal stable isotope records of the Eocene-Oligocene climate transition, *Paleoceanography*, *11*, 251– 266.

Zachos, J.C., N.J. Shackleton, J.S. Revenaugh, P. Heiko, and B.P. Flower (2001), Climate response to orbital forcing across the Oligocene-Miocene boundary, *Science*, *292*, 274–278.

Ziveri, P., R.C. Thunell, and D. Rio (1995), Export production of coccolithophores in an upwelling region: Results from San Pedro Basin, Southern California Borderlands, *Mar. Micropal.*, *24*, 335-358.

Supplementary data

Plate 2-1. Scanning Electron Microscope (SEM) pictures showing that the studied samples are dominated by diatoms and radiolarian (organisms producing a siliceous test) and that coccoliths are generally well preserved. **(a-b)** Sample 511-5R4-63 (38.42 mbsf), **(c)** Sample 511-15R1-93 (129.43 mbsf), **(d-e)** Sample 511-17R1-68 (148.18 mbsf), **(f-h)** Sample 511-20R1-66 (176.66 mbsf).

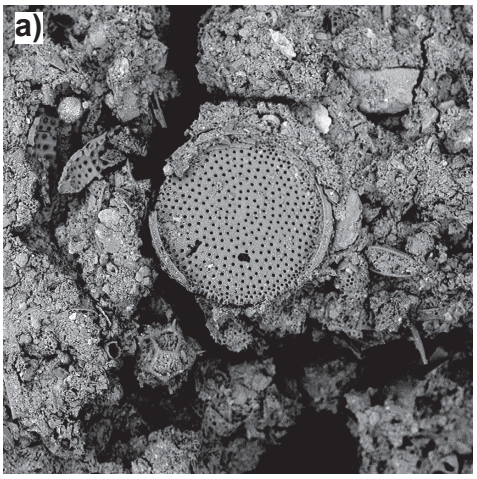
a)
130 µm

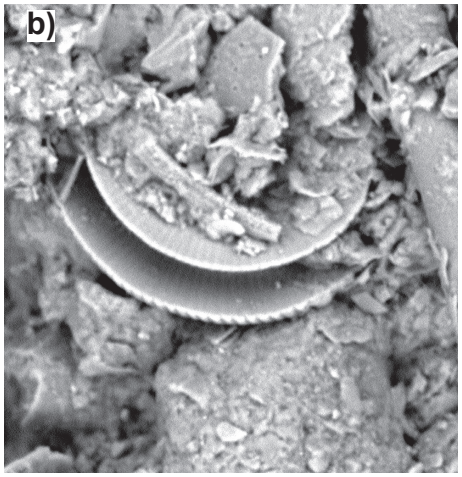
b)
8 µm

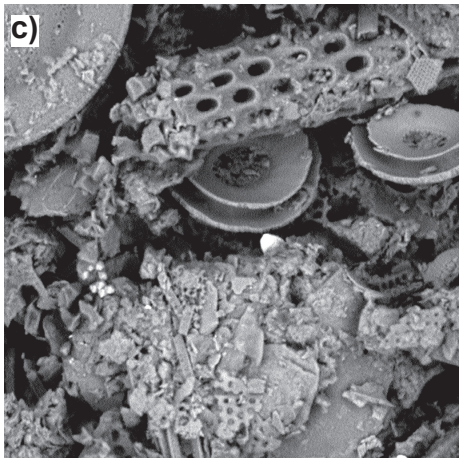
c)
10 µm

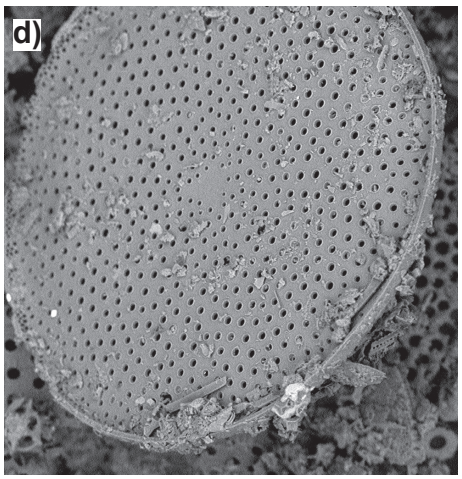
d)
50 µm

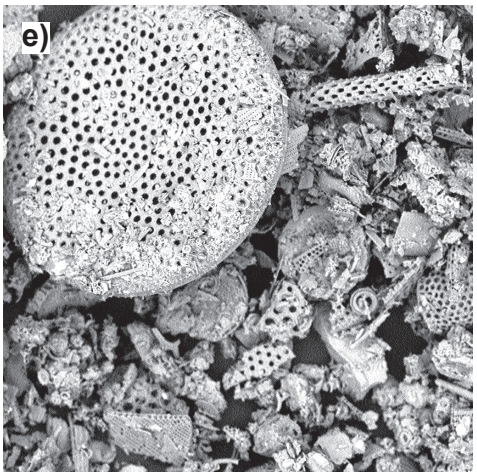
e)
80 µm

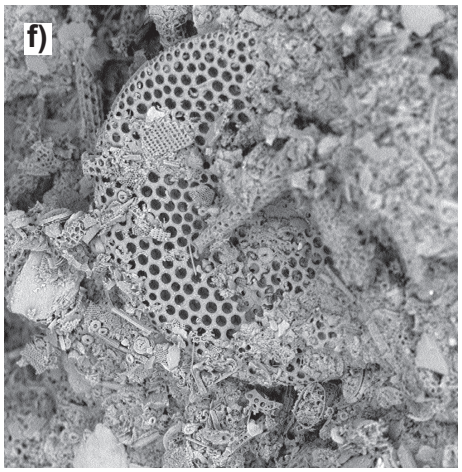
f)
70 µm

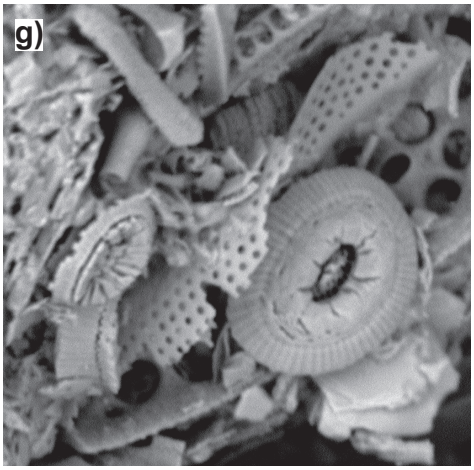
g)
8 µm

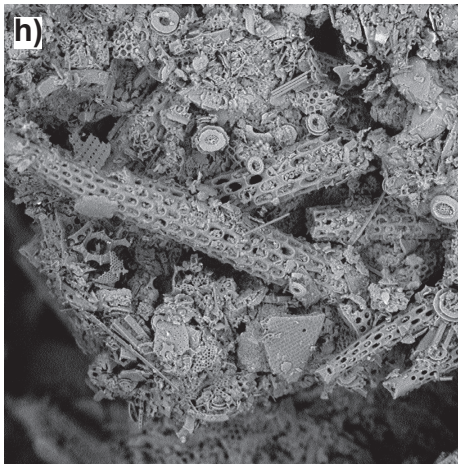
h)
40 µm

Chapitre 3

Changements globaux dans les assemblages de Noëlaerhabdaceae et implications pour les estimations de pCO_2 à la transition Oligocène-Miocène

Ce chapitre s'intéresse à la transition Oligocène-Miocène (25-16 Ma) au Site DSDP (Deep Sea Drilling Project) 516, situé dans la gyre subtropicale de l'Atlantique Sud sur le Rio Grande Rise. Au Miocène, le Site DSDP 516 se trouvait à 1313 m de profondeur, bien au dessus de la profondeur de compensation des carbonates (CCD), permettant ainsi une bonne préservation des assemblages de nannofossiles. De plus, le taux de sédimentation relativement élevé (17 m/Ma) à ce site a permis un enfouissement rapide et une bonne préservation de la matière organique en comparaison avec d'autres sites océaniques profonds.

Si de nombreuses études ont souligné un renouvellement important dans les assemblages de nannofossiles calcaires (coccolithes et *incertae sedis*) au cours de la transition Oligocène-Miocène (Pujos, 1985; Olafsson, 1989; Young, 1998), peu se sont intéressées aux assemblages de Noëlaerhabdaceae. La première partie de ce chapitre **(3.1)** présente donc une étude sur les variations d'abondances absolues des assemblages de Noëlaerhabdaceae à différentes latitudes de l'Océan Atlantique et de l'Océan Pacifique autour de la limite Oligocène-Miocène (Sites DSDP 516, 608 et 588). Pour les trois sites étudiés, les assemblages de nannofossiles sont caractérisés par des proportions élevées successives de *Cyclicargolithus*, *Dictyococcites* et *Reticulofenestra*. Le déclin synchrone de *Cyclicargolithus* aux trois sites étudiés correspond probablement à un événement global. Les causes possibles de ce turnover taxonomique à long terme sont explorées. D'une part, un événement climatique global, en relation avec les glaciations du Miocène inférieur, pourrait avoir déclenché le déclin du taxon *Cyclicargolithus*. La niche écologique laissée vacante suite à la diminution en abondance de *Cyclicargolithus* a pu alors être exploitée par les réticulofénestrés (*Dictyococcites* et *Reticulofenestra*) qui deviennent dominants dans les assemblages après 20 Ma. D'autre part, ce turnover global pourrait refléter une succession évolutive graduelle et être le résultat de pressions sélectives, comme une compétition accrue entre *Cyclicargolithus* et réticulofénestrés. Une diversification au sein des réticulofénestrés, indiquée par l'augmentation de la variation de taille au sein de ce groupe dès ~20 Ma, aurait pu contribuer au déclin de *Cyclicargolithus*.

Dans la deuxième partie de ce chapitre **(3.2)**, la comparaison entre les concentrations en alcénones et les abondances relatives et absolues des différentes espèces de Noëlaerhabdaceae permet d'identifier l'espèce *Cyclicargolithus floridanus* comme étant un producteur majeur d'alcénones au Site DSDP 516 à la transition Oligocène-Miocène. Contrairement aux hypothèses précédentes, *Reticulofenestra* n'était pas le producteur d'alcénones prédominant pendant l'intervalle de temps étudié. La distribution des différents types d'alcénones ($MeC_{37:2}$, $EtC_{38:2}$, and $MeC_{38:2}$) ne change pas malgré des changements distincts dans la

composition des espèces, suggérant des distributions similaires en alcénones di-insaturées au sein de la famille des Noëlaerhabdaceae pendant l'Oligocène supérieur-Miocène inférieur. La grande taille de cellule de *Cyclicargolithus* peut avoir des implications sur les reconstructions de pressions partielles de CO_2 basées sur les alcénones. Nos résultats soulignent l'importance d'une identification la plus précise possible des producteurs d'alcénones pour des périodes (>1,85 Ma) pré-datant la première apparition des producteurs actuels.

Il est à noter que la trop faible concentration en alcénones, atteignant souvent la limite de détection, dans les sédiments des Sites DSDP 588 et 608 n'a malheureusement pas permis l'identification des producteurs d'alcénones à la transition Oligocène-Miocène du Pacifique Sud et de l'Atlantique Nord.

3.1. Changements globaux dans les assemblages de Noëlaerhabdaceae autour de la limite Oligocène-Miocène

Global shifts in Noelaerhabdaceae assemblages during the late Oligocene-early Miocene

Julien Plancq[a*], Emanuela Mattioli[a], Jorijntje Henderiks[b], Vincent Grossi[a]

[a] Laboratoire de Géologie de Lyon (UMR 5276), CNRS, Université Lyon 1, Ecole Normale Supérieure Lyon, Campus scientifique de la DOUA, Villeurbanne, France

[b] Uppsala University, Department of Earth Sciences, Paleobiology Program, Villavägen 16, 752 36 Uppsala, Sweden

[*] Corresponding author : Julien Plancq, Laboratoire de Géologie de Lyon, UMR 5276, CNRS, Université Lyon 1, Campus de la DOUA, Bâtiment Géode, 69622 Villeurbanne Cedex, France. Tel.: +33 4 72431544.
E-mail address: julien.plancq@pepsmail.univ-lyon1.fr (J. Plancq)

Submitted to Marine Micropaleontology

Abstract

This study investigates abundance variations in Noelaerhabdaceae assemblages during the late Oligocene-early Miocene at different latitudes of the Atlantic and Pacific oceans (DSDP Sites 516, 608 and 588). Nannofossil assemblages were characterized at the three studied sites by the successive high proportion of *Cyclicargolithus*, *Dictyococcites* and *Reticulofenestra*. Local paleoceanographic changes, such as the input of nutrient-poor water masses, might explain shifts in ecological prominence within the Noelaerhabdaceae at DSDP Site 516 (Southern Atlantic). But the similar timing of a decline in *Cyclicargolithus* at the three studied sites more likely corresponds to a global process. Here, we explore possible causes for this long-term taxonomic turnover. A global change in climate, associated with early Miocene glaciations, could have triggered a decline in fitness of the taxon *Cyclicargolithus*. The ecological niche made vacant because of the decrease in *Cyclicargolithus* could then have been exploited by *Reticulofenestra*/*Dictyococcites* that became prominent in the assemblages

after 20 Ma. Alternatively, this global turnover might reflect a gradual evolutionary succession and be the result of other selection pressures, such as increased competition between *Cyclicargolithus* and *Reticulofenestra*/*Dictyococcites*. A diversification within *Reticulofenestra*/*Dictyococcites*, indicated by an expansion in the size variation within this group since ~20 Ma, may have contributed to the decreased fitness of *Cyclicargolithus*.

Keywords: Noelaerhabdaceae; *Cyclicargolithus* decline; late Oligocene; early Miocene; climate; evolution.

1. Introduction

The Noelaerhabdaceae are a family of coccolithophores dominant in most Neogene calcareous nannofossil assemblages and includes the two most prominent modern coccolithophores and alkenone producers, namely *Emiliania huxleyi* and *Gephyrocapsa oceanica*, known to produce blooms in today's oceans. Those large scale blooms have important implications for the global carbon cycle through processes of photosynthesis, calcification and respiration (Rost and Riebesell, 2004). During the Pleistocene, distinct intervals of dominance are recorded within the gephyrocapsids (e.g., Matsuoka and Okada, 1990; Bollmann et al., 1998; Flores and Marino, 2002; Flores et al., 2003; Baumann and Freitag, 2004; Barker et al., 2006) while *E. huxleyi* rose to global dominance ~270 thousand years ago (ka) (Thierstein et al., 1977). The cosmopolitan distribution of the Noelaerhabdaceae family, which is believed to represent the main lineage of ancient alkenone producers, was sustained throughout most of the Cenozoic. Comparatively, our knowledge about the ecological preference or assemblage dynamics of the Oligocene and Miocene representatives of the Noelaerhabdaceae is relatively poor (Haq, 1980; Rio et al., 1990, Young, 1990; Kameo and Sato, 2000).

Several studies have shown that the late Oligocene-early Miocene period is marked by an important turnover of calcareous nannofossils, with first and last occurrences that are of biostratigraphic interest (Olafsson, 1989; Pujos, 1985; Young, 1998). For example, the early definition of the Oligocene-Miocene boundary relied on the last occurrence of *Dictyococcites bisectus* (*Reticulofenestra bisecta* of some authors; Berggren et al., 1985). However, only a few studies have estimated absolute abundances of the different genera of Noelaerhabdaceae during this period (e.g., Olafsson, 1989; Henderiks and Pagani, 2007; Plancq et al., 2012) and

the paleoecological affinities of most species are still poorly known. The late Oligocene to early Miocene was a period of relative global warmth interrupted by large, transient Antarctic glaciations (named "Oi-2" and "Mi-1" events) as attested by significant oxygen isotopic ($\delta^{18}O$) increases (0.50 to >1.0 ‰) in benthic foraminiferal records (e.g., Miller et al., 1991, 1996; Zachos et al., 2001a,b; Billups et al., 2002). The opening and deepening of the Drake Passage and the subsequent intensification of the Antarctic Circumpolar Current (ACC) may have been coincident with the Oligocene-Miocene boundary and are believed to constitute important events in the Antarctic ice sheet expansion (e.g., Barker and Thomas, 2004; von der Heydt and Dijkstra, 2006), although the timing of this opening and causes of the inception of the glacial history of Antarctica are still being debated (Scher and Martin, 2006; Livermore et al., 2007; Cramer et al, 2009). The paleoceanographic changes associated with these cooling events could have influenced the composition of the nannofossil assemblages, which are largely controlled by variations in the temperature and nutrient characteristics of the upper water column (e.g., McIntyre and Bé, 1967; Okada and Honjo, 1973; Winter and Siesser, 1994).

In the present study, we investigate the relative and absolute abundances of three Noelaerhabdaceae genera - *Cyclicargolithus*, *Reticulofenestra* and *Dictyococcites* - in sediments from three Deep Sea Drilling Project (DSDP) sites covering the late Oligocene-early Miocene. These three sites are located in the North and South Atlantic and South-West Pacific, in areas corresponding to subtropical gyres. Results highlight similar variations in Noelaerhabdaceae assemblages at all studied sites, with an apparent global decline in *Cyclicargolithus*, a dominant species in Oligocene sediments, at ~20 million years ago (Ma). This overall turnover cannot be explained by local paleoceanographic changes alone, and suggests the influence of global abiotic and/or biotic selection pressures.

2. Material and methods

2.1. Studied sites and sampling strategy

The investigated time interval spans the latest Oligocene and the early Miocene (26-16 Ma). Deep Sea Drilling Project (DSDP) Sites 516, 608 and 588 located in South Atlantic, North Atlantic and South-West Pacific respectively (Fig. 3-1), were selected for their continuous sedimentation and good nannofossil preservation (e.g., Barker et al., 1983; Lohman, 1986; Takayama and Sato, 1987; Plancq et al., 2012).

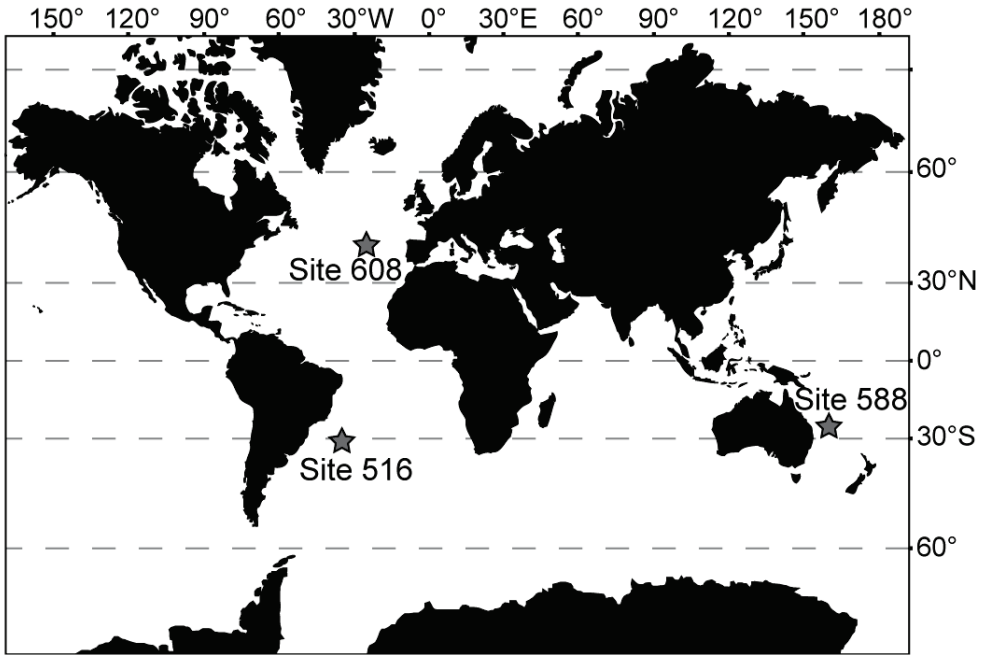

Figure 3-1. Location of the studied DSDP Sites 608, 516 and 588.

DSDP Leg 94 Site 608 (42°50N; 23°05W) is located on the eastern side of the North Atlantic Ridge on the southern flank of the King's Trough tectonic complex, at 3526 m water depth in the temperate subtropical North Atlantic gyre (Ruddiman et al., 1987). During the Miocene, Site 608 was at ca. 43°N (Wright et al., 1992) and nannofossil-foraminifera ooze deposition prevailed. Twenty-four samples were selected for this study with a temporal resolution of one sample per 330 kyr (ca. one sample every 3 meters).

DSDP Leg 90 Site 588 (26°06S; 161°E) was drilled on the Lord Howe Rise at 1533 m water depth in the South-West Pacific Ocean (Kennett et al., 1986). During the Miocene, this site was located at ca. 32.5°S (Wright et al., 1992), within a subtropical oligotrophic regime providing a steady nannofossil-foraminifera chalk sedimentation and upper water column stability (Flower and Kennett, 1993). Twenty-six samples were selected with a temporal resolution of one sample per 320 kyr (ca. one sample every 3 meters).

DSDP Leg 72 Site 516 (30°16S; 35°17W) is located on the upper flanks of the Rio Grande Rise at 1313 m water depth in the South Atlantic subtropical gyre (Belkin and Gordon, 1996). This gyre has been located at this latitude since the early Miocene (Barker et al., 1983). Sediments are primarily composed of nannofossil-foraminifera and nannofossil oozes. The thirty-six samples used for the present study are the same as those studied by Plancq et al. (2012). The temporal resolution is one sample per 220 kyr (ca. one sample every 4 meters).

The age models for the three DSDP sites used in this study are the ones presented by Pagani et al. (1999) and Henderiks and Pagani (2007). All age datums were recalibrated to the latest geological timescale (Gradstein et al., 2012) and are presented in Table 3-1.

Table 3-1. Age model parameters

FAD = first appearance datum; LAD = last appearance datum. Datum levels identified by (1) Berggren et al. (1985), (2) Wei and Wise (1989), (3) Hodell and Woodruff (1994), (4) Wright et al. (1992), (5) Gartner (1992), and (6) Clement and Robinson (1987).

Site/Hole	Datum	Depth (m)	Age (Ma)	Reference
516	LAD *Sphenolithus heteromorphus*	71.1	13.57	1
516	LAD *Praeorbulina sciana*	72.2	14.5	1
516	FAD *Praeorbulina glomerosa*	88.3	16.28	1
516	FAD *Praeorbulina sciana*	98.1	16.4	1
516	FAD *Fohsella birnageae*	103	16.7	1
516	LAD *Catapsydrax dissimilis*	109.6	17.5	1
516	LAD *Globorotalia kugleri*	178	21.14	1
516F	FAD *Discoaster druggi*	198	22.86	1
516F	FAD *Globorotalia kugleri*	208.2	23	1
516F	FAD *Globigerinoides primordius (common)*	215	23.5	1
516F	LAD *Sphenolithus ciperoensis*	256.3	24.43	2
588C	CM3	316.1	16.02	3
588C	Mi-1b	337.8	17.65	4
588C	CM-O/M (end)	368.9	22.4	3
588C	Mi-1	388.8	23.03	4
588C	CM-O/M (beginning)	390	23.4	3
608	LAD *Helicosphaera ampliaperta*	327.66	14.91	5
608	Mi-2	331.4	16.08	4
608	Chron C5B/C5C	332.23	15.97	6
608	Chron C5C/C5D	344.69	17.23	6
608	Mi-1b	349.16	17.65	4
608	FAD *Sphenolithus heteromorphus*	353.46	17.71	5
608	Chron C5D/C5E	353.94	18.21	6
608	LAD *Sphenolithus belemnos*	354.96	17.95	5
608	base Chron C6n	362.74	19.72	6
608	Chron C6A/C6AA	394.21	21.08	6
608	Chron C6AA/C6B	408.23	21.77	6
608	Mi-1	411.36	23.03	4
608	Chron C8/C9	449.64	26.43	6
608	LAD *Sphenolithus distensis*	455.08	26.84	5

2.2. Micropaleontological analyses

Slides for calcareous nannofossil quantitative analysis were prepared following the random settling method (Beaufort, 1991; modified by Geisen et al., 1999). A small amount of dried sediment powder (5 mg) was mixed with water (with basic pH, over-saturated with respect to calcium carbonate) and the homogenized suspension was allowed to settle for 24 hours onto a cover slide. The slide was dried and mounted on a microscope slide with Rhodopass. Coccolith quantification was performed using a polarizing optical ZEISS microscope (magnification 1000x). A standard number of 500 calcareous nannofossils (coccoliths and nannoliths) were counted in a variable number of fields of views (between 10 and 30 according to the richness of the sample). Each slide was counted twice and the reproducibility achieved was high (coefficient of variation: 10%).

Absolute abundance of nannofossils per gram of sediment was calculated using the formula:

$$X = (N.V)/(M.A.H) \quad (1)$$

where X is the number of calcareous nannofossils per gram of sediment; N the number of nannofossils counted in each sample; V the volume of water used for the dilution in the settling device (cm^3); M the weight of powder used for the suspension (g); A the surface considered for nannofossil counting (cm^2); H the height of the water over the cover slide in the settling device (2.1 cm). Relative abundances (percentages) of nannofossil genera were also calculated from the total nannofossil content.

The calculation of fluxes permits to overcome the effects of a variable sedimentary dilution and to effectively compare data from different intervals in a time-series. The formula introduced by Davies et al. (1995) was first used to calculate the mass accumulation rates (MAR):

$$MAR = T. [BD-(P.W)] \quad (2)$$

where MAR is the mass accumulation rate ($g/m^2/yr$), T the sedimentation rate (m/yr), BD the wet bulk density (g/m^3), P the porosity (weight percent) and W the seawater density (1.025 g/cm^3).

Fluxes of nannofossils (specimens/m^2/yr) were then obtained by multiplying the MAR with nannofossil abundances (specimens/g sediment).

Scanning electron microscope (SEM) images were taken using a field emission electron microscope Zeiss Supra35VP, equipped with detectors for secondary and back-scattered electrons.

3. Taxonomy used for the Noelaerhabdaceae

The taxonomy used to distinguish the different species within the Noelaerhabdaceae is somewhat arbitrary, since it is primarily based on the coccolith size (Young, 1998). The differentiation at the genus level of the three genera of the Noelaerhabdaceae (*Reticulofenestra*, *Dictyococcites* and *Cyclicargolithus*) is also subject to discussion. *Dictyococcites* is often considered as a junior synonym of *Reticulofenestra* and the two genera are grouped either as reticulofenestrids (e.g., Henderiks and Pagani, 2007; Henderiks, 2008) or more simply as *Reticulofenestra* (e.g., Young, 1998; Bolton et al., 2010). Nevertheless, *Cyclicargolithus* represents a very characteristic genus easily distinguishable from other reticulofenestrids due to its distinct shape (see Plate 3-1). In the present study, *Dictyococcites*, *Reticulofenestra* and *Cyclicargolithus* were distinguished on the basis of distinctive morphological features (see taxonomic remarks) and abundance variations are presented at the genus level to establish the broad-scale patterns and facilitate a first-order comparison between the investigated sites. Relative variations in size-defined morphospecies (see taxonomic remarks), as well as previously published biometric datasets on *Reticulofenestra*, *Dictyococcites* and *Cyclicargolithus* (Henderiks and Pagani, 2007; Plancq et al., 2012) at Site 516, further confirm our hypotheses of the long-term turnover within this prominent fossil group.

4. Results

Mean absolute abundances of nannofossils at DSDP Sites 608, 516 and 588 are of the same order of magnitude ($4.2x10^9$, $5.0x10^9$ and $5.4x10^9$ nannofossils/g of sediment, respectively) and do not show any significant stratigraphic trend across the late Oligocene-early Miocene (data not shown). Delicate coccoliths that are prone to dissolution, such as *Syracosphaera* and *Pontosphaera*, are observed with pristine structures in all the samples investigated by light microscopy, indicating a good state of preservation of coccoliths at the three sites. Preservation of small coccoliths is also good, and coccospheres are commonly recorded (Plate 3-1). Observed coccolith assemblages are systematically dominated by four genera, which together account for more than 80% of the total nannofossil assemblage: *Reticulofenestra*, *Dictyococcites*, *Cyclicargolithus* (all belonging to the Noelaerhabdaceae), and *Coccolithus*

(Figs. 3-2, 3-3 and 3-4). These taxonomic groups are present throughout the investigated time interval. The same morphospecies occur at all three sites. In particular, *C. floridanus*, *R. pseudoumbilicus*, *R. minutula*, *R. haqii*, *R. minuta*, *D. antarcticus*, *D. hesslandii*, *Dictyococcites* smaller than 3 µm constitute on average more than 80% of the total nannofossil assemblage. Light microscopy and scanning electron microscopy (Plate 3-1) attest for a good preservation of Noelaerhabdaceae coccoliths.

Remarkably, for each genus of the Noelaerhabdaceae, relative abundances and fluxes show comparable temporal and quantitative variations at all sites (Figs. 3-2 and 3-3). *Cyclicargolithus* represents on average 27% of the total nannofossil assemblage before 20 Ma whereas it shows a sharp decrease in abundance (7% of the total nannofossil assemblage) after 20 Ma. *Dictyococcites* shows significant quantitative variations throughout the studied time interval. Two peaks of maximum abundances are observed between 25 and 23 Ma and between 20 and 18 Ma (36% of the total nannofossil assemblage), whereas two sharp decreases are observed between 23 and 21.5 Ma (28%) and after 18 Ma (18%). These variations are less obvious at Site 608, where no maximum is observed between 25 and 23 Ma, likely due to a lower resolution sampling during this period (Fig. 3-2). Finally, *Reticulofenestra* represents ca. 12% of the total nannofossil assemblage before 20 Ma but shows a progressive increase in abundance thereafter (29.5%), reaching more than 30% of the total nannofossil assemblage around 17 Ma.

Unlike Noelaerhabdaceae, abundances of *Coccolithus, Helicosphaera* and of the nannoliths *Sphenolithus* and *Discoaster* show distinct variations between the Atlantic and the Pacific oceans (Fig. 3-4). At both Atlantic sites, *Coccolithus* abundance is relatively constant (14.6% of the total nannofossil assemblage, for Site 516; 25% of the total nannofossil assemblage, for Site 608) but shows a peak in abundance (36.5% for Site 516 and 46.6% for Site 608) between 20.5 and 18.5 Ma. The abundance of *Sphenolithus* is also relatively constant throughout the studied time interval (2% for Site 516; 8% for Site 608), and only shows a peak at ca. 17 Ma. This peak is less prominent at Site 516 (9.6%) than at Site 608 (21%). In the South-West Pacific (Site 588), *Coccolithus* is present in smaller proportions (10%) compared to both Atlantic sites (Fig. 3-4). Two small peaks of *Coccolithus* are observed at 20.2 Ma (17.8%) and at 18.4 Ma (20.7%) while the abundance of *Sphenolithus* shows no clear stratigraphic trend. The abundance of *Discoaster* is relatively constant throughout the studied time interval (5%), and only shows a peak (26%) at ca. 19 Ma at DSDP Site 608. *Helicosphaera* shows low abundances (1.4%) and no peculiar stratigraphic trend (Fig. 3-4).

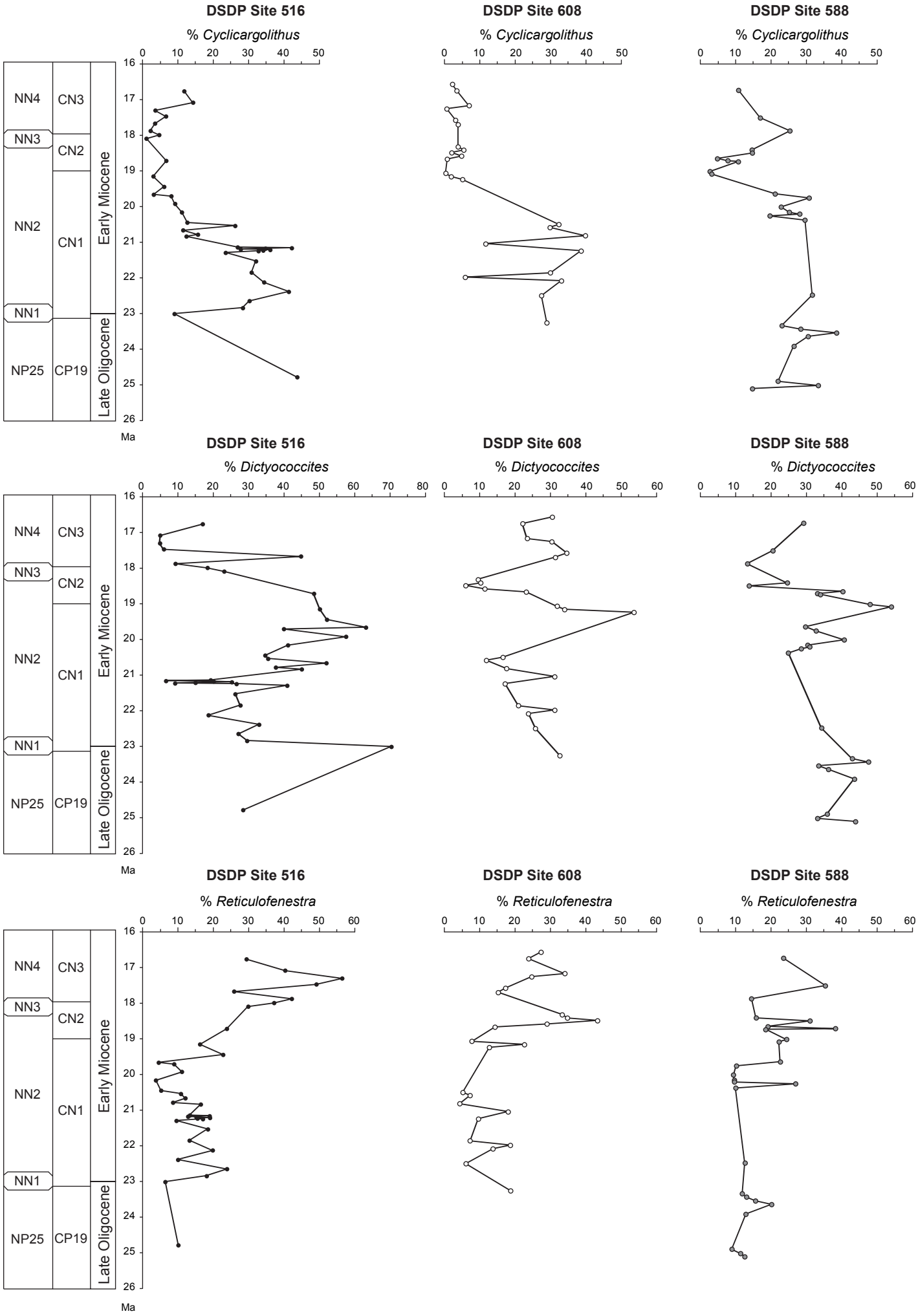

Figure 3-2. Relative (%) abundances of the Noelaerhabdaceae genera (*Cyclicargolithus*, *Dictyococcites* and *Reticulofenestra*) during the late Oligocene-early Miocene for each studied sites. Nannofossil zonations of Martini (1971) and of Okada and Bukry (1980) are reported.

When considering relative abundances of different morphospecies within the Noelaerhabdaceae (Fig. 3-5), which represents on average more than 80% of the total nannofossil assemblage, a distinct pattern of succession of prominent taxa occurs. Namely, *Cyclicargolithus floridanus* (which is dominant with respect to *C. abisectus* showing average relative abundances lower than 2%) is very abundant in the three studied sites before 20 Ma, with relative abundance fluctuations around 30%. It then fluctuates but shows generally values lower than 10%. *Reticulofenestra minuta* and *Dictyococcites* spp. (smaller than 3 μm) also show some of the highest values of relative abundance in the interval between 26 and 20 Ma, although a slightly different pattern is observed at the three sites. In the interval between 20 and 18.7 Ma, the morphospecies of intermediate size, namely *R. minutula* and *D. hesslandii* did emerge as well as *D. antarcticus*. Finally, in the interval between 18.7 and 16 Ma, the larger morphospecies (> 5 μm) *R. pseudoumbilicus* shows abundance peaks up to 30% of the Noelaerhabdaceae.

The assemblage data for Site 516 are in agreement with those reported by Henderiks and Pagani (2007), although the apparent timing in assemblage shifts is slightly different due to different sample spacing in the two studies. Also, the biometric data of Henderiks and Pagani (2007) and Plancq et al. (2012) for DSDP Site 516 show an increase in size in the reticulofenestrids that is in agreement with the morphospecies shifts we observe in the three sites.

5. Discussion

Similar variations in Noelaerhabdaceae abundances are observed during the late Oligocene-early Miocene in the South and North Atlantic and in the South-West Pacific (DSDP Sites 516, 608 and 588, respectively). At the three sites, nannofossil assemblages are successively characterized by high abundances of *Cyclicargolithus* between 26 and 20 Ma, *Dictyococcites* between 20 and 18.7 Ma, and *Reticulofenestra* afterwards (Fig. 3-5). Within each genus, the number of morphospecies and their relative abundances have varied over time and, to a lesser extent, between regions. We will first discuss our results at genus level and eventually we will discuss different-sized morphospecies changes.

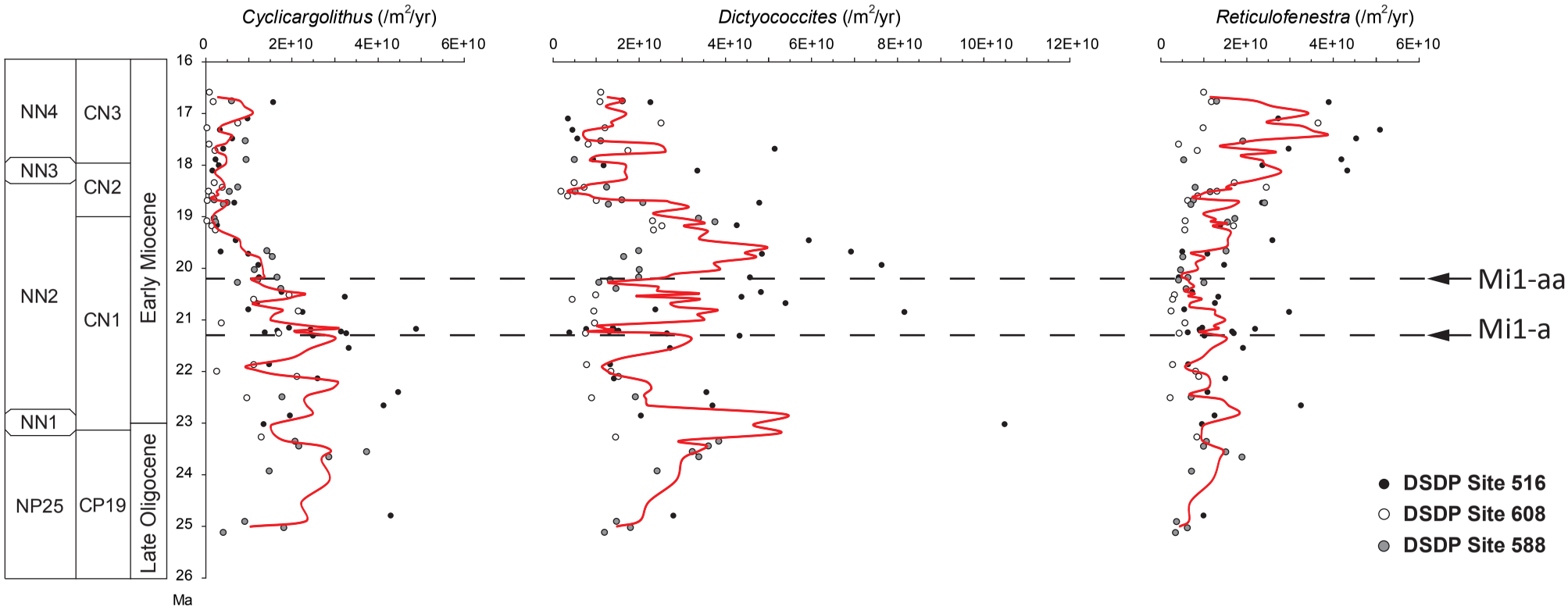

Figure 3-3. Fluxes (coccoliths/m^2/yr) of the Noelaerhabdaceae genera (*Cyclicargolithus*, *Dictyococcites* and *Reticulofenestra*) during the late Oligocene-early Miocene. Trend curves are 3-points moving average through combined data from all three investigated sites. The glacial Mi-1a and Mi-1aa events (dashed lines) are also reported (Pagani et al., 2000; Pekar and DeConto, 2006).

5.1. Changes in local paleoceanography and in calcareous nannofossil assemblages

The abundance changes within the Noelaerhabdaceae may represent distinct ecological responses of the different genera and species to local paleoceanographic changes. Although ecological preferences of Neogene nannofossils are poorly understood especially for the Miocene, some hypotheses have been developed on the grounds of distribution patterns and statistical tests (e.g., Wei and Wise, 1990; Kameo and Sato, 2000; Monechi et al., 2000).

Henderiks and Pagani (2007) already discussed shifts in nannofossil assemblages at DSDP Site 516 (Southern Atlantic) in response to paleoceanographic changes inferred from oxygen isotopic ($\delta^{18}O$) values of foraminiferal tests and carbon isotopic ($\delta^{13}C$) compositions of diunsaturated C_{37} alkenones (Pagani et al., 2000). The influx of warm, low-nutrient surface waters from low latitudes may explain the decrease in *Cyclicargolithus* abundance between ~21 and 20.5 Ma. This is consistent with the inferred ecological preference of this taxon, which was apparently more abundant in mid paleo-latitudes (e.g., Wei and Wise, 1990) and showed affinities for high-nutrient conditions (Monechi et al., 2000).

At ~20.3 Ma, the input of cold, nutrient-rich waters, induced an increased productivity of *Coccolithus*, and the subsequent prominence of *Dictyococcites* (Figs. 3-2, 3-3 and 3-4). An abundance increase of the genus *Dictyococcites* supports the presence of cold-water masses (Haq, 1980; Pujos, 1985; Kameo and Sato, 2000) during that time. *Coccolithus* is documented to thrive at mid- and high-latitudes in both modern and ancient settings (Wei and Wise, 1990; Wells and Okada, 1997; Cachão and Moita, 2000). This input of cold water has been interpreted as a consequence of the opening of the Drake Passage to deeper-water resulting in an intensification of the Antarctic Circumpolar Current (ACC), and a northward progression of the Polar Frontal Zone (PFZ) (Barker and Burrell, 1977; Pagani et al., 2000). However, the opening of the Drake Passage and a rapid deepening of the ACC may have occurred in the late Eocene, at about 39-37 Ma (Scher and Martin, 2006; Livermore et al., 2007; Cramer et al., 2009). In addition, Lagabrielle et al. (2009) have suggested a short-term closure of the Drake Passage in the late Oligocene.

Following the cooling event, a re-establishment of surface water stratification (with warmer waters) then induced the decline of *Dictyococcites* coupled to an increase of *Reticulofenestra* and *Sphenolithus* (Figs. 3-2, 3-3 and 3-4) after 19.5 Ma. The *Reticulofenestra* spp. were more abundant at mid-to-high paleo-latitudes and were likely characteristic of mesotrophic, temperate water masses, while *Sphenolithus* appears to have been characteristic

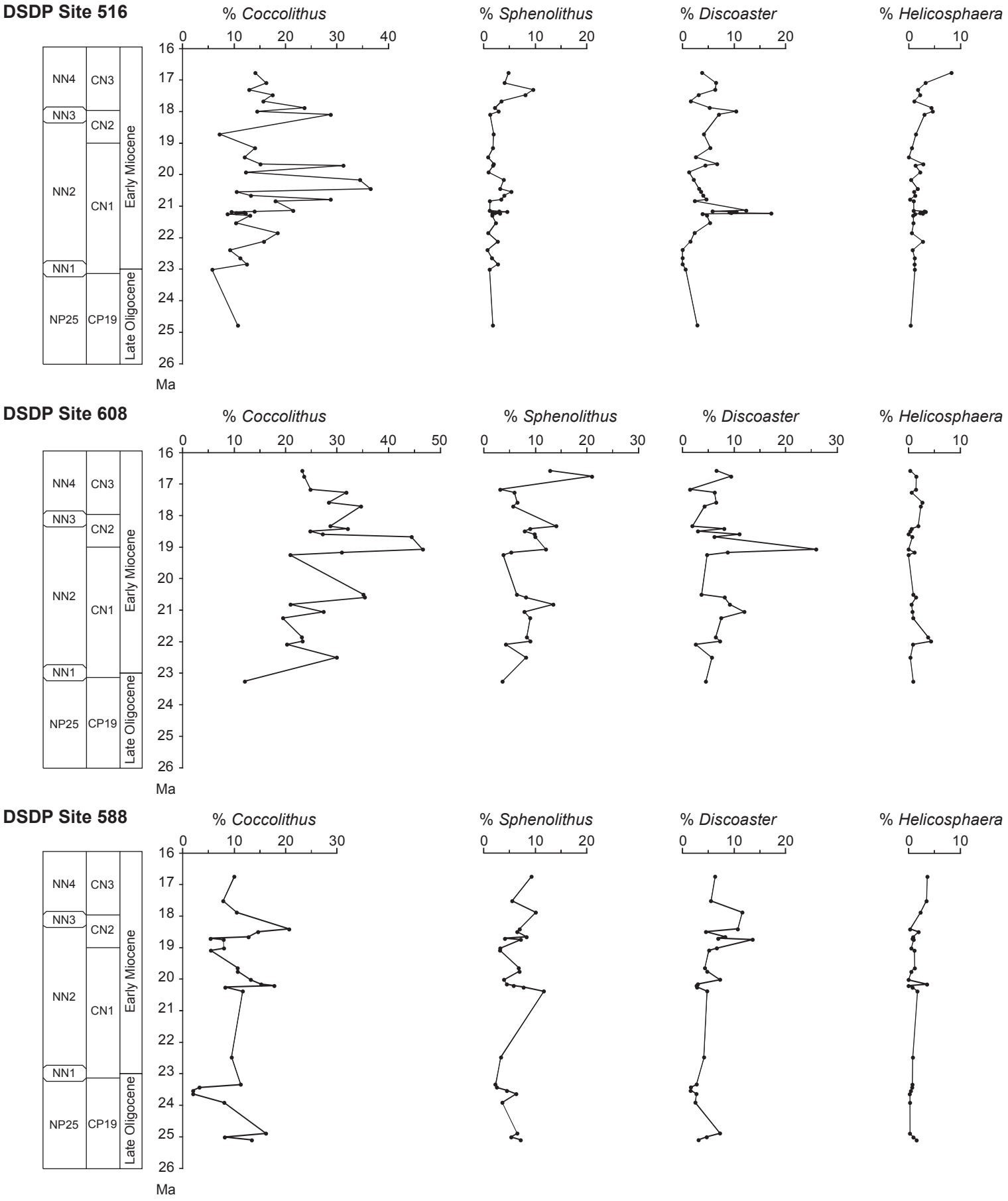

Figure 3-4. Relative (%) abundances of *Coccolithus*, *Helicosphaera* and of the nannoliths *Sphenolithus* and *Discoaste*r at DSDP Sites 516, 608 and 588 during the late Oligocene-early Miocene.

of warm/oligotrophic paleo-environments (e.g., Wei and Wise, 1990; Persico and Villa, 2004; Villa et al., 2008).

Noelaerhabdaceae assemblage shifts observed in the North Atlantic (DSDP Site 608) and the South-West Pacific (DSDP Site 588) are remarkably similar to those observed at Site 516, with a prominent decrease in *C. floridanus* proportions occurring at 20 Ma and the parallel increase in some medium- and large-size reticulofenestrids (Fig. 3-5). However, DSDP Site 608 is located at low latitudes in the Northern Hemisphere, in a paleoceanographic setting far-removed from the AAC and from the PFZ, and paleoceanographic conditions at the Pacific Site 588 should have been particularly different from the two Atlantic sites during the studied time interval as suggested by the different trends observed in *Coccolithus* and *Sphenolithus* abundances (Fig. 3-4). Thus, the Noelaerhabdaceae variation pattern observed at the three sites cannot be explained by regional paleoceanographic changes alone.

5.2. Changes in climate and in calcareous nannofossil assemblages

The decline of *Cyclicargolithus* around 20 Ma (Figs. 3-2, 3-3 and 3-5) may correspond to a more global feature. Haq (1980) did observe a similar feature in the Atlantic Ocean, with a decrease in *Cyclicargolithus* assemblage between 22.5 and 18 Ma. The successive dominance of *Cyclicargolithus* and *Reticulofenestra*/*Dictyococcites* may represent a passive ecological replacement in communities in response to a global shift in climate during the late Oligocene-early Miocene. The major decline of *Cyclicargolithus* would have allowed the expansion (and possibly diversification, see below) of *Reticulofenestra*/*Dictyococcites* into its vacant ecological niche, explaining the dominance of these species from 20 Ma onwards (Figs. 3-2, 3-3 and 3-5).

Several Antarctic glaciations, called “Oi-2” and “Mi-1” events, occurred during the late Oligocene to early Miocene period as attested by excursions in $\delta^{18}O$ values of benthic foraminifers (e.g., Miller et al., 1991; Wright and Miller, 1992). Interestingly, and despite the limited temporal resolution of the present study, the onset of the decline of *Cyclicargolithus* appears to have coincided with Mi-1a and Mi-1aa glacial events (Fig. 3-3) that occurred at about 21.3 and 20.2 Ma respectively (as shown by a ~0.5 ‰ increase in $\delta^{18}O$ values of benthic foraminifers; Wright and Miller, 1992; Paul et al., 2000; Billups et al., 2002; Pekar and DeConto, 2006). The onset of such events could have changed the oceanic circulation and surface water characteristics influencing the ecology and thus composition of the nannofossil assemblages. For example, at DSDP Site 516, Pagani et al. (2000) hypothesized that the Mi-1a event led to an intensification of gyre circulation in South Atlantic and thus to a higher

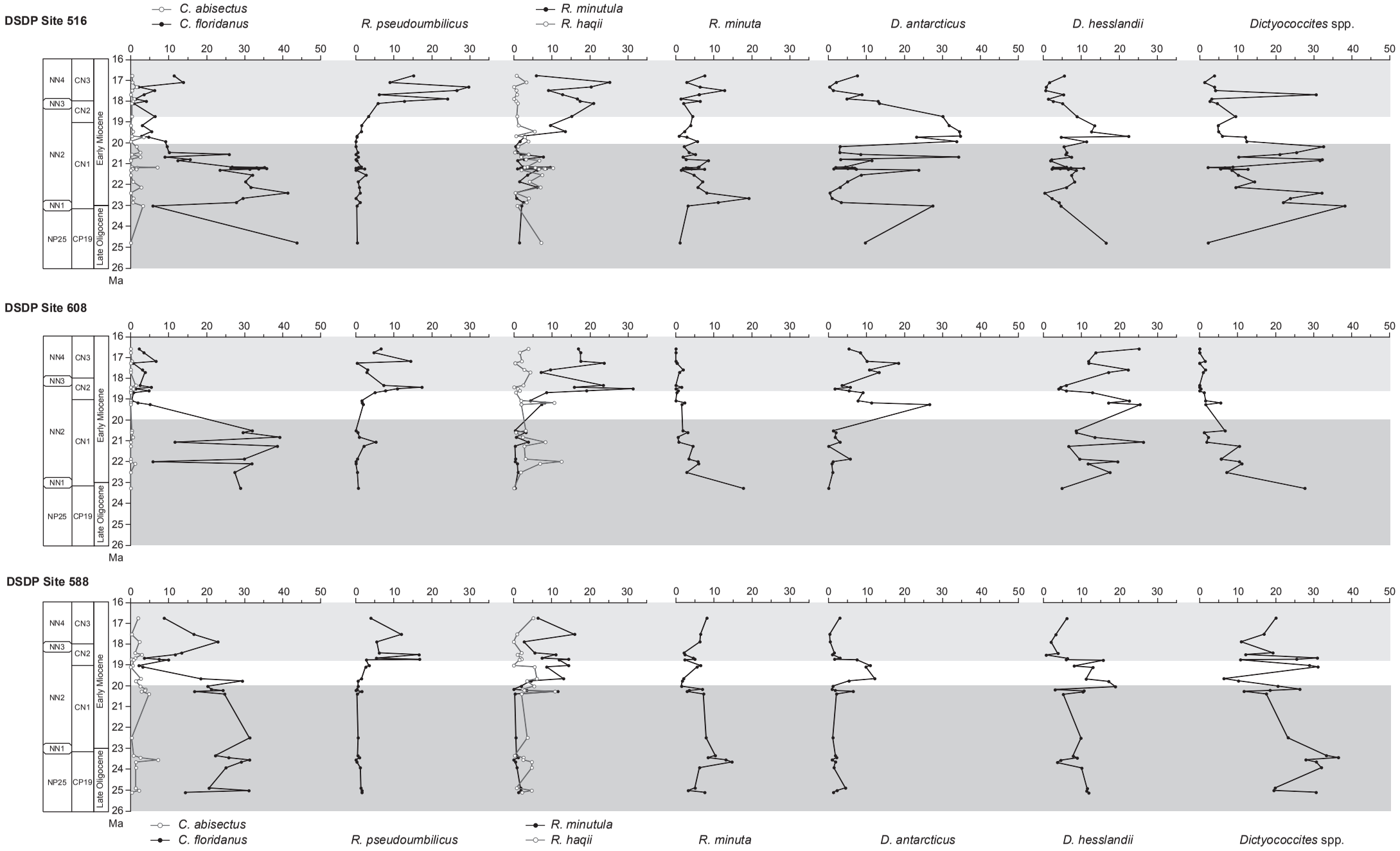

Figure 3-5. Relative abundances (%) of the different species within the Noelaerhabdaceae at DSDP Sites 516, 608 and 588 during the late Oligocene-early Miocene. Gray colors indicate different time intervals in which, although small differences are observed between the three sites, concomitant changes in the relative abundance of species occur.

influx of warm, low-nutrient waters from lower latitudes, which may have triggered the decline of *Cyclicargolithus* observed at this site. The Mi-1a event is recorded in $\delta^{18}O$ data at DSDP Sites 608 and 588 (Kennett, 1985; Woodruff and Savin, 1989; Wright et al., 1992; Norris et al., 1994), but evidence is lacking for a global change in oceanic circulation that could have affected the paleoceanography of the North Atlantic and South-West Pacific. Peculiar orbital configuration (high-amplitude variability in obliquity) coupled to variability in atmospheric carbon dioxide may explain the onset of Mi-1 events (e.g. Zachos et al., 2001b; Pälike et al., 2006). For example, the Mi-1a event may have accounted for a ~50 ppmv decrease in partial pressure of atmospheric carbon dioxide (pCO_2) as recorded in the ^{13}C content of alkenones at DSDP Sites 516, 588 and 608 (Pagani et al., 1999, 2000) and, at a more global scale, by stomatal frequency data (stomatal index) from multiple tree species (Kürschner et al., 2008). Atmospheric CO_2 is believed to have a strong influence on the long-term climate evolution. Nevertheless, considering the error propagation of the available proxies, atmospheric CO_2 concentrations are actually surprisingly stable during the Miocene and it seems difficult to relate a global shift in climate with an apparent small fluctuation in pCO_2 (Pagani et al., 1999, 2000). This remains puzzling and debated in light of the climatic and ecological events that occurred during the Miocene (e.g., Pagani, 2002; Pagani et al., 2009; LaRiviere et al., 2012).

Supplementary evidence is thus needed to support the hypothesis that the global turnover in Noelaerhabdaceae assemblages is linked to a global climatic change (variations in oceanic circulation and/or influence of atmospheric pCO_2).

5.3. Changes within the Noelaerhabdaceae

Alternatively, the successive dominance of *Cyclicargolithus* and *Reticulofenestra*/*Dictyococcites* could be the result of other selection pressures within the phytoplankton communities. The Oligocene-Miocene transition is characterized by an important turnover in nannofossils assemblages, notably within the Noelaerhabdaceae with the last occurrence of *Reticulofenestra bisecta* (Okada and Bukry, 1980; Berggren et al., 1985; Young, 1998). Climatic perturbations could have sped up the race for being the fittest species and the steady increase in abundance of *Reticulofenestra*/*Dictyococcites* might be the effect of an active competition between the two groups (*Cyclicargolithus*, mainly *C. floridanus*, and *Reticulofenestra*/*Dictyococcites*) rather than a passive exploitation by these species of the ecological niche made vacant because of the decrease of *Cyclicargolithus*. Biometry data suggests a distinct diversification in *Reticulofenestra*/*Dictyococcites* after 20

Ma at Site 516 (Henderiks and Pagani, 2007; Plancq et al., 2012). Our results show that, in the three studied sites after 20 Ma, there is an increase in the relative abundance of morphospecies of intermediate and large size that mirrors the decline in *C. floridanus* (Fig. 3-5). This increase in abundance of large morphospecies of *Reticulofenestra*/*Dictyococcites* that became more prominent with time may correspond to a cryptic speciation within the group. In fact, minor size differences can characterize cryptic species in modern coccolithophores (for a synthesis, see Geisen et al., 2004). Interestingly, such a succession in species dominance has been observed within other members of the Noelaerhabdaceae family, in particular within the *Gephyrocapsa* complex during the Quaternary, whose biometric changes have been interpreted in terms of evolutionary adaptation for lack of a clear linkage to concurrent changes in climate and/or preservation (e.g., Matsuoka and Okada, 1989; 1990; Bollmann et al., 1998). A diversification in *Reticulofenestra*/*Dictyococcites* may have induced the steady decline (occurring over ~1 Ma; Fig. 3-5) of *Cyclicargolithus floridanus*, although this taxon maintained competitive populations until its extinction occurring 8 Myr later (last occurrence at 11.85 Ma; Gradstein et al., 2012).

6. Conclusion

Similar relative and absolute abundance variations in Noelaerhabdaceae assemblages are observed during the late Oligocene-early Miocene at different latitudes of Atlantic and Pacific oceans, with the successive prominence of *Cyclicargolithus floridanus*, *Dictyococcites antarcticus*/*D. hesslandii*, and *Reticulofenestra minutula/R. pseudoumbilicus*. We explored the paleoenvironmental factors that may have triggered the observed assemblage turnover, in spite of a poor knowledge of ecological preferences of the Oligocene-Miocene species/genera and of the rather arbitrary, size-defined taxonomy of the Noelaerhabdaceae family. The decline of *Cyclicargolithus* recorded at the three studied sites may correspond to a global climatic shift (variations in oceanic circulation or influence and/or atmospheric pCO_2) eventually coupled to variations in local paleoceanographic conditions. The subsequent dominance of *Reticulofenestra*/*Dictyococcites* in assemblages from 20 Ma is paired with a diversification in sizes, and may be the result of an evolutionary process such as competition between the two groups (*Cyclicargolithus* and *Reticulofenestra*/*Dictyococcites*. The present study confirms that changes in nannofossil assemblages are a good proxy for the reconstruction of global evolutionary patterns that may be related to paleoenvironmental

changes. However, morphospecies biometry and paleoceanographic studies at higher temporal resolution, depicting both paleoecological and evolutionary patterns, will be needed to reinforce the presented hypotheses for the global shifts in Noelaerhabdaceae assemblages.

Acknowledgements

We would like to thank Jeremy Young and Giuliana Villa for their constructive comments and critical review. This study used Deep Sea Drilling Project samples provided by the Integrated Ocean Drilling Program. We thank the curators from the Bremen Core Repository and the Kochi Core Center for their efficiency. Yannick Donnadieu (LSCE, France) is kindly acknowledged for stimulating discussions.

References

Backman, J., 1980. Miocene-Pliocene nannofossils and sedimentation rates in the Hatton-Rockall Basin, NE Atlantic Ocean. Stockholm Contributions in Geology 36, 1-91.

Barker, P.F., Burrell, J., 1977. The opening of the Drake Passage. Marine Geology 25, 15–34.

Barker P.F., Carlson, R.L., Johnson, D.A., the Shipboard Scientific Party, 1983. Site 516: Rio Grande Rise. Initial Rep. Deep Sea Drill. Proj. 72, 155-338, doi:10.2973/dsdp.proc.72.105.

Barker, P.F., Thomas, E., 2004. Origin, signature and palaeoclimatic influence of the Antarctic circumpolar current. Earth Science Reviews 66, 143-162.

Barker, S., Archer, D., Booth, L., Elderfield, H., Henderiks, J., Rickaby, R.E.M., 2006. Globally increased pelagic carbonate production during the Mid-Brunhes dissolution interval and the CO_2 paradox of MIS 11. Quaternary Science Reviews 25, 3278-3293.

Baumann, K-H., Freitag, T., 2004. Pleistocene fluctuations in the northern Benguela Current system as revealed by coccolith assemblages. Marine Micropaleontology 52, 195-215.

Beaufort, L., 1991. Adaptation of the random settling method for quantitative studies of calcareous nannofossils. Micropaleontology 37, 415–418.

Belkin, I.M., Gordon, A.L., 1996. Southern Ocean fronts from the Greenwich meridian to Tasmania. Journal of Geophysical Research 101, 3675– 3696.

Berggren, W.A., Kent, D.V., Flynn, J., Van Couvering, J.A., 1985. Cenozoic geochronology. Geological Society of America Bulletin 96, 1407–1418.

Billups, K., Channell, J.E.T., Zachos, J., 2002. Late Oligocene to early Miocene geochronology and paleoceanography from the subantarctic South Atlantic. Paleoceanography 17 (1), 1004, doi:10.1029/2000PA000568.

Bollmann, J., Baumann , K.H., Thierstein, H.R., 1998. Global dominance of *Gephyrocapsa* coccoliths in the late Pleistocene: selective dissolution, evolution, or global environmental change? Paleoceanography 13, 517-529.

Bolton, C.T., Lawrence, K.T., Gibbs, S.J., Wilson, P.A., Cleaveland, L.C., Timothy, D., Herbert, T.D., 2010. Glacial-interglacial productivity changes recorded by alkenones and microfossils in late Pliocene eastern equatorial Pacific and Atlantic upwelling zones. Earth and Planetary Science Letters 295, 401-411.

Bukry, D., 1971. Cenozoic calcareous nannofossils from the Pacific Ocean. Transactions of the San Diego Society of Natural History 16, 303-327.

Cachão, M., Moita, M.T., 2000. *Coccolithus pelagicus*, a productivity proxy related to moderate fronts off Western Iberia. Marine Micropaleontology 39, 131– 155.

Clement, B.M., Robinson, F., 1987. The magnetostratigraphy of Leg 94 sediments. Initial Reports of Deep Sea Drilling Project 94, 635-650.

Cramer, B.S., Toggweiler, J.R., Wright, J.D., Katz, M.E., Miller, K.G., 2009. Ocean overturning since the Late Cretaceous : inferences from a new benthic foraminiferal isotope compilation. Paleoceanography 24, doi: 10.1029/2008PA001683.

Davies, T.A., Kidd, R.B., Ramsay-Anthony, T.S., 1995. A time-slice approach to the history of Cenozoic sedimentation in the Indian Ocean. In: T.A. Davies, M.F. Coffin, and S.W. Wise (Eds.), Selected Topics Relating to the Indian Ocean Basins and Margins, Sedimentary Geology 96, 157–179.

Flores, J.A., Marino, M., 2002. Pleistocene calcareous nannofossil stratigraphy for ODP Leg 177 (Atlantic sector of the Southern Ocean). Marine Micropaleontology 45, 191–224.

Flores, J.A., Marino, M., Sierro, F.J., Hodell, D.A., Charles, C.D., 2003. Calcareous plankton dissolution pattern and coccolithophore assemblages during the last 600 kyr at ODP Site 1089 (Cape Basin, South Atlantic): paleoceanographic implications. Paleogeography, Paleoclimatology, Paleoecology 196, 409-426.

Flower, B.P., Kennett, J.P., 1993. Middle Miocene ocean–climate transition: high resolution oxygen and carbon isotopic records from DSDP Site 588A, southwest Pacific. Paleoceanography 8, 811–843.

Gartner, S., 1992. Miocene nannofossil chronomogy in the North Atlantic, DSDP Site 608. Marine Micropaleontology 18, 307-331.

Geisen, M., Bollmann, J., Herrle, J.O., Mutterlose, J., Young, J.R., 1999. Calibration of the random settling technique for calculation of absolute abundance of calcareous nannoplankton. Micropaleontology 45 (4), 437-442.

Geisen, M., Young, J.R., Probert, I., Saez, A.G., Baumann, K.-H., Bollmann, J., Cros, L., de Vargas, C., Medlin, L.K., Sprengel, C., 2004. Species level variations in coccolithophores. In: H.R. Thierstein, and J.R. Young (Eds.), Coccolithophores, from molecular processes to global impact, Springer, 327-367 pp.

Gradstein, F.M., Ogg, J.G., Schmitz, M., Ogg, G., 2012. The Geologic Time Scale 2012. Elsevier, 1176 pp.

Haq, B.U., 1976. Coccoliths in cores from the Bellinghausen abyssal plain and Antarctic continental rise (DSDP Leg 35). Initial Reports of Deep Sea Drilling Project 35, 557-567.

Haq, B.U., 1980. Biogeographic history of Miocene calcareous nannoplankton and paleoceanography of the Atlantic Ocean. Micropaleontology 26 (4), 414-443.

Henderiks, J., 2008. Coccolithophore size rules-reconstructing ancient cell geometry and cellular calcite quota from fossil coccoliths. Marine Micropaleontology 67, 143-154.

Henderiks, J., Pagani, M., 2007. Refining ancient carbon dioxide estimates: significance of coccolithophore cell size for alkenone-based pCO_2 records. Paleoceanography 22, PA3202, doi: 10.1029/2006PA001399.

Hodell, D.A.,Woodruff, F., 1994. Variations in the strontium isotopic ratio of seawater during the Miocene: stratigraphic and geochemical implications. Paleoceanography 9, 405-426.

Jordan, R.W., Cros, L., Young, J.R., 2004. A revised classification scheme for living haptophytes. Micropaleontology 50, 55-79.

Kameo, K., Sato, T., 2000. Biogeography of Neogene calcareous nannofossils in the Caribbean and the eastern equatorial Pacific-floral response to the emergence of the Isthmus of Panama. Marine Micropaleontology 39, 201-218.

Kennett, J.P., 1985. Miocene to early Pliocene oxygen and carbon isotope stratigraphy in the southwest Pacific, Deep Sea Drilling Project Leg 90. Initial Reports of Deep Sea Drilling Project 90, 1383-1411, doi:10.2973/dsdp.proc.90.142.

Kennett, J.P., von der Borch, C.C., the Shipboard Scientific Party, 1986. Site 588: Lord Howe Rise, 26°S. Initial Reports of Deep Sea Drilling Project 90, 139-252, doi:10.2973/dsdp.proc.90.104.

Kürschner, W.M., Kvaček, Z., Dilcher, D.L., 2008. The impact of Miocene atmospheric carbon dioxide fluctuations on climate and the evolution of terrestrial ecosystems. Proceedings of the National Academy of Science U.S.A. 105 (2), 449-453.

Lagabrielle, Y., Goddéris, Y., Donnadieu, Y., Malavieille, J., Suarez, M., 2009. The tectonic history of Drake Passage and its possible impacts on global climate. Earth and Planetary Science Letters 279, 197-211.

LaRiviere, J.P., Ravelo, A.C., Crimmins, A., Dekens, P.S., Ford, H.L., Lyle, M., Wara, M.W., 2012. Late Miocene decoupling of oceanic warmth and atmospheric carbon dioxide forcing. Nature 486, 97-100.

Livermore, R., Hillenbrand, C-D., Meredith, M., Eagles G., 2007. Drake Passage and Cenozoic climate: an open shut case? Geochemistry, Geophysics, Geosystems 8(1), doi: 10.1029/2005GC001224.

Lohman, W.H., 1986. Calcareous nannoplankton biostratigraphy of the southern Coral sea, Tasman Sea, and southwestern Pacific Ocean, Deep Sea Drilling Project Leg 90: Neogene and Quaternary. Initial Reports of Deep Sea Drilling Project 90, 763-793, doi:10.2973/dsdp.proc.90.112.

Martini, E., 1971. Standard Tertiary and Quaternary calcareous nannoplankton zonation. In: Farinacci, A. (Ed.), Proceedings of the second planktonic conference 2, 739-785 pp.

Matsuoka, H., Okada, H., 1989. Quantitative analysis of Quaternary nannoplankton in the subtropical northwestern Pacific Ocean. Marine Micropaleontology 14, 97-118.

Matsuoka, H., Okada, H., 1990. Time-progressive morphometrical changes of the genus *Gephyrocapsa* in the Quaternary sequence of the tropical Indian Ocean, Site 709. In: Duncan, R.A., Backman, J., Peterson, L.C. et al. (Eds.), Proceedings of the Ocean Drilling Program Scientific Results 115, 255-270.

McIntyre, A., Bé, A.W.H., 1967. Modern coccolithophores of the Atlantic Ocean-I. Placolith and cyrtoliths. Deep-Sea Research 14, 561-597.

Miller, K.G., Wright, J.D., Fairbanks, R.G., 1991. Unlocking the ice house: Oligocene to Miocene oxygen isotopes, eustasy, and margin erosion. Journal of Geophysical Research 96, 6829-6848.

Miller, K.G., Mountain, G.S., and Leg 150 Shipboard Party and Members of the New Jersey Coastal Plan Drilling Project, 1996. Drilling and dating New Jersey Oligocene-Miocene sequences: ice volume, global sea level, and EXXON records. Science 271, 1092-1095.

Monechi, S., Buccianti, A., Gardin, S., 2000. Biotic signals from nannoflora across the iridium anomaly in the upper Eocene of the Massignano section: evidence from statistical analysis. Marine Micropaleontology 39, 219-237.

Norris, R.D., Corfield, R.M., Cartlidge, J.E., 1994. Evolutionary ecology of *Globorotalia* (*Globoconella*) (planktic foraminifera). Marine Micropaleontology 23, 121-145.

Okada, H., Bukry, D., 1980. Supplementary modification and introduction of code numbers to the low-latitude coccolith biostratigraphic zonation (Bukry, 1973; 1975). Marine Micropaleontology 5, 321-325.

Okada, H., Honjo, S., 1973. The distribution of oceanic coccolithophorids in the Pacific. Deep-Sea Research 20, 335–374.

Olafsson, G., 1989. Quantitative calcareous nannofossil biostratigraphy of upper Oligocene to middle Miocene sediment from ODP Hole 667A and middle Miocene sediment from DSDP site 574. Proceedings of the Ocean Drilling Program Scientific Results 108, 9-22.

Pagani, M., 2002. The alkenone-CO_2 proxy and ancient atmospheric carbon dioxide. Philosophical Transactions of the Royal Society A 360, 609-632.

Pagani, M., Arthur, M.A., Freeman, K.H., 1999. Miocene evolution of atmospheric carbon dioxide. Paleoceanography 14 (3), 273-292.

Pagani, M., Arthur, M.A., Freeman, K.H., 2000. Variations in Miocene phytoplankton growth rates in the southwest Atlantic: evidence for changes in ocean circulation. Paleoceanography 15, 486-496.

Pagani, M., Caldeira, K., Berner, R., Beerling, D.J., 2009. The role of terrestrial plants in limiting atmospheric CO_2 decline over the past 24 million years. Nature 460, 85-89.

Pälike, H., Frazier, J., Zachos, J.C., 2006. Orbitally forced palaeoclimatic records from the equatorial Atlantic Ceara Rise. Quaternary Science Reviews 25, 3138-3149.

Paul, H.A., Zachos, J.C., Flower, B.P., Tripati, A., 2000. Orbitally induced climate and geochemical variability across the Oligocene/Miocene boundary. Paleoceanography 15, 471-485.

Pekar, S.F., DeConto, R.M., 2006. High-resolution ice-volume estimates for the early Miocene: evidence for a dynamic ice sheet in Antarctica. Palaeogeography, Palaeoclimatology, Palaeoecology 231, 101-109.

Persico, D., Villa, G., 2004. Eocene–Oligocene calcareous nannofossils from Maud Rise and Kerguelen Plateau (Antarctica): paleoecological and paleoceanographic implications. Marine Micropaleontology 52, 153-179.

Plancq, J., Grossi, V., Henderiks, J., Simon, L., Mattioli, E., 2012. Alkenone producers during late Oligocene-early Miocene revisited. Paleoceanography 27, PA1202, doi: 10.1029/2011PA002164.

Pujos, A., 1985. Late Eocene to Pleistocene medium-sized and small-sized Reticulofenestrids. In: H. Stradner, and K. Perch-Nielsen (Eds.), Proc. INA meeting, Vienna 1985, Abhandlungen der Geologischen Bundesanstalt 39, 239–277.

Rost, B., Riebesell, U., 2004. Coccolithophores and the biological pump: responses to environmental changes. In: H.R. Thierstein, and J.R. Young (Eds), Coccolithophores – From Molecular Processes to Global Impact, Springer, New York, 76-99.

Ruddiman, W.F., Kidd, R.B., Thomas, E., the Shipboard Scientific Party, 1987. Site 608. Initial Reports of Deep Sea Drilling Project 94, 149-246, doi:10.2973/dsdp.proc.94.104.

Scher, H.D., Martin, E.E., 2006. Timing and climatic consequences of the opening of Drake Passage. Science 312, 428-430.

Takayama, T., Sato, T., 1987. Coccolith biostratigraphy of the North Atlantic Ocean, Deep Sea Drilling Project Leg 94. Initial Reports of Deep Sea Drilling Project 94, 651-702, doi:10.2973/dsdp.proc.94.113.

Theodoridis, S.A., 1984. Calcareous nannofossil biozonation of the Miocene and revision of the helicoliths and discoasters. Utrecht Micropaleontological Bulletins 32, 32-271.

Thierstein, H.R., Geitzenauer, K.R., Molfino, B., Shackleton, N.J., 1977. Global synchroneity of late Quaternary coccolith datum levels: Validation by oxygen isotopes. Geology 5, 400-404.

Villa, G., Fioroni, C., Pea, L., Bohaty, S., Persico, D., 2008. Middle Eocene–late Oligocene climate variability: Calcareous nannofossil response at Kerguelen Plateau, Site 748. Marine Micropaleontology 69, 173-192.

von der Heydt, A., Dijkstra, H.A., 2006. Effect of ocean gateways on the global ocean circulation in the late Oligocene and early Miocene. Paleoceanography 21, PA10111, doi:10.1029/2005PA001149.

Wei, W., Wise, S.W., 1989. Paleogene calcareous nannofossils magnetobiochronology: results from South Atlantic DSDP Site 516. Marine Micropaleontology 14, 119-152.

Wei, W., Wise, S.W., 1990. Biogeographic gradients of middle Eocene-Oligocene calcareous nannoplankton in the South Atlantic Ocean. Palaeogeography, Palaeoclimatology, Palaeoecology 79, 29-61.

Wells, P., Okada, H., 1997. Response of nannoplankton to major changes in sea-surface temperature and movements of hydrological fronts over Site DSDP 594 (south Chatham Rise, southeastern New Zeland), during the last 130 Kyr. Marine Micropaleontology. 32, 341–363.

Winter, A., Siesser, W., 1994. Coccolithophores. Cambridge University Press, Cambridge, 242 pp.

Woodruff, F., Savin, S.M., 1989. Miocene deep water oceanography. Paleoceanography 4, 87-140.

Wright, J.D., Miller, K.G., 1992. Miocene stable isotope stratigraphy, site 747, Kerguelen Plateau. Proceedings of the Ocean Drilling Program Scientific Results 120, 855-866.

Wright, J.D., Miller, K.G., Fairbanks, R.G., 1992. Early and middle Miocene stable isotopes: implications for deepwater circulation and climate. Paleoceanography 7, 357-389.

Young, J.R., 1990. Size variation of Neogene *Reticulofenestra* coccoliths from Indian Ocean DSDP cores. Journal of Micropaleontology 9, 71-86.

Young, J.R., 1998. Neogene. In: P.R. Bown (Ed.), Calcareous Nannofossil Biostratigraphy. Chapman and Hall, Cambridge, U.K, pp. 225-265.

Young, J.R., Bown, P.R., 1997. Cenozoic calcareous nannoplankton classification. Journal of Nannoplankton Research 19, 36-47.

Young, J.R., Geisen, M., Cros, L., Kleijne, A., Probert, I., Sprengel, C., Ostergaard, J.B., 2003. A guide to extant coccolithophore taxonomy. Journal of Nannoplankton Research Special Issue 1, 1–132.

Zachos, J.C., Pagani, M., Sloan, L., Thomas, E., Billups, K., 2001a. Trends, rhythms, and aberrations in global climate 65 Ma to present. Science 292, 686-693.

Zachos, J.C., Shackleton, N.J., Revenaugh, J.S., Pälike, H., Flower, B.P., 2001b. Climate response to orbital forcing across the Oligocene-Miocene boundary. Science 292, 274-278.

Appendix A. Taxonomic remarks

Taxonomy used in the present work follows haptophyte phylogeny as revised by Young and Bown (1997), Young et al. (2003) and Jordan et al. (2004).

A1. Family Noelaerhabdaceae Jerkovic 1970 emend. Young & Bown 1997

This is the dominant family in most Neogene assemblages, and includes the extant genera *Emiliania* and *Gephyrocapsa*.

A1.1. Genus Reticulofenestra Hay, Mohler and Wade 1966

Elliptical to sub-circular reticulofenestrids with a prominent open central area and with no slits in the distal shield. The rather simple morphology of *Reticulofenestra* makes subdivision into species notoriously problematic. The conventional taxonomy is primarily based on size. This is unsatisfactory and arbitrary, but of stratigraphic value (Backman, 1980; Young, 1990). In this study, a subdivision of four species based on size and central area opening size was employed during the assemblage counts:

Reticulofenestra haqii Backman 1978: morphospecies 3-5 µm in length, with a central opening shorter than 1.5 µm.

Reticulofenestra minuta Roth 1970: morphospecies smaller than 3 µm.

Reticulofenestra minutula (Gartner, 1967) Haq and Berggren, 1978: morphospecies 3-5 µm in length with a central opening longer than 1.5 µm.

Reticulofenestra pseudoumbilicus (Gartner 1967) Gartner 1969: larger morphospecies (> 5~~–7~~ µm).

A1.2. Genus Dictyococcites (Black 1967) emend. Backman 1980

Elliptical reticulofenestrids with a large central area closed (or virtually closed) in line with the distal shield. The central area of the distal shield frequently shows a median furrow or a minute pore, but not large enough to suggest that they belong to *Reticulofenestra*. Although *Dictyococcites sensu* Black (1967) can be regarded as a heavily calcified, junior synonym of *Reticulofenestra*, the emended diagnosis of Backman (1980) allows consistent separation of this genus from *Reticulofenestra*.

Dictyococcites sp.: small morphospecies (< 3 µm) with a closed central area.

Dictyococcites antarcticus Haq 1976: in contrast with *D. hesslandii*, the specimens of *D. antarcticus* (4-8 µm) show no pore but a narrow and elongated rectangular central area (named "furrow" in Haq, 1976 and "straight band" in Backman, 1980). The straight extinction band along the major axis occupies at least one half of the total length of the elliptical central area (Backman, 1980).

Dictyococcites hesslandii (Haq 1966) Haq and Lohmann, 1976: the central area of the distal shield exhibits a small pore, from which extinction bands radiate (3-8 µm).

A1.3. Genus Cyclicargolithus Bukry 1971

Circular to sub-circular reticulofenestrids with a small central area and high tube-cycles. Although Theodoridis (1984) regarded *Cyclicargolithus* as a junior synonym of *Reticulofenestra*, the diagnosis of Bukry (1971) allows consistent separation of this genus from *Reticulofenestra*.

Cyclicargolithus abisectus (Müller 1970) Wise 1973: large species (>10 µm).

Cyclicargolithus floridanus (Roth and Hay in Hay et al., 1967) Bukry 1971: species smaller than 10 µm.

A2. Other coccoliths recorded in this study

Calcidiscus leptoporus (Murray and Blackman, 1898) Loeblich and Tappan, 1978

Coccolithus miopelagicus Bukry, 1971

Coccolithus pelagicus (Wallich 1877) Schiller 1930

Helicosphaera spp. Kamptner 1954

Pontosphaera spp. Lohmann 1902

Syracosphaera pulchra Lohmann 1902

Umbilicosphaera spp. Lohmann 1902

A3. Nannoliths

Discoaster spp. Tan, 1927

Sphenolithus spp. Deflandre in Grassé 1952

Plate 3-1. Images in cross-polarized light (POL) and scanning electron microscope (SEM) of the three genera of the Noelaerhabdaceae during the late Oligocene-early Miocene. **a)** *Reticulofenestra minutula*, POL (1000x), Sample 608-39H3-127 and 588C-5R2-25. **b-c)** *Reticulofenestra minuta*, SEM, Sample 588C-2R6-100. **d)** *Reticulofenestra pseudoumbilicus*, SEM, Sample 516F-10R1-122. **e)** *Dictyococcites* sp., POL (1000x), Sample 516-27H3-79. **f)** *Dictyococcites antarcticus*, POL (1000x), Sample 588C-4R5-33. **g)** *Dictyococcites hesslandii*, SEM, Sample 588C-11R1-111. **h)** *Dictyococcites antarcticus*, SEM, 516F-10R1-122. **i)** *Dictyococcites* sp., SEM, Sample 588C-11R1-111. **j)** *Dictyococcites hesslandii* (coccosphere), SEM, Sample 516-26H2-18. **k-l)** *Cyclicargolithus floridanus*, POL (1000x), Sample 516-26H2-18 and 588C-2R6-100. **m-n)** *Cyclicargolithus floridanus*, SEM, Sample 588C-2R6-100 and 516F-10R1-53. Scale bars: 1μm.

a) *Reticulofenestra minutula*

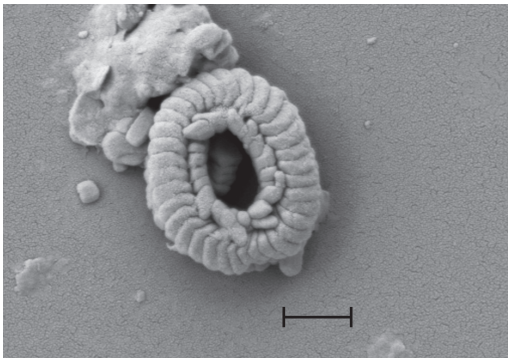

b) *Reticulofenestra minuta*

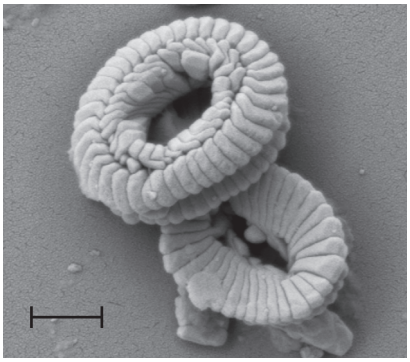

c) *Reticulofenestra minuta*

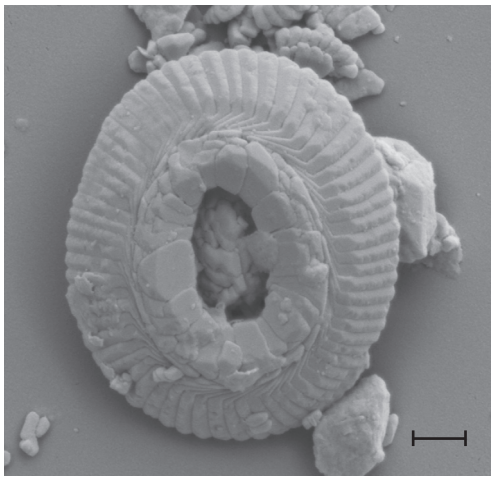

d) *Reticulofenestra pseudoumbilicus*

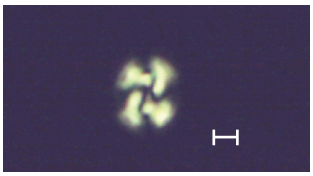

e) *Dictyococcites* sp.

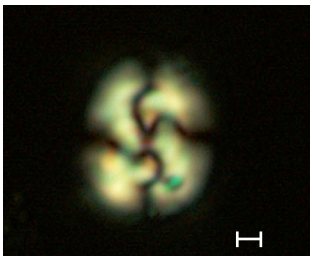

f) *Dictyococcites antarcticus*

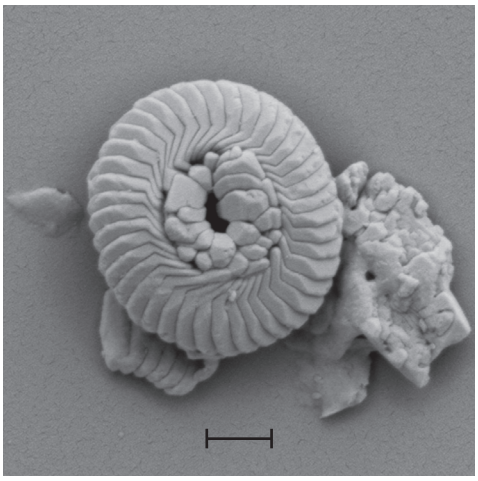

g) *Dictyococcites hesslandii*

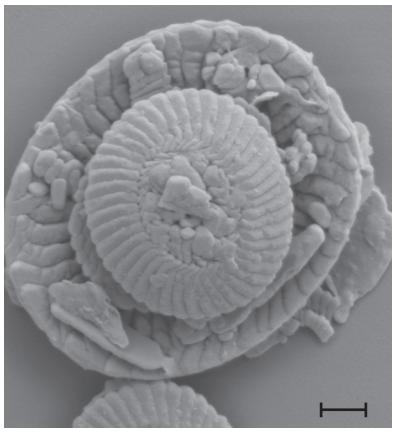

h) *Dictyococcites antarcticus*

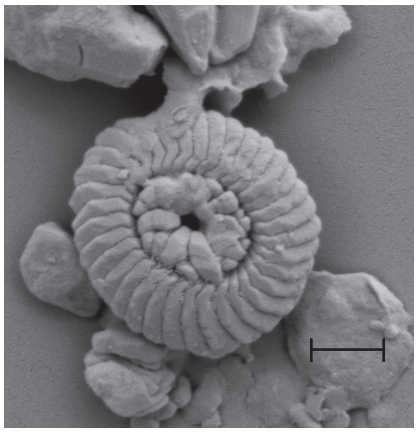

i) *Dictyococcites* sp.

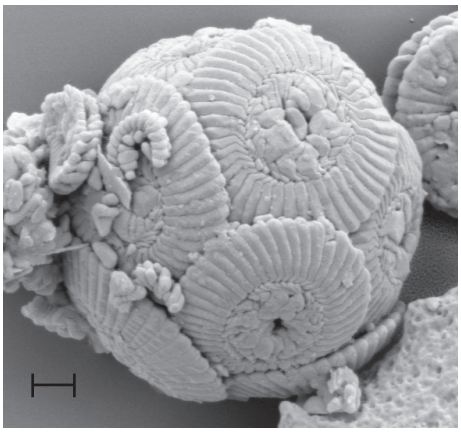

j) *Dictyococcites hesslandii* (coccosphere)

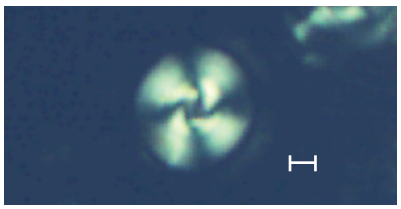

k) *Cyclicargolithus floridanus*

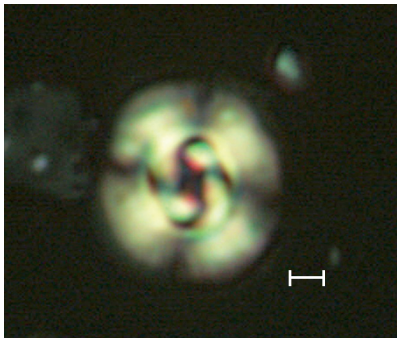

l) *Cyclicargolithus floridanus*

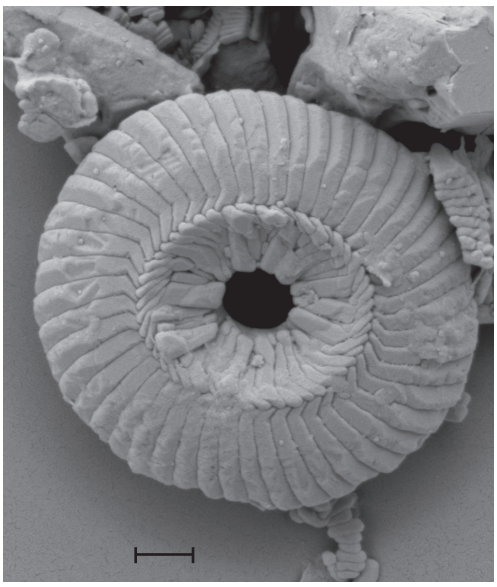

m) *Cyclicargolithus floridanus*

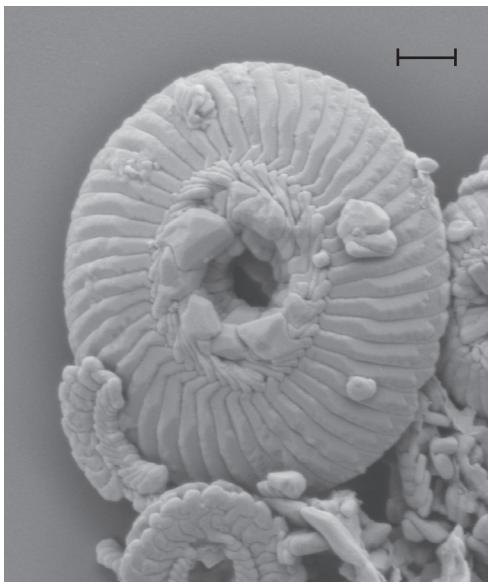

n) *Cyclicargolithus floridanus*

3.2. Réévaluation des producteurs d'alcénones à l'Oligocène-Miocène

Published in Paleoceanography, vol. 27, 2012.

Alkenone producers during late Oligocene–early Miocene revisited

Julien Plancq,[1] Vincent Grossi,[1] Jorijntje Henderiks,[2] Laurent Simon,[3] and Emanuela Mattioli[1]

Received 10 May 2011; revised 8 September 2011; accepted 16 November 2011; published 18 January 2012.

[1] This study investigates ancient alkenone producers among the late Oligocene–early Miocene coccolithophores recorded at Deep Sea Drilling Project (DSDP) Site 516. Contrary to common assumptions, *Reticulofenestra* was not the most important alkenone producer throughout the studied time interval. The comparison between coccolith species-specific absolute abundances and alkenone contents in the same sedimentary samples shows that *Cyclicargolithus* abundances explain 40% of the total variance of alkenone concentration and that the species *Cyclicargolithus floridanus* was a major alkenone producer, although other related taxa may have also contributed to the alkenone production at DSDP Site 516. The distribution of the different alkenone isomers ($MeC_{37:2}$, $EtC_{38:2}$, and $MeC_{38:2}$) remained unchanged across distinct changes in species composition, suggesting similar diunsaturated alkenone compositions within the Noelaerhabdaceae family during the late Oligocene–early Miocene. However, the overall larger cell size of *Cyclicargolithus* may have implications for the alkenone-based reconstruction of past partial pressure of CO_2. Our results underscore the importance of a careful evaluation of the most likely alkenone producers for periods (>1.85 Ma) predating the first occurrence of contemporary alkenone producers (i.e., *Emiliania huxleyi* and *Gephyrocapsa oceanica*).

Citation: Plancq, J., V. Grossi, J. Henderiks, L. Simon, and E. Mattioli (2012), Alkenone producers during late Oligocene–early Miocene revisited, *Paleoceanography*, *27*, PA1202, doi:10.1029/2011PA002164.

1. Introduction

[2] Alkenones are long-chain (C_{35}–C_{40}) lipids whose biosynthesis in modern oceans is restricted to a few extant unicellular haptophyte algae belonging to the Isochrysidales clade, which includes the calcifying haptophytes (coccolithophores) *Emiliania huxleyi* and *Gephyrocapsa oceanica* [*Marlowe et al.*, 1984; *Volkman et al.*, 1980, 1995]. A few noncalcifying Isochrysidales, such as *Isochrysis galbana*, also produce alkenones but they are restricted to coastal areas and are not considered as an important source of alkenone in the open ocean [*Marlowe et al.*, 1990].

[3] Diunsaturated and triunsaturated C_{37} alkenones ($C_{37:2}$ and $C_{37:3}$, respectively) are ubiquitous and abundant in marine sediments, and have been intensively used for paleoceanographic reconstructions [e.g., *Brassell et al.*, 1986; *Jasper and Hayes*, 1990; *Eglinton et al.*, 1992; *Bard et al.*, 1997; *Cacho et al.*, 1999; *Martrat et al.*, 2004; *Bolton et al.*, 2010].

[1]Laboratoire de Géologie de Lyon, UMR 5276, CNRS, Université Lyon 1, Ecole Normale Supérieure Lyon, Villeurbanne, France.
[2]Paleobiology Program, Department of Earth Sciences, Uppsala University, Uppsala, Sweden.
[3]Laboratoire d'Ecologie des Hydrosystèmes Naturels et Anthropisés, UMR 5023, CNRS, Université Claude Bernard Lyon, Villeurbanne, France.

0883-8305/12/2011PA002164

The production of $C_{37:2}$ and $C_{37:3}$ alkenones is linked to the coccolithophore growth temperature [*Brassell et al.*, 1986; *Prahl and Wakeham*, 1987] and the so-called alkenone unsaturation index $U^{K'}_{37}$ (defined as the ratio $[C_{37:2}]/([C_{37:2}] + [C_{37:3}])$) has been used as a proxy to reconstruct past sea surface temperatures, especially during the Quaternary period [e.g., *Müller et al.*, 1998; *Eltgroth et al.*, 2005; *Pahnke and Sachs*, 2006]. The carbon isotopic composition of the $C_{37:2}$ alkenone ($\delta^{13}C_{37:2}$) is also used to evaluate the carbon isotopic fractionation ($\varepsilon_{p37:2}$) that occurred during marine haptophyte photosynthesis in order to estimate concentration of CO_2 in past ocean surface waters ($[CO_{2(aq)}]$) and partial pressure of atmospheric CO_2 (paleo-pCO_2) [e.g., *Jasper and Hayes*, 1990; *Jasper et al.*, 1994; *Bidigare et al.*, 1997, 1999; *Pagani et al.*, 1999; *Pagani*, 2002; *Seki et al.*, 2010].

[4] The alkenone-based proxies have been calibrated on modern coccolithophores in culture (*E. huxleyi* and *G. oceanica*) and on Quaternary sediments [e.g., *Conte et al.*, 1995, 1998; *Müller et al.*, 1998; *Popp et al.*, 1998; *Riebesell et al.*, 2000]. However, the temperature calibration of the $U^{K'}_{37}$ index is species-dependent [e.g., *Volkman et al.*, 1995; *Conte et al.*, 1998] and includes variability due to physiological factors such as nutrients and light availability [e.g., *Epstein et al.*, 1998; *Prahl et al.*, 2003]. Nutrient-limited chemostat cultures show that the carbon isotopic composition of alkenones and $\varepsilon_{p37:2}$ values vary with $[CO_{2(aq)}]$ and physiological factors such as growth rate (μ) and cell size [*Laws et al.*, 1995; *Popp et al.*, 1998]. However, nutrient-

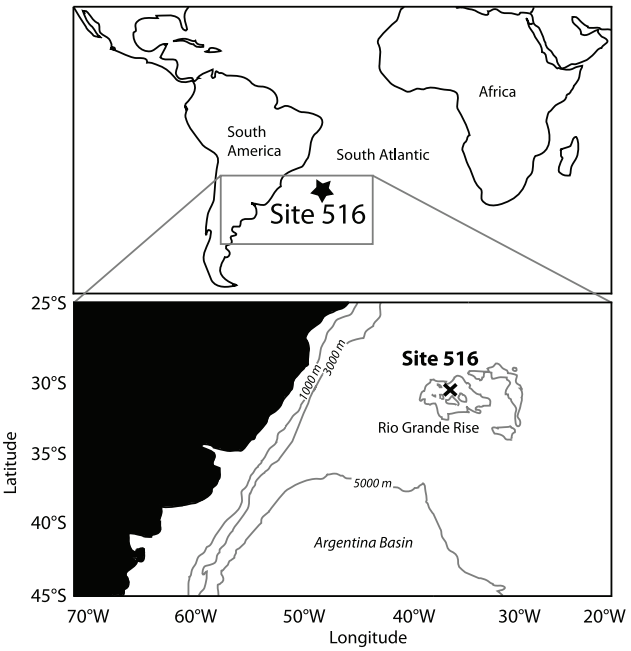

Figure 1. Location of DSDP Site 516 at the Rio Grande Rise (adapted from *Henderiks and Pagani* [2007]).

replete batch cultures produce much lower $\varepsilon_{p37:2}$ values and a different relationship between $\varepsilon_{p37:2}$ and $\mu/[CO_{2(aq)}]$ [*Riebesell et al.*, 2000].

[5] There is a huge gap between the first sedimentary record of alkenones in the Cretaceous at ~120 Ma [*Farrimond et al.*, 1986; *Brassell et al.*, 2004] and the first occurrence of modern alkenone producers (0.27 Ma for *E. huxleyi* [*Thierstein et al.*, 1977] and 1.85 Ma for *G. oceanica* [*Pujos-Lamy*, 1977]). Since *E. huxleyi* and *G. oceanica* cannot be responsible for alkenone production during most of the Cenozoic and the Mesozoic, the biological sources of alkenones preserved in pre-Quaternary sediments need to be elucidated in order to better constrain paleoenvironmental reconstructions based on these biomarkers.

[6] Based on the consistent cooccurrence of *Reticulofenestra* coccoliths and alkenones in marine sediments dating back to the Eocene (45 Ma), *Marlowe et al.* [1990] suggested that the most probable Cenozoic alkenone producers are to be found within the genus *Reticulofenestra*, which belongs to the Noelaerhabdaceae family like *Emiliania* and *Gephyrocapsa*. However, this study did not compare alkenone concentrations with *Reticulofenestra* absolute abundances. More recently, *Bolton et al.* [2010] argued that *Reticulofenestra* species were the main alkenone producers during the late Pliocene, based on a correlation between *Reticulofenestra* abundances and C_{37} alkenone concentrations in sediments. Yet, other alkenones (e.g., C_{38}) were not considered.

[7] Here, we investigate the cooccurrence of alkenones and coccolithophore genera and species during the late Oligocene–early Miocene by comparing nannofossil assemblages and species-specific absolute abundances with alkenone contents (C_{37} and C_{38} alkenones) in sediments from the Deep Sea Drilling Project (DSDP) Site 516. This allows a detailed characterization of ancient alkenone producers and a reappraisal of paleoceanographic and paleo-pCO_2 reconstructions for the investigated period.

2. Material and Methods

2.1. Sampling

[8] DSDP Leg 72 Site 516 is located on the upper flanks of the Rio Grande Rise at 1313 m water depth in the South Atlantic subtropical gyre (Figure 1). Site 516 is situated north of the Northern Subtropical Front [*Belkin and Gordon*, 1996] and other front zones of the South Atlantic. During the Miocene, carbonate-rich sediments were deposited well above the lysocline and the calcite compensation depth (CCD), at water depths similar to today [*Barker*, 1983]. Studies by *Pagani et al.* [2000a, 2000b] and *Henderiks and Pagani* [2007] demonstrated the simultaneous presence of Noelaerhabdaceae coccoliths and alkenones in DSDP Site 516 sediment samples. However, these studies neither reported alkenone concentrations nor absolute abundances of coccoliths. We therefore selected a total of 35 sediment samples from Holes 516 and 516F. The sample depths slightly differ from those studied by *Henderiks and Pagani* [2007]. The time interval investigated spans the latest Oligocene and the early Miocene (25–16 Ma) and includes a period (~21–19 Ma) of major paleoceanographic changes [*Pagani et al.*, 2000b]. The age model for DSDP Site 516 used in this study is the one presented by *Henderiks and Pagani* [2007].

2.2. Total Organic Carbon Analyses

[9] Subsamples (~100 mg of ground bulk sediment) were acidified in situ with HCl 2N in precleaned (combustion at 450°C) silver capsules until effervescence ceased, dried in an oven (50°C) and wrapped in tin foil before analyses. Total organic carbon (TOC) analyses were performed with a Thermo FlashEA 1112 elemental analyzer using aspartic acid (36.09% of carbon) and nicotinamid (59.01% of carbon) as calibration standards (n = 5 with variable weight for each standard). Accuracy was checked using in-house reference material analyzed with the samples (fine ground low carbon sediment; 0.861 ± 0.034% of carbon (standard deviation; n = 12)). All samples were analyzed twice and the reproducibility achieved for duplicate analyses was better than 10% (coefficient of variation).

2.3. Alkenone Analyses

[10] Samples (~10 g) were ground and extracted by way of sonication (5×) using 50 mL of Dichloromethane (DCM)/Methanol (MeOH) (2:1 v/v). Following evaporation of the solvents, the total lipid extract was separated into three fractions using chromatography over a column of inactivated (4% H_2O) silica, with hexane (Hex), Hex/ethyl acetate (7:3 v/v) and DCM/MeOH (1:1 v/v) as eluents. The second fraction, containing alkenones, was dried under N_2, silylated (pyridine/N,O-bis(trimethylsilyl)trifluoroacetamide or BSTFA, 2:1 v/v, 60°C for 1 h) and dissolved in hexane for analysis by gas chromatography (GC/FID) and gas chromatography/mass spectrometry (GC/MS).

[11] Alkenones were identified by GC/MS using a MD800 Voyager spectrometer interfaced to an HP6890 gas

chromatograph equipped with an on-column injector and a DB-5MS column (30 m × 0.25 mm × 0.25 μm). The oven temperature was programmed from 60°C (1 min) to 130°C at 20°C min^{-1}, and then to 310°C (20 min) at 4°C min^{-1}. Helium was used as the carrier gas at constant flow (1.1 mL min^{-1}).

[12] Alkenone abundances were determined by GC/FID using hexatriacontane (n-C_{36} alkane) as internal standard. The GC was a HP-6890 Series gas chromatograph configured with an on-column injector and a HP5 (30 m × 0.32 mm × 0.25 μm) capillary column. Helium was used as the carrier gas at constant flow and the oven temperature program was the same as for GC-MS analyses. Samples were injected twice and the reproducibility achieved for duplicate alkenone quantifications was less than 10% (coefficient of variation).

2.4. Micropaleontological Analyses

[13] Slides for calcareous nannofossil quantitative analysis were prepared following the random settling method [*Beaufort*, 1991b] (modified by *Geisen et al.* [1999]). A small amount of dried sediment powder (5 mg) was mixed with water (with basic pH, oversaturated with respect to calcium carbonate) and the homogenized suspension was allowed to settle for 24 h onto a cover slide. The slide was dried and mounted on a microscope slide with Rhodopass. Coccolith quantification was performed using a polarizing optical ZEISS microscope (magnification 1000×). A standard number of 500 calcareous nannofossils (coccoliths and nannoliths) were counted in a variable number (between 10 and 30) of field of views. In order to test the reproducibility of our quantification, each slide was counted twice and the reproducibility achieved was high (coefficient of variation: 10%).

[14] Absolute abundance of nannofossils per gram of sediment was calculated using the formula

$$X = (N*V)/(M*A*H), \quad (1)$$

where X is the number of calcareous nannofossils per gram of sediment; N the number of nannofossils counted in each sample; V the volume of water used for the dilution in the settling device (mL); M the weight of powder used for the suspension (g); A the surface considered for nannofossil counting (cm^2); H the height of the water over the cover slide in the settling device (2.1 cm). Species-specific relative abundances (percentages) were also calculated from the total nannofossil content.

[15] Coccolith size is a proxy for cell size in ancient Noelaerhabdaceae [*Henderiks*, 2008]. *Henderiks and Pagani* [2007] have already evaluated the size variability within the reticulofenestrids (namely species of the genera *Reticulofenestra* and *Dictyococcites*) at Site 516 and its implications for the interpretation of measured alkenone-based $\varepsilon_{p37:2}$ values. Here, we pair the reticulofenestrid size data with the mean size variability of *Cyclicargolithus* in the same 24 samples studied by *Henderiks and Pagani* [2007]. In each sample, 100 individual *Cyclicargolithus* coccoliths were measured from four replicate slides, rendering statistically robust estimates of mean size and its variance [*Henderiks and Törner*, 2006].

2.5. Comparison Between Alkenone and Nannofossil Contents

[16] Our working hypothesis is that, under good preservation conditions, the alkenone concentration should be related to the number of coccoliths of alkenone-producing taxa in sediments. A similar assumption has already been used to identify biological sources of alkenones in sediments of late Quaternary [e.g., *Müller et al.*, 1997; *Weaver et al.*, 1999] and Pliocene age [e.g., *Bolton et al.*, 2010; *Beltran et al.*, 2011]. Here, we compare major trends of absolute and relative abundances of coccolith genera to variations in total alkenone concentrations.

[17] Simple and multiple linear regression analyses (significance threshold $\alpha = 0.05$) were used to determine the relationships between alkenone contents and relative/absolute abundances of coccolith genera, and between $\varepsilon_{p37:2}$ (data from *Pagani et al.* [2000b]), abundances of coccolith genera and mean sizes. The normality of the input data and residual distributions was checked using a Shapiro-Wilk test. All statistical analyses were performed using the JMP version 8.0.1 (SAS institute) software.

3. Taxonomy Used for the Noelaerhabdaceae Family

[18] Since the early publication of *Marlowe et al.* [1990], the genus *Reticulofenestra* has been considered by different authors as the most probable alkenone producer during the Cenozoic. However, species of the genus *Reticulofenestra* are generally considered to have a high morphological plasticity, and the *Dictyococcites* and *Cyclicargolithus* genera are often considered as junior synonyms of *Reticulofenestra* [e.g., *Theodoridis*, 1984; *Marlowe et al.*, 1990; *Young*, 1990; *Aubry*, 1992; *Beaufort*, 1992; *Henderiks and Pagani*, 2007; *Henderiks*, 2008]. Consequently, these genera have often been grouped either as reticulofenestrids (*Reticulofenestra* + *Dictyococcites* [e.g., *Henderiks and Pagani*, 2007; *Henderiks*, 2008]) or more simply as *Reticulofenestra* (*Reticulofenestra* + *Dictyococcites* + *Cyclicargolithus* [e.g., *Aubry*, 1992]). This grouping can result in misleading conclusions when trying to precisely define ancient species involved in alkenone production. A taxonomic revision is beyond the scope of this work and *Dictyococcites*, *Reticulofenestra* and *Cyclicargolithus* are distinguished here on the basis of distinctive morphological features in optical microscope (Table 1 and Appendix A).

4. Results

4.1. TOC

[19] The studied samples are characterized by a low total organic carbon content (0.06% on average; Figure 2a). Higher values are recorded at the base of the studied interval and a slight trend to decreasing values is observed from 25 to 20 Ma, with a mean TOC content of 0.08% and 0.04% before and after 20.5 Ma, respectively (Figure 2a).

4.2. Alkenones

[20] One C_{37} and two C_{38} alkenones are present in all the samples studied. These were identified as heptatriacontadien-2-one ($MeC_{37:2}$), octatriacontadien-3-one ($EtC_{38:2}$) and octatriacontadien-2-one ($MeC_{38:2}$), respectively. $MeC_{37:2}$,

Table 1. Distinctive Morphological Features Used to Distinguish the Three Noelaerhabdaceae Genera (*Reticulofenestra, Dictyococcites,* and *Cyclicargolithus*) at DSDSP Site 516 During the Late Oligocene–Early Miocene

Noelaerhabdaceae Genus	Distinctive Morphological Features
Reticulofenestra	Elliptical coccoliths with a prominent open central area and with no slits in the distal shield [*Hay et al.*, 1966].
Dictyococcites	Elliptical coccoliths with a large central area closed or virtually closed in line with the distal shield. The central area of the distal shield frequently shows a median furrow or a minute pore [*Backman*, 1980].
Cyclicargolithus	Circular to subcircular coccoliths with a small central area and high tube cycles [*Bukry*, 1971]. Larger coccolith size range than *Reticulofenestra* and *Dictyococcites* [*Henderiks*, 2008].

$EtC_{38:2}$, and $MeC_{38:2}$ alkenones account for 55%, 33%, and 12% of total alkenone content, respectively, and no significant variation of these proportions is observed through the time interval studied.

[21] The total amount of these ketones is relatively low (0.03 μg per gram of sediment on average), with a maximum of 0.13 μg per gram of sediment at about 23 Ma (Figure 2b), and values attaining the detection limit at around 20 and 17 Ma. A general trend to decreasing alkenone content is seen from 25 to 16 Ma but three periods of increasing total alkenone content are observed at about 23, 22–21.5 and 19.5–17.5 Ma (Figure 2b). This overall distribution matches with that of TOC (Figures 2a and 2b). The same variations are observed when each alkenone is considered individually. Similar trends also occur when alkenone content is expressed relative to TOC (Figure 2c). In Figure 3, quantitative alkenone data expressed per gram of sediment are compared to absolute and relative abundances of Noelaerhabdaceae coccoliths.

4.3. Coccolith Assemblages

[22] Coccoliths are well preserved in all investigated samples since delicate coccoliths that are prone to dissolution, such as *Syracosphaera* and *Pontosphaera*, are commonly observed with pristine structures. This indicates that coccolith assemblages are not importantly biased by selective dissolution in the water column or diagenetic effects, in agreement with previous studies at Site 516 [*Henderiks and Pagani*, 2007].

[23] The mean absolute abundance of nannofossils is 5.0×10^9 nannofossils per gram of sediment and does not show any significant stratigraphic trend across the late Oligocene–early Miocene (Figure 2d). Coccolith assemblages are dominated by four genera, which account for 70%–80% of the total assemblage, namely: *Reticulofenestra*, *Dictyococcites*, *Cyclicargolithus*, all belonging to the Noelaerhabdaceae family, and *Coccolithus*. No significant stratigraphic trend across the late Oligocene–early Miocene is observed when all the Noelaerhabdaceae are combined (Figure 2e). The mean absolute abundance of Noelaerhabdaceae is 3.4×10^9 coccoliths per gram of sediment (Figure 2e).

[24] For each genus of Noelaerhabdaceae, relative and absolute abundances show similar variations through time (Figures 3b, 3c, and 3d). Three shifts in coccolith assemblages can be distinguished: (1) Between 25 and 20.5 Ma, coccolith assemblages are dominated by *Cyclicargolithus* representing on average 30% (1.4×10^9 specimens per gram of sediment) of the total nannofossil assemblage, whereas *Dictyococcites* represents ~25% (1.3×10^9) and *Reticulofenestra* ~15% (0.7×10^9); (2) between 20.5 and 17.5 Ma, coccolith assemblages show a dominance of *Dictyococcites* (40%; 2.3×10^9) and an increase (from 15% to 45%; 0.95×10^9 to 2.0×10^9) in the proportion of *Reticulofenestra*, whereas *Cyclicargolithus* shows a sharp decrease in abundance (8%; 0.42×10^9); and (3) assemblages between 17.5 and 16 Ma are characterized by the dominance of

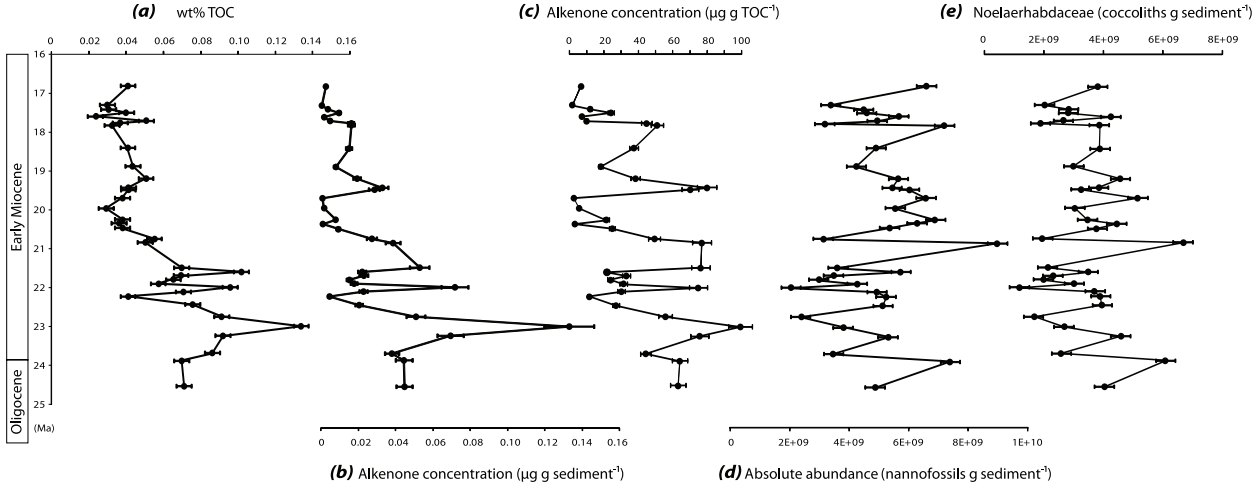

Figure 2. (a) Total organic carbon content (wt % TOC), (b) total alkenone content (μg per gram of sediment), (c) total alkenone content relative to TOC (μg per gram of TOC), (d) absolute abundance of nannofossils (specimens per gram of sediment), and (e) absolute abundance of Noelaerhabdaceae (coccoliths per gram of sediment) at DSDP Site 516 during the late Oligocene–early Miocene. Error bars represent coefficients of variation.

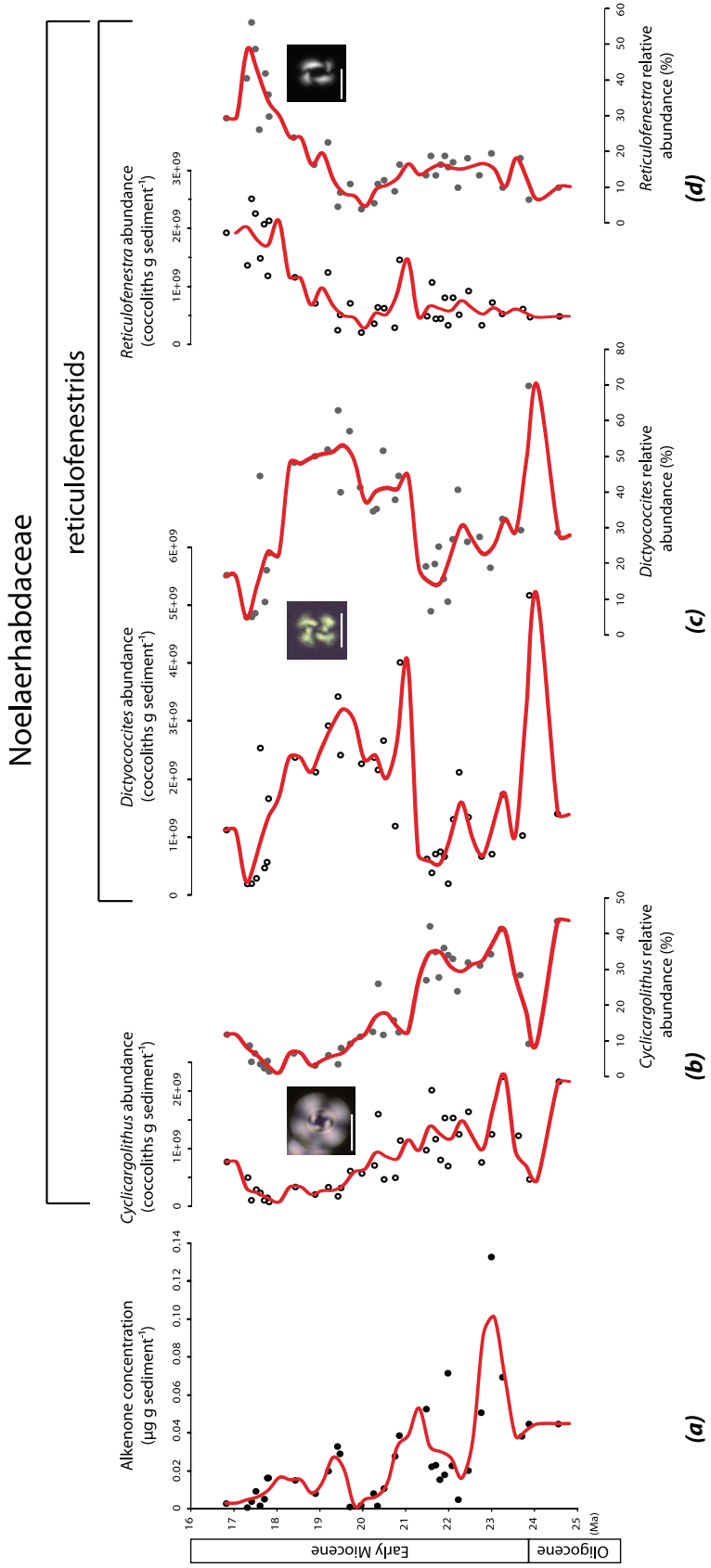

Figure 3. Comparison between alkenone concentration and Noelaerhabdaceae distribution at DSDP Site 516 during the late Oligocene–early Miocene. (a) Total alkenone content (μg per gram of sediment) and absolute and relative abundances of (b) *Cyclicargolithus*, (c) *Dictyococcites*, and (d) *Reticulofenestra*. Relative abundances are relative to the total nannofossil contents. Trend curves are moving average curves calculated using a 0.5 Ma window size and a 0.25 Ma time step. Scale bars on nannofossil pictures equal 4 μm.

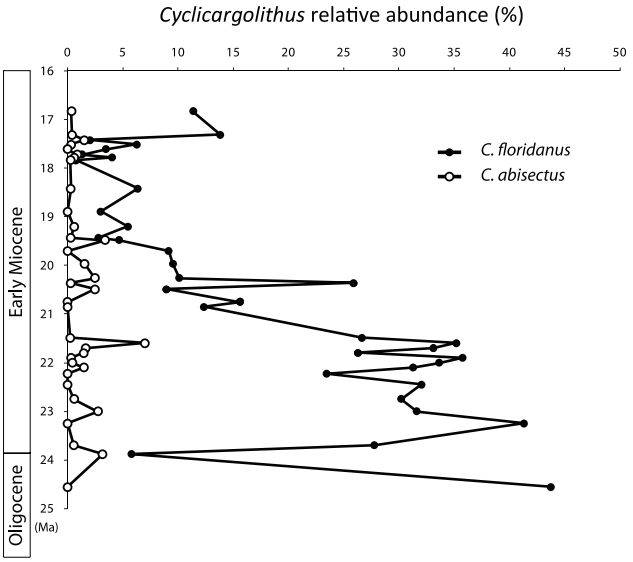

Figure 4. Relative abundances of *Cyclicargolithus* species *C. floridanus* and *C. abisectus* at DSDP Site 516. It should be noted that *C. floridanus* is entirely responsible for the *Cyclicargolithus* abundance trend.

Reticulofenestra (45%; 2.0×10^9) with smaller amounts of both *Cyclicargolithus* (9%; 0.44×10^9) and *Dictyococcites* (8%; 0.42×10^9). In general, *Dictyococcites* and *Cyclicargolithus* abundances show opposite trends (Figures 3b and 3c). This record is consistent with the results of *Henderiks and Pagani* [2007] although the apparent timing in assemblage shifts is slightly different due to different sample spacing.

[25] The coccolith size of *Cyclicargolithus*, which is strongly linearly correlated to its cell diameter [*Henderiks*, 2008], ranges between 4 and 12 μm (N = 2454). Mean size per sample varies between 6.13 μm $\pm$ 0.24 (95% confidence mean) in the late Oligocene and 8.45 μm $\pm$ 0.18 (95% confidence mean) in the early Miocene.

5. Discussion

5.1. Alkenone Producers at DSDP Site 516

[26] Significant correlations between the abundance of coccoliths of the main alkone producers (namely *E. huxleyi* and *G. oceanica*) and the alkenone concentration have been observed in late Quaternary sediments [e.g., *Müller et al.*, 1997; *Weaver et al.*, 1999]. Based on this observation, parallel distributions of reticulofenestrid coccoliths and alkenone contents have been used to identify past biological sources of alkenones in Pliocene sediments [e.g., *Bolton et al.*, 2010; *Beltran et al.*, 2011]. The similar variations at DSDP Site 516 between the absolute abundance of *Cyclicargolithus* coccoliths and the total alkenone content (Figure 3) suggests a significant contribution of this genus to alkenone production between 25 and 16 Ma. More precisely, alkenone production is supported by the species *C. floridanus* which is entirely responsible for the *Cyclicargolithus* abundance trend (Figure 4). Although reticulofenestrids are sometimes considered as species having high morphological plasticity which may bias their taxonomy [e.g., *Beaufort*, 1991a], *C. floridanus* represents a very characteristic morphospecies easily distinguishable from other reticulofenestrids due to its larger size and distinct subcircular shape.

[27] Processes of degradation in the water column and in sediments may affect alkenone and coccolith records differently, leading to misleading interpretations of the sedimentary record. In the present case, several observations argue against the effects of such potential preservation biases.

[28] First, records of coccolith assemblages can be skewed by the dissolution of susceptible species during settling and sedimentary burial [*Roth and Coulbourn*, 1982; *Gibbs et al.*, 2004; *Young et al.*, 2005]. Such selective coccolith dissolution is not observed within the studied nannofossil groups at DSDP Site 516 [*Henderiks and Pagani*, 2007; this study]. Sediments from Site 516 are calcareous oozes with little evidence of dissolution or cementation precipitation [*Barker et al.*, 1983], and no significant secondary calcite overgrowth is observed on coccoliths [*Ennyu et al.*, 2002]. An important effect of diagenesis affecting the recorded coccolith assemblages can thus be excluded.

[29] Second, a majority of organic matter produced in the surface oceans is generally remineralized before and after reaching the seafloor. The concentrations of TOC and alkenones in sediments are thus a function of preservation conditions and represent only a fraction of the original export productivity. Nevertheless, the relatively high sedimentation rate (17 m/Ma) and the relatively shallow water depth (1313 m) of DSDP Site 516 [*Barker et al.*, 1983] induced a limited oxidation and a relatively rapid burial of organic matter into the sediments compared to other oceanic settings [*Mukhopadhyay et al.*, 1983]. Moreover, the paleodepth of the studied site did not change significantly during the time span investigated. Changes in TOC and alkenone concentrations in sediments may also reflect varying sedimentation rate. However, the sedimentation rate calculated according to the age model of the studied interval does not show significant variations [*Pagani et al.*, 2000b; *Henderiks and Pagani*, 2007]. Thus the observed overall decrease in TOC since ~21.5 Ma (Figure 2a) likely reflects a decrease in primary productivity in response to paleoceanographic changes (mainly linked to temperature and nutrient concentrations [*Pagani et al.*, 2000b; *Henderiks and Pagani*, 2007]) rather than changes in sedimentary dilution or organic matter degradation. Despite the fact that alkenones represent only a very small fraction of TOC, the significant covariation observed between TOC and total alkenone content (Figures 2a and 2b; $R^2 = 0.69$, $p < 0.0001$) suggests that alkenone distribution also reflects variations in the abundance of alkenone producers rather than an erratic degradation of alkenones relative to TOC. It should be noted that these biolipids are generally considered less prone to degradation than other phytoplankton-derived lipids [*Sun and Wakeham*, 1994; *Gong and Hollander*, 1997, 1999]. In addition, the association between organic matter and the calcium carbonate of coccoliths might have produced a physical and chemical protection against remineralization [*Armstrong et al.*, 2002], as coccoliths have very likely acted as ballast and reduced the residence time of organic matter within the water column [*Klaas and Archer*, 2002].

[30] Finally, the apparent similar variations between the abundance of *Cyclicargolithus* and the total alkenone content are supported by statistical analyses which show that, among all tested Noelaerhabdaceae genera, only absolute

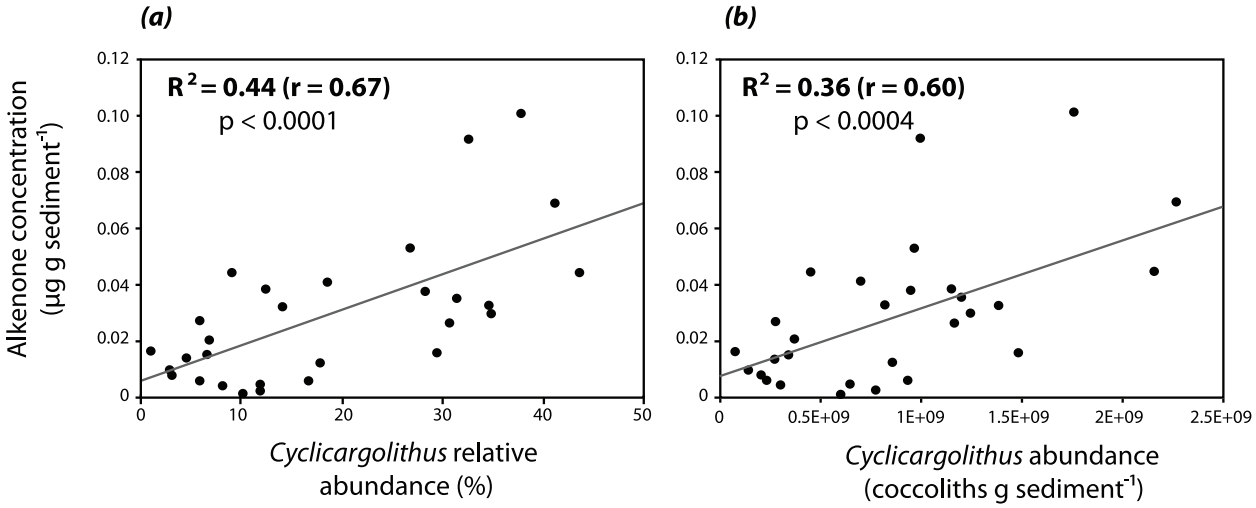

Figure 5. Correlations (linear regressions; $\alpha = 0.05$) between alkenone content (μg per gram of sediment) and (a) relative and (b) absolute abundances of *Cyclicargolithus* during the late Oligocene–early Miocene at DSDP Site 516.

and relative abundances of this genus produce significant and positive linear correlations with the total alkenone content (R^2 = 0.36–0.44, $p < 0.0005$; Figure 5). Such a correlation is unlikely the result of diagenetic processes. Still, it is possible that a better preservation of the calcite of coccoliths compared to alkenones has led to an underestimation of the contribution of *Cyclicargolithus* to alkenone production. This may partly explain why *Cyclicargolithus* represents only 40% of the total variance of alkenone concentration. However, other taxa may have also contributed to the alkenone production at DSDP Site 516 since *Cyclicargolithus* has a limited stratigraphical range (from ~40 Ma to ~13 Ma [*Young*, 1998]). The continuous cooccurrence of the *Reticulofenestra* genus and alkenones throughout the Cenozoic sediment record is the main argument to infer it is the most probable ancient alkenone producer [e.g., *Marlowe et al.*, 1990]. In the present study, the quantitative distribution of *Reticulofenestra* shows an inverse trend compared to that of alkenone concentrations (Figures 3a and 3d). Moreover, when considering *Reticulofenestra* plus *Cyclicargolithus* abundances in a multiple linear regression calculated versus alkenone concentrations, the fit does not increase ($R^2 = 0.45$, $p < 0.001$) with respect to *Cyclicargolithus* alone ($R^2 = 0.44$, $p < 0.0005$). These observations suggest a weak contribution of the genus *Reticulofenestra* to alkenone production in the time interval considered, although a contribution of this genus cannot be completely excluded. Abundances of *Dictyoccocites* (Figure 3c) do not significantly correlate either with the general trend of alkenone concentrations. However, a contribution of *Dictyococcites* to alkenone production cannot be excluded especially after 20.5 Ma where a small increase in alkenone content coincides with a sharp increase in *Dictyococcites* (Figures 3a and 3c). It is also possible that noncalcifying haptophytes, for which there is no mineralized fossil record, have contributed to the alkenone production at DSDP Site 516 although extant noncalcifying alkenone producers (e.g., *Isochrysis galbana*) are not considered as an important source of alkenones in modern open ocean sediments [*Marlowe et al.*, 1990].

[31] It is worth noticing that no change in the proportion of the different alkenone isomers ($MeC_{37:2}$, $EtC_{38:2}$, and $MeC_{38:2}$) is observed throughout the entire time interval considered in this study. This may imply that all alkenone-producing species produced the same type of alkenones during the late Oligocene–Early Miocene, which may not be surprising since the alkenone compositions of modern coccolithophorids (essentially *G. oceanica* and *E. huxleyi*) are rather similar [*Volkman et al.*, 1995]. It is possible, however, that the original distribution of alkenones at DSDP Site 516 contained alkenone isomers with more than two unsaturations, since triunsaturated and tetraunsaturated alkenones are known to be far more reactive toward diagenetic processes than their diunsaturated homologues [e.g., *Grimalt et al.*, 2000; *Rontani and Wakeham*, 2008].

5.2. Paleoenvironmental Implications

[32] Past atmospheric CO_2 concentrations (pCO_2) can be estimated from the carbon isotopic fractionation between ambient CO_2 and the algal cell ($\varepsilon_{p37:2}$) that occurred during marine haptophyte photosynthesis [*Jasper and Hayes*, 1990; *Jasper et al.*, 1994; *Bidigare et al.*, 1997, 1999; *Pagani et al.*, 1999], based on the expression

$$\varepsilon_{p37:2} = \varepsilon_f - b/[CO_{2(aq)}], \quad (2)$$

where $\varepsilon_{p37:2}$ is calculated from the difference between the carbon isotopic compositions of diunsturated C_{37} alkenone ($\delta^{13}C_{37:2}$) and foraminifera carbonate ($\delta^{13}C_{foram}$) [see *Pagani et al.*, 1999]. ε_f is the carbon isotope fractionation due to all carbon-fixing reactions (here assuming ε_f = 25‰ [*Popp et al.*, 1998]) and '*b*' represents the sum of physiological factors, including growth rate and cell geometry, that affect total carbon isotope discrimination [*Laws et al.*, 1995; *Popp et al.*, 1998]. The magnitude of term '*b*' is estimated by the phosphate concentration of the surface ocean [*Bidigare et al.*, 1997, 1999; *Pagani et al.*, 1999]. In oligotrophic settings, it is generally assumed that the influence of

Table 2. Pairwise Linear Regressions Between Alkenone $\delta^{13}C$ ($\delta^{13}C_{37:2}$), $\varepsilon_{p37:2}$, *Cyclicargolithus* and Reticulofenestrids Mean Cell Size, and the Ratio of *Cyclicargolithus* to Noelaerhabdaceae

	$\delta^{13}C_{37:2}$	$\varepsilon_{p37:2}$	Reticulofenestrid Mean Size	*Cyclicargolithus* Mean Size	Mix Mean Size
$\varepsilon_{p37:2}$	$R = -0.96$ $p < 0.0001$				
Reticulofenestrid mean size	$R = 0.68$ $p = 0.0003$	$R = -0.68$ $p = 0.0003$			
Cyclicargolithus mean size	$R = 0.69$ $p = 0.0002$	$R = -0.67$ $p = 0.0004$	$R = 0.75$ $p < 0.0001$		
Mix mean size	$R = 0.33$ $p = 0.112$	$R = -0.36$ $p = 0.085$	$R = 0.86$ $p < 0.0001$	$R = 0.50$ $p = 0.013$	
Cyclicargolithus/ Noelaerhabdaceae	$R = -0.67$ $p = 0.0003$	$R = 0.62$ $p = 0.0013$	$R = -0.34$ $p = 0.099$	$R = -0.60$ $p = 0.002$	$R = -0.17$ $p = 0.419$

haptophyte growth rates on $\varepsilon_{p37:2}$ is negligible [e.g., *Pagani et al.*, 2005].

[33] Considering that larger phytoplankton cells, with higher carbon cell quota relative to surface area, fractionate less than smaller cells under similar $CO_{2(aq)}$ and low growth rates [e.g., *Laws et al.*, 1995; *Popp et al.*, 1998], *Henderiks and Pagani* [2007] applied a cell size correction to the term '*b*' in order to revise pCO_2 trends reconstructed by *Pagani et al.* [2000b] at DSDP Site 516. This correction was based on the cell diameter of reticulofenestrids, namely *Reticulofenestra* and *Dictyococcites*, considered as the most probable alkenone producers during the Cenozoic. Indeed, a significant correlation exists between alkenone $\delta^{13}C_{37:2}$ (and therefore $\varepsilon_{p37:2}$) and reticulofenestrid mean size ($R = 0.68$, $p = 0.0003$; Table 2). Yet, the present study suggests that another major alkenone producer at

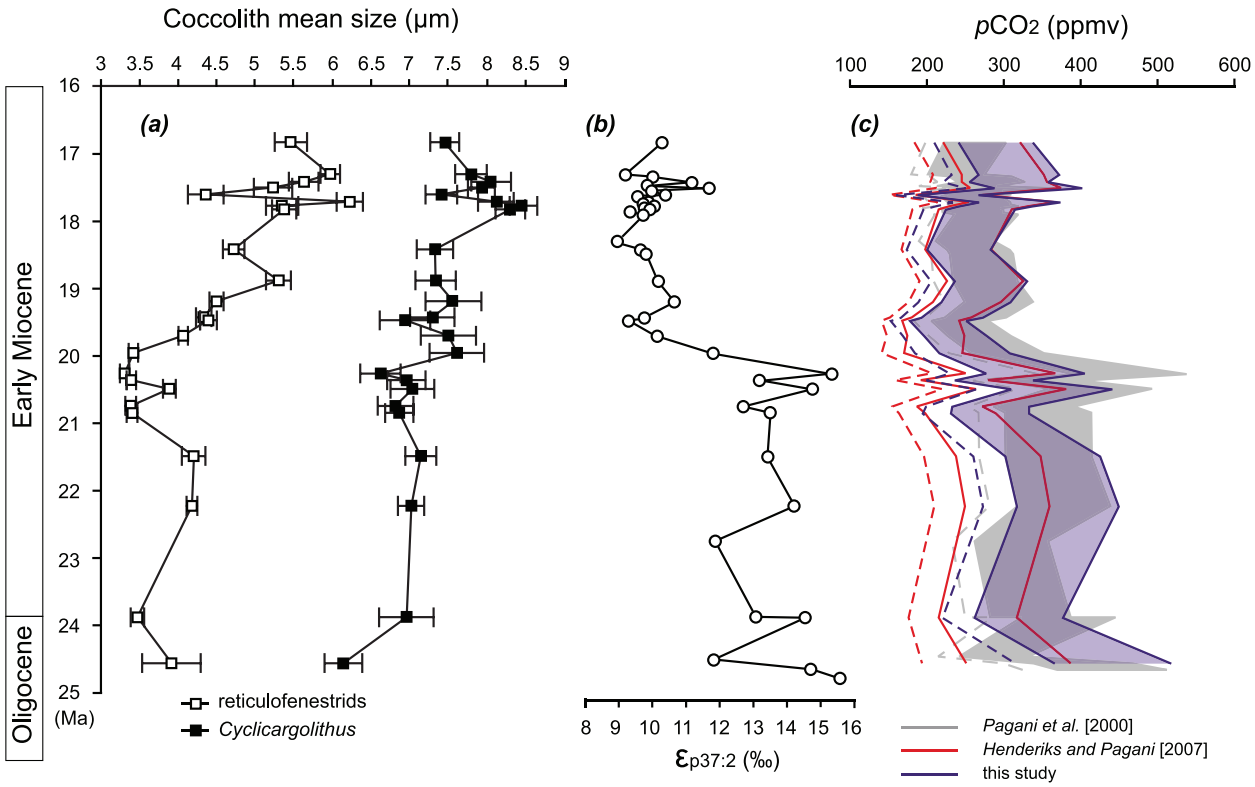

Figure 6. (a) Mean size variability at Site 516 of reticulofenestrids (*Reticulofenestra* plus *Dictyococcites*) and *Cyclicargolithus*, as determined in the 24 samples studied by *Henderiks and Pagani* [2007] (error bars indicate 95% confidence intervals); (b) alkenone-derived $\varepsilon_{p37:2}$ record [from *Pagani et al.*, 2000b]; (c) revised pCO_2 estimates after cell size corrections (see detailed methods in work by *Henderiks and Pagani* [2007]) including *Cyclicargolithus* (blue) compared to pCO_2 estimates of *Pagani et al.* [2000b] (grey) and *Henderiks and Pagani* [2007] (red). Shaded bands and lines depict minimum and maximum estimates with propagated 95% confidence levels of input factors. Dashed lines represent minimum estimates assuming no diagenetic alteration of biogenic carbonates used to determine paleo-SST [see *Pagani et al.*, 2005].

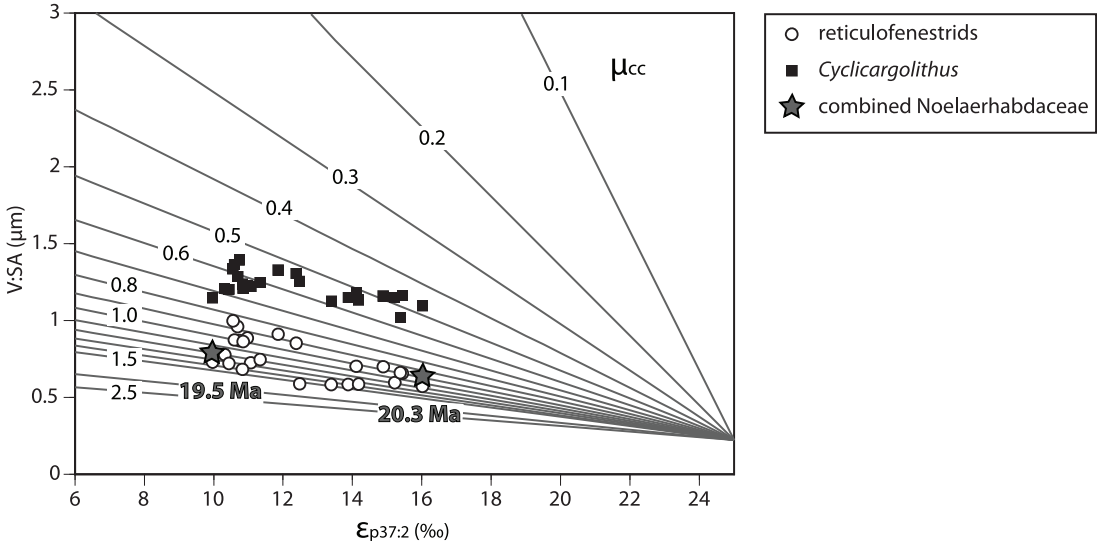

Figure 7. Relationship between $\varepsilon_{p37:2}$ (‰), cell volume to surface area ratios (V:SA; μm), and growth rates (μ_{cc}; d^{-1}), calculated with constant $CO_{2(aq)}$ = 10 μmol kg^{-1} [after *Henderiks and Pagani*, 2007]. The contoured growth rates represent values under continuous light chemostat experiments and need to be corrected for the effect of day length and respiration in natural settings [*Bidigare et al.*, 1997, 1999]. The stars depict the 6‰ decrease in $\varepsilon_{p37:2}$ between 20.3 and 19.5 Ma, which, under constant CO_2, corresponds to an increase in Noelaerhabdaceae cell sizes and growth rates.

this site was *Cyclicargolithus*, which had an overall larger cell diameter than the reticulofenestrids (Figure 6a). We have thus reevaluated the interpretation of published $\varepsilon_{p37:2}$ values (Figure 6b) [*Pagani et al.*, 2000b] and reestimated paleo-pCO_2 values considering the mean cell size of *Cyclicargolithus*. Prior to 20 Ma, this results in higher pCO_2 estimates (max. 340–550 ppmv) compared to values presented by *Henderiks and Pagani* [2007] due to the relatively high proportions and larger size of *Cyclicargolithus*. After 20 Ma, *Cyclicargolithus* is less common than large reticulofenestrids, resulting in pCO_2 estimates (<400 ppmv) that are similar to those determined by *Henderiks and Pagani* [2007]. Overall, the new pCO_2 estimates stay within the ranges previously reported by *Pagani et al.* [2000b] (Figure 6c).

[34] Relative differences in growth rates between reticulofenestrids and *Cyclicargolithus* can be evaluated using the following model [*Henderiks and Pagani*, 2007]:

$$\mu/\left[CO_{2(aq)}\right] = \left(\varepsilon_{p37:2} - \varepsilon_f\right)/K_{V:SA,} \quad (3)$$

where the term '*b*' from equation (2) is now expressed by specific growth rate (μ) and a constant ($K_{V:SA}$) that is defined by the cell volume to surface area ratio (V:SA) of eukaryotic species [*Popp et al.*, 1998]

$$K_{V:SA} = 49 - 222(V:SA). \quad (4)$$

[35] Under constant $[CO_{2(aq)}]$, and assuming no vital effects in $\varepsilon_{p37:2}$ between different haptophytes, similar values of $\varepsilon_{p37:2}$ could be generated by large cells (high V:SA) with low growth rates and/or small cells with high growth rates (Figure 7). In this scenario, our reconstructions indicate that *Cyclicargolithus* had 30% to 60% lower specific growth rates than the reticulofenestrids.

[36] Without access to cell geometry data and detailed nannofossil data, *Pagani et al.* [2000b] initially calculated an overall ~60% increase in haptophyte growth rates to explain the distinct 6‰ decrease in $\varepsilon_{p37:2}$ observed after ~20 Ma (Figure 6b). Here we combine the *Cyclicargolithus* and reticulofenestrid data (based on their mean size and respective proportions relative to the total Noelaerhabdaceae abundance), and show that the 6‰ shift in $\varepsilon_{p37:2}$ is supported by an increase (~23%) in mean cell size (V:SA) and by an overall increase in mean growth rates of ~24% (Figure 7). The distinct 6‰ shift in $\varepsilon_{p37:2}$ may thus be partly explained by changes in the major alkenone producers with different growth rates under similar CO_2 conditions: from assemblages dominated by slow-growing *Cyclicargolithus* to dominantly reticulofenestrids with higher growth rates. Pairwise correlations (Table 2) show that there is a significant correlation between $\delta^{13}C_{37:2}$ (and therefore $\varepsilon_{p37:2}$) and reticulofenestrid mean size (R = 0.68, $p < 0.001$); $\delta^{13}C_{37:2}$ and *Cyclicargolithus* mean size (R = 0.69, p = 0.0002); and $\delta^{13}C_{37:2}$ and the *Cyclicargolithus*/Noelaerhabdaceae abundance ratio (R = −0.67, p = 0.0003). Finally, the observed variability in alkenone $\delta^{13}C_{37:2}$ and $\varepsilon_{p37:2}$ are best explained by a multiple linear regression linking the $\delta^{13}C_{37:2}$ to changes in mean Noelaerhabdaceae cell size and in the *Cyclicargolithus*/Noelaerhabdaceae abundance ratio (R = 0.81; $p < 0.0001$).

6. Conclusion

[37] A comparison of nannofossil and alkenone absolute contents in Atlantic sediment samples (DSDP Site 516) spanning the late Oligocene to early Miocene suggests that the species *Cyclicargolithus floridanus* was a major alkenone

producer between 25 and 20.5 Ma, explaining at least 40% of the total alkenone content at this site. The contribution to alkenone production by large *Dictyococcites* is supported in younger sediments whereas that of *Reticulofenestra* species appears less pronounced. These observations challenge previous statements that *Reticulofenestra* was the most important alkenone producer during the late Oligocene–early Miocene. The relatively high proportions of *Cyclicargolithus* before 20 Ma and its larger cell size lead to higher paleo-pCO_2 estimates than those previously determined without considering this genus. Finally, the variability in alkenone $\delta^{13}C_{37:2}$ and $\varepsilon_{p37:2}$ are explained by changes in mean cell size as well as changes in the major alkenone producers with different growth rates. This highlights the importance of a careful evaluation of the most likely alkenone producers before using alkenone-based proxies for paleoenvironmental reconstructions.

Appendix A: Taxonomic Remarks

[38] Taxonomy used in the present work follows Haptophyte phylogeny as revised by *Young and Bown* [1997] and *Sáez et al.* [2004].

A1. Noelaerhabdaceae Family

[39] *Noelaerhabdaceae* (*Jerkovic* [1970], emended by *Young and Bown* [1997]) is the dominant family in most Neogene assemblages, considered as the Cenozoic ancestor of the modern alkenone producers *Emiliania* and *Gephyrocapsa*.

A1.1. Genus *Reticulofenestra*

[40] Elliptical to subcircular coccoliths with a prominent open central area and with no slits in the distal shield. The rather simple morphology of *Reticulofenestra* [*Hay et al*., 1966] makes subdivision into species notoriously problematic. The conventional taxonomy is primarily based on size. This is unsatisfactorily and arbitrary, but of stratigraphic value [*Backman*, 1980; *Young et al.*, 2003]. In this study, a subdivision of four size-defined species was employed during the assemblage counts: (1) *Reticulofenestra haqii* [*Backman*, 1978]: morphospecies 3–5 μm in length, with a central opening shorter than 1.5 μm; (2) *Reticulofenestra minuta* [*Roth*, 1970]: morphospecies smaller than 3 μm; (3) *Reticulofenestra minutula* [*Gartner*, 1967; *Haq and Berggren*, 1978]: morphospecies 3–5 μm in length with a central opening longer than 1.5 μm; and (4) *Reticulofenestra pseudoumbilicus* [*Gartner*, 1967, 1969]: larger morphospecies (5–7 μm).

A1.2. Genus *Dictyococcites*

[41] Elliptical coccoliths with a large central area closed (or virtually closed) in line with the distal shield. The central area of the distal shield frequently shows a median furrow or a minute pore, but not large enough to suggest that they belong to *Reticulofenestra*. Although *Dictyococcites sensu* [*Black*, 1967] can be regarded as a heavily calcified, junior synonym of *Reticulofenestra*, the emended diagnosis of *Backman* [1980] clearly separates this genus from *Reticulofenestra*.

[42] *Dictyococcites* spp. are small morphospecies (<3 μm) with a supposed closed central area.

[43] *Dictyococcites antarcticus* [*Haq*, 1976]: in contrast with *D. hesslandii*, the specimens of *D. antarcticus* (4–8 μm) show no pore but a narrow and elongated rectangular central area (named "furrow" by *Haq* [1976] and "straight band" by *Backman* [1980]). The straight extinction band along the major axis occupies at least one half of the total length of the elliptical central area [*Backman*, 1980].

[44] *Dictyococcites hesslandii* [*Haq*, 1966; *Haq and Lohmann*, 1976]: for these specimens, the central area of the distal shield exhibits a small pore, from which extinction bands radiate (3–8 μm). Two morphometric size classes were distinguished in this study (3–5 μm and >5 μm).

A1.3. Genus *Cyclicargolithus*

[45] This genus is represented by circular to subcircular coccoliths with a small central area and high tube cycles. Although *Theodoridis* [1984] assigned *Cyclicargolithus* as a junior synonym of *Reticulofenestra*, the emended diagnosis of *Bukry* [1971] clearly separates this genus from *Reticulofenestra*.

[46] *Cyclicargolithus abisectus* [*Müller*, 1970; *Wise*, 1973] are large species (>10 μm).

[47] *Cyclicargolithus floridanus* [*Hay et al.*, 1967; *Bukry*, 1971] are species smaller than 10 μm.

A2. Other Coccoliths

[48] Other coccoliths that do not belong to the Noelaerhabdaceae family and found in the studied samples are listed here: *Calcidiscus leptoporus* [*Murray and Blackman*, 1898; *Loeblich and Tappan*, 1978], *Coccolithus miopelagicus* [*Bukry*, 1971], *Coccolithus pelagicus* [*Wallich*, 1877; *Schiller*, 1930], *Helicosphaera* spp. [*Kamptner*, 1954], *Pontosphaera* spp. [*Lohmann*, 1902], *Syracosphaera pulchra* [*Lohmann*, 1902], and *Umbilicosphaera* spp. [*Lohmann*, 1902].

A3. Nannoliths

[49] Nannoliths are thought to be related to coccoliths but have peculiar structures. Nannoliths found in the studied samples are *Discoaster* spp. [*Tan*, 1927] and *Sphenolithus* spp. [*Grassé*, 1952].

[50] **Acknowledgments.** We would like to thank two anonymous reviewers for their constructive comments and critical review. This study used Deep Sea Drilling Project samples provided by the Integrated Ocean Drilling Program. We thank Walter Hale from the Bremen Core Repository for his efficiency.

References

Armstrong, R. A., C. Lee, J. I. Hedges, S. Honjo, and S. G. Wakeham (2002), A new mechanistic model for organic carbon fluxes in the ocean based on the quantitative association of POC with ballast minerals, *Deep Sea Res. Part II*, *49*, 219–236, doi:10.1016/S0967-0645(01)00101-1.

Aubry, M. P. (1992), Paleogene calcareous nannofossils from the Kerguelen Plateau, Leg 120, *Proc. Ocean Drill. Program Sci. Results*, *120*, 471–491, doi:10.2973/odp.proc.sr.120.149.1992.

Backman, J. (1978), Late Miocene–early Pliocene nannofossil biochronology and biogeography in the Vera Basin, SE Spain, *Stockholm Contrib. Geol.*, *32*, 93–114.

Backman, J. (1980), Miocene-Pliocene nannofossils and sedimentation rates in the Hatton-Rockall basin, NE Atlantic Ocean, *Stockholm Contrib. Geol.*, *36*(1), 1–91.

Bard, E., F. Rostek, and C. Sonzogni (1997), Interhemispheric synchrony of the last deglaciation inferred from alkenone paleothermometry, *Nature*, *385*, 707–710, doi:10.1038/385707a0.

Barker, P. F. (1983), Tectonic evolution and subsidence history of the Rio Grande Rise, *Initial Rep. Deep Sea Drill. Proj.*, *72*, 953–976, doi:10.2973/dsdp.proc.72.151.1983.

Barker, P. F. et al. (1983), Site 516: Rio Grande Rise, *Initial Rep. Deep Sea Drill. Proj.*, *72*, 155–338, doi:10.2973/dsdp.proc.72.105.1983.

Beaufort, L. (1991a), Dynamique du nannoplancton calcaire au cours du Néogène: Implication climatiques et océanographiques, MS thesis, 173 pp., Lab de Geol. de Lyon, Univ. Lyon, Lyon, France.

Beaufort, L. (1991b), Adaptation of the random settling method for quantitative studies of calcareous nannofossils, *Micropaleontology*, *37*, 415–418, doi:10.2307/1485914.

Beaufort, L. (1992), Size variations in late Miocene *Reticulofenestra* and implication for paleoclimatic interpretation, *Mem. Sci. Geol.*, *43*, 339–350.

Belkin, I. M., and A. L. Gordon (1996), Southern Ocean fronts from the Greenwich meridian to Tasmania, *J. Geophys. Res.*, *101*, 3675–3696, doi:10.1029/95JC02750.

Beltran, C., J.-A. Flores, M.-A. Sicre, F. Baudin, M. Renard, and M. de Rafélis (2011), Long chain alkenones in the early Pliocene Sicilian sediments (Trubi Formation–Punta di Maiata section): Implications for the alkenone paleothermometry, *Palaeogeogr. Palaeoclimatol. Palaeoecol.*, *308*, 253–263, doi:10.1016/j.palaeo.2011.03.017.

Bidigare, R. R., et al. (1997), Consistent fractionation of ^{13}C in nature and in the laboratory: Growth-rate effects in some haptophyte algae, *Global Biogeochem. Cycles*, *11*, 279–292, doi:10.1029/96GB03939.

Bidigare, R. R., et al. (1999), Correction to "Consistent fractionation of ^{13}C in nature and in the laboratory: Growth-rate effects in some haptophyte algae," *Global Biogeochem. Cycles*, *13*, 251– 252, doi:10.1029/1998GB900011.

Black, M. (1967), New names for some coccolith taxa, *Proc. Geol. Soc. Lond.*, *1640*, 139–145.

Bolton, C. T., K. T. Lawrence, S. J. Gibbs, P. A. Wilson, L. C. Cleaveland, D. Timothy, and T. D. Herbert (2010), Glacial-interglacial productivity changes recorded by alkenones and microfossils in late Pliocene eastern equatorial Pacific and Atlantic upwelling zones, *Earth Planet. Sci. Lett.*, *295*, 401–411, doi:10.1016/j.epsl.2010.04.014.

Brassell, S. C., G. Eglinton, I. T. Marlowe, U. Pflaumann, and M. Sarnthein (1986), Molecular stratigraphy: A new tool for climatic assessment, *Nature*, *320*, 129–133, doi:10.1038/320129a0.

Brassell, S. C., M. Dumitrescu, and the ODP Leg 198 Shipboard Scientific Party (2004), Recognition of alkenones in a lower Aptian porcellanite from the west-central Pacific, *Org. Geochem.*, *35*, 181–188, doi:10.1016/j.orggeochem.2003.09.003.

Bukry, D. (1971), Cenozoic calcareous nannofossils from the Pacific Ocean, *Trans. San Diego Soc. Nat. Hist.*, *16*, 303–327.

Cacho, I., J. O. Grimalt, C. Pelejero, M. Canals, F. J. Sierro, J. A. Flores, and N. J. Shackleton (1999), Dansgaard-Oeschger and Heinrich event imprints in Alboran Sea paleotemperatures, *Paleoceanography*, *14*, 698–705, doi:10.1029/1999PA900044.

Conte, M. H., A. Thompson, and G. Eglinton (1995), Lipid biomarker diversity in the coccolithophorid *Emiliania huxleyi* (Prymnesiophycea) and the related species *Gephyrocapsa oceanica*, *J. Phycol.*, *31*, 272–282, doi:10.1111/j.0022-3646.1995.00272.x.

Conte, M. H., A. Thompson, D. Lesley, and R. P. Harris (1998), Genetic and physiological influences on the alkenone/alkenoate versus growth temperature relationship in *Emiliania huxleyi* and *Gephyrocapsa oceanica*, *Geochim. Cosmochim. Acta*, *62*(1), 51–68, doi:10.1016/S0016-7037(97)00327-X.

Eglinton, G., S. A. Bradshaw, A. Rosell, M. Sarnthein, U. Pflaumann, and R. Tiedemann (1992), Molecular record of secular sea surface temperature changes on 100-year timescales for glacial terminations I, II and IV, *Nature*, *356*, 423–426, doi:10.1038/356423a0.

Eltgroth, M. L., R. L. Watwood, and G. V. Wolfe (2005), Production and cellular localisation of neutral long-chain lipids in the haptophyte algae *Isochrysis galbana* and *Emiliania huxleyi*, *J. Phycol.*, *41*, 1000–1009, doi:10.1111/j.1529-8817.2005.00128.x.

Ennyu, A., M. A. Arthur, and M. Pagani (2002), Fine-fraction carbonate stable isotopes as indicators of seasonal shallow mixed-layer paleohydrography, *Mar. Micropaleontol.*, *46*, 317–342, doi:10.1016/S0377-8398(02)00079-8.

Epstein, B. L., S. D'Hondt, J. G. Quinn, J. Zhang, and P. E. Hargraves (1998), An effect of dissolved nutrient concentrations on alkenone-based temperature estimates, *Paleoceanography*, *13*(2), 122–126, doi:10.1029/97PA03358.

Farrimond, P., G. Eglinton, and S. C. Brassell (1986), Alkenones in Cretaceous black shales, Blake-Bahama basin, western North Atlantic, *Org. Geochem.*, *10*, 897–903, doi:10.1016/S0146-6380(86)80027-4.

Gartner, S. (1967), Calcareous nannofossils from Neogene of Trinidad, Jamaica, and Gulf of Mexico, *Univ. Kans. Paleontol. Contrib.*, *28*, 1–7.

Gartner, S. (1969), *Hayella* Roth and *Hayella* Gartner, *Micropaleontology*, *15*, 490.

Grassé, P. P. (1952), *Traité de Zoologie, Anatomie, Systématique, Biologie*, vol. 1, 1071 pp., Masson, Paris.

Geisen, M., J. Bollmann, J. O. Herrle, J. Mutterlose, and J. R. Young (1999), Calibration of the random settling technique for calculation of absolute abundance of calcareous nannoplankton, *Micropaleontology*, *45*(4), 437–442.

Gibbs, S., N. Shackleton, and J. R. Young (2004), Identification of dissolution patterns in nannofossil assemblages: A high-resolution comparison of synchronous records from Ceara rise, ODP Leg 154, *Paleoceanography*, *19*, PA1029, doi:10.1029/2003PA000958.

Gong, C., and D. J. Hollander (1997), Differential contribution of bacteria to sedimentary organic matter in oxic and anoxic environments, Santa Monica basin, California, *Org. Geochem.*, *26*, 545–563, doi:10.1016/S0146-6380(97)00018-1.

Gong, C., and D. J. Hollander (1999), Evidence for the differential degradation of alkenones under contrasting bottom water oxygen conditions: Implication for paleotemperature reconstruction, *Geochim. Cosmochim. Acta*, *63*, 405–411, doi:10.1016/S0016-7037(98)00283-X.

Grimalt, J. O., J. Rullkötter, M.-A. Sicre, R. Summons, J. Farrington, H. R. Harvey, M. Goñi, and K. Sawada (2000), Modifications of the C_{37} alkenone and alkenoate composition in the water column and sediment: Possible implications for sea surface temperature estimates in paleoceanography, *Geochem. Geophys. Geosyst.*, *1*(11), 1031, doi:10.1029/2000GC000053.

Hay, W. W., H. Mohler, and M. E. Wade (1966), Calcareous nannofossils from Nal'chik (northwest Caucasus), *Eclogae Geol. Helv.*, *56*, 379–399.

Haq, B. U. (1966), Electron microscope studies on some upper Eocene calcareous nannoplankton from Syria, *Stockholm Contrib. Geol.*, *15*, 23–37.

Haq, B. U. (1976), Coccoliths in cores from the Bellinghausen abyssal plain and Antarctic continental rise (DSDP Leg 35), *Initial Rep. Deep Sea Drill. Proj.*, *35*, 557–567.

Haq, B. U., and W. A. Berggren (1978), Late Neogene calcareous plankton biochronology of the Rio Grande Rise (South Atlantic Ocean), *J. Paleontol.*, *52*, 1167–1194.

Haq, B. U., and G. P. Lohmann (1976), Early Cenozoic calcareous nannoplankton biogeography of the Atlantic Ocean, *Mar. Micropaleontol.*, *1*, 119–197.

Hay, W. W., H. P. Mohler, P. H. Roth, and R. R. Schmidt (1967), Calcareous nannoplankton zonation of the Cenozoic of the Gulf Coast and Caribbean-Antillean area, and transoceanic correlation, *Trans. Gulf Coast Assoc. Geol. Soc.*, *17*, 428–480.

Henderiks, J. (2008), Coccolithophore size rules—Reconstructing ancient cell geometry and cellular calcite quota from fossil coccoliths, *Mar. Micropaleontol.*, *67*, 143–154, doi:10.1016/j.marmicro.2008.01.005.

Henderiks, J., and M. Pagani (2007), Refining ancient carbon dioxide estimates: Significance of coccolithophore cell size for alkenone-based pCO_2 records, *Paleoceanography*, *22*, PA3202, doi:10.1029/2006PA001399.

Henderiks, J., and A. Törner (2006), Reproducibility of coccolith morphometry: Evaluation of spraying and smear slide preparation techniques, *Mar. Micropaleontol.*, *58*, 207–218, doi:10.1016/j.marmicro.2005.11.002.

Jasper, J. P., and J. M. Hayes (1990), A carbon isotope record of CO_2 levels during the late Quaternary, *Nature*, *347*, 462–464, doi:10.1038/347462a0.

Jasper, J. P., J. M. Hayes, A. C. Mix, and F. G. Prahl (1994), Photosynthetic fractionation of ^{13}C and concentrations of dissolved CO_2 in the central equatorial Pacific during the last 255,000 years, *Paleoceanography*, *9*, 781–798, doi:10.1029/94PA02116.

Jerkovic, L. (1970), Noelaerhabdus nov. gen. type d'une nouvelle famille de coccolithphorides fossiles, Noelaerhabdaceae du Miocène supérieur de Yougoslavie, *C. R. Acad. Sci*, *270*, 468–470.

Kamptner, E. (1954), Untersuchungen uber den feinbau der coccolithen, *Arch. Protistenkd.*, *100*, 1–90.

Klaas, C., and D. E. Archer (2002), Association of sinking organic matter with various types of mineral ballast in the deep sea: Implications for the rain ratio, *Global Biogeochem. Cycles*, *16*(4), 1116, doi:10.1029/2001GB001765.

Laws, E. A., B. N. Popp, R. R. Bidigare, M. C. Kennicutt, and S. A. Macko (1995), Dependence of phytoplankton carbon isotopic composition on growth rate and $[CO_2]_{aq}$: Theoretical considerations and experimental results, *Geochim. Cosmochim. Acta*, *59*, 1131–1138, doi:10.1016/0016-7037(95)00030-4.

Loeblich, A. R., and H. Tappan (1978), The coccolithophorid genus *Calcidiscus* Kamptner and its synonyms, *J. Paleontol.*, *52*, 1390–1392.

Lohmann, H. (1902), Die Coccolithophoridae, eine monographie der coccolithen bildenden flagellaten, zugleich ein beitrat zur kenntnis des Mittelmeerauftriebs, *Arch. Protistenkd.*, *1*, 89–165.

Marlowe, I. T., S. C. Brassell, G. Eglinton, and J. C. Green (1984), Long chain unsaturated kenones and esters in living algae and marine sediments, *Org. Geochem.*, *6*, 135–141, doi:10.1016/0146-6380(84)90034-2.

Marlowe, I. T., S. C. Brassell, G. Eglinton, and J. C. Green (1990), Long-chain alkenones and alkyl alkenoates and the fossil coccolith record of marine sediments, *Chem. Geol.*, *88*, 349–375, doi:10.1016/0009-2541(90)90098-R.

Martrat, B., J. O. Grimalt, C. Lopez-Martinez, I. Cacho, F. J. Sierro, J. A. Flores, R. Zahn, M. Canals, J. H. Curtis, and D. A. Hodell (2004), Abrupt temperature changes in the western Mediterranean over the past 250,000 years, *Science*, *306*, 1762–1765, doi:10.1126/science.1101706.

Mukhopadhyay, P. K., J. Rullkötter, and D. H. Welte (1983), Facies and diagenesis of organic matter in sediments from the Brazil basin and the Rio Grande Rise, Deep Sea Drilling Project Leg 72, *Initial Rep. Deep Sea Drill. Proj.*, *72*, 821–828, doi:10.2973/dsdp.proc.72.138.1983.

Müller, C. (1970), Nannoplankton-zonen der unteren-meeresmolasse Bayerns, *Geol. Bavarica*, *63*, 107–118.

Müller, P. J., M. Cepek, G. Ruhland, and R. R. Schneider (1997), Alkenone and coccolithophorid species changes in late Quaternary sediments from the Walvis Ridge: Implications for the alkenone paleotemperature method, *Palaeogeogr. Palaeoclimatol. Palaeoecol.*, *135*, 71–96, doi:10.1016/S0031-0182(97)00018-7.

Müller, P. J., G. Kirst, G. Rulhand, I. von Storch, and A. Rosell-Melé (1998), Calibration of the alkenone paleotemperature index $U^{K'}_{37}$ based on core-tops from the eastern South Atlantic and the global ocean (60°N–60°S), *Geochim. Cosmochim. Acta*, *62*(10), 1757–1772, doi:10.1016/S0016-7037(98)00097-0.

Murray, G., and V. H. Blackman (1898), On the nature of the coccospheres and rhabdospheres, *Philos. Trans. R. Soc. B*, *190*, 427–441.

Pagani, M. (2002), The alkenone-CO_2 proxy and ancient atmospheric CO_2, in *Understanding Climate Change: Proxies, Chronology, and Ocean–atmosphere Interactions: Papers of a Theme*, *Philos. Trans. R. Soc. A*, 360, 609–632.

Pagani, M., M. A. Arthur, and K. H. Freeman (1999), Miocene evolution of atmospheric carbon dioxide, *Paleoceanography*, *14*(3), 273–292, doi:10.1029/1999PA900006.

Pagani, M., K. H. Freeman, and M. A. Arthur (2000a), Isotope analyses of molecular and total organic carbon from Miocene sediments, *Geochim. Cosmochim. Acta*, *64*, 37–49, doi:10.1016/S0016-7037(99)00151-9.

Pagani, M., M. A. Arthur, and K. H. Freeman (2000b), Variations in Miocene phytoplankton growth rates in the southwest Atlantic: Evidence for changes in ocean circulation, *Paleoceanography*, *15*, 486–496, doi:10.1029/1999PA000484.

Pagani, M., J. C. Zachos, K. H. Freeman, B. Tripple, and S. Bohaty (2005), Marked decline in atmospheric carbon dioxide concentrations during the Paleogene, *Science*, *309*, 600–603, doi:10.1126/science.1110063.

Pahnke, K., and J. P. Sachs (2006), Sea surface temperatures of southern midlatitudes 0–160 kyr B.P., *Paleoceanography*, *21*, PA2003, doi:10.1029/2005PA001191.

Popp, B. N., E. A. Laws, R. R. Bidigare, J. E. Dore, K. L. Hanson, and S. G. Wakeham (1998), Effect of phytoplankton cell geometry on carbon isotopic fractionation, *Geochim. Cosmochim. Acta*, *62*, 69–77, doi:10.1016/S0016-7037(97)00333-5.

Prahl, F. G., and S. G. Wakeham (1987), Calibration of unsaturation patterns in long-chain ketone compositions for paleotemperature assessment, *Nature*, *330*, 367–369, doi:10.1038/330367a0.

Prahl, F. G., G. V. Wolfe, and M. A. Sparrow (2003), Physiological impacts on alkenone paleothermometry, *Paleoceanography*, *18*(2), 1025, doi:10.1029/2002PA000803.

Pujos-Lamy, A. (1977), Essai d'établissement d'une biostratigraphie du nannoplancton calcaire dans le Pleistocène de l'Atlantique Nord-oriental, *Boreas*, *6*, 323–331, doi:10.1111/j.1502-3885.1977.tb00297.x.

Riebesell, U., A. T. Revill, D. G. Hodsworth, and J. K. Volkman (2000), The effects of varying CO_2 concentration on lipid composition and carbon isotope fractionation in *Emiliania huxleyi*, *Geochim. Cosmochim. Acta*, *64*, 4179–4192, doi:10.1016/S0016-7037(00)00474-9.

Rontani, J. F., and S. G. Wakeham (2008), Alteration of alkenone unsaturation ratio with depth in the Black Sea: Potential roles of stereomutation and aerobic biodegradation, *Org. Geochem.*, *39*(9), 1259–1268, doi:10.1016/j.orggeochem.2008.06.002.

Roth, P. H. (1970), Oligocene calcareous nannoplankton biostratigraphy, *Eclogae Geol. Helv.*, *63*, 799–881.

Roth, P. H., and W. T. Coulbourn (1982), Floral and solution patterns of coccoliths in surface sediments of the North Pacific, *Mar. Micropaleontol.*, *7*, 1–52, doi:10.1016/0377-8398(82)90014-7.

Sáez, A. G., I. Probert, J. R. Young, B. Edvardsen, W. Eikrem, and L. K. Medlin (2004), A review of the phylogeny of the Haptophyta, in *Coccolithophores: From Molecular Processes to Global Impact*, edited by H. R. Thierstein and J. R. Young, pp. 251–269, Springer, Berlin.

Schiller, J. (1930), *Coccolithineae, Dr. L. Rabenhorst's Kryptogamen-Flora von Deutschland, Osterreich und der Schweiz Ser.*, vol. 10, edited by L. Rabenhorst, pp. 89–273, Akad. Verl., Leipzig, Germany.

Seki, O., G. L. Foster, D. N. Schmidt, A. Mackensen, K. Kawamura, and R. D. Pancost (2010), Alkenone and boron-based Pliocene pCO_2 records, *Earth Planet. Sci. Lett.*, *292*, 201–211, doi:10.1016/j.epsl.2010.01.037.

Sun, M. Y., and S. G. Wakeham (1994), Molecular evidence for degradation and preservation of organic matter in the anoxic Black Sea basin, *Geochim. Cosmochim. Acta*, *58*, 3395–3406, doi:10.1016/0016-7037(94)90094-9.

Tan, S. H. (1927), Over de samenstelling en het onstaan van krijt en mergelgesteenten van de Molukken, *Jaarbk. Mijnwezen Ned. Indie*, *55*, 111–122.

Theodoridis, S. (1984), *Calcareous Nannofossil Biozonation of the Miocene and Revision of the Helicoliths and Discoasters*, *Utrecht Micropaleontol. Bull. Ser.*, vol. 32, 1–271, State Univ. of Utrecht, Utrecht, Germany.

Thierstein, H. R., K. R. Geitzenauer, B. Molfino, and N. J. Shackleton (1977), Global synchroneity of late Quaternary coccolith datum levels: Validation by oxygen isotopes, *Geology*, *5*, 400–404, doi:10.1130/0091-7613(1977)5<400:GSOLQC>2.0.CO;2.

Volkman, J. K., G. Eglinton, E. D. S. Corner, and T. E. V. Forsberg (1980), Long-chain alkenes and alkenones in the marine coccolithphorid *Emiliania huxleyi*, *Phytochemistry*, *19*, 2619–2622, doi:10.1016/S0031-9422(00)83930-8.

Volkman, J. K., S. M. Barrett, S. I. Blackburn, and E. L. Sikes (1995), Alkenones in *Gephyrocapsa oceanica*: Implications for studies of paleoclimate, *Geochim. Cosmochim. Acta*, *59*, 513–520, doi:10.1016/0016-7037(95)00325-T.

Wallich, G. C. (1877), Observations on the coccosphere, *Ann. Mag. Nat. Hist.*, *19*, 342–350.

Weaver, P. P. E., M. R. Chapman, G. Eglinton, M. Zhao, D. Rutledge, and G. Read (1999), Combined coccolith, foraminiferal, and biomarker reconstruction of paleoceanographic conditions over the past 120 kyr in the northern North Atlantic (59°N, 23°W), *Paleoceanography*, *14*, 336–349, doi:10.1029/1999PA900009.

Wise, S. W. (1973), Calcareous nannofossils from cores recovered during Leg 18, Deep Sea Drilling Project: Biostratigraphy and observations on diagenesis, *Initial Rep. Deep Sea Drill. Proj.*, *18*, 569–615.

Young, J. R. (1990), Size variation of Neogene *Reticulofenestra* coccoliths from Indian Ocean DSDP cores, *J. Micropaleontol.*, *9*, 71–85, doi:10.1144/jm.9.1.71.

Young, J. R. (1998), Neogene, in *Calcareous Nannofossil Biostratigraphy*, edited by P. R. Bown, pp. 225–265, Chapman and Hall, Cambridge, U. K., doi:10.1007/978-94-011-4902-0_8

Young, J. R., and P. R. Bown (1997), Cenozoic calcareous nannoplankton classification, *J. Nannoplankton Res.*, *19*, 36–47.

Young, J. R., M. Geisen, L. Cros, A. Kleijne, I. Probert, C. Sprengel, and J. B. Ostergaard (2003), A guide to extant coccolithophore taxonomy, *J. Nannoplankton Res. Spec. Issue 1*, 1–132.

Young, J. R., M. Geisen, and I. Probert (2005), A review of selected aspects of coccolithophore biology with implications for palaeobiodiversity estimation, *Micropaleontology*, *51*(4), 267–288, doi:10.2113/gsmicropal.51.4.267.

V. Grossi, E. Mattioli, and J. Plancq, Laboratoire de Géologie de Lyon, UMR 5276, CNRS, Université Lyon 1, Ecole Normale Supérieure Lyon, Batiment Géode, 2 rue Raphaël Dubois, Campus scientifique de la DOUA, Villeurbanne F-69622, France. (julien.plancq@pepsmail.univ-lyon1.fr)

J. Henderiks, Paleobiology Program, Department of Earth Sciences, Uppsala University, Villavägen 16, SE-752 36 Uppsala, Sweden.

L. Simon, Laboratoire d'Ecologie des Hydrosystèmes Naturels et Anthropisés, UMR 5023, CNRS, Université Claude Bernard Lyon 1, 6 rue Dubois, Campus scientifique de la DOUA, Villeurbanne F-69622, France.

Chapitre 4

Changements environnementaux et formation de sapropèles au Pliocène supérieur du sud-ouest de la Sicile mis en évidence par les alcénones et les assemblages de nannofossiles

Ce chapitre s'intéresse au Pliocène supérieur (Piacenzien; 3,6-2,6 Ma) des coupes de Punta Grande et Punta Piccola, affleurant au sud-ouest de la Sicile. Ces coupes font partie de la coupe composite Capo Rossello qui est considérée comme la référence pour la calibration orbitale du Pliocène méditerranéen (e.g., Hilgen, 1991; Lourens et al., 1996). Le Pliocène supérieur de Sicile est un cas d'étude particulièrement intéressant puisqu'il est caractérisé d'une part par l'apparition de deux nouveaux genres de Noëlaerhabdaceae, *Pseudoemiliania* et *Gephyrocapsa* (Kamptner, 1943; Gartner, 1969; Young, 1998), et d'autre part par la présence cyclique de niveaux riches en matière organique (sapropèles).

La comparaison entre les flux des différentes espèces de coccolithes et du contenu en alcénones de la coupe composite Punta Grande/Punta Piccola suggère que *Reticulofenestra minutula* était un producteur majeur d'alcénones à ce site, bien que la contribution d'autres espèces de Noëlaerhabdaceae apparentées (comme *Pseudoemiliania lacunosa*) ne puisse être exclue. Un changement dans le profil de distribution des alcénones, montrant des proportions plus élevées des alcénones $EtC_{38:2}$ et $EtC_{39:2}$ dans certaines sapropèles (S102, S107 et S112), pourrait témoigner de conditions de stress, tel qu'un appauvrissement en nutriments pendant le dépôt de ces niveaux particuliers. Le fait que *R. minutula* soit phylétiquement proche des espèces productrices actuelles d'alcénones permet l'utilisation de l'index $U^{K'}_{37}$ dans ces sédiments pliocènes pour l'estimation des températures des eaux océaniques de surface (SSTs).

Les variations de SSTs reconstruites à partir de l'$U^{K'}_{37}$, des flux de carbone organique total (COT) et des flux de nannofossiles, sont utilisées pour discuter des conditions environnementales caractérisant le Pliocène supérieur de Punta Grande/Punta Piccola. Cette coupe comprend deux séries de sapropèles qui semblent avoir des mécanismes de formation distincts. La formation des sapropèles S101-S112 peut s'expliquer par une meilleure préservation de la matière organique, due au développement d'une stratification thermohaline de la colonne d'eau et la formation d'eaux de fond appauvries en oxygène, tandis que les sapropèles A3-A5 ont probablement été formées à cause d'une augmentation de la productivité primaire.

Paleoenvironmental changes and related sapropel formation during the Piacenzian (late Pliocene) of the Punta Grande/Punta Piccola composite section (southwest Sicily) as inferred from alkenones and nannofossil assemblages

Julien Plancq*, Emanuela Mattioli, Bernard Pittet and Vincent Grossi

Laboratoire de Géologie de Lyon : Terre, Planètes, Environnement (UMR 5276), CNRS, Université Lyon 1, Ecole Normale Supérieure Lyon, Campus scientifique de la DOUA, Villeurbanne Cedex, France.

* Corresponding author : Laboratoire de Géologie de Lyon, UMR 5276, CNRS, Université Lyon 1, Campus de la DOUA, Bâtiment Géode, 69622 Villeurbanne Cedex, France. Tel.: +33 4 72431544.
E-mail address: plancq@pepsmail.univ-lyon1.fr (J. Plancq)

In preparation

Abstract

A careful evaluation of the most likely ancient alkenone producers is essential to ensure the reliability of alkenone-based sea-surface temperature (SST) estimates in sediments predating the first occurrence of modern alkenone producers (i.e. *Emiliania huxleyi* and *Gephyrocapsa oceanica*). This study investigates ancient alkenone producers among the late Pliocene (Piacenzian) coccolithophores at Punta Grande/Punta Piccola composite section (southwest Sicily, western Mediterranean). The comparison between coccolith species-specific fluxes and alkenone contents shows that *Reticulofenestra minutula* was a major alkenone producer, although the contribution to alkenone production of other Noelaerhabdaceae species (such as *Pseudoemiliania lacunosa*) is likely. Interestingly, a change in alkenone profile, with higher proportions of $EtC_{38:2}$ and $EtC_{39:2}$ alkenones, in some sapropels (S102, S107 and S112) may attest for stressing growth conditions, like significant nutrient depletion, during the deposition of these peculiar levels. The fact that *R. minutula* is phyletically close to modern alkenone producer species allows the application of the $U^{K'}_{37}$ index to late Pliocene sediments for estimation of sea surface temperatures. Variations in alkenone-based SST, coupled with variations in total organic carbon (TOC) and nannofossil fluxes, are thus used to discuss the environmental conditions prevailing during the late Pliocene of the Punta Grande/Punta

Piccola composite section. This section exhibits two series of organic-rich sedimentary layers (so-called sapropels) which can be explained by distinct mechanisms of formation. Whereas sapropels S101-S112 are likely due to a better preservation of organic matter, due to the development of a thermohaline stratification of the water column and to oxygen depleted bottom waters, sapropels A3-A5 were likely formed thanks to enhanced primary productivity.

1. Introduction

In modern oceans, alkenones are produced by a few extant unicellular haptophyte algae belonging to the Isochrysidales clade, which includes the cosmopolitan calcifying haptophytes (coccolithophores) *Emiliania huxleyi* and *Gephyrocapsa oceanica* (Marlowe et al., 1984; Volkman et al., 1980, 1995). Certain non-calcifying Isochrysidales, such as *Isochrysis galbana*, also produce alkenones but they are restricted to coastal areas and are not considered as an important source of alkenone in the open ocean (Marlowe et al., 1990). The alkenone unsaturation index $U^{K'}_{37}$ exploits the link between the production of di- and tri-unsaturated C_{37} alkenones ($C_{37:2}$ and $C_{37:3}$, respectively) and the producing species growth temperature (Brassell et al., 1986; Prahl and Wakeham, 1987), and has been used as a proxy to reconstruct past sea-surface temperatures, especially during the Quaternary period (e.g., Müller et al., 1998; Eltgroth et al., 2005; Pahnke and Sachs, 2006; Bolton et al., 2010).

The alkenone-based temperature proxy has been calibrated on coccolithophore cultures (*E. huxleyi* and *G. oceanica*) and Quaternary sediments (e.g. Conte et al., 1995, 1998; Müller et al., 1998; Popp et al., 1998; Riebesell et al., 2000), but there is a huge gap between the first record of alkenones in the Cretaceous at ~120 Ma (Farrimond et al., 1986; Brassell et al., 2004) and the first occurrence of the modern alkenone producers (-0.27 Ma for *E. huxleyi*, Thierstein et al., 1977, and -1.85 Ma for *G. oceanica,* Pujos-Lamy, 1977). Since *E. huxleyi* and *G. oceanica* cannot be responsible for alkenone production during most of the Cenozoic, the biological sources of alkenones preserved in pre-Quaternary sediments need to be elucidated in order to better constrain paleoenvironmental reconstructions based on the alkenone paleothermometer. Based on the consistent co-occurrence of *Reticulofenestra* coccoliths and alkenones in marine sediments dating back to the Eocene (45 Ma), Marlowe et al. (1990) suggested that the most probable Cenozoic alkenone producers are to be found within the genus *Reticulofenestra*, which belongs to the Noelaerhabdaceae Family, the same as *Emiliania* and *Gephyrocapsa*. So far, only a few studies have interpreted *Reticulofenestra* species as alkenone producers during the early Pliocene (Beltran et al., 2011) and the early Pleistocene (Bolton et al., 2010). Recently, we demonstrated that another genus of the

Noelaerhabdaceae Family, namely *Cyclicargolithus*, was a major alkenone producer during the late Oligocene-early Miocene at Deep Sea Drilling Project (DSDP) Site 516 in the South Atlantic Ocean (Plancq et al., 2012).

The Piacenzian stage (late Pliocene; 3.6-2.59 Ma; Gradstein et al., 2012) of the Punta Grande/Punta Piccola composite section (southwest Sicily) constitutes an interesting case study. First, it represents a key period for the evolution of the Noelaerhabdaceae family with the first occurrence of the two genera *Pseudoemiliania* and *Gephyrocapsa* (Kamptner, 1943; Gartner, 1969; Young, 1998). Second, late Pliocene deposits from this section are characterized by carbonate-rich and carbonate-poor alternations, with regular intercalations of dark layers rich in organic matter (sapropels). Several studies have suggested that the formation of these sapropels was due to enhanced freshwater supplies to the Mediterranean Sea by river runoff linked to strengthening in the precessionally-controlled African monsoon (e.g., Cita et al., 1977; Rossignol-Strick, 1985; Béthoux, 1993; Foucault and Mélières, 1995, 2000; Combourieu Nebout et al., 2004). This increased continental influx promoted an increased primary productivity and, finally, an enhanced organic matter input to marine sediments (Pedersen and Calvert, 1990; Calvert and Pedersen, 1992) or, alternatively, improved organic matter preservation because of enhanced sea-water stratification and production of anoxic bottom waters (e.g., Cita et al., 1977; Béthoux, 1993). Also, a combination of the two processes (enhanced preservation and productivity) has been suggested (e.g., Rohling, 1994). Many of these paleoenvironmental, chemical and mineralogical studies have been performed on the late Pliocene (Piacenzian) sapropels from the Punta Piccola section. However, these studies have only been focused on a restricted number of sapropel layers (S104-S107) and the characterization of long-term paleoenvironmental changes throughout the Piacenzian has received little attention.

We thus propose to compare variations in sea-surface temperatures (SSTs) derived from the alkenone temperature proxy $U^{K'}_{37}$ with changes in nannofossil assemblages to describe paleoenvironmental changes throughout the Piacenzian of these Sicilian sections. Beltran et al. (2007) used the $U^{K'}_{37}$ at Punta Piccola section, but they only studied a limited time interval comprised between 3.01 and 2.95 Ma and they did not definitely identify the alkenone producers. Here, we investigate alkenone producers by comparing Noelaerhabdaceae species-specific fluxes with alkenone concentrations in the same sediments from the Punta Grande/Punta Piccola composite section. This allows the identification of *Reticulofenestra minutula* as being the major alkenone producers during the Piacenzian. The applicability of the $U^{K'}_{37}$ index to reconstruct temperature changes in Pliocene sediments is also discussed.

Then, variations in SSTs, coupled with variations in TOC and in nannofossil fluxes, allow characterizing long-term changes environmental conditions throughout the Piacenzian of this Sicilian section, and distinguishing two distinct mechanisms for the formation of sapropels S101-S112 and sapropels A3-A5.

2. Materials and methods

2.1. Geological setting and sampling

The Capo Rossello composite section (Cita and Gartner, 1973), located in the Caltanissetta basin (south-west of Sicily), is considered as the reference for the orbital calibration of the Pliocene timescale, thanks to an excellent stratigraphy based on magnetic and isotopic data, and on calcareous nannofossil record, and contains the stratotypes of both the Zanclean and the Piacenzian stages (Rio et al., 1984; Hilgen, 1991; Langereis and Hilgen, 1991; Lourens et al., 1996). The Punta Grande and Punta Piccola sections, outcropping along the south-west Sicilian coast near Agrigento (Figure 4-1), represent the upper part of the Capo Rossello composite section and contain the GSSP (Global Stratotype Section and Point) of the Zanclean/Piacenzian (early/late Pliocene) boundary, defined at the top of the lithological cycle 77 of Hilgen (1991) with an age of 3.6 Ma (Castradori et al., 1998). During the Pliocene, the studied sites were situated in an open marine slope-basin setting in the Sicily sill, at a water-depth of about 600-800 m (Brolsma, 1978; Sprovieri, 1986; Sgarrella et al., 2012).

The Punta Grande and Punta Piccola sections were logged and a total of 61 samples were collected with an average sampling spacing of 80 cm; biomarker and nannofossil analyses were conducted on the same samples (Figure 4-1). The Punta Grande section and the lower part (first 14 m) of the Punta Piccola section are characterized by marls and marly limestones of the Trubi Formation, that show cyclically deposited sequences (of approximately 1 m thickness), each corresponding to four successively grey, white, beige and white colored marly facies (Hilgen, 1987, 1991; Figure 4-1). The uppermost part of the Punta Piccola section comprises regular alternations of grey marls and light-grey marly limestones of the Monte Narbone Formation, with the cyclical occurrence of dark laminated (sapropel) marl layers noted S101 to S112 and A1 to A5 (Hilgen, 1991; Lourens et al., 1996; Sprovieri et al., 2006; Figure 4-1). The studied time interval spans the Piacenzian (late Pliocene; Lourens et al., 1996), from the Zanclean/Piacenzian boundary (3.6 Ma) to the Piacenzian/Gelasian boundary coincident with the sapropel A5 mid-point (2.59 Ma) (Figure 4-1).

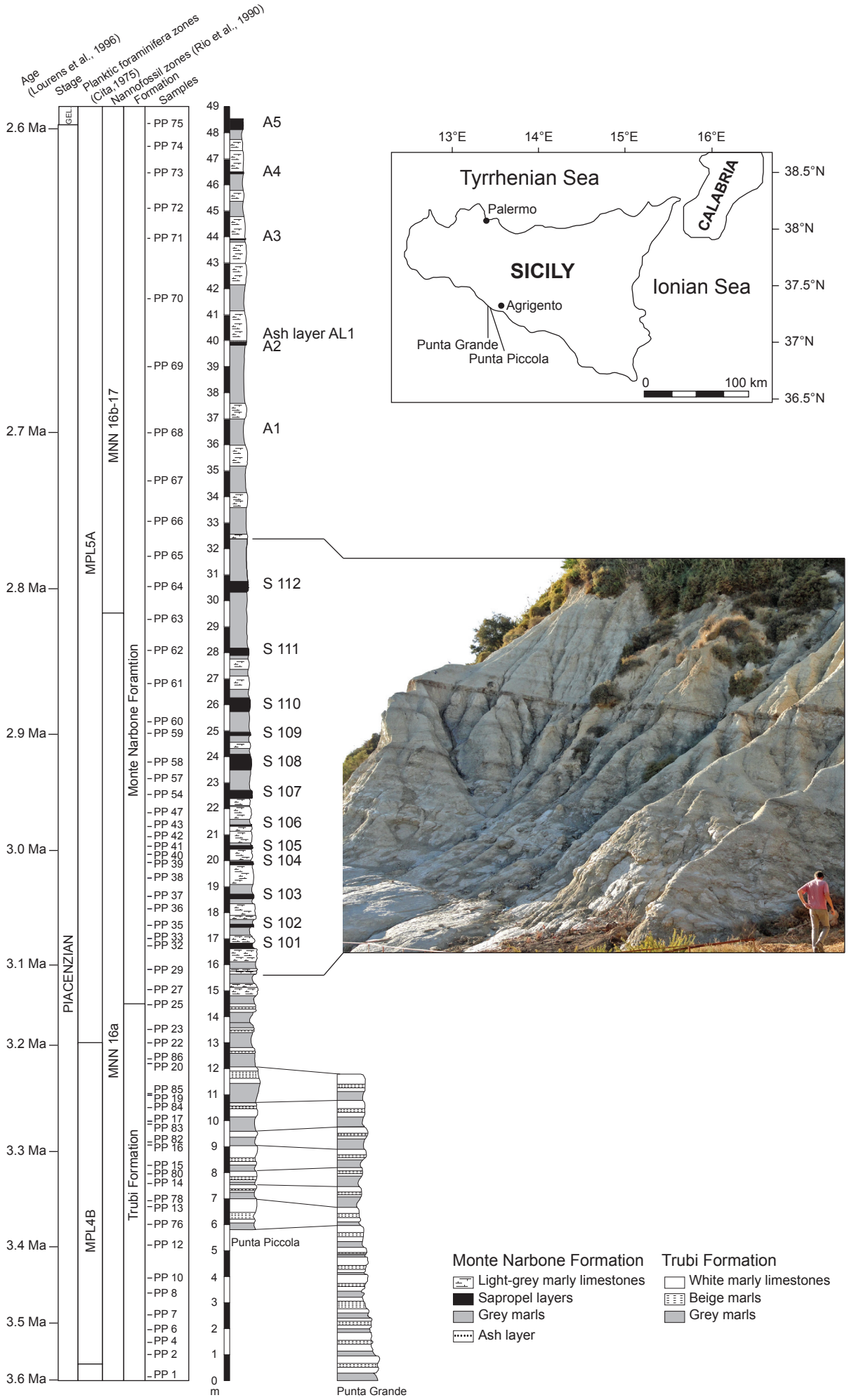

Figure 4-1. Location, picture and schematic log of the Punta Grande and Punta Piccola sections.

The Punta Grande/Punta Piccola composite section comprises the planktic foraminifera zones MPL4B and MPL5A (Cita, 1975) and the nannofossil zones MNN 16a and MNN 16b-17 (Rio et al., 1990). The sedimentation rate significantly increased at the top of the section, from 3.8 cm/kyr between 0 and 34.5 m (between 3.6 and ~2.7 Ma) to 11.7 cm/kyr between 34.5 and 48.4 m (between ~2.7 Ma and 2.6 Ma).

2.2. Micropaleontological analyses

Slides for calcareous nannofossil quantitative analysis were prepared following the Random Settling method (Beaufort, 1991; modified by Geisen et al., 1999). A small amount of dried sediment powder (10 mg) was mixed with water (with basic pH, over-saturated with respect to calcium carbonate) and the homogenised suspension was allowed to settle for 24 hours onto a cover slide. The slide was dried and mounted on a microscope slide with Rhodopass. Coccolith quantification was performed using a polarizing optical ZEISS microscope (magnification 1000x). A standard number of 400 calcareous nannofossils (coccoliths and nannoliths) were counted in a variable number (between 15 and 30) of fields of view.

Absolute abundance of nannofossils per gram of sediment was calculated using the formula:

$$X = (N.V)/(M.A.H) \quad (1)$$

where X is the number of calcareous nannofossils per gram of sediment; N the number of nannofossils counted in each sample; V the volume of water used for the dilution in the settling device (475 cm^3); M the weight of powder used for the suspension (g); A the surface considered for nannofossil counting (cm^2); H the height of the water over the cover slide in the settling device (2.1 cm). Species-specific relative abundances (percentages) were also calculated from the total nannofossil content.

2.3. Total Organic Carbon (TOC) analyses

Sub-samples (ca. 50 mg of ground samples) were acidified *in-situ* with HCl 2N in pre-cleaned (combustion at 450°C) silver capsules until effervescence ceased, dried in an oven (50°C) and wrapped in tin foil before analyses. Duplicate TOC analyses were performed with a Thermo FlashEA 1112 elemental analyzer using aspartic acid (36.09% of carbon) and nicotinamid (59.01% of carbon) as calibration standards. Accuracy was checked using in-house reference material (fine grounded low carbon sediment). The reproducibility achieved for duplicate analyses of all samples was better than 10% (coefficient of variation).

2.4. Alkenone analyses

Samples (ca. ~30g) were ground and extracted by way of sonication (5 x) using 40 mL of Dichloromethane (DCM). Following evaporation of the solvents, the total lipid extract was separated into four lipid fractions of increasing polarity by using chromatography over a solid phase extraction (SPE) silica-NH2 cartridge (0.5 g packing) with hexane (Hex), Hex/DCM (3:1 v/v), DCM/acetone (9:1 v/v) and Methanol (MeOH) as eluents, respectively. Alkenones, contained in the second fraction, were identified and quantified by gas chromatography/mass spectrometry (GC/MS) and gas chromatography (GC/FID), respectively. GC/MS analyses were performed on a MD800 Voyager spectrometer interfaced to an HP6890 gas chromatograph equipped with an on-column injector and a DB-5MS column (30 m x 0.25 mm x 0.25 μm). The oven temperature was programmed from 60°C (1 min) to 130°C at 20°C/min, and then to 310°C (20 min) at 4°C/min. Helium was used as the carrier gas at constant flow. GC/FID analyses were performed on a HP-6890 Series gas chromatograph configured with an on-column injector and a HP5 (30 m x 0.32 mm x 0.25 μm) capillary column. Helium was used as the carrier gas at constant flow and the oven temperature program was the same as for GC/MS analyses.

Alkenone concentrations were determined by GC/FID using hexatriacontane (*n*-C_{36} alkane) as internal standard. The global calibration of Conte et al. (2006), which is based on surface water data covering a wide range of modern-day oceanic environments and alkenone-synthesizing populations, was used to convert $U^{K'}_{37}$ values into sea-surface temperatures (SSTs). The internal precision of the temperature estimate is 0.2°C.

Following quantifications of alkenones, some alkenone fractions were reduced to the corresponding unsaturated alcohols (alkenols) using $NaBH_4$ as described by Rontani et al. (2011). The reduction of alkenones to their corresponding alkenols allows detecting small amounts of alkenones since alkenols display better chromatographic characteristics. Briefly, fractions containing alkenones were reduced in diethyl ether–methanol (2:1, v/v) using excess $NaBH_4$ (10 mg/mg extract). After addition of a saturated solution of ammonium chloride, alkenols were extracted with DCM (x 3) and the combined extracts were filtered over anhydrous Na_2SO_4, evaporated to dryness under N_2, silylated [pyridine/N,O-bis(trimethylsilyl)trifluoroacetamide (BSTFA), 2:1 v/v] and dissolved in hexane for analysis by GC/MS.

2.5. Data treatment

To overcome the effects of a variable sedimentary dilution on nannofossil and organic matter concentrations, coccolith abundances, TOC and alkenone amounts were expressed in fluxes (Figures 4-2 and 4-4). Fluxes (/cm^2/yr) were determined by multiplying the density of the calcite (g/cm^3) and the sedimentation rate (cm/yr) with the coccolith absolute abundances (specimens/g of sediment), organic matter content (g/g of sediment) and alkenone concentration (µg/g of sediment).

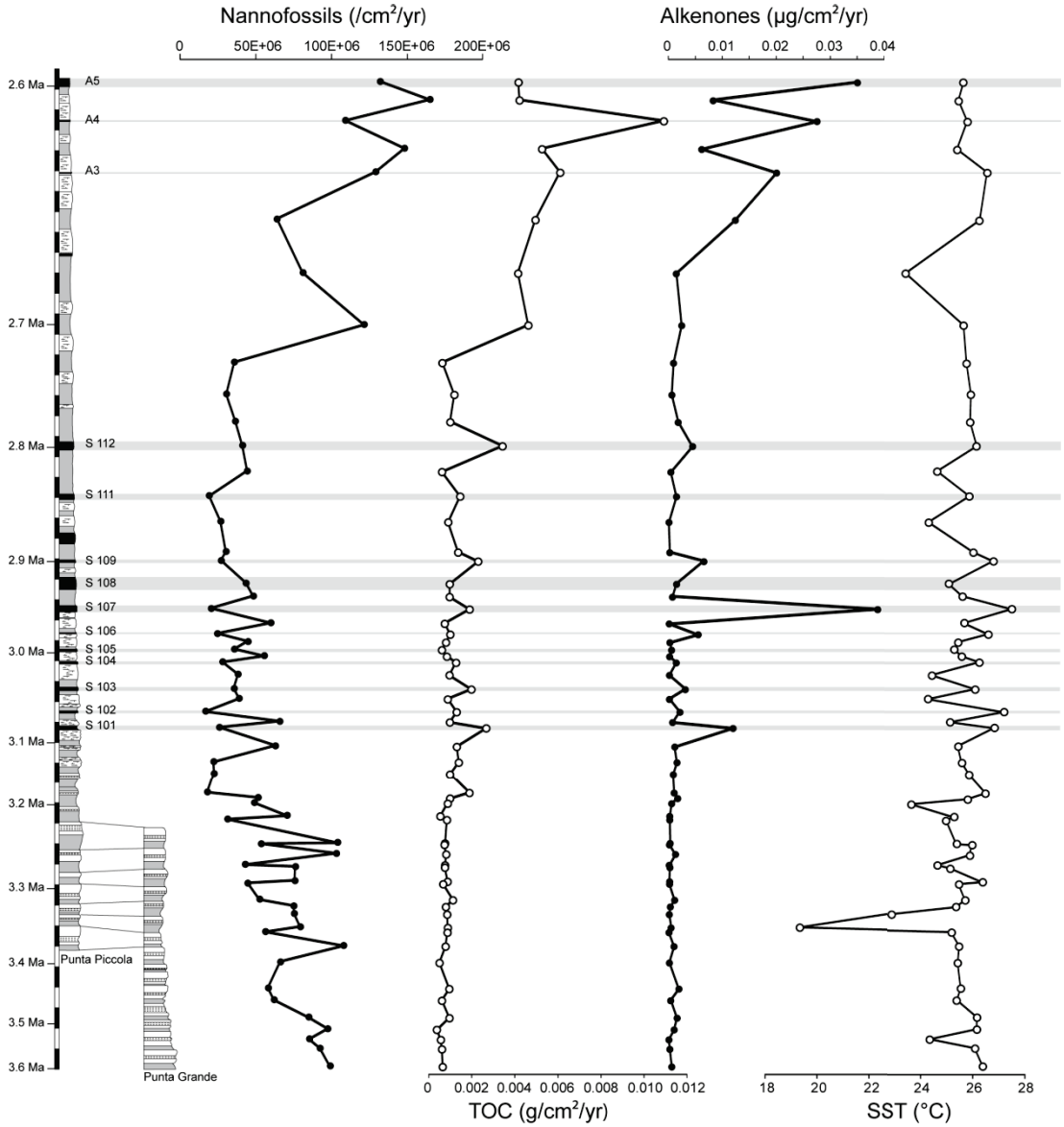

Figure 4-2. Variations in nannofossil flux (/cm^2/yr), total organic carbon (TOC) flux (g/cm^2/yr), total alkenone flux (µg/cm^2/yr), and alkenone-based sea-surface temperature (SST) values (°C) during the Piacenzian of Punta Grande/Punta Piccola composite section. Grey-shaded bands indicate sapropels studied in the present work (S101-S112 and A3-A5). The calibration used to convert $U^{K'}_{37}$ values into SSTs is the one presented by Conte et al. (2006).

3. Results

3.3. Coccolith assemblages

Coccoliths are well preserved in all samples investigated since delicate coccoliths that are prone to dissolution, such as *Syracosphaera* and *Pontosphaera*, are commonly observed with pristine structures.

The nannofossil flux (in average $61x10^6$ nannofossils/cm^2/yr) shows a significant stratigraphic trend across the Piacenzian. Between 3.6 and 3.1 Ma, fluxes are highly variable but a decreasing trend can be observed (from ~$96x10^6$ to ~$41x10^6$ nannofossils/cm^2/yr; Figure 4-2). Between 3.1 and 2.8 Ma, low fluxes are recorded ($38x10^6$ nannofossils/cm^2/yr in average), with even lower values in sapropels (in average of $27x10^6$ nannofossils/cm^2/yr) but they progressively increase afterwards (between 2.8 and 2.6 Ma) with values reaching $165x10^6$ nannofossils/cm^2/yr at the top of the section (Figure 4-2). Lower fluxes are observed in sapropels A4 and A5, but not in layer A3 (Figure 4-2).

Coccolith assemblages are dominated by two genera belonging to the Noelaerhabdaceae Family, namely *Reticulofenestra* and *Dictyococcites*, which account in average for 70% of the total nannofossil assemblage. *Reticulofenestra* is represented by the species *R. pseudoumbilicus*, *R. minutula* and *R. minuta*, and *Dictyococcites* by *D. antarcticus*, *D. hesslandii* and *Dictyococcites* spp. (specimens smaller than 3µm). The genus *Pseudoemiliania* is present in lower proportions (4% of the total nannofossil assemblage) and is only represented by the species *P. lacunosa*. Small *Gephyrocapsa* species (< 3µm) are also identified but these are statistically insignificant (<0.1%). The nannolith *Discoaster* spp. is present in low proportions (2% of the total nannofossil assemblage) but shows increased abundances (up to 10.5%) in sapropels S101, S102, S107 and S111 (Figure 4-3). Other nannofossil taxa (the coccoliths *Coccolithus*, *Umbilicosphaera*, *Helicosphaera*, *Pontosphaera*, *Calcidiscus*, *Scyphosphaera*, and the nannolith *Sphenolithus*) account together for 25% in average of the total nannofossil assemblage. These results are in disagreement with the study of Beltran et al. (2007) who reported that Punta Piccola sediments were dominated by *Pseudoemiliania lacunosa* and small *Reticulofenestra* species (< 5µm). These discrepancies are probably due to a much lower sampling resolution considered by Beltran et al. (2007) and to different preparation techniques and taxonomic concepts (see taxonomic remarks).

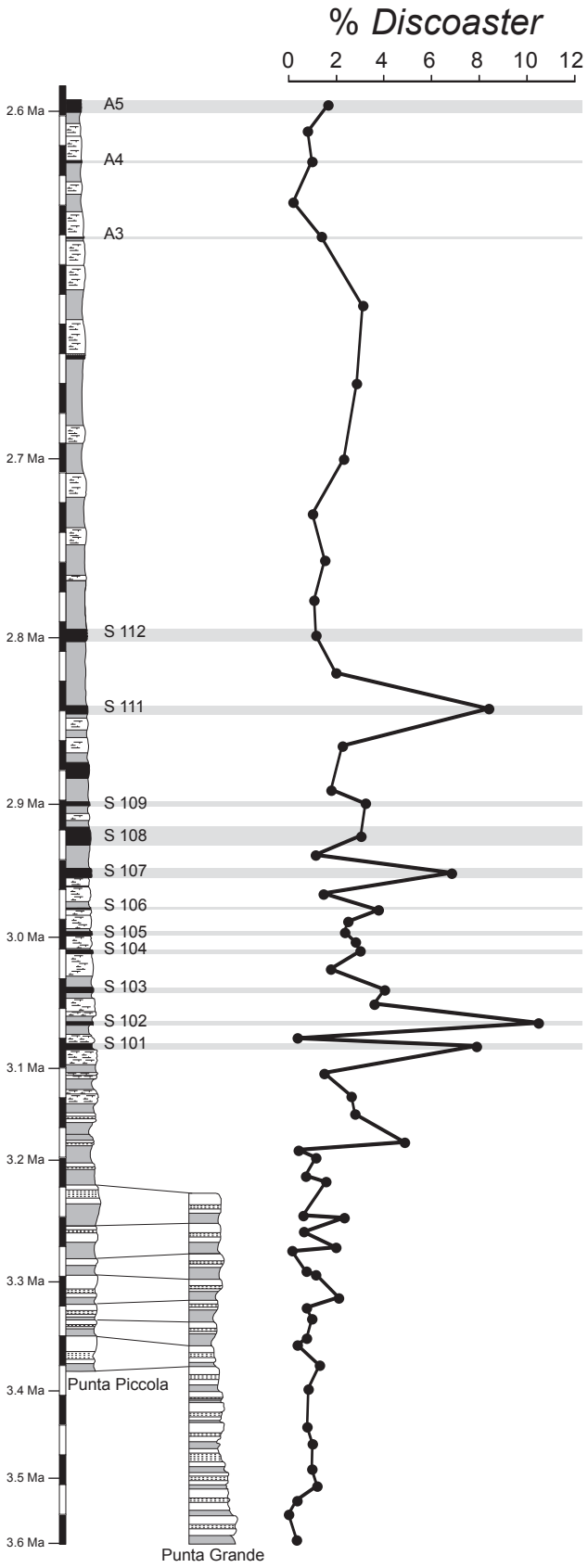

Figure 4-3. Variations in the relative proportions (%) of the oligotrophic nannolith *Discoaster* during the Piacenzian of Punta Grande/Punta Piccola composite section.

Fluxes of *Reticulofenestra* and *Dictyococcites* show overall similar temporal variations (Figure 4-4). The species *R. minutula* and *Dictyococcites* spp. also show similar variations since they are dominant within the *Reticulofenestra* and *Dictyococcites* pools, respectively (Figure 4-4).

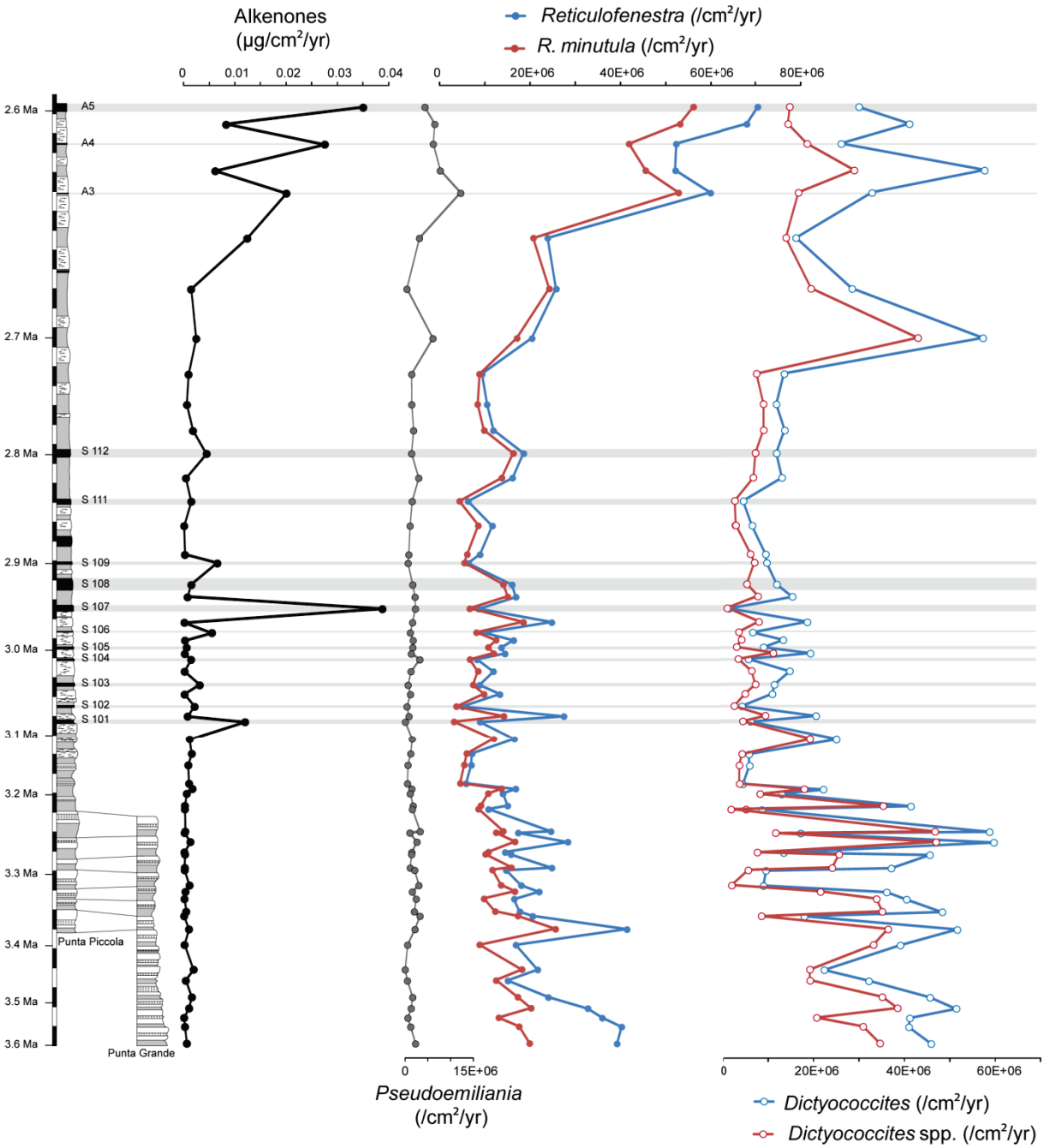

Figure 4-4. Comparison between total alkenone flux (µg/cm^2/yr) and fluxes (specimens/cm^2/yr) of the three dominant Noelaerhabdaceae genera in nannofossil assemblages (*Pseudoemiliania*, *Reticulofenestra* and *Dictyococcites*) during the Piacenzian of Punta Grande/Punta Piccola composite section. The species *R. minutula* and *Dictyococcites* spp. also show similar variations since they are dominant within the *Reticulofenestra* and *Dictyococcites* pools, respectively. The genus *Pseudoemiliania* is only represented by the species *P. lacunosa*.

Between 3.6 and 3.1 Ma, fluxes are highly variable (in average $21x10^6$ specimens/cm^2/yr for *Reticulofenestra* and $31x10^6$ specimens/cm^2/yr for *Dictyococcites*) but a strong decrease is observed at around 3.2 Ma, especially within the *Dictyococcites* genus (Figure 4-4). Fluxes are then significantly lower between 3.1 and 2.8 Ma (in average $13x10^6$ and $11x10^6$ specimens/cm^2/yr for *Reticulofenestra* and *Dictyococcites*, respectively), with even lower values recorded in sapropels (Figure 4-4). A significant increase is then recorded between 2.8 and 2.6 Ma, which is more pronounced for *Reticulofenestra* (up to $71x10^6$ specimens/cm^2/yr) compared to *Dictyococcites* (up to $58x10^6$ specimens/cm^2/yr). The genus *Pseudoemiliania* (only represented by the species *P. lacunosa*) presents relatively constant fluxes between 3.6 and 2.8 Ma ($2x10^6$ specimens/cm^2/yr), but a slight increasing trend is observed between 2.8 and 2.6 Ma (with values up to $12x10^6$ specimens/cm^2/yr) (Figure 4-4). Interestingly, contrarily to sapropels S101 to S112, overall higher coccolith fluxes (especially for *Reticulofenestra*) are recorded in sapropels A3-A5 (Figure 4-4).

3.2. TOC

The total organic carbon content of the samples show relatively low mean values (0.4%; 0.0016 g/cm^2/yr) with higher values (0.6%; 0.0031 g/cm^2/yr) recorded in the sapropels of the Monte Narbone Formation (except for S105, S108 and A5) (Figure 4-2).

TOC fluxes are relatively constant (0.0011 g/cm^2/yr) between 3.6 and 2.75 Ma (except in sapropels where TOC flux slightly increases, but they progressively increase upwards (from 2.75 to 2.6 Ma) with values reaching 0.0106 g/cm^2/yr at ~2.58 Ma (Figure 4-2).

3.3. Alkenones

Five major alkenones were present in all the samples, namely: heptatriacontatrien-2-one ($MeC_{37:3}$), heptatriacontadien-2-one ($MeC_{37:2}$), octatriacontadien-3-one ($EtC_{38:2}$), octatriacontadien-2-one ($MeC_{38:2}$) and nonatriacontatrien-3-one ($EtC_{39:2}$). The alkenone distribution differs in sapropels S102, S107 and S112 with higher proportions of $EtC_{38:2}$ (and also of $EtC_{39:2}$) and reduced proportions of $MeC_{37:2}$ (Figure 4-5). As previously demonstrated (Rontani et al., 2001, 2011), $NaBH_4$ reduction and silylation of alkenones to alkenol silyl ethers did not modify the distribution of the major alkenones present in the Punta Grande and Punta Piccola sediments, but allowed the identification of three additional alkenones (under their alkenol form), namely a $EtC_{40:x}$ alkenone and two co-eluting Me- and $EtC_{41:x}$ alkenones (Figure 4-5).

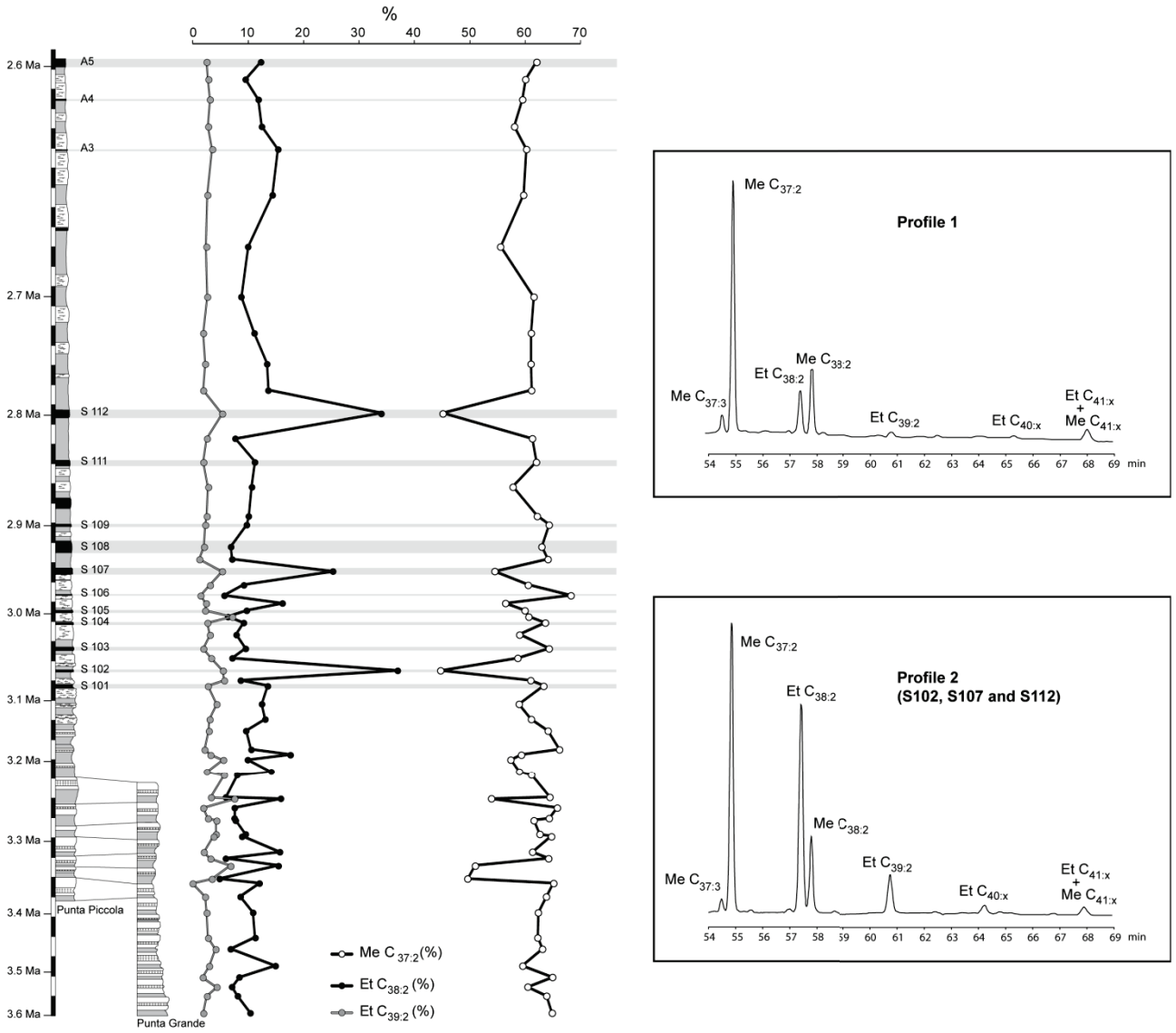

Figure 4-5. Variations in the relative proportions (%) of $MeC_{37:2}$, $EtC_{38:2}$ and $EtC_{39:2}$ alkenones at Punta Grande/Punta Piccola composite section. Almost all the studied sample show a similar alkenone distribution (Profile 1), except sapropels S102, S107 and S112 characterized by a distinct alkenone distribution with higher $EtC_{38:2}$ and $EtC_{39:2}$ alkenones (Profile 2). Profiles 1 and 2 presented in this figure are obtained after $NaBH_4$ reduction (Rontani et al., 2011), allowing the detection of $EtC_{40:x}$, $EtC_{41:x}$ and $MeC_{41:x}$ alkenones.

Overall, fluxes of alkenones match with those of TOC ($R^2 = 0.42$; $p < 0.0001$). The total flux of these ketones is relatively low (0.0035 µg/cm^2/yr in average), but higher values are recorded in the sapropels, reaching up to 0.0358 µg/cm^2/yr for sapropelic layer S107 (Figure 4-2). Alkenone fluxes remain relatively constant (0.0019 µg/cm^2/yr) between 3.6 and 2.8 Ma

(except peaks observed in the sapropels), but they increase afterwards with values reaching 0.0351 µg/cm^2/yr (Figure 4-2).

The $U^{K'}_{37}$ ratios show higher values in sapropels (between 0.88 and 0.96) compared with non-sapropels (between 0.63 and 0.93). No significant stratigraphic trend is observed in sea-surface temperature estimates throughout the studied time interval. SSTs range between 25.3°C and 27.5°C for the sapropels and between 19.3°C and 26.5°C for the non-sapropelic intervals (Figure 4-2). These results are in good agreement with those of Beltran et al. (2007), who only studied cycles 104 to 107 of Langereis and Hilgen (1991), and with paleoclimatic modelling experiments for this period (e.g., Haywood et al., 2000, 2002). It should be noted that sapropels S101-S112 record almost systematically higher temperatures compared with non-sapropels (1°C of difference in average) while no significant increase in temperature is observed within sapropels A3-A5 (Figure 4-2).

4. Discussion

4.1. Putative alkenone producers at Punta Grande/Punta Piccola composite section and applicability of the $U^{K'}_{37}$ index to Pliocene sediments

In order to ensure the applicability of the $U^{K'}_{37}$ index in Pliocene sediments, it is essential to identify ancient alkenone producers. Nannofossil species-specific abundances were thus compared with the alkenone content of the same samples of the Punta Grande/Punta Piccola composite section. A similar approach has already been used to identify alkenone producers in sediments of late Quaternary (e.g. Müller et al., 1997; Weaver et al., 1999), Pliocene (e.g. Bolton et al., 2010; Beltran et al., 2011) and Oligocene-Miocene ages (Plancq et al., 2012).

The overall similar variations between the total alkenone content and the abundances of *Reticulofenestra* of the present composite section (Figure 4-4) suggest that this genus contributed significantly to alkenone production during the Piacenzian. More precisely, alkenone production seems to have been mainly supported by *Reticulofenestra minutula*, which accounts for the majority of the *Reticulofenestra* genus abundance trend (Figure 4-4). This is in good agreement with the results of Beltran et al. (2011) who argued that the alkenone production during the early Pliocene of Sicily (between 4.66 and 4.38 Ma) was mainly supported by *Reticulofenestra* species smaller than 5 µm (corresponding to *R. minuta* and *R. minutula*). Bolton et al. (2010) also identified the genus *Reticulofenestra* as the

principal alkenone producer during the late Pliocene (2.6-2.4 Ma) of the eastern equatorial Pacific and Atlantic oceans.

Still, it is possible that a better preservation of coccoliths compared to alkenones has led to an underestimation of the contribution of *Reticulofenestra minutula* to alkenone production. Even though alkenones are among the most refractory biolipids to degradation (Sun and Wakeham, 1994; Gong and Hollander, 1997, 1999), a significant loss of alkenones occurs in the water column and during early sediment diagenesis (e.g., Prahl et al., 1989; Conte et al., 1992; Madureira et al., 1995). This may partly explain why *R. minutula* only explains 27% of the total variance of alkenone concentration, as attested by a linear regression between *R. minutula* and alkenone fluxes ($R^2 = 0.27$, $p < 0.0001$).

This low correlation coefficient might also be explained by the discrepancy between alkenone and coccolith contents in sapropels S101 to S112, where higher alkenone concentrations are coupled to lower coccolith abundances. Indeed, a better correlation ($R^2 = 0.37$, $p < 0.0001$) is obtained when sapropels are not considered. Such discrepancies could be explained by an ecological response to environmental factors. Using cultures of *Emiliania huxleyi*, Sorrosa (2012) showed that a change of growth temperature from 20°C to 10°C enhanced the alkenone production and reduced the cell number (and thus the number of coccoliths). Here, alkenone-based temperature estimates systematically increase in sapropels S101 to S112 (see section 3.3), suggesting that variations in temperature are not responsible for the discrepancies observed between alkenones and coccoliths. Besides that, a distinct alkenone profile, with higher proportions of $EtC_{38:2}$ and $EtC_{39:2}$ alkenones coupled to lower proportions of $MeC_{37:2}$ alkenone, is observed in sapropels S102, S107 and S112 (Figure 4-5). Interestingly, this change in alkenone profiles may testify for the occurrence of stressing conditions during the formation of these peculiar levels. Culture experiments of *E. huxleyi* and *G. oceanica* have indeed shown that, under nutrient depletion, relative proportions of MeC_{37} alkenones decrease while those of Me- and EtC_{38} and EtC_{39} ethyl increase, and that the cellular alkenone concentration increases steadily by a factor of three (Conte et al., 1998; Epstein et al., 1998; Prahl et al., 2003; Eltgroth et al., 2005). These experimental observations, which confirm the role of alkenones as intracellular energy storages (Pond and Harris, 1996; Epstein et al., 2001), would thus suggest that very oligotrophic (nutrient depletion) conditions in surface Mediterranean waters occurred during the deposition of the sapropels S102, S107 and S112. This interpretation is coherent with the record of high alkenone concentrations and low nannofossil abundances in these peculiar levels.

It is also possible that other taxa have contributed to alkenone production. The lack of correlation between alkenone content and other Noelaerhabdaceae species (*P. lacunosa*, *R. pseudoumbilicus*, *R. minuta*, *D. antarcticus*, *D. hesslandii* and *Dictyococcites* spp.) does not necessarily demonstrate that they did not contribute to alkenone production at Punta Piccola. This assumption is further supported by a multiple linear regression which shows a positive and significant correlation between all the Noelaerhabdaceae species and the alkenone content ($R^2 = 0.49$; $p < 0.0001$). Also the contribution to alkenone production of non-calcifying haptophytes, for which there is no mineralized fossil record, cannot be totally excluded at Punta Grande/Punta Piccola composite section.

The use of the $U^{K'}_{37}$ index to reconstruct paleo sea-surface temperatures in Pliocene sediments raises some questions since *R. minutula* may have reacted differently to variations in temperature compared to the contemporary alkenone producers (*Emiliania huxleyi* and *Gephyrocapsa oceanica*). A genetic relationship between ancient and modern alkenone producers can be inferred by using alkenone indices such as the U^{K}_{38Me} index (defined as the ratio between $C_{38:2}$ and $C_{38:3}$ methyl alkenones; Conte and Eglinton, 1993) and the U^{K}_{38Et} index (defined as the ratio between $C_{38:2}$ and $C_{38:3}$ ethyl alkenones; Conte et al., 1998). For example, Beltran et al. (2011) used these indices in early Pliocene sediments to show that *R. minutula* and *R. minuta* are genetically related to modern producers. Here, the absence of $C_{38:3}$ ethyl and methyl alkenones in the studied samples does not allow the calculation of these specific alkenone indices. However, the work of Beltran et al. (2011) as well as molecular (Fujiwara et al., 2001; Sáez et al., 2004) and micropaleontological data (Marlowe et al., 1990; Young, 1990, 1998; Young and Bown, 1997) already suggested very close evolutionary relationships between *E. huxleyi* and *G. oceanica* and their Cenozoic ancestors, such as *Reticulofenestra* and *Pseudoemiliania*. In addition, even though a few studies showed that the calibration of the $U^{K'}_{37}$ ratio is species-dependent (e.g., Conte et al., 1995, 1998; Epstein et al., 1998; Popp et al., 1998; Yamamoto et al., 2000), genetically-related factors are believed to have only a little impact on the alkenone unsaturation of the open-ocean producers (Müller et al., 1997, 1998; Villanueva et al., 2002; Conte et al., 2006). Since *Reticulofenestra* species are phyletically close to modern alkenone producers, the $U^{K'}_{37}$ index can be used with confident in late Pliocene sediments.

4.2. Environmental changes and related sapropel formation at Punta Grande/Punta Piccola composite section

We used variations in nannofossil assemblages, total organic carbon (TOC) content and alkenone-based sea-surface temperatures to characterize long-term changes in environmental conditions and to discuss environmental conditions prevailing during the formation of sapropels S101-S112 and sapropels A3-A5. This allowed distinguishing three intervals throughout the Piacenzian of Punta Grande/Punta Piccola composite section. In addition, two distinct mechanisms are proposed for the formation of sapropels S101-S112 and sapropels A3-A5.

4.2.1. Before the occurrence of sapropel layers (~3.6-3.1 Ma)

This interval is characterized by alternations of marls and marly limestones without the occurrence of sapropel layers (Figure 4-1). Nannofossil fluxes, in particular the mesotrophic species *Reticulofenestra minutula* and *Dictyococcites* spp. (smaller than 3 μm) (Flores et al., 2005), show relatively high fluxes with important fluctuations (Figures 4-2 and 4-4) whereas abundances of the oligotrophic nannolith *Discoaster* (e.g., Flores et al., 1992, 1995; Vázquez et al., 2000) are low. Nannofossil assemblages would thus suggest overall mesotrophic conditions but the relatively low TOC fluxes rather indicate intermediate levels of primary productivity during this period. Benthic foraminiferal assemblages corroborate these observations, since they indicate an oligotrophic environment with short periods of enhanced productivity (Sgarrella et al., 2012). Besides this, the decreasing trend observed in nannofossil flux would attest for a progressive change in trophic conditions (from relatively mesotrophic to oligotrophic) throughout this time interval. SSTs show no peculiar stratigraphic trend during this period (Figure 4-2), but a sharp decrease in SST (19°C) is recorded at ~3.35 Ma. This cooling may correspond to a sporadic event of upwelling of deep and cold waters, which could have brought nutrients to the surface waters. However, this hypothesis is not supported by higher nannofossil or TOC fluxes (attesting for higher primary productivity). More data would be thus needed to explain this sharp SST decrease.

4.2.2. First occurrence of sapropel layers, S101-S112 (3.1-2.8 Ma)

This interval comprises regular alternations of grey marls and light-grey marly limestones, with the cyclical occurrence of sapropel layers noted S101 to S112. High variations are observed in SSTs, TOC and nannofossil fluxes between sapropel and non-sapropel levels.

However, the overall low nannofossil flux would attest for more oligotrophic conditions during this time interval with respect to the previous interval.

Sapropels S101-S112 are characterized by a systematic increase in alkenone-based reconstructed SSTs (except for S105 and S108), suggesting warmer conditions during their formation. This is in good agreement with previous studies that argued for higher temperatures in relation to these dark layers based on vegetation marker analyses (Combourieu Nebout et al., 2004), alkenone unsaturation index (Beltran et al., 2007) and foraminiferal assemblages (e.g., Sprovieri et al., 2006). The deposition of these sapropels has also been related to times of precession minima, implying stronger summer conditions as a consequence of enhanced insolation (Hilgen, 1991; Lourens et al., 1996).

Previous studies (e.g., Van Os et al., 1994; Daux et al., 2006) supported the hypothesis of an enhanced primary productivity during the formation of sapropels S101-S112 at Punta Piccola. For instance, Daux et al. (2006), based on manganese concentrations, suggested that the deposition of the sapropelic layer S107 took place under oxygenated bottom waters, implying that their high organic matter content is more likely the result of higher organic production, in response to important supply of continental nutrients, rather than the result of enhanced organic matter preservation due to water column stratification. In the present study, variations in nannofossil fluxes are not in agreement with an increase in productivity during the formation of S101 to S112. Conversely, the systematic decrease in nannofossil fluxes, and particularly in the mesotrophic species *R. minutula*, *R. minuta* and *Dictyococcites* spp. (Flores et al., 2005), likely indicates the development of oligotrophic sea-surface waters (Figure 4-4). This is supported by an increase in the relative abundance of the oligotrophic nannolith *Discoaster* (e.g., Flores et al., 1992, 1995; Vázquez et al., 2000) in most sapropels S101 to S112 (Figure 4-3). It is important to notice that this change in nannofossil assemblages is unlikely the result of enhanced dissolution within sapropel layers. Several studies have evidenced dissolution of foraminifera and calcareous nannofossils in eastern Mediterranean sapropels (e.g., Negri et al, 2003; Principato et al., 2005; Crudeli et al, 2006) and *Discoaster* is thought to be more resistant to dissolution than *R. minutula or Dictyococcites* spp. (Lohman and Carlson, 1981). At Punta Grande/Punta Piccola composite section, observations under optical and scanning electron microscopes show well preserved calcareous nannofossils in both sapropel and non-sapropel layers, with only a small degree of etching and/or overgrowth (Sprovieri et al., 2006; Beltran et al., 2007, 2009; this study). This implies that the abundance decrease in *R. minutula-R. minuta* coupled to the abundance increase in *Discoaster* is more likely an ecological response to oligotrophic conditions rather than enhanced dissolution.

The development of oligotrophy in sea-surface waters probably resulted from an effective thermohaline stratification of the water column and a lack of nutrient recycling in surface waters where photosynthesis occurred. A thermohaline stratification within sapropels S101-S112 is supported by (1) a systematic increase in alkenone-based SSTs (Figure 4-2) and (2) $\delta^{18}O$ depletions in planktonic foraminiferal shells attesting for the development of a low-salinity surface layer, subsequent to increased freshwater input (Vergnaud-Grazzini et al., 1977; Gudjonsson and van der Zwaan, 1985; Thunell and Williams, 1989; Tang and Stott, 1993; Beltran et al., 2007). This thermohaline stratification might also be responsible for an enhanced preservation of organic matter in sapropels, because it promoted reduced ventilation at the water-sediment interface. Anoxia may have never been reached in the bottom waters but benthic foraminiferal assemblages testify for hypoxic conditions (Sgarrella et al., 2012), which would explain the systematic higher TOC and alkenone contents recorded in these layers (Figure 4-2).

4.2.3. Sapropel layers A3-A5 (2.8-2.6 Ma)

Between 2.8 and 2.6 Ma, SSTs are more stable. The progressive but significant increases in nannofossil fluxes, especially for the mesotrophic species *R. minutula*, and in alkenones and TOC fluxes (Figure 4-2) suggest a progressive increase in primary productivity under eutrophic conditions. This change from oligotrophic to eutrophic conditions has already been observed with planktic foraminifera and may reflect paleoceanographic changes linked to the intensification of Northern Hemisphere glaciations occurring at ~2.7 Ma (Lourens et al., 1996; Sprovieri et al., 2006).

Unlike sapropels S101-S112, sapropels A3-A5 are not characterized by significant increases in SSTs and in the relative abundance of *Discoaster* spp. (Figures 4-2 and 4-3). Also, *Reticulofenestra* and *Dictyococcites* species do not show a systematic abundance decrease within these peculiar levels. These observations do not support an effective thermohaline stratification of the water column as observed for sapropels S101-S112. High *Reticulofenestra* fluxes in sapropel A3 and A5 (Figure 4-4) would attest for an increased productivity during the deposition of these dark layers, probably linked to increased terrigenous input to marine sedimentation. This interpretation is supported by planktic and benthic foraminiferal assemblages that indicate eutrophic sub-surface waters, even though periods of surface water stratification have also been suggested to sporadically occur (Sprovieri et al., 2006; Sgarrella et al., 2012).

The mechanisms responsible for the formation of sapropels A3-A5 seem thus to be distinct from those explaining the formation of sapropels S101-S112. First, sapropels A3-A5 were formed under overall enhanced primary productivity and thermohaline stratification whereas overall sea-surface oligotrophy prevailed during the formation of sapropels S101-S112. In addition, the input of freshwater into the Mediterranean Sea likely induced a thermohaline stratification intensifying sea surface oligotrophy, and also explaining the formation of sapropels S101-S112. This stratification was probably not effective during the deposition of sapropels A3-A5, suggesting that their formation is more likely the result of enhanced productivity.

5. Conclusion

The comparison between nannofossil and alkenone fluxes in the Piacenzian (late Pliocene) of the Punta Grande/Punta Piccola composite section shows that the species *Reticulofenestra minutula* was a major alkenone producer between 3.6 and 2.6 Ma. Also, the contribution to alkenone production of related Noelaerhabdaceae species (such as *Pseudoemiliania lacunosa*) cannot be totally excluded at Punta Grande/Punta Piccola. Interestingly, a change in alkenone profile, with higher proportions of $EtC_{38:2}$ and $EtC_{39:2}$ alkenones, is observed in some sapropels (S102, S107 and S112), which likely attests for a physiological adaptation in response to a nutrient depletion (very oligotrophic surface waters). The major alkenone producer in these Sicilian sections (*R. minutula*) is phyletically close to modern alkenone producers, implying that genetic differences between ancient and modern producers are expected to have only a minimal influence on the alkenone unsaturation ratio $U^{K'}_{37}$. This allows the application of the $U^{K'}_{37}$ index in these Pliocene sediments.

Variations in alkenone-based sea-surface temperatures (SSTs), nannofossil assemblages and total organic carbon (TOC) content allow distinguishing three intervals of varying sea-surface trophic conditions: meso-oligotrophic conditions between 3.6 and 3.1 Ma, more oligotrophic conditions between 3.1 and 2.8 Ma, and meso-eutrophic conditions between 2.8 and 2.6 Ma. Variations in SSTs, TOC and nannofossils also testify for two distinct mechanisms for the formation of sapropels S101-S112 and for sapropels A3-A5. Thus, a better preservation of organic matter, due to the development of thermohaline stratification and hypoxic (oxygen depleted) bottom waters, likely occurred during the deposition of S101-S112 layers, while an enhanced primary productivity better explains the formation of A3-A5 layers.

Appendix A: Taxonomic remarks

Taxonomy used in the present work follows Haptophyte phylogeny as revised by Young and Bown (1997) and Sáez et al. (2004).

A1. Noelaerhabdaceae Family

Noelaerhabdaceae (Jerkovic, 1970 emended by Young and Bown, 1997) is the dominant Family in most Neogene assemblages and is considered as the Cenozoic ancestor of the modern alkenone producers *Emiliania* and *Gephyrocapsa*.

A1.1. Genus *Reticulofenestra* Hay, Mohler and Wade 1966

Elliptical to sub-circular coccoliths with a prominent open central area and with no slits in the distal shield. The rather simple morphology of *Reticulofenestra* makes subdivision into species notoriously problematic. The conventional taxonomy is primarily based on size. This is unsatisfactorily and arbitrary, but of stratigraphic value (Backman, 1980; Young et al., 2003). In this study, a subdivision of four size-defined species was employed during the assemblage counts:

Reticulofenestra haqii Backman 1978: morphospecies 3-5 μm in length, with a central opening shorter than 1.5 μm.

Reticulofenestra minuta Roth 1970: morphospecies smaller than 3 μm.

Reticulofenestra minutula (Gartner, 1967) Haq and Berggren, 1978: morphospecies 3-5 μm in length with a central opening longer than 1.5 μm.

Reticulofenestra pseudoumbilicus (Gartner 1967) Gartner 1969: larger morphospecies (5-7 μm).

A1.2. Genus *Dictyococcites* (Black 1967) emend. Backman 1980

Elliptical coccoliths with a large central area closed (or virtually closed) in line with the distal shield. The central area of the distal shield frequently shows a median furrow or a minute pore, but not large enough to suggest that they belong to *Reticulofenestra*. Although *Dictyococcites sensu* Black (1967) can be regarded as a heavily calcified, junior synonym of *Reticulofenestra*, the emended diagnosis of Backman (1980) clearly separates this genus from *Reticulofenestra*.

Dictyococcites spp.: small morphospecies (< 3 μm) with a supposedly closed central area.

Dictyococcites antarcticus Haq 1976: in contrast with *D. hesslandii*, the specimens of *D. antarcticus* (4-8 μm) show no pore but a narrow and elongated rectangular central area (named "furrow" in *Haq*, 1976 and "straight band" in *Backman*, 1980). The straight extinction band along the major axis occupies at least one half of the total length of the elliptical central area [*Backman*, 1980].

Dictyococcites hesslandii (Haq 1966) Haq and Lohmann, 1976: the central area of the distal shield exhibits a small pore, from which extinction bands radiate (3-8 μm). Two morphometric size classes were distinguished in this study (3-5 μm and >5 μm).

A1.3. Genus *Pseudoemiliania* Gartner 1969

Circular to sub-circular coccoliths with a variable number of slits in the distal shield. Only one species has been identified in this study:

Pseudoemiliania lacunosa (Kamptner, 1963) Gartner, 1969

A1.4. Genus *Gephyrocapsa* Kamptner 1943

Elliptical coccoliths with a structure similar to those of *Reticulofenestra*, but with conjunct bridge, formed from inner tube-elements spanning the central area.

Small *Gephyrocapsa*: morphospecies smaller than 3 μm.

A2. Other coccoliths

Calcidiscus leptoporus (Murray and Blackman, 1898) Loeblich and Tappan, 1978

Calcidiscus macintyrei (Bukry and Bramlette, 1969) Loeblich and Tappan, 1978

Coccolithus pelagicus (Wallich 1877) Schiller 1930

Helicosphaera spp. Kamptner 1954

Pontosphaera spp. Lohmann 1902

Rhabdosphaera spp. Haeckel 1894

Scyphosphaera spp. Lohmann 1902

Syracosphaera pulchra Lohmann 1902

Umbilicosphaera spp. Lohmann 1902

A3. Nannoliths

Discoaster Tan, 1927

Sphenolithus Deflandre in Grassé 1952

Acknowledgements

We warmly thank Antonio Caruso (University of Palermo, Italy) and Agata Di Stefano (University of Catania, Italy) for their help during the field trip in Sicily. We are also grateful to Laurent Simon (University of Lyon, France) who performed the TOC analyses.

References

Beaufort, L. (1991), Adaptation of the random settling method for quantitative studies of calcareous nannofossils, *Micropaleontology*, *37*, 415–418.

Beltran, C., M. de Rafélis, F. Minoletti, M. Renard, M.A. Sicre, and U. Ezat (2007), Coccolith $\delta^{18}O$ and alkenone records in middle Pliocene orbitally controlled deposits: high frequency temperature and salinity variations of sea surface water, *Geochem. Geophys. Geosyst.*, *8*. doi:10.1029/2006GC001483.

Beltran, C., M. de Rafélis, A. Person, F. Stalport, and M. Renard (2009), Multiproxy approach for determination of nature and origin of carbonate micro-particles so-called “micarb” in pelagic sediments, *Sed. Geol.*, *213*, 64–76.

Beltran, C., J.-A. Flores, M.-A. Sicre, F. Baudin, M. Renard, and M. de Rafélis (2011), Long chain alkenones in the Early Pliocene Sicilian sediments (Trubi Formation-Punta di Maiata section): implications for the alkenone paleothermometry, *Palaeogeogr. Palaeoclim. Palaeoecol*, *308* (3–4), 253–263.

Béthoux, J.P. (1993), Mediterranean sapropel formation, dynamic and climatic viewpoints, *Oceanologica Acta*, *16*, 127-133.

Bolton, C.T., K.T., Lawrence, S.J. Gibbs, P.A. Wilson, L.C. Cleaveland, D. Timothy, and T.D. Herbert (2010), Glacial-interglacial productivity changes recorded by alkenones and microfossils in late Pliocene eastern equatorial Pacific and Atlantic upwelling zones, *Earth Planet. Sci. Lett.*, *295*, 401-411.

Brassell, S.C., G. Eglinton, I.T. Marlowe, U. Pflaumann, and M. Sarnthein (1986), Molecular stratigraphy: a new tool for climatic assessment, *Nature*, *320*, 129-133.

Brassell, S.C., M. Dumitrescu, and the ODP Leg 198 Shipboard Scientific Party (2004), Recognition of alkenones in a lower Aptian porcellanite from the west-central Pacific, *Org. Geochem.*, *35*, 181-188.

Brolsma, M.J. (1978), Quantitative foraminiferal analysis and environmental interpretation of the Pliocene and topmost Miocene on the South coast of Sicily, *Utrecht Micropaleontol. Bull.*, *18*, 159 pp.

Calvert, S.E., and T.F. Pedersen (1992), Organic carbon accumulation and preservation in marine sediments: How important is anoxia? In *Productivity, accumulation and preservation of organic matter in recent and ancient sediments,* edited by J.K. Whelan, and J.W. Farrington, Columbia Univ. Press, New York, pp. 231-263.

Castradori, D., D. Rio, F.J. Hilgen, and L.J. Lourens (1998), The Global Standard Stratotype section and Point (GSSP) of the Piacenzian Stage (Middle Pliocene), *Episodes 21*, 88–93.

Cita, M.B. (1975), The Miocene-Pliocene boundary. History and definition, in *Late Neogene Epoch Boundaries*, edited by T. Saito, and L.H. Burckle, Spec. Publ., 1. Micropaleontol. Press, pp. 1–30.

Cita, M.B., and S. Gartner (1973), Studi sul Pliocene e sugli strati del passagio dal Miocene al Pliocene, IV. The stratotype Zanclean. Foraminiferal and nannofossil biostratigraphy, *Riv. Ital. Paleont. Stratigr.*, *79*, 503–558.

Cita, M. B., C. Vergnaud-grazzini, C. Robert, H. Chamley, N. Ciaranfi, and S. d'Onofrio (1977), Paleoclimatic record of a long deep sea core from the eastern Mediterranean, *Quat. Res.*, *8*, 205-235.

Combourieu-Nebout, N., A. Foucault, and F. Mélières (2004), Vegetation markers of palaeoclimate cyclical changes in the Pliocene of Punta Piccola (Sicily, Italy), *Palaeogeogr. Palaeoclim. Palaeoecol.*, *214*, 55–66.

Conte, M.H., and G. Eglinton (1993), Alkenone and alkenoate distributions within the euphotic zone of the eastern North Atlantic: correlation with production temperature, *Deep Sea Res. I*, *40*, 1935–1961.

Conte, M.H., G. Eglinton, and L.A.S. Madureira (1992), Long-chain alkenones and alkyl alkenoates as paleotemperature indicators: their production, flux and early sedimentary diagenesis in the Eastern North Atlantic, *Org. Geochem.*, *19*, 287–298.

Conte, M.H., M.-A. Sicre, C. Rühlemann, J.C. Weber, S. Schulte, D. Schulz-Bull, and T. Blanz (2006), Global calibration of the alkenone unsaturation index $U^{k'}_{37}$ with surface water production temperature and a comparison of the coretop integrated production temperatures recorded by $U^{k'}_{37}$ with overlying sea surface temperatures, *Geochem. Geophys. Geosyst.*, *72*, 1–22.

Conte, M.H., A. Thompson, and G. Eglinton (1995), Lipid biomarker diversity in the coccolithophorid *Emiliania huxleyi* (Prymnesiophycea) and the related species *Gephyrocapsa oceanica*, *J. Phycol.*, *31*, 272–82.

Conte, M.H., A. Thompson, D. Lesley, and R.P. Harris (1998), Genetic and physiological influences on the alkenone/alkenoate versus growth temperature relationship in *Emiliania huxleyi* and *Gephyrocapsa oceanica*, *Geochim. Cosmochim. Acta*, *62* (1), 51-68.

Crudeli, D., J.R. Young, E. Erba, M. Geisen, P. Ziveri, G.J. de Lange, and C.P. Slomp (2006), Fossil record of holococcoliths and selected hetero-holococcolith associations from the Mediterranean (Holocene-Late Pleistocene): Evaluation of carbonate diagenesis and paleoecological-paleocenographic implications, *Palaeogeogr. Palaeoclimatol. Palaeoecol*., *237* (2-4), 191-212.

Daux, V., A. Foucault, F. Mélières, and M. Turpin (2006), Sapropel-like Pliocene sediments of Sicily deposited under oxygenated bottom water, *Bull. Soc. Géol.*, *177*, 79–88.

Eltgroth, M.L., R.L. Watwood, and G.V. Wolfe (2005), Production and cellular localization of neutral long-chain lipids in the Haptophyte algae *Isochrysis galbana* and *Emiliania huxleyi*, *J. Phycology*, *41*, 1000-1009.

Epstein, B.L., S. D'Hondt, J.G. Quinn, J. Zhang, and P.E. Hargraves (1998), An effect of dissolved nutrient concentrations on alkenone-based temperature estimates, *Paleoceanography*, *13*, 122–126.

Epstein, B.L., S. D'Hondt, and P.E. Hargraves (2001), The possible role of C_{37} alkenones in *Emiliania huxleyi*, *Org. Geochem.*, *32*, 867-875.

Farrimond, P., G. Eglinton, and S.C. Brassell (1986), Alkenones in Cretaceous black shales, Blake-Bahama Basin, western North Atlantic, *Org. Geochem.*, *10*, 897-903.

Flores, J.-A., F.J. Sierro, G.M. Filippelli, M.Á. Bárcena, M. Pérez-Folgado, A. Vázquez, and R. Utrilla (2005), Surface water dynamics and phytoplankton communities during deposition of cyclic late Messinian sapropel sequences in the western Mediterranean, *Mar. Micropaleontol.*, *56*, 50-79.

Flores, J.A., F.J. Sierro, and G. Glaçon (1992), Calcareous plankton analysis in the preevaporitic sediments of the ODP site 654 (Tyrrhenian Sea, Western Mediterranean), *Micropaleontology*, *38*, 279–288.

Flores, J.A., F.J. Sierro, and I. Raffi (1995), Evolution of the calcareous nannofossil assemblage as a response to the paleoceanographic changes in the eastern equatorial Pacific Ocean from 4 to 2 Ma (Leg 138, Sites 849 and 852), *Proc. ODP Sci. Res.*, *138*, 163–176.

Foucault, A., and F. Mélières (1995), Nature et origine des cycles sédimentaires métriques du Pliocène de l'ouest méditerranéen d'après l'étude du contenu terrigène de la Formation Narbone (Punta Piccola, Sicile, Italie), *C. R. Acad. Sci. Paris, 321*, 869–876.

Foucault, A., and F. Mélières (2000), Palaeoclimatic cyclicity in central Mediterranean Pliocene sediments: the mineralogical signal, *Palaeogeogr. Palaeoclimatol. Palaeoecol.*, *158*, 311–323.

Fujiwara, S., M. Tsuzuki, M. Kawachi, N. Minaka, and I. Inouye (2001), Molecular phylogeny of the Haptophyta based on the *rbc*L gene and sequence variation in the spacer region of the rubisco operon, *J. Phycol.*, *37*, 121-129.

Gartner, S. (1969), *Hayella* Roth and *Hayella* Gratner, *Micropaleontology*, *15*, 490.

Geisen, M., J. Bollmann, J.O. Herrle, J. Mutterlose, and J.R. Young (1999), Calibration of the random settling technique for calculation of absolute abundance of calcareous nannoplankton, *Micropaleontology*, *45* (4), 437-442.

Gong, C., and D.J. Hollander (1997), Differential contribution of bacteria to sedimentary organic matter in oxic and anoxic environments, Santa Monica Basin, California, *Org. Geochem.*, *26*, 545-563.

Gong, C., and D.J. Hollander (1999), Evidence for the differential degradation of alkenones under contrasting bottom water oxygen conditions: Implication for paleotemperature reconstruction, *Geochim. Cosmochim. Acta*, *63*, 405-411

Gradstein, F.M., J.G Ogg, M. Schmitz, and G. Ogg (2012), *The Geologic Time Scale 2012*, Elsevier, 2012, 1176 pp.

Gudjonsson, L., and G.J. Van der Zwaan (1985), Anoxic events in the Pliocene Mediterranean, *Proc. K. Ned. Akad. Wet., Ser. B*, *88*, 69–82.

Haywood, A.M., B.W. Sellwood, and P.J. Valdes (2000), Regional warming: Pliocene (3 Ma) paleoclimate of Europe and the Mediterranean, *Geology*, *28*, 1063-1066.

Haywood, A.M., P.J. Valdes, and B.W. Sellwood (2002), Magnitude of climate variability during middle Pliocene warmth: a palaeoclimate modelling study, *Palaeogeogr. Palaeoclimatol. Palaeoecol*., *188*, 1-24.

Hilgen, F.J. (1987), Sedimentary rhythms and high resolution chronostratigraphic correlations in the Mediterranean Pliocene, *Newsl. Stratigr.*, *17*, 109–127.

Hilgen, F.G. (1991), Extension of the astronomically calibrated (polarity) time scale to the Miocene/Pliocene boundary, *Earth Planet. Sci. Lett.*, *104*, 349–368.

Kamptner, E. (1943), Zur revision der coccolithineen-spezies *Pontosphaera huxleyi* Lohm., *Akademie der Wissenschafen in Wien, Mathematisch-Naturwissenschaftliche Klasse*, 80, 43-49.

Langereis, C.G., and F.J. Hilgen (1991), The Rossello composite: a Mediterranean and global reference section for the Early to early Late Pliocene, *Earth Planet. Sci. Lett.*, *104*, 211-225.

Lohman, G.P., and J.J. Carlson (1981), Oceanographic significance of Pacific late Miocene calcareous nannoplankton, *Mar. Micropaleontol.*, *6*, 553-579.

Lourens, L.J., A. Antonarakou, F.J. Hilgen, AA.M. Van Hoof, C. Vergnaud-Grazzini, and W.J. Zachariasse (1996), Evaluation of the Plio-Pleistocene Astronomical Timescale, *Paleoceanography*, *11*, 391-413.

Madureira, L.A.S., M.H. Conte, and G. Eglinton (1995), Early diagenesis of lipid biomarker compounds in North Atlantic sediments, *Paleoceanography*, *10*, 627–642.

Marlowe, I.T., S.C. Brassell, G. Eglinton, and J.C. Green (1984), Long chain unsatured kenones and esters in living algae and marine sediments, *Org. Geochem.*, *6*, 135-141.

Marlowe, I.T., S.C. Brassell, G. Eglinton, and J.C. Green (1990), Long-chain alkenones and alkyl alkenoates and the fossil coccolith record of marine sediments, *Chem. Geol.*, *88*, 349-375.

Müller, P.J., M. Cepek, G. Ruhland, and R.R. Schneider (1997), Alkenone and coccolithophorid species changes in Late Quaternary sediments from the Walvis Ridge: Implications for the alkenone paleotemperature method, *Palaeogeogr. Palaeoclimatol. Palaeoecol*., *135*, 71–96.

Müller, P.J., G. Kirst, G. Rulhand, I. von Storch, and A. Rosell-Melé (1998), Calibration of the alkenone paleotemperature index $U^{K'}_{37}$ based on core-tops from the eastern South Atlantic and the global ocean (60°N-60°S), *Geochim. Cosmochim. Acta*, *62* (10), 1757-1772.

Negri, A., C. Morigi, and S. Giunta (2003), Are productivity and stratification important to sapropel deposition? Microfossil evidence from late Pliocene insolation cycle 180 at Vicra, Calabria, *Palaeogeogr. Palaeoclimatol. Palaeoecol*., *190*, 243-255.

Pahnke, K., and J.P. Sachs (2006), Sea surface temperatures of southern midlatitudes 0-160 kyr B.P, *Paleoceanography*, *21*, PA2003, doi:10.1029/2005PA001191.

Pedersen, T.F., and S.E. Calvert (1990), Anoxia vs. productivity: What controls the formation of organic-carbon-rich sediments and sedimentary rocks? *Am. Assoc. Petr. Geol. Bull., 74*, 454–466.

Plancq, J., V. Grossi, J. Henderiks, L. Simon, and E. Mattioli (2012), Alkenone producers during late Oligocene–early Miocene revisited, *Paleoceanography*, *27*, PA1202, doi:10.1029/2011PA002164.

Pond, D.W., and R.P. Harris (1996), The lipid composition of the coccolithophore *Emiliania huxleyi* and its possible ecophysiological significance, *J. Mar. Biol. Ass. UK*, *76*, 579-594.

Popp, B.N., E.A. Laws, R.R. Bidigare, J.E. Dore, K.L. Hanson, and S.G. Wakeham (1998), Effect of phytoplankton cell geometry on carbon isotopic fractionation, *Geochim. Cosmochim. Acta*, *62*, 69–77.

Prahl, F.G., G.J. de Lange, M. Lyle, and M.A. Sparrow (1989), Post-depositional stability of long chain alkenones under contrasting redox conditions, *Nature*, *341*, 434–437.

Prahl, F.G., and S.G. Wakeham (1987), Calibration of unsaturation patterns in long-chain ketone compositions for paleotemperature assessment, *Nature*, *330*, 367-369.

Prahl, F.G., G.V. Wolfe, and M.A. Sparrow (2003), Physiological impacts on alkenone paleothermometry, *Paleoceanography*, *18*, 1025. doi:10.1029/2002PA000803.

Principato, M.S., D. Crudeli, P. Ziveri, C.P. Slomp, C. Corselli, E. Erba, and G.J. de Lange (2006), Phyto and zooplankton paleofluxes during the deposition of sapropel S1 (eastern Mediterranean): Biogenic carbonate preservation and paleoecological implications, *Palaeogeogr. Palaeoclimatol. Palaeoecol*., *235* (1-3), 8-27.

Pujos-Lamy, A. (1977), Essai d'établissement d'une biostratigraphie du nannoplancton calcaire dans le Pleistocène de l'Atlantique Nord-oriental, *Boreas*, *6*, 323-331.

Riebesell, U., A.T. Revill, D.G. Hodsworth, and J.K. Volkman (2000), The effects of varying CO_2 concentration on lipid composition and carbon isotope fractionation in *Emiliania huxleyi*, *Geochim. Cosmochim. Acta*, *64*, 4179-4192.

Rio, D., R. Sprovieri, and I. Raffi (1984), Calcareous plankton biostratigraphy and biochronology of the Pliocene-Lower Pleistocene succession of the Capo Rossello area, Sicily, *Mar. Micropaleontol.*, *9*, 135–180.

Rio, D., R. Sprovieri, R. Thunell, C. Vergnaud Grazzini, and G. Glaçon (1990), Pliocene-Pleistocene paleoenvironmental history of the Western Mediterranean: a synthesis of ODP Site 653 results, *Proc. ODP Sci. Res.*, *107*, 695–704.

Rohling, E.J. (1994), Review and new aspects concerning the formation of eastern Mediterranean sapropels, *Mar. Geol. 122*, 1-28.

Rontani, J.-F., D. Marchand, and J.K. Volkman (2001), $NaBH_4$ reduction of alkenones to the corresponding alkenols: a useful tool for their characterisation in natural samples, *Org. Geochem.*, *32*, 1329–1341.

Rontani, J.-F., S.G. Wakeham, F.G. Prahl, F. Vaultier, and J.K. Volkman (2011), Analysis of trace amounts of alkenones in complex environmental samples by way of $NaBH_4/NaBD_4$ reduction and silylation, *Org. Geochem.*, *42*, 1299–1307.

Rossignol-Strick, M. (1985), Mediterranean Quaternary sapropels, an immediate response of the African monsoon to variations of insolation, *Palaeogeogr. Palaeoclimatol. Palaeoecol.*, *49*, 237–263.

Sáez, A.G., I. Probert, J.R. Young, B. Edvardsen, W. Eikrem, and L.K. Medlin (2004), A review of the phylogeny of the Haptophyta, in *Coccolithophores: From molecular processes to global impact*, edited by H.R. Thierstein and J.R. Young, J.R., pp. 251–269, Springer-Verlag, Berlin Heidelberg.

Sgarrella, F., V. Di Donato, and R. Sprovieri (2012), Benthic foraminiferal assemblage turnover during intensification of the Northern Hemisphere glaciation in the Piacenzian Punta Piccola section, *Palaeogeogr. Palaeoclimatol. Palaeoecol.*, *330-334*, 59–74.

Sorrosa, J., 2012. Regulation by temperature in coccolithophorids; growth, calcification and alkenone synthesis. *Lambert Academic Publishing, U.K.*, 62 pp.

Sprovieri, R. (1986), Paleotemperature changes and speciation among benthic foraminifera in the Mediterranean Pliocene, *Boll. Soc. Paleontol. It.*, *24* (1), 13–21.

Sprovieri, R., M. Sprovieri, A. Caruso, N. Pelosi, S. Bonomo, and L. Ferraro (2006), Astronomic forcing on the planktonic foraminifera assemblage in the Piacenzian Punta Piccola section (southern Italy), *Paleoceanography*, *21*, PA4204, doi:10.1029/2006PA001268.

Sun, M.Y., and S.G. Wakeham (1994), Molecular evidence for degradation and preservation of organic matter in the anoxic Black Sea Basin, *Geochim. Cosmochim. Acta*, *58*, 3395-3406.

Tang, C.M., and L.D. Stott (1993), Seasonal salinity changes during Mediterranean sapropel deposition 9 000 years B.P.: Evidence from isotopic analyses of individual planktonic foraminifera, *Paleoceanography*, *8*, 473-493.

Thierstein, H.R., K.R. Geitzenauer, B. Molfino, and N.J. Shackleton (1977), Global synchroneity of late Quaternary coccolith datum levels: validation by oxygen isotopes, *Geology*, *5*, 400-404.

Thunell, R.C., and D.F. Williams (1989), Glacial-Holocene salinity changes in the Mediterranean Sea: Hydrographic and depositional effects, *Nature*, *338*, 493-496.

Van Os, B.J.H., L.J. Lourens, F.J. Hilgen, and G.J. De Lange (1994), The formation of Pliocene sapropels and carbonate cycles in the Mediterranean: diagenesis, dilution, and productivity, *Paleoceanography*, *9* (4), 601–617.

Vázquez, A., R. Utrilla, I. Zamarrenño, F.J. Sierro, J.A. Flores, and G. Francés (2000), Precession related sapropels of the Messinian Sorbas Basin (south Spain): paleoenvironmental significance, *Palaeogeogr. Palaeoclimatol. Palaeoecol.*, *158*, 353–370.

Vergnaud-Grazzini, C., W.B.F. Ryan, and M.B. Cita (1977), Stable isotope fractionation, climatic change and episodic stagnation in the eastern Mediterranean during the late Quaternary, *Mar. Micropaleontol*., *2*, 353-370.

Villanueva, J., J.A. Flores, and J.O. Grimalt (2002), A detailed comparison of the $U^{k'}_{37}$ and coccolith records over the past 290 kyears: implications to the alkenone paleotemperature method, *Org. Geochem.*, *33*, 897-905.

Volkman, J.K., G. Eglinton, E.D.S. Corner, and T.E.V. Forsberg (1980), Long-chain alkenes and alkenones in the marine coccolithphorid *Emiliania huxleyi*, *Phytochemistry*, *19*, 2619-2622.

Volkman, J.K., S.M. Barrett, S.I. Blackburn, and E.L. Sikes (1995), Alkenones in *Gephyrocapsa oceanica*: Implications for studies of paleoclimate, *Geochim. Cosmochim. Acta*, *59*, 513–520.

Weaver, P.P.E., M.R. Chapman, G. Eglinton, M. Zhao, D. Rutledge, and G. Read (1999), Combined coccolith, foraminiferal, and biomarker reconstruction of paleoceanographic conditions over the past 120 kyr in the northern North Atlantic (59°N, 23°W), *Paleoceanography*, *14*, 336-349.

Yamamoto, M., Y. Shiraiwa, and I. Inouye (2000), Physiological responses of lipids in *Emiliania huxleyi* and *Gephyrocapsa oceanica* (Haptophyceae) to growth status and their implications for alkenone paleothermometry, *Org. Geochem.*, *31*, 799-811.

Young, J.R. (1990), Size variation of Neogene *Reticulofenestra* coccoliths from Indian Ocean DSDP Cores, *J. Micropaleontol.*, *9*, 71–86.

Young, J.R. (1998), Neogene, in *Calcareous Nannofossil Biostratigraphy*, edited by P.R. Bown, pp. 225-265, British Micropalaeontology Society Publication Series, Kluver Academic Publishers, Cambridge.

Young, J.R., and P.R. Bown (1997), Cenozoic calcareous nannoplankton classification, *J. Nannoplankton Res.*, *19*, 36–47.

Chapitre 5

Conclusions et Perspectives

5.1. Conclusions

Le but de ce travail de thèse était de tenter d'identifier les producteurs d'alcénones au Cénozoïque, et d'appréhender si cette identification est essentielle pour assurer l'utilisation des proxys de température ($U^{K'}_{37}$) et de pCO_2 ($\varepsilon_{p37:2}$) basés sur ces lipides. Pour ce faire, la comparaison des profils de variations des concentrations en alcénones et des abondances (relatives et absolues) des différentes espèces de Noëlaerhabdaceae dans les mêmes sédiments a été entreprise dans trois cas d'études, correspondant à des périodes clés de l'évolution des Noëlaerhabdaceae. Les données issues de l'analyse des alcénones et des assemblages de nannofossiles ont été ensuite utilisées pour des reconstitutions paléo-environnementales et plaéocéanographiques. Les principaux résultats de ce travail sont:

1) A l'Eocène-Oligocène (34,8-30,7 Ma), les producteurs d'alcénones au Site DSDP 511 (Atlantique Sud) ne peuvent pas être clairement identifiés, bien que la contribution de certaines espèces de *Reticulofenestra* (*R. dictyoda*, *R. minuta*) soit probable. Toutefois, l'utilisation du proxy de température basé sur les alcénones reste possible, puisque les valeurs de températures d'eaux océaniques de surface (SST) dérivées de l'$U^{K'}_{37}$ sont cohérentes avec celles dérivées d'autres proxys de température ($\delta^{18}O$, TEX_{86}). Ainsi, les variations de SST, couplées aux variations des concentrations en biomarqueurs lipidiques (alcénones et diols à longues chaînes) et en carbonate de calcium, mettent en évidence un refroidissement progressif associé à une augmentation de la productivité primaire au Site 511 autour de la limite Eocène-Oligocène. Ces conditions sont à mettre en relation avec le développement de conditions d'upwelling certainement associé à la mise en place du courant circumpolaire antarctique.

2) A l'Oligocène-Miocène (25-16 Ma), le genre *Cyclicargolithus* (plus précisément l'espèce *C. floridanus*) est identifié comme un producteur majeur d'alcénones au Site DSDP 516 (Atlantique Sud). La grande taille de cellule de *Cyclicargolithus*, qui influence le fractionnement isotopique du carbone (ε_p), a pour conséquence une ré-estimation à la hausse des valeurs de paléo-pCO_2, qui avaient été estimées auparavant en prenant uniquement en compte les réticulofénestrés (*Reticulofenestra* et *Dictyococcites*) qui ont une petite taille de cellule. La transition Oligocène-Miocène est par ailleurs caractérisée

par le déclin du genre *Cyclicargolithus* (observé simultanément en Atlantique Sud, en Atlantique Nord et dans le Pacifique Sud), probablement dû à un événement climatique global (glaciation) et/ou à une pression évolutive (compétition avec les réticulofénestrés).

3) Au Pliocène supérieur (3,6-2,6 Ma) du sud-ouest de la Sicile, l'espèce *Reticulofenestra minutula* est identifiée un comme producteur majeur d'alcénones, bien que la contribution d'autres espèces, telle que *Pseudoemiliania lacunosa*, ne puisse être exclue. Des différences entre les concentrations en alcénones et les abondances en coccolithes sont observées dans les niveaux à sapropèles, où de plus fortes concentrations en alcénones sont accompagnées de plus faibles abondances de coccolithes. Ces différences pourraient être expliquées par la mise en place d'une stratification thermohaline, entraînant une oligotrophie des eaux de surface et un appauvrissement en oxygène des eaux de fond lors de la formation de ces couches particulières, comme le suggèrent les variations des SST dérivées de l'$U^{K'}_{37}$, les concentrations en matière organique totale et les variations d'assemblages de nannofossiles. Dans ces sédiments pliocènes, l'utilisation de l'$U^{K'}_{37}$ est justifiée par le fait que *Reticulofenestra* est proche phylétiquement des producteurs actuels, minimisant ainsi les possibles biais génétiques sur la calibration du proxy de température.

L'ensemble des résultats de ce travail de thèse permet d'énoncer les conclusions générales suivantes :

Quelles étaient les espèces productrices d'alcénones au cours du Cénozoïque ? L'hypothèse de Marlowe et collaborateurs (1990) est-elle vérifiée et généralisable ?

L'identification des producteurs, quand elle est possible, montre que la production d'alcénones n'est pas restreinte à une seule espèce ou à un seul genre, mais à plusieurs qui sont très proches phylétiquement des producteurs actuels comme le suggèrent les données moléculaires (Fujiwara et al., 2001; Sáez et al., 2004) et micropaléontologiques (Young, 1990, 1998; Young et Bown, 1997). L'identification de *Cyclicargolithus floridanus* comme producteur majeur d'alcénones autour de la limite Oligocène-Miocène démontre que, contrairement à l'hypothèse de Marlowe et collaborateurs (1990), *Reticulofenestra* n'est pas le seul genre responsable de la production d'alcénones pendant tout le Cénozoïque. Cette production semble avoir pu être assurée par plusieurs genres au cours de l'histoire évolutive des Noëlaerhabdaceae. Ceci est d'autant plus vraisemblable que *Cyclicargolithus* a une répartition stratigraphique limitée (de ~40 Ma à ~13 Ma [Young, 1998]). De plus, ce genre est

un taxon caractéristique des moyennes latitudes (Wei et Wise, 1990) où il domine les assemblages. Il ne peut donc pas être responsable de la production d'alcénones aux hautes latitudes où il est rare. La question initiale « *qui étaient les producteurs d'alcénones ?* » pourrait alors être reformulée par « *qui étaient les producteurs majeurs d'alcénones ?* ». Par ailleurs, la contribution d'espèces non-calcifiantes est également envisageable, mais elle reste hypothétique à cause de l'absence d'enregistrement sédimentaire de ces espèces.

L'identification formelle des producteurs anciens d'alcénones est-elle essentielle pour l'utilisation des proxys basés ces lipides ($U^{K'}_{37}$ et $\varepsilon_{p37:2}$) dans des sédiments pré-datant l'apparition des producteurs actuels ?

Pour les reconstructions de paléo-pCO_2, il apparaît essentiel d'identifier le plus précisément possible les producteurs anciens d'alcénones. La taille de cellule des espèces productrices a en effet une influence directe sur les valeurs du fractionnement isotopique du carbone ($\varepsilon_{p37:2}$) et, *in fine*, sur les valeurs estimées de pCO_2. Une estimation plus juste des paléo-pCO_2 inclut donc l'identification des producteurs d'alcénones, la quantification de leurs abondances respectives et la détermination de la taille de leur cellule par une étude biométrique des coccolithes. En revanche, pour le paléo-thermomètre $U^{K'}_{37}$, l'identification des producteurs d'alcénones ne semble pas primordiale. Cette constatation tend à confirmer l'idée que les facteurs génétiques ont un impact minime sur la calibration de l'$U^{K'}_{37}$ (Müller et al., 1997, 1998; Villanueva et al., 2002). Cependant, certaines études (e.g ; Huguet et al., 2006; Kim et al., 2009) montrent des différences significatives entre les températures estimées à partir de l'$U^{K'}_{37}$ et celles reconstruites à partir des tétraéthers d'archées (TEX_{86}), soulignant l'importance des approches multi-proxys pour s'assurer de la fidélité des paléo-thermomètres.

Ce travail de thèse a également permis de compléter l'enregistrement sédimentaire de la distribution des alcénones au cours du Cénozoïque (Table 5-1). Les sédiments de l'Oligocène-Miocène (Site 516) ou de l'Eocène-Oligocène (Site 511) sont caractérisés par des profils d'alcénones ne présentant qu'un nombre limité d'alcénones en comparaison à des études antérieures (Table 5-1). Ceci est probablement dû à des concentrations trop faibles de certaines alcénones (par exemple $EtC_{39:2}$) pour être détectées par chromatographie en phase gazeuse. En revanche, les sédiments du Pliocène supérieur de Sicile ont mis en évidence une plus grande diversité de longueurs de chaîne des alcénones. Cette diversité a pu être étudiée grâce, notamment, à la transformation des alcénones en alcénols par le borohydrure de sodium ($NaBH_4$) suivie d'une étape de silylation. Les alcénols présentent en effet de meilleurs

facteurs de réponse en spectrométrie de masse, diminuant ainsi significativement la limite de détection des alcénones. Cette méthode, pour la première fois appliquée à des échantillons très anciens, a ainsi permis l'identification d'alcénones en C_{41} ($MeC_{41:x}$ et $EtC_{41:x}$[1]), qui n'avaient pas été détectées avant réduction et qui ont rarement ou encore jamais été décrites dans le registre sédimentaire. En effet, à ce jour, seule une alcénone en MeC_{41} (di-insaturée) a été reportée dans des sédiments riches en matière organique (black shales) datant du Cénomanien (95 Ma, Crétacé supérieur; Farrimond et al., 1986) alors que l'alcénone en EtC_{41} est ici, semble-t-il, reportée pour la première fois dans le registre sédimentaire. Il est probable que la lacune d'enregistrement de ce type d'alcénones dans les sédiments cénozoïques et quaternaires soit liée à un biais de détection, puisque les alcénones en C_{41} sont déjà présentes en faibles concentrations chez certaines espèces actuelles (Table 5-1). Ce résultat démontre donc que la réduction des alcénones en alcénols est une approche prometteuse pour une meilleure caractérisation des profils d'alcénones dans les sédiments anciens.

[1] Le nombre de double liaisons n'a pas pu être clairement déterminé, mais il s'agit probablement d'alcénones di-insaturées.

Nombre de carbones Nombre d'insaturations Position C=O	36 2 Et	37 2 Me	37 3 Me	37 4 Me	38 2 Me	38 3 Me	38 4 Me	38 2 Et	38 3 Et	38 4 Et	39 2 Me	39 3 Me	39 4 Me	39 2 Et	39 3 Et	39 4 Et	40 2 Et	40 3 Et	40 4 Et	40 2 Me	41 2 Et	41 2 Me	Nombre de carbones Nombre d'insaturations Position C=O
Producteurs actuels																							
Emiliania huxleyi		+	+	+	+	+		+	+	+				+	+								Marlowe et al., 1984
Gephyrocapsa oceanica		+	+		+	+		+	+			+		+	+								Volkman et al., 1995
Chrysotila lamellosa		+	+	+				+	+	+	+	+					+	+					Rontani et al., 2004
Isochrysis galbana		+	+	+				+	+					+	+								Marlowe et al., 1984
Sédiments quaternaires																							
Méditerranée		+	+		+	+		+	+														Cacho et al., 1999
Atlantique N (hautes lat.)		+	+	+	+	+		+	+														Rosell-Melé et al., 1994
Mer du Nord		+	+		+	+		+	+					+	+								Volkman et al., 1980
Atlantique N (basses lat.)		+	+		+	+		+	+					+	+								Brassell et al., 1986
Baie Walvis		+	+		+	+		+	+					+	+								Volkman et al., 1980
Sédiments tertiaires																							
Pliocène supérieur (Sicile)		**+**	**+**		**+**			**+**						**+**			**+**				**+**	**+**	**Cette étude**
Pliocène		+	+	+	+	+	+	+	+	+				+	+								Marlowe et al., 1984
Pliocène		+	+		+			+							+		+						Marlow et al., 2001
Oligocène/Miocène (Atl. S)		**+**			**+**			**+**															**Plancq et al., 2012**
Miocène		+	+		+	+		+	+					+	+								Brassell et al., 1980
Oligocène		+	+	+	+	+	+	+	+	+													Marlowe et al., 1984, 1990
Eocène/Oligocène (Atl. S)		**+**	**+**					**+**	**+**														**Cette étude**
Eocène (hautes lat.)		+	+	+	+	+	+	+	+	+													Marlowe et al., 1984, 1990
Eocène (basses lat.)		+	+		+			+															Marlowe et al., 1990
Paléocène																	+						Yamamoto et al., 1996
Sédiments crétacés																							
Cénomanien		+						+			+						+			+		+	Farrimond et al., 1986
Albien		+						+			+						+						Farrimond et al., 1986
Aptien	+	+						+			+												Brassell et al., 2004

Table 5-1. Compilation (non exhaustive) de la présence des différents types d'alcénones dans le registre sédimentaire et chez les espèces productrices actuelles (modifié d'après Brassell et al., 2004). Les données en rouge sont celles obtenues au cours de ce travail de thèse. A noter que la distribution pour le Pliocène supérieur de Sicile a été obtenue après réduction des alcénones au $NaBH_4$.

5.2. Perspectives

Si notre double approche quantitative (alcénones/nannofossiles) a permis d'apporter de nouvelles informations sur les producteurs potentiels d'alcénones dans les périodes pré-datant l'apparition des producteurs actuels, une étude détaillée de la distribution et de la structure des alcénones dans les sédiments cénozoïques apparaît nécessaire. La comparaison de la structure de ces lipides entre l'actuel et le registre sédimentaire devrait permettre de mieux contraindre la contribution de certains producteurs ou des changements de producteurs dans les sédiments pré-quaternaires. D'une part, l'application de la méthode de réduction au $NaBH_4$ des alcénones en alcénols correspondants (Rontani et al., 2011) apparaît être prometteuse pour mieux préciser les profils de distribution de ces molécules dans les sédiments anciens (cf. 5.1. Conclusions). D'autre part, la détermination de la position des doubles liaisons devrait apporter des informations sur l'évolution des voies de biosynthèse et sur l'identité des producteurs anciens. Des études sur les alcénones actuelles di- et tri-insaturées ont en effet permis de distinguer trois « familles d'alcénones » sur la base de l'espacement entre les doubles liaisons, suggérant des voies de biosynthèse différentes (Xu et al., 2001; Lopez et al., 2005; Prahl et al., 2006; Rontani et al., 2006; Lopez et Grimalt, 2006). Dans les sédiments DSDP de l'Eocène-Oligocène (Site 511) et de l'Oligocène-Miocène (Site 516), le peu de matériel disponible (15 g par échantillon) et les faibles concentrations en alcénones ne permettront malheureusement pas d'envisager l'étude de la position des doubles liaisons, car la méthode utilisée (oxydation au tétroxyde d'osmium) nécessite une grande quantité de matériel. Par contre, ces analyses pourront être effectuées sur les alcénones des sédiments pliocènes de Sicile qui ont été amplement échantillonnés (environ 50 g) et qui contiennent parfois de fortes quantités de ces biomarqueurs. Il sera donc déterminant de voir si un changement de structure d'alcénones se produit dans les niveaux à sapropèles, dont certains sont caractérisés par un changement de profil de distribution de ces lipides. Les résultats permettront alors de préciser si ce changement de profil est également dû à un changement de producteur d'alcénones, et pas uniquement à une réponse physiologique du même producteur aux variations des conditions environnementales responsables du dépôt de ces niveaux sédimentaires particuliers.

Dans les sédiments de Punta Grande/Punta Piccola, l'étude de la variation des températures dérivées de l'$U^{K'}_{37}$ a permis de mettre en évidence une augmentation de température dans les

niveaux à sapropèles (S101-S112) du Pliocène supérieur. Toutefois, une comparaison avec des températures estimées avec d'autres proxys est primordiale pour mieux s'assurer de la fiabilité des résultats et interprétations basés sur l'$U^{K'}_{37}$ (cf. Chapitre 4). La mesure du TEX_{86} (basé sur les tétraéthers d'archées; Schouten et al., 2002) et du LDI (basé sur les diols à longues chaînes produits par des diatomées; Rampen et al., 2012) dans ces échantillons pliocènes est programmée[2]. D'éventuelles différences de températures estimées à partir des trois proxys permettraient de discuter 1) de l'influence possible de facteurs physiologiques sur l'$U^{K'}_{37}$ jusque là essentiellement mise en évidence à partir de cultures *in vitro* (e.g ., Epstein et al., 1998; Prahl et al., 2003), et 2) de la robustesse de chacun de ces proxys de température, encore peu utilisés simultanément pour les reconstitutions paléo-environnementales.

Dans ce travail de thèse, l'identification des producteurs anciens d'alcénones a été entreprise pour trois périodes clés de l'évolution des Noëlaerhabdaceae au cours du Cénozoïque. D'autres périodes clés semblent importantes à étudier, comme celle comprenant la première apparition des producteurs actuels, notamment *Gephyrocapsa oceanica*. L'étude de la coupe de Faro Rossello (sud ouest de la Sicile) représente ainsi une perspective très intéressante puisqu'elle couvre un intervalle de temps (environ 1,86-1,55 Ma, Pléistocène) comprenant la première apparition de *Gephyrocapsa oceanica*. Des échantillons de cette coupe ont déjà été prélevés dans le cadre de nos travaux, et les résultats préliminaires de l'analyse du contenu en alcénones et des assemblages de Noëlaerhabdaceae sont présentés en Figure 5-1. A ce jour, la comparaison entre les profils d'alcénones et des différentes espèces de coccolithes ne permet pas d'identifier clairement le(s) producteur(s) majeur(s) d'alcénones sur ce site, bien que certaines similitudes puissent être observées avec *Dictyococcites* spp. et *Gephyrocapsa* (>3 μm) (Figure 5-1). L'étude de la distribution et de la structure des alcénones sera nécessaire pour mettre en évidence un changement éventuel de producteurs et/ou des variations environnementales pendant l'intervalle de temps étudié. Cette approche qualitative sera plus particulièrement intéressante au sommet de la coupe (40-52 m), puisque c'est dans cet intervalle, où les concentrations en alcénones diminuent, qu'a lieu la première apparition de *G. oceanica* >5.5 μm (Caruso, 2004).

[2] Les mesures du TEX_{86} seront réalisées en collaboration avec le Professeur Antoni Rosell-Melé (Université Autonome de Barcelone, Espagne) dans le cadre d'un stage post-doctoral de 2-3 mois (mai-juillet 2013) financé par l'EAOG (European Association of Organic Geochemists).

Pour mieux comparer les alcénones « anciennes » avec les alcénones « actuelles », l'étude de la composition et de la structure précise des alcénones des espèces productrices actuelles, telles qu'*Emiliania huxleyi* ou *Gephyrocapsa oceanica*, au stade diploïde (calcifiantes) et au stade haploïde (non-calcifiantes) est essentielle. A ce jour, de nombreux travaux ont analysé le contenu en alcénones d'*E. huxleyi* ou de *G. oceanica* au stade diploïde (e.g., Volkman et al., 1980a,b, 1995; Prahl et al., 2006), mais l'étude des formes haploïdes reste rare (Conte et al., 1995). Pourtant, pour *E. huxleyi*, le passage de formes diploïdes calcifiantes à des formes haploïdes non-calcifiantes a été observé à plusieurs reprises dans certaines conditions de culture (Houdan et al., 2004; Frada et al., 2008). L'étude de la composition en alcénones des stades haploïde et diploïde d'*E. huxleyi* ou de *G. oceanica* permettra de déterminer si le passage d'un stade à l'autre s'accompagne d'une modification de la distribution des différentes alcénones. Si tel est le cas, la comparaison des profils « actuels » et « anciens » constituera une aide précieuse pour déceler la contribution d'espèces non-calcifiantes, pour lesquelles il n'y a pas d'enregistrement sédimentaire. Il sera également primordial de vérifier que le passage du stade diploïde à haploïde ne modifie pas l'$U^{K'}_{37}$.

Enfin, au cours de ce travail qui n'avait pas vocation à effectuer une révision taxonomique, les différents genres des Noëlaerhabdaceae ont été distingués sur des critères morphologiques (voir Annexe 2). Nous avons ainsi considéré séparément les genres *Dictyococcites* et *Reticulofenestra*. Cette distinction est discutable, puisque certains auteurs considèrent que *Dictyococcites* est un *Reticulofenestra* plus calcifié, et donc que ces deux genres n'en forment en réalité qu'un seul (e.g., Young, 1990; Aubry, 1992; Henderiks et Pagani, 2007). Ces différentes considérations taxonomiques peuvent engendrer des discussions au sujet des espèces anciennes productrices d'alcénones ou rendre difficile la comparaison de différentes études entre elles. Un consensus sur la taxonomie de la famille des Noëlaerhabdaceae au Cénozoïque (qui pourrait représenter un projet de thèse) apparaît nécessaire non seulement dans le cadre des résultats obtenus dans ce travail de thèse mais aussi pour les études micropaléontologiques en général.

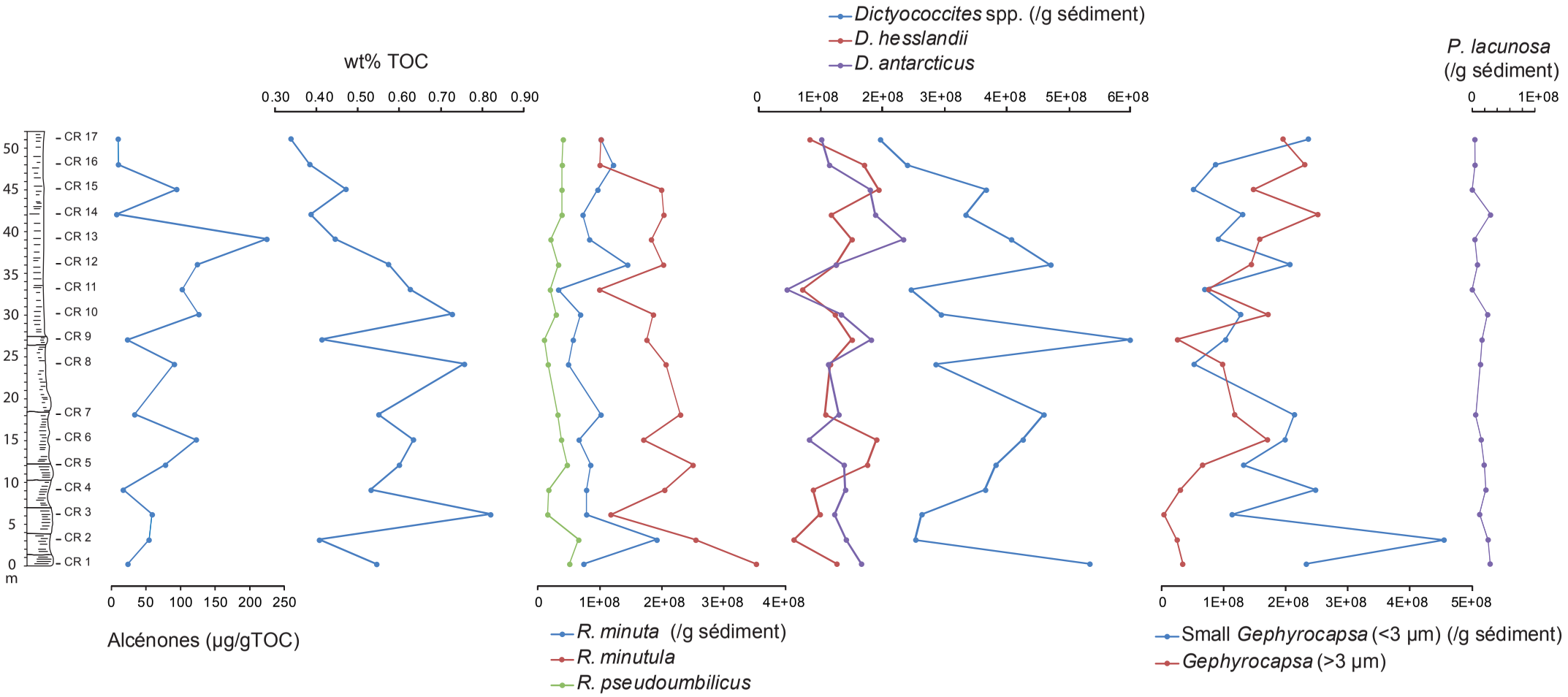

Figure 5-1. Profils de variations des alcénones (µg/g TOC), de la matière organique totale (TOC; wt %) et des différentes espèces de Noëlaerhabdaceae (spécimens/g de sédiments) à Faro Rosello au Pléistocène.

Références

Aubry, M.P., 1992. Paleogene calcareous nannofossils from the Kerguelen Plateau, Leg 120. Proceedings of the Ocean Drilling Program Scientific Results 120, 471–491, doi:10.2973/odp.proc.sr.120.149.1992.

Brassell, S.C., Dumitrescu, M., ODP Leg 198 Shipboard Scientific Party, 2004. Recognition of alkenones in a lower Aptian porcellanite from the west-central Pacific. Organic Geochemistry 35, 181-188.

Caruso, A., 2004. Climatic changes during Late Pliocene and early Pleistocene at Capo Rossello (Sicily, Italy): response from planktonic foraminifera. In: Coccioni, R., et al. (Eds), Proceedings of the first Italian Meeting on Environmental Micropaleontology, Grzybowski Foundation Special Publication 9, pp. 17-36.

Conte, M.H., Thompson, A., Eglinton, G., Green, J.C., 1995. Lipid biomarker diversity in the coccolithophorid *Emiliania huxleyi* (Prymnesiophyceae) and the related species *Gephyrocapsa oceanica*. Journal of Phycology 31 (2), 272-282, doi: 10.1111/j.0022-3646.1995.00272.x.

Epstein, B.L., D'Hondt, S., Quinn, J.G., Zhang, J., Hargraves, P.E., 1998. An effect of dissolved nutrient concentrations on alkenone-based temperature estimates. Paleoceanography 13, 122–126.

Farrimond, P., Eglinton, G., Brassell, S.C., 1986. Alkenones in Cretaceous black shales, Blake-Bahama Basin, western North Atlantic. Organic Geochemistry 10, 897-903.

Frada, M., Probert, I., Allen, M.J., Wilson, W.H., de Vargas, C., 2008. The "Cheshire Cat" escape strategy of the coccolithophore *Emiliania huxleyi* in response to viral infection. Proceedings of the National Academy of Sciences 105 (41), 15944-15949.

Fujiwara, S., Tsuzuki, M., Kawachi, M., Minaka, N., Inouye, I., 2001. Molecular phylogeny of the Haptophyta based on the *rbc*L gene and sequence variation in the spacer region of the rubisco operon. Journal of Phycology 37, 121-129.

Henderiks, J., Pagani, M., 2007. Refining ancient carbon dioxide estimates: Significance of coccolithophore cell size for alkenone-based pCO_2 records. Paleoceanography 22, PA3202, doi:10.1029/2006PA001399.

Houdan, A., Billard, C., Marie, D., Not, F., Sáez, A.G., Young, J.R., Probert, I., 2004. Holococcolithophore-heterococcolithphore (Haptophyta) life cycles: flow cytometric analysis of relative ploidy levels. Systematics and Biodiversity 1 (4), 453-465.

Huguet, C., Kim, J.-H., Sinninghe Damsté, J.S., Schouten, S., 2006. Reconstruction of glacial–interglacial sea surface temperature in the Arabian Sea using organic proxies. Paleoceanography 21, PA3003. doi:10.1029/2005PA001215.

Kim, J.-H., Huguet, C., Zonneveld, K.A.F., Versteegh, G.J.M., Roeder, W., Sinninghe Damsté, J.S., Schouten, S., 2009. An experimental field study to test the stability of lipids used for the TEX86 and UK'37 paelothermometers. Geochimica et Cosmochimica Acta 73, 2888-2898.

Lopez, J.F., de Oteyza, T.G., Teixidor, P., Grimalt, J.O., 2005. Long chain alkenones in hypersaline and marine coastal microbial mats. Organic Geochemistry 36, 861-872.

Lopez, J.F., Grimalt, J.O., 2006. Reassessment of the structural composition of the alkenone distributions in natural environments using an improved method for double bond location based on GC-MS analysis of cyclopropylimines. Journal of American Society for Mass Spectrometry 17, 710-720.

Marlowe, I.T., Brassell, S.C., Eglinton, G., Green, J.C., 1990. Long-chain alkenones and alkyl alkenoates and the fossil coccolith record of marine sediments. Chemical Geology 88, 349-375.

Müller, P.J., Cepek, M., Ruhland, G., Schneider, R.R., 1997. Alkenone and coccolithophorid species changes in Late Quaternary sediments from the Walvis Ridge: Implications for the alkenone paleotemperature method. Palaeogeography Palaeoclimatology Palaeoecology 135, 71–96.

Müller, P.J., Kirst, G., Rulhand, G., von Storch, I., Rosell-Melé, A., 1998. Calibration of the alkenone paleotemperature index $U^{K'}_{37}$ based on core-tops from the eastern South Atlantic and the global ocean (60°N-60°S). Geochimica et Cosmochimica Acta 62 (10), 1757-1772.

Prahl, F.G., Rontani, J.-F., Volkman, J.K., Sparrow, M.A., Royer, I.M., 2006. Unusual C_{35} and C_{36} alkenones in a paleoceanographic benchmark strain of *Emiliania huxleyi*. Geochimica et Cosmochimica Acta 70, 2856-2867.

Prahl, F.G., Wolfe, G.V., Sparrow, M.A., 2003. Physiological impacts on alkenone paleothermometry. Paleoceanography 18, doi:10.1029/2002PA000803.

Rampen, S.W., Willmott, V., Kim, J.-H., Uliana, E., Mollenhauer, G., Schefuβ, E., Sinninghe Damsté, J.S., Schouten, S., 2012. Long chain 1,13- and 1,15-diols as a potential proxy for palaeotemperature reconstruction. Geochimica et Cosmochimica Acta 84, 204-216.

Rontani, J.-F., Prahl, F.G., Volkman, J.K., 2006. Re-examination of the double bond position in alkenones and derivatives: biosynthetic implications. Journal of Phycology 42, 800-813.

Rontani, J.-F., Wakeham, S.G. Prahl, F.G., Vaultier, F., Volkman J.K., 2011. Analysis of trace amounts of alkenones in complex environmental samples by way of $NaBH_4/NaBD_4$ reduction and silylation. Organic Geochemistry 42, 1299–1307.

Sáez, A.G., Probert, I., Young, J.R., Edvardsen, B., Eikrem, W., Medlin, L.K., 2004. A review of the phylogeny of the Haptophyta. In: Thierstein, H.R., Young, J.R. (Eds), Coccolithophores: From molecular processes to global impact. Springer-Verlag, Berlin Heidelberg, pp. 251–269.

Schouten, S., Hopmans, E.C., Schefuβ, E., Sinninghe Damsté, J.S., 2002. Distributional variations in marine crenarchaeotal membrane lipids: a new tool for reconstructing ancient sea water temperatures? Earth and Planetary Science Letters 204, 267-274.

Villanueva, J., Flores, J.A., Grimalt J.O., 2002. A detailed comparison of the $U^{k'}_{37}$ and coccolith records over the past 290 kyears: implications to the alkenone paleotemperature method. Organic Geochemistry 33, 897-905.

Volkman, J.K., Barrett, S.M., Blackburn, S.I., Sikes, E.L., 1995. Alkenones in *Gephyrocapsa oceanica*: Implications for studies of paleoclimate. Geochimica et Cosmochimica Acta 59, 513-520.

Volkman, J.K., Eglinton, G., Corner, E.D.S., Forsberg, T.E.V., 1980a. Long-chain alkenes and alkenones in the marine coccolithphorid *Emiliania huxleyi*. Phytochemistry 19, 2619-2622.

Volkman, J.K., Eglinton, G., Corner, E.D.S., Sargent, J., 1980b. Novel unsaturated straight-chain C_{37}-C_{39} methyl and ethyl ketones in marine sediments and a coccolithophore *Emiliania huxleyi*. In: Douglas, A.G., Maxwell, J.R. (Eds), Advances in Organic Geochemistry 1979, Pergamon Press, Oxford, pp. 219-228.

Wei, W., Wise, S.W., Jr., 1990. Biogeographic gradients of middle Eocene-Oligocene calcareous nannoplankton in the South Atlantic Ocean. Palaeogeography Palaeoclimatology Palaeoecology 79, 29-61.

Xu, L., Reddy, C.M., Farrington, J.W., Frysinger, G.S., Gaines, R.B., Johnson, C.G., Nelson, R.K., Eglinton, T.I., 2001. Identification of a novel alkenone in Black Sea sediments. Organic Geochemistry 32, 633-645.

Young, J.R., 1990. Size variation of Neogene *Reticulofenestra* coccoliths from Indian Ocean DSDP Cores. Journal of Micropaleontology 9, 71–86.

Young, J.R., 1998. Neogene. In: Bown, P.R. (Ed.), Calcareous Nannofossil Biostratigraphy, British Micropalaeontology Society Series, pp. 225-265.

Young, J.R., Bown, P.R., 1997. Cenozoic calcareous nannoplankton classification. Journal of Nannoplankton Research 19, 36-47.

Annexes

Annexe 1. Méthodes

Dans cette annexe sont décrites les principales méthodes de micropaléontologie et de géochimie organique utilisées au cours de ce travail de thèse.

1. Méthodes de micropaléontologie quantitative

1.1. Préparation des lames pour l'étude au microscope optique

La méthode utilisée pour la préparation des lames est celle des boîtes de décantation (ou random settling technique), initialement décrite par Beaufort (1991) et modifiée par Geisen et al. (1999). Elle présente l'avantage de préserver l'assemblage originel et de permettre d'évaluer l'abondance absolue des nannofossiles par gramme de roche.

Chaque échantillon est dans un premier temps réduit en une poudre parfaitement homogène à l'aide d'un pilon et d'un mortier en agate. La présence de micrograins de quartz ou de pyrite empêche la fragmentation mécanique des nannofossiles. La poudre est ensuite mise à sécher à 50°C dans une étuve pendant environ 24h. Ensuite, environ 5 mg de poudre de chaque échantillon, pesés avec une balance de précision, sont mis en suspension dans un tube gradué avec de l'eau savonneuse (savon de Marseille) et passés aux ultrasons pendant maximum 2 minutes. Les ultrasons désagrègent complètement les éventuels agrégats; l'eau savonneuse permet d'éviter la formation d'agrégats argileux et, grâce à l'augmentation du pH, empêche la corrosion des coccolithes par l'eau lors de la phase suivante de décantation.

La suspension (475 ml) est par la suite homogénéisée dans un bécher à l'aide d'un agitateur magnétique pendant environ 10 minutes. Puis, celle-ci est versée dans une boîte de décantation contenant en son centre une lamelle couverte par la suspension à hauteur de 2.1 cm (Figure A1-1) et sur laquelle se déposeront, de manière homogène et aléatoire, toutes les particules en suspension. La boîte est alors laissée à température ambiante et dans un environnement calme pendant 24h, permettant la décantation de toutes les particules.

L'eau est enfin évacuée par un drain au goutte-à-goutte. Une fois sèche, la lamelle est collée à l'aide de résine (Rhodopass) sur une lame de microscope.

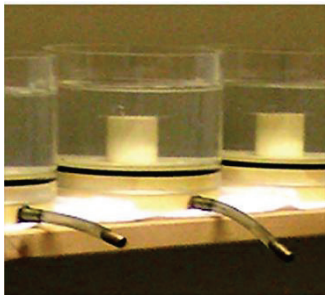

(a)

(b)

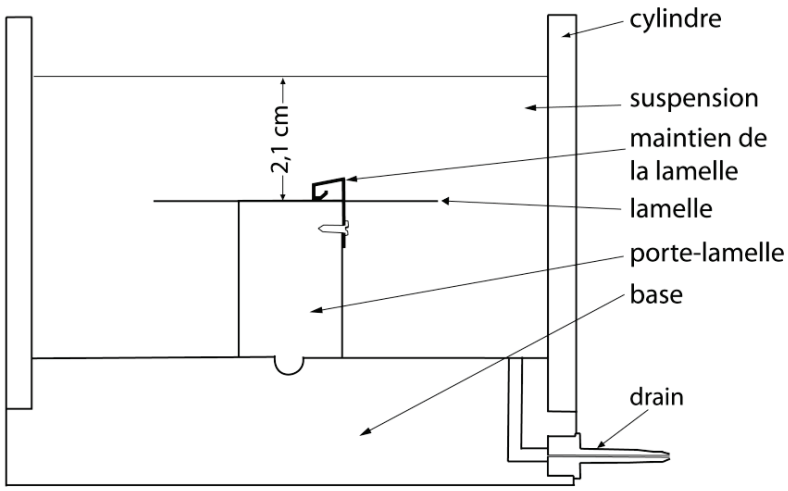

Figure A1-1. (a) Photographie (Maillot S.) et **(b)** schéma d'une boîte de décantation (modifié d'après Geisen et al., 1999).

1.2. Quantification absolue et relative des assemblages de nannofossiles

Pour la quantification absolue des nannofossiles calcaires par gramme de roche, chaque lame est observée au microscope optique ZEISS à lumière polarisante avec un grossissement de 1000. Tous les nannofossiles, coccolithes et nannolithes (par exemple *Sphenolithus* spp.), sont identifiés sur la base de la taxonomie standard (Young et Bown, 1997; Sáez et al., 2004 ; voir annexe taxonomique), et comptés par champs de vue successifs (un champ de vue représente un diamètre de 200 μm).

Dans cette étude, le comptage a été arrêté en moyenne à 500 coccolithes (300 pour les lames les plus pauvres). En effet, d'après les abaques publiés par Dennison et Hay (1967), dans un échantillon où 200 fossiles ont été décomptés, la probabilité de ne pas observer une espèce rare dont l'abondance relative est de 1% est égale à 15%. Autrement dit, les chances d'observer une espèce rare sont satisfaisantes (85%).

L'abondance absolue X de nannofossiles par gramme de roche peut ensuite être calculée grâce à l'équation suivante :

$$X = (N \times V) / (M \times A \times H)$$

Avec N: nombre total de nannofossiles comptés
A: surface étudiée (cm^2)
V: volume d'eau utilisée pour la dilution (cm^3)
M: poudre de roche pesée (g)
H: hauteur d'eau au-dessus de la lame (cm)

L'abondance absolue de chaque taxon est également calculée suivant la formule ci-dessus, où N correspond au nombre de spécimens du taxon considéré.

Enfin, l'abondance relative de chaque taxon est calculée par rapport au nombre total de coccolithes.

1.3. Calcimétrie

La calcimétrie est une mesure indirecte du taux de carbonate de calcium ($CaCO_3$) contenu dans un échantillon. Elle repose sur la quantification de dioxyde de carbone (CO_2) dégagé lors de la dissolution d'environ 300 mg de poudre d'échantillon par 10 mL d'acide chlorhydrique (HCl, 1N). La quantité de CO_2 dégagée est proportionnelle au pourcentage de $CaCO_3$ contenu dans l'échantillon. Les mesures de calcimétrie sont réalisées à l'aide d'un calcimètre Dietrich-Frühling^{TM}.

Le volume de CO_2 dégagé est influencé par les conditions de pression et de température. Pour s'en extraire, l'équation suivante est appliquée :

$$\mathbf{V_{CO2} = (V \times (P-Ps) \times 273) / (760 \times (273+T))}$$

Avec V_{CO2}: Volume de CO_2 normalisé (mL)
V: Volume de CO_2 dégagé et mesuré (en mL ± 0,2 ml)
Ps: Facteur de correction de la pression de saturation (en Torr)
P: Pression atmosphérique (en mm de Hg)
T: Température (en °C)

Ce volume est ensuite converti en pourcentage de CO_2 grâce à l'équation:

$$\mathbf{\% CO_2 = (V_{CO2} \times 44 \times 100) / (22414 \times M)}$$

Avec M: Masse de poudre utilisée (en g)

Le pourcentage de carbonate de calcium est enfin calculé à partir du pourcentage de CO_2:

$$\mathbf{\%CaCO_3 = \%CO_2 \times 2{,}273 \times f}$$

Avec f: facteur de correction.

Le facteur de correction f tient compte des erreurs d'origine logistique (balance, calcimètre…) et des erreurs de mesures de l'opérateur (pesées et lecture des volumes de gaz). Ce facteur est

déterminé après avoir fait une dizaine de mesures à partir d'une même poudre de $CaCO_3$ pur à 98%. Les valeurs trouvées sont ensuite comparées avec le standard.

2. Méthodes de géochimie organique

2.1. Analyse du carbone organique total (COT)

Dans un premier temps, le carbone inorganique (carbonate de calcium) des échantillons est éliminé par attaques acides successives. Environ 100 mg de poudre d'échantillon réduit en poudre sont acidifiés *in situ* avec de l'acide chlorhydrique (HCl 2N) dans des capsules en argent (résistantes aux attaques acides) jusqu'à l'arrêt d'effervescence, séchés à l'étuve (50°C) et enroulés dans des capsules en étain (pour faciliter la combustion) avant les analyses.

L'échantillon est ensuite placé dans un analyseur élémentaire où il subit une combustion (950°C) en présence d'O_2 et de catalyseur d'oxydation, transformant le carbone en CO_2. Les gaz libérés par la combustion (N_2, CO_2, H_2O) sont séparés sur colonne chromatographique, et détectés par un détecteur non spécifique TCD (Thermal Conductivity Detector). L'acide aspartique ($C_7H_7NO_4$; 36,09% de carbone) et le nicotinamide ($C_6H_6N_2O_4$; 59,01% de carbone) sont utilisés comme standards de calibration pour la quantification du COT. Un matériel de référence interne (sédiment pauvre en carbone; 0,861 ± 0,034% de carbone) est analysé en parallèle les échantillons pour déterminer la précision analytique. Tous les échantillons sont dupliqués.

Toutes les analyses de COT ont été effectuées avec un analyseur élémentaire Thermo FlashEA 1112 au Laboratoire d'Ecologie des Hydrosystèmes Naturels et Anthropisés (LEHNA, UMR 5023, Université Claude Bernard Lyon 1) en collaboration avec Laurent Simon.

2.2. Analyse des biomarqeurs lipidiques

2.2.1. Extraction

Les échantillons sont extraits 5 fois à la sonde à ultrasons en utilisant 50 mL de Dichlorométhane (DCM). Les 5 extraits sont regroupés dans un même ballon et l'extrait total est concentré à l'évaporateur rotatif (Rotavap). L'extrait est transféré dans un pilulier taré et le solvant résiduel est évaporé sous flux d'azote (N_2).

2.2.2. Séparation

Les échantillons sont ensuite séparés en fractions de polarité croissante par chromatographie d'adsorption sur gel de silice.

- Pour les échantillons du Site DSDP 516 (Oligocène-Miocène), les séparations ont été effectuées à l'aide de colonnes en verre (pipettes Pasteur) remplies aux 3/4 par un gel de silice (Kiesegel 60) désactivé à 4% d'H_2O (Figure A1-2). L'extrait total repris dans un volume minimum (200 µL) d'Hexane (Hex) est déposé en tête de colonne et trois fractions sont éluées avec des solvants de polarité croissante:

F1 (hydrocarbures): Hexane (6 mL)

F2 (cétones, esters et alcools): Hex/actétate d'éthyle (AE) (7:3, v/v; 10 mL)

F3 (acides gras et lipides plus polaires): DCM/Méthanol (MeOH) (1:1, v/v; 10 mL)

- Pour tous les autres échantillons, les séparations ont été réalisées sur colonnes SPE (Solid Phase Extraction) en verre contenant 0,5 g de silice-NH_2 (aminopropyl) (Figure A1-2). Pour ces colonnes quatre fractions sont éluées avec des solvants de polarité croissante:

F1 (hydrocarbures): Hexane (4 mL)

F2 (cétones et esters): Hex/DCM (3:1, v/v; 6 mL)

F3 (alcools): DCM/Acétone (9:1, v/v; 5 mL)

F4 (acides gras et lipides plus polaires): MeOH (6 mL)

Avantages/inconvénients des colonnes SPE: Les colonnes SPE étant prêtes à l'emploi lors de leur achat, elles présentent un gain de temps considérable pour le traitement des échantillons par rapport aux colonnes avec du gel de silice désactivé à 4% d'H_2O qui nécessite un temps assez long de préparation (le gel de silice est préalablement activé à 130°C pendant 4 heures avant d'être désactivé). Toutefois, des irrégularités entre les lots de cartouches (les colonnes SPE sont vendues par lot de 30 ou 50 pièces) peuvent entraîner une mauvaise séparation. Une partie des alcénones, normalement contenues dans la fraction F2, peut alors se retrouver dans la fraction F3. Avant l'analyse d'échantillons, il est recommandé de tester chaque lot de colonnes pour éventuellement adapter le protocole d'élution.

Chaque fraction éluée est récupérée dans un pilulier taré et évaporée à sec sous flux de N_2.

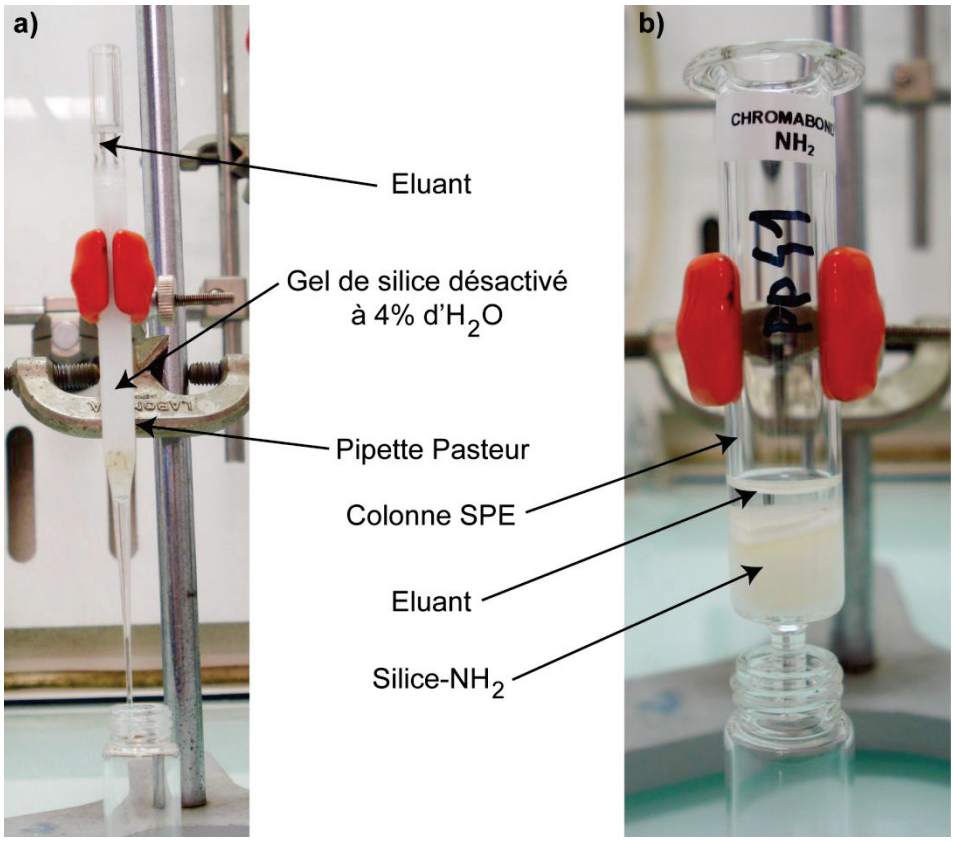

Figure A1-2. Photographies **a)** d'une colonne de silice (désactivée à 4% d'H_2O) et **b)** d'une colonne SPE (Solid Phase Extraction) utilisées pour la séparation des biomarqueurs.

2.2.3. Silylation

La silylation consiste à convertir les groupements hydroxyles (–OH) des alcools et des acides gras en éther de triméthylsilyle (TMS) par réaction avec le BSTFA (N,O-bis(triméthylsilyl)-trifluoroacétamide):

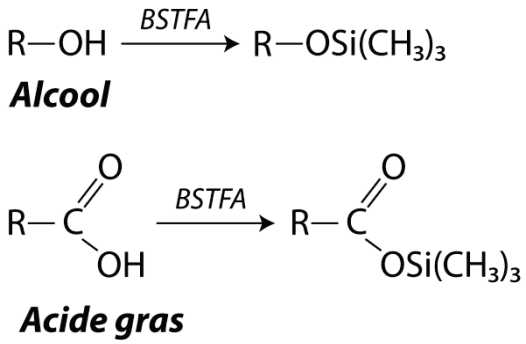

Ce traitement améliore la résolution des alcools et acides gras (contenus dans les fractions F3 et F4) et facilite leur identification par spectrométrie de masse.

Protocole: la fraction sèche est reprise dans 100 µL de pyridine et 50 µL de BSTFA et est mise à réagir à 50°C pendant 45 min. Le réactif est ensuite évaporé sous flux d'azote.

2.2.4. Réduction des alcénones par $NaBH_4$

La méthode de réduction au borohydrure de sodium ($NaBH_4$), introduite par Rontani et al. (2001), consiste à réduire les alcénones en alcénols correspondants qui, après silylation, présentent un meilleur facteur de réponse en spectrométrie de masse et qui sont mieux séparés chromatographiquement. Cette méthode permet donc de détecter des alcénones présentes en faibles quantités dans un échantillon. La réduction se fait selon la réaction suivante:

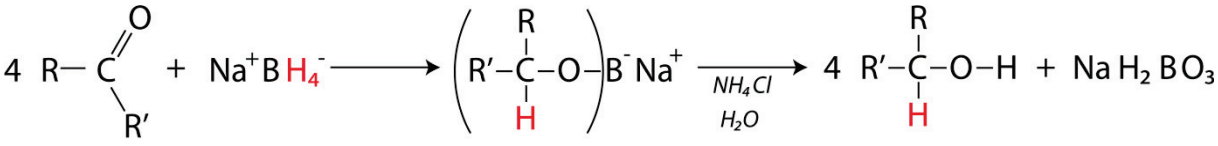

Protocole: le protocole suivi est celui décrit par Rontani et al. (2011). La fraction F2 (contenant les alcénones) est reprise dans 5mL d'un mélange d'éther diéthylique (Et_2O) et de méthanol (4:1, v/v). Quelques milligrammes de $NaBH_4$ (10 mg/mg d'extrait) sont ajoutés et le mélange est laissé à réagir à température ambiante pendant 1 heure avec un agitateur magnétique. Ensuite, 10 mL d'une solution saturée de chlorure d'ammonium (NH_4Cl) sont ajoutés goutte à goutte et les alcénols sont extraits 3 fois avec de l'Hex/DCM (4:1, v/v). Les extraits sont regroupés, séchés au sulfate de sodium anhydre (Na_2SO_4), filtrés et transférés dans un pilulier. La fraction réduite est ensuite silylée comme décrit précédemment (paragraphe 2.2.3).

2.2.5. Quantification des biomarqueurs lipidiques

Les alcénones ont été quantifiées par chromatographie en phase gazeuse-détection à ionisation de flamme (CPG-FID) après ajout d'un étalon interne (hexatriacontane ; *n*-C_{36} alcane). La quantité de chaque alcénone individuelle est alors déterminée par la relation suivante :

$$\mathbf{Q_{anal.} = (Q_{stdint.} \times A_{anal.})/A_{stdint.}}$$

Avec $Q_{anal.}$: Quantité d'alcénone

$Q_{stdint.}$: Quantité de standard interne ajoutée

$A_{stdint.}$: Aire du pic du standard interne

$A_{anal.}$: Aire du pic d'alcénone

Les diols ont été quantifiées par étalonnage externe en chromatographie phase gazeuse-spectrométrie de masse (CPG-SM). Cinq solutions étalons sont préparées par dilution successive à partir d'une solution mère de 1,2-dipalmitoyl glycerol et analysées en CPG-SM. Une droite d'étalonnage reliant de manière linéaire concentrations de l'étalon et aires des pics de l'étalon peut ainsi être tracée. Les aires de pics des diols sont ensuite déterminées en CPG-SM et les concentrations correspondantes sont obtenues en utilisant l'équation de la droite d'étalonnage.

2.2.6. Chromatographie en phase gazeuse-détection à ionisation de flamme (CPG-FID)

L'échantillon est repris dans un volume adéquat de solvant (Hexane) et 1 µL est injecté dans l'injecteur à l'aide d'une seringue. Le CPG-FID utilisé est un HP-6890 équipé d'un injecteur de type « on-column » et d'une colonne capillaire HP-5 (5% phényl-méthylpolysiloxane ; 30m x 0,32mm x 0,25µm). L'hélium est utilisé comme gaz vecteur à débit constant (1,1 mL/min). La température du four est maintenue à 60°C pendant 1 minute, puis programmée de 60°C à 130°C à 20°C/min, puis à 4°C/min de 130°C à 310°C, température à laquelle il est maintenu pendant 20 minutes.

2.2.7. Chromatographie en phase gazeuse- spectrométrie de masse (CPG-SM)

Les analyses sont réalisées avec un spectromètre de masse Finnigan MD800 Voyager simple quadripole fonctionnant en impact électronique (EI) et couplé à un CPG HP-6890 équipé d'un injecteur « on-column » et d'une colonne capillaire DB-5MS (5% phényl-méthylpolysiloxane ; 30m x 0,25mm x 0,25µm). La température de la source du spectromètre de masse est de 200°C, la température de l'interface de 280°C, et le potentiel d'ionisation est de 70 eV. L'hélium est utilisé comme gaz vecteur à débit constant (1,1 mL/min) et la programmation de température du four est la même que celle utilisée en CPG-FID.

Références

Beaufort, L., 1991. Adaptation of the random settling method for quantitative studies of calcareous nannofossils. Micropaleontology 37, 415–418.

Dennison, J., Hay, W.W., 1967. Estimating the needed sampling area for subaquatic ecologic studies. Journal of Paleontology 41, 706-708.

Geisen, M., Bollmann, J, Herrle, J.O., Mutterlose, J., Young, J.R., 1999. Calibration of the random settling technique for calculation of absolute abundance of calcareous nannoplankton. Micropaleontology 45 (4), 437-442.

Rontani, J.-F., Marchand, D., Volkman, J.K., 2001. $NaBH_4$ reduction of alkenones to the corresponding alkenols: a useful tool for their characterisation in natural samples. Organic Geochemistry 32, 1329–1341.

Rontani, J.-F., Wakeham, S.G. Prahl, F.G., Vaultier, F., Volkman J.K., 2011. Analysis of trace amounts of alkenones in complex environmental samples by way of $NaBH_4$/$NaBD_4$ reduction and silylation. Organic Geochemistry 42, 1299–1307.

Sáez, A.G., Probert, I., Young, J.R., Edvardsen, B., Eikrem, W., Medlin, L.K., 2004. A review of the phylogeny of the Haptophyta. In: Thierstein, H.R., Young, J.R. (Eds), Coccolithophores: From molecular processes to global impact. Springer-Verlag, Berlin Heidelberg, pp. 251–269.

Young, J.R., Bown, P.R., 1997. Cenozoic calcareous nannoplankton classification. Journal of Nannoplankton Research 19, 36-47.

Annexe 2. Remarques taxonomiques sur la famille des Noëlaerhabdaceae

La famille des Noëlaerhabdaceae est une famille typique et dominante dans la plupart des assemblages de nannofossiles du Cénozoïque. Avant l'apparition d'*Emiliania* et *Gephyrocapsa*, cette famille est représentée par les genres *Cyclicargolithus* (Eocène inférieur-Oligocène moyen), *Reticulofenestra* (Eocène inférieur-actuel), *Dictyococcites* (Eocène inférieur-Pleistocène ?) et *Pseudoemiliania* (Pliocène supérieur-Pléistocène moyen). Cependant, la différenciation taxonomique des genres *Reticulofenestra*, *Dictyococcites* et *Cyclicargolithus* est sujette à discussion. Les espèces du genre *Reticulofenestra* sont généralement considérées comme ayant une grande variabilité morphologique, et les genres *Dictyococcites* et *Cyclicargolithus* sont souvent regardés comme étant synonymes de *Reticulofenestra* (e.g., Theodoris, 1984; Marlowe et al., 1990; Young, 1990; Aubry, 1992; Beaufort 1992; Henderiks et Pagani, 2007; Henderiks, 2008). Par conséquent, ces genres ont été regroupés par les auteurs soit comme réticulofénestrés (*Reticulofenestra* + *Dictyococcites*) soit tout simplement comme *Reticulofenestra*. De plus, la morphologie relativement simple de *Reticulofenestra* ou *Dictyococcites* rend la subdivision en espèces problématique, si bien que la taxonomie conventionnelle se base sur la taille du coccolithe. Bien qu'arbitraire, cette subdivision en morphoespèces est très utile en biostratigraphie (Backman, 1980; Young et al., 2003). Dans ce travail de thèse, *Reticulofenestra*, *Dictyococcites* et *Cyclicargolithus* ont été séparés sur la base de caractéristiques morphologiques. La taxonomie utilisée suit la phylogénie des Haptophytes présentée par Young et Bown (1997) et Sáez et al. (2004).

Les principaux termes morphologiques utilisés pour la description des coccolithes sont présentés en Figure A2-1.

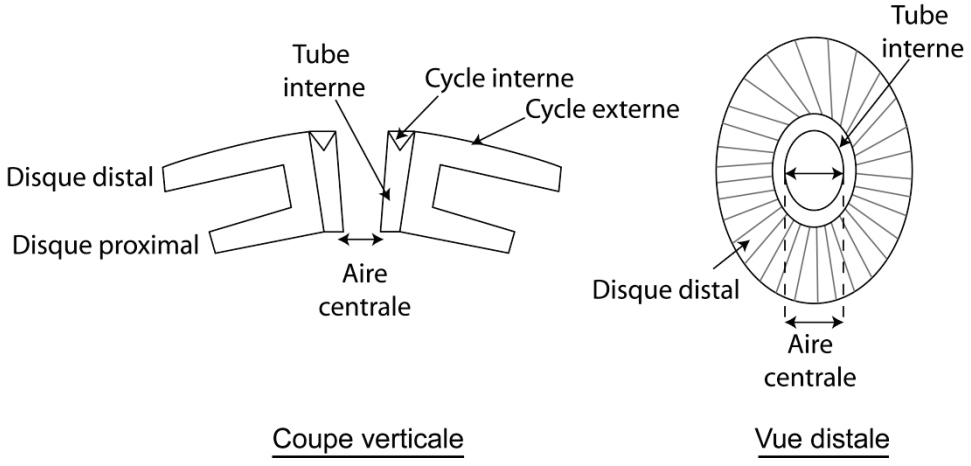

Figure A2-1. Termes clés pour la description morphologique des coccolithes (schéma modifié d'après Bown et Young, 1998).

Les différentes espèces reconnues tout au long de ce travail de thèse (couvrant l'Eocène, Oligocène et Pliocène) sont présentées ci-dessous. Elles ont été distinguées sur la base de critères morphologiques observés au microscope otique et présentés dans la littérature.

Famille *Noëlaerhabdaceae* Jerkovic, 1970 emend. Young & Bown 1997

Genre *Reticulofenestra* Hay, Mohler and Wade 1966

Coccolithes elliptiques à sub-circulaires avec une aire centrale largement ouverte et pas de fentes sur le disque distal.

Reticulofenestra clatrata Muller, 1970: coccolithes de taille moyenne avec de grandes marges et une grande aire centrale occupée par une plaque perforée et divisée par une suture médiane.
Reticulofenestra daviesii (Haq, 1968) Haq, 1971: coccolithes de taille moyenne (5-8 µm) avec des septes qui délimitent des gros pores dans l'aire centrale.
Reticulofenestra dictyoda Stradner in Stradner and Edwards, 1968: coccolithes elliptiques petits à grands (3-14 µm) avec une large aire centrale.
Reticulofenestra haqii Backman, 1978: morphoespèces de 3-5 µm de longueur avec une ouverture de l'aire centrale inférieure à 1.5 µm.
Reticulofenestra hillae Bukry and Percival, 1971: grands coccolithes elliptiques (> 12 µm) avec un cycle interne du disque distal épais, qui se développe autour d'une petite ouverture centrale ne dépassant pas le tiers de la longueur du coccolithe.
Reticulofenestra minuta Roth, 1970: morphoespèces plus petites que 3 µm.
Reticulofenestra minutula (Gartner, 1967) Haq and Berggren, 1978: morphoespèces de 3-5 µm de longueur avec une ouverture de l'aire centrale supérieure à 1.5 µm.
Reticulofenestra pseudoumbilicus (Gartner, 1967) Gartner, 1969: grandes morphoespèces (5-7 µm).
Reticulofenestra umbilicus (Levin, 1965) Martini and Ritzkowski, 1968: très grands coccolithes elliptiques (> 14 µm, comme décrit par Backman and Hermelin, 1986) avec une large aire centrale.

Genre *Dictyococcites* (Black, 1967) emend. Backman, 1980

Coccolithes elliptiques avec une large aire centrale fermée ou presque fermée. L'aire centrale du disque distal montre fréquemment un sillon médian ou un pore circulaire, mais pas assez large pour suggérer une aire centrale ouverte, caractéristique d'après les auteurs du genre *Reticulofenestra*. Bien que *Dictyococcites sensu* Black (1967) puisse être considéré comme une *Reticulofenestra* fortement calcifiée, la diagnose émendée de Backman (1980) distingue clairement ce genre de *Reticulofenestra*.

Dictyococcites antarcticus Haq, 1976: coccolithes de taille moyenne (4-8 μm) avec une aire centrale rectangulaire étroite et allongée (appelé "furrow", sillon, dans Haq, 1976 ou "straight band", bande droite dans Backman, 1980). Ce sillon mesure au moins la moitié de la longueur totale de l'aire centrale (Backman, 1980).
Dictyococcites bisectus (Hay et al., 1966) Bukry and Percival, 1971 = *Reticulofenestra bisecta* (Hay et al., 1966) Roth, 1970: coccolithes elliptiques très biréfringents (< 10 μm) avec une aire centrale du disque distal fermée.
Dictyococcites hesslandii (Haq, 1966) Haq and Lohmann, 1976: coccolithes de taille moyenne (3-8 μm) avec une aire centrale du disque distal montrant un petit pore, à partir duquel les bandes d'extinction rayonnent.
Dictyococcites stavensis (Levin and Joerger, 1976) = *Reticulofenestra stavensis* (Levin and Joerger, 1967) Varol, 1989: coccolithes elliptiques très biréfringents (> 10 μm) avec une aire centrale du disque distal fermée.
Dictyococcites spp.: petites morphoespèces (< 3 μm) avec une aire centrale fermée.

Genre *Cyclicargolithus* Bukry, 1971

Coccolithes circulaires à sub-circulaires avec une petite aire centrale et un tube intern élevé. Bien que Theodoridis (1984) assimile *Cyclicargolithus* comme *Reticulofenestra*, la diagnose émendée de Bukry (1971) sépare clairement ce genre de *Reticulofenestra*.

Cyclicargolithus abisectus (Müller, 1970) Wise, 1973: grandes espèces (>10 μm).
Cyclicargolithus floridanus (Roth and Hay in Hay et al., 1967) Bukry, 1971: espèces plus petites que 10 μm.

Genre *Pseudoemiliania* Gartner, 1969

Coccolithes circulaires à sub-circulaires avec un nombre variable de fentes dans le disque distal. Une seule espèce a été identifiée lors de ce travail de thèse:

Pseudoemiliania lacunosa (Kamptner, 1963) Gartner, 1969

Genre *Gephyrocapsa* Kamptner, 1943

Coccolithes elliptiques avec une structure similaire à celle de *Reticulofenestra*, mais avec un pont formé par les éléments du tube interne qui se rejoignent au milieu de l'aire centrale.

Small *Gephyrocapsa*: morphoespèces plus petites que 3 μm.

Références

Aubry, M.P., 1992. Paleogene calcareous nannofossils from the Kerguelen Plateau, Leg 120. Proceedings of the Ocean Drilling Program Scientific Results 120, 471–491, doi:10.2973/odp.proc.sr.120.149.1992.

Backman, J., 1980. Miocene-Pliocene nannofossils and sedimentation rates in the Hatton-Rockall basin, NE Atlantic Ocean. Stockholm Contribution in Geology 36 (1), 1–91.

Beaufort, L., 1992. Size variations in late Miocene Reticulofenestra and implication for paleoclimatic interpretation. Memorie di Scienze Geologiche 43, 339–350.

Black, M., 1967. New names for some coccolith taxa. Proceedings of the Geological Society of London 1640, 139–145.

Bown, P.R., Young, J.R., 1998. Introduction. In: Bown, P.R. (Ed.), Calcareous Nannofossil Biostratigraphy. British Micropalaeontology Society Publication Series, Kluver Academic Publishers, Cambridge, pp. 5.

Bukry, D., 1971. Cenozoic calcareous nannofossils from the Pacific Ocean. Transactions of the San Diego Society Natural History 16, 303–327.

Henderiks, J., 2008. Coccolithophore size rules—Reconstructing ancient cell geometry and cellular calcite quota from fossil coccoliths. Marine Micropaleontology 67, 143–154, doi:10.1016/j.marmicro.2008.01.005.

Henderiks, J., Pagani, M., 2007. Refining ancient carbon dioxide estimates: Significance of coccolithophore cell size for alkenone-based pCO_2 records. Paleoceanography 22, PA3202, doi:10.1029/2006PA001399.

Marlowe, I.T., Brassell, S.C., Eglinton, G., Green, J.C., 1990. Long-chain alkenones and alkyl alkenoates and the fossil coccolith record of marine sediments. Chemical Geology 88, 349-375.

Sáez, A.G., Probert, I., Young, J.R., Edvardsen, B., Eikrem, W., Medlin, L.K., 2004. A review of the phylogeny of the Haptophyta. In: Thierstein, H.R., Young, J.R. (Eds), Coccolithophores: From molecular processes to global impact. Springer-Verlag, Berlin Heidelberg, pp. 251–269.

Theodoridis, S., 1984. Calcareous Nannofossil Biozonation of the Miocene and revision of the *Helicoliths* and *Discoasters*. Utrecht Micropaleontology Bulletin Series 32, 1–271.

Young, J.R., 1990. Size variation of Neogene *Reticulofenestra* coccoliths from Indian Ocean DSDP Cores. Journal of Micropaleontology 9, 71–86.

Young, J.R., Bown, P.R., 1997. Cenozoic calcareous nannoplankton classification. Journal of Nannoplankton Research 19, 36-47.

Young, J.R., Geisen, M., Cros, L., Kleijne, A., Probert, I., Sprengel, C., Ostergaard, J.B., 2003. A guide to extant coccolithophore taxonomy. Journal of Nannoplankton Research Special Issue 1, 1–132.

Planche A2-1. Images au microscope à lumière polarisée (1000x) des différentes espèces de Noëlaerhabdaceae identifiées au cours de ce travail de thèse. Barres d'échelle: 1µm.

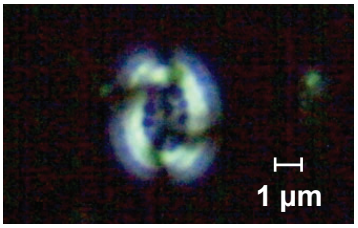

a) *Reticulofenestra clatrata*
Echantillon 511-9R2-56

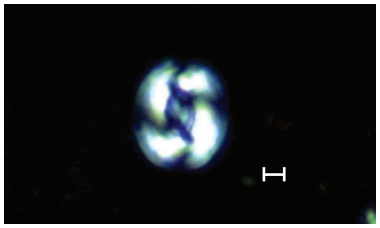

b) *Reticulofenestra daviesii*
Echantillon 511-9R2-56

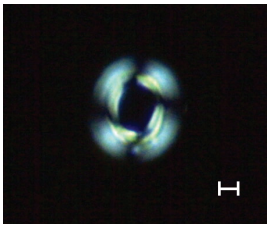

c) *Reticulofenestra dictyoda*
Echantillon 511-20R2-80

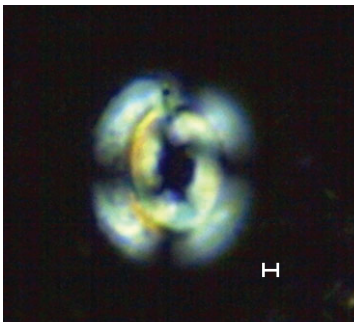

d) *Reticulofenestra hillae*
Echantillon 511-20R2-80

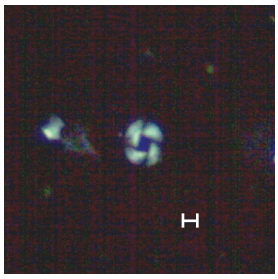

e) *Reticulofenestra minuta*
Echantillon 511-20R2-80

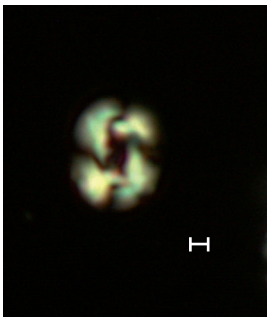

f) *Reticulofenestra minutula*
Echantillon 608-39H3-127

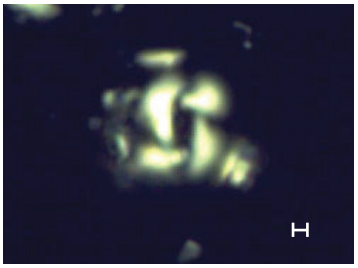

h) *Reticulofenestra pseudoumbilicus*
Echantillon 516-27H3-79

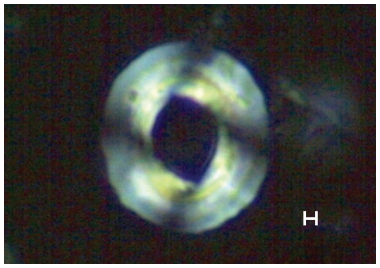

g) *Reticulofenestra umbilicus*
Echantillon 511-9R2-56

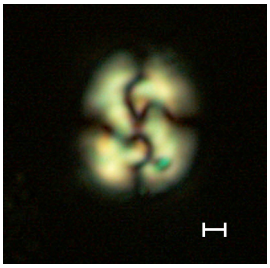

i) *Dictyococcites antarcticus*
Echantillon 588C-4R5-33

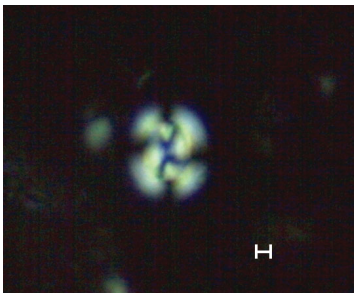

j) *Dictyococcites bisectus*
Echantillon 511-9R2-56

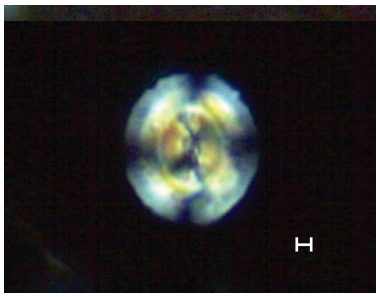

k) *Dictyococcites stavensis*
Echantillon 511-20R2-80

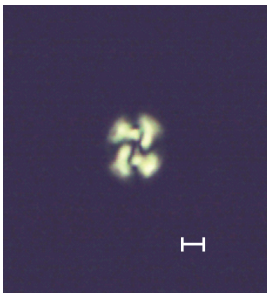

l) *Dictyococcites spp.*
Echantillon 516-27H3-79

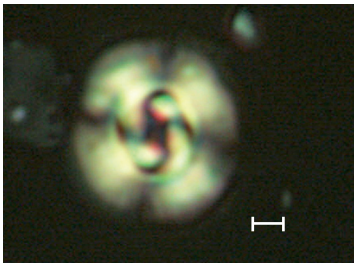

m) *Cyclicargolithus floridanus*
Echantillon 516-26H2-18

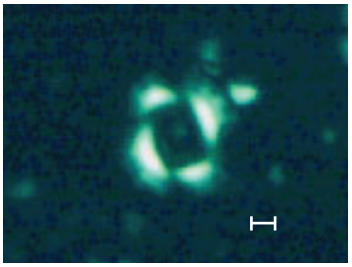

n) *Pseudoemiliania lacunosa*
Echantillon PP84

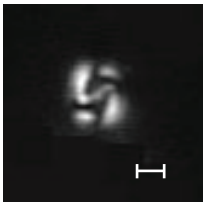

o) *Small Gephyrocapsa*
Image tirée du site internet Nannotax

Planche A2-1.